DEVELOPMENT OF AN AUTOMATED WHEELCHAIR TIEDOWN AND OCCUPANT RESTRAINT SYSTEM

KATHLEEN D. KLINICH, MIRIAM A. MANARY, KYLE J. BOYLE,

NICHOLE R. ORTON, JINGWEN HU

UMTRI | TRANSPORTATION RESEARCH INSTITUTE
UNIVERSITY OF MICHIGAN

Technical Report Documentation Page

1. Report No. UMTRI-2021-2	2. Government Accession No.	3. Recipient's Catalog No.
4. Title and Subtitle Development of an Automated Wheelchair Tiedown and Occupant Restraint System		5. Report Date September 2021
		6. Performing Organization Code
7. Author(s) Klinich, Kathleen D., Manary, Miriam. A., Boyle, Kyle J., Orton, Nichole R., Hu, Jingwen		8. Performing Organization Report No.
9. Performing Organization Name and Address University of Michigan Transportation Research Institute 2901 Baxter Rd. Ann Arbor MI 48109		10. Work Unit No. (TRAIS)
		11. Contract or Grant No. DTNH2215D00017:
12. Sponsoring Agency Name and Address National Highway Traffic Safety Administration 1200 New Jersey Avenue SE Washington, DC, 20590		13. Type of Report and Period Covered Final, October 2019-December 2021
		14. Sponsoring Agency Code

16. Abstract

This project developed an automated wheelchair tiedown and restraint system (AWTORS) that could be safely and independently used in an automated vehicle (AV) by someone using a wheelchair as vehicle seating. The project used past research, computational modeling, prototype construction, volunteer evaluation, and dynamic testing to demonstrate feasibility. Computational modeling was used to optimize placement of the wheelchair station, locate the wheelchair anchorages relative to the occupant, optimize belt anchor locations, and determine airbag characteristics for front and side impacts. Frontal simulations showed improved injury measures with a Self-Conforming Rearseat AirBag (SCaRAB), particularly with suboptimal belt geometry. Side impact simulations showed adequate protection in nearside crashes with standard curtain airbags and outboard shoulder belt location. However, changes to belt geometry were insufficient to keep the occupant within the wheelchair during farside impacts, leading to design of a Center Airbag To Contain Humans (CATCH). Models of power and manual wheelchairs were developed and used to choose restraint and geometry parameters for sled testing. The concept for securing the wheelchair to the vehicle used hardware meeting specifications of the Universal Docking Interface Geometry (UDIG) that have been included in RESNA and ISO standards. Vehicle anchorages meeting the specifications were constructed, as were attachment designs for a commercial manual and power wheelchair. The occupant restraint portion of the AWTORS included an automatic seatbelt donning mechanism based on a past UMTRI prototype, but with geometric improvements. Volunteer testing was performed with 8 wheelchair users. Using the two study wheelchairs equipped with UDIG anchors, the study evaluated the usability of four wheelchair seating stations with different geometries, each with two different belt conditions. Data included videos of ingress and egress, scans of volunteer posture, and questionnaires to document the time spent docking the wheelchair and donning the seatbelt, belt fit, comfort, and potential usability issues. Average time for entry, docking, and donning was less than 2 minutes in all conditions. For three-quarters of trials, participants would recommend use of the docking and donning systems. The preparation of test fixtures for volunteer testing identified challenges in implementing optimal geometry defined through simulations. Ten frontal sled tests were performed to demonstrate differences with belt geometry and airbag presence, as well as to check the durability of UDIG anchors and attachments. Eight farside impacts were run to evaluate different versions of the CATCH bag, as well as to check durability of UDIG attachments in side impact.

17. Key Word Wheelchair, transportation, UDIG, occupant restraint, automated vehicles		18. Distribution Statement	
19. Security Classif. (of this report) Unclassified	20. Security Classif. (of this page) Unclassified	21. No. of Pages 261	22. Price

Form DOT F 1700.7 (8-72) Reproduction of completed page authorized

This report includes the same technical content as DOT HS 813 275. However, the title differs from the DOT report; it emphasizes that the "Wheelchair Tiedowns" and "Occupant Restraint Systems" are both separate, important components needed to travel safely while seated in a wheelchair.

Contents

List of Figures

List of Tables

Introduction

For people with disabilities who do not drive, automated vehicles (AVs) would provide a welcome opportunity for independent travel. According to the American Community Survey (ACS), the overall percentage of people with disability in the United States in 2017 was 12.7% (Erickson et al., 2018). Among the six categories of disabilities identified by the ACS, the highest prevalence across all ages was the 6.9% reported as having an ambulatory disability, which increases rapidly with age. In the 2017 National Household Travel Survey, 25.5 million people over age 5 report disabilities that limit their ability to travel (Brumbaugh, 2018). Of these, 11.6% use manual wheelchairs, 3.9% use power wheelchairs, and 4.4% use scooters, indicating that about five million people use wheeled mobility devices in the United States.

The Americans with Disabilities Act (2010) and its interpretation as the ADA Accessibility Guidelines (36 CFR Part 1192, 2017) through the U.S. Access Board[1] provides detailed transportation requirements that are translated into regulations by the U.S. Department of Transportation. These establish necessary minimum levels of accessibility and accommodations that are required in compliant public transportation, including requirements for assistance by a driver or other operator. However, these requirements do not consider the scenario where an individual with a disability travels in a public vehicle without a driver or other operator.

Some people who use wheelchairs cannot transfer to conventional vehicle seating and must remain seated in their wheelchairs for motor vehicle travel. In these situations, it is necessary to secure the wheelchair to the vehicle and provide occupant protection with a Wheelchair Tiedown and Occupant Restraint System (WTORS). For this population to fully realize the promise of independent AV transportation, a WTORS must be crashworthy for use in smaller vehicles, able to be used without third-party assistance, and able to accommodate a wide range of wheelchair types.

This report describes a project to develop an automated WTORS that could be safely and independently used in an AV by people who remain seated in their wheelchairs for travel. The Literature Review chapter reviews the literature related to wheelchair transportation safety, with a focus on topics that are relevant for providing the opportunity for safe, independent use of automated vehicles to people who use wheelchairs. The Design Concept and Approach chapter describes initial strategies on design space, prototype concepts, computational modeling, volunteer assessment, and dynamic testing. The Computational Modeling Chapter details the methods of validating frontal and side impact wheelchair models, optimization of restraint systems, and simulations of feasible geometry. The Design and Prototype chapter provides details of the hardware development for the wheelchair attachments, vehicle anchorages, and automated belt donning arm, as well as considerations for implementing usable wheelchair seating stations. The Volunteer Assessment Chapter details the methods and

---

[1] The full name of this agency is the Architectural and Transportation Barriers Compliance Board, an independent Federal agency created in 1973 and devoted to accessibility for people with disabilities. It is commonly referred to as the U.S. Access Board.

results of hardware evaluation by eight volunteers who were regular wheelchair users. The Dynamic Testing chapter reports methods and results to evaluate prototypes in ten frontal and eight farside impacts. Finally, the Discussion addresses some of the remaining challenges to implementing safe and independent AWTORS for use in AVs.

Literature Review

Wheelchair Transportation Safety Basics

A best-practices travel recommendation for individuals who use wheelchairs and travel in passenger vehicles is to transfer to the original production vehicle seats and make use of the vehicle's occupant protection systems (ANSI/RESNA 2017d). An AV intended to be used in this way would also need an automated method of stowing and securing a wheelchair and transfer aids.

People for whom transfer from their wheelchairs is infeasible or impractical can use adapted vehicles, which are configured to allow use of a wheelchair as vehicle seating. Vehicle adaptations include increasing cabin height by 200 to 250 mm (8 to 10 in), ramps or lifts to facilitate ingress and egress, modified controls for those who can drive, specialized hardware to secure the wheelchair to the vehicle, and a method of protecting the occupant in a crash that is compatible with wheelchair use. The last two elements are commonly referred to as the Wheelchair Tiedown and Occupant Restraint System (WTORS). In addition, people using wheelchairs as vehicle seating should choose wheelchair, WTORS, and accessories that have been crash tested according to voluntary guidelines prescribed in ANSI/RESNA Volume 4 WC18 and WC19 (2017) (see relevant standards section.) Since 2000, the University of Michigan Transportation Research Institute (UMTRI) has developed, maintained, and distributed the online "Ride Safe" brochure available at the portal at http://wc-transportation-safety.umtri.umich.edu/ridesafe-brochure to educate consumers and caregivers on these best practice recommendations for traveling in wheelchairs.

Wheelchair Securement Systems

To travel solo in a private vehicle while using a wheelchair as vehicle seating, individuals must firmly secure the wheelchair to the vehicle. The most common strategy for people who drive while seated in wheelchairs involves customized hardware added to the bottom of wheelchairs that dock into securement systems mounted on the vehicle floors. An example is shown in Figure 1. Good function of these systems depends on maintaining close alignment of the mating hardware to allow effective docking to occur between the wheelchair and vehicle. However, day-to-day differences in wheelchair tire pressure or added wheelchair cargo can be enough to obstruct the process. A recent study showed that half of users needed multiple attempts to dock their wheelchairs in these securement systems (van Roosmalen et al., 2013). In addition, this design of wheelchair docking system usually reduces the ground clearance of the wheelchair and increases difficulty of traversing over door thresholds and uneven surfaces. Such systems are also customized for a particular pairing of a single user and a single private

vehicle and are not adaptable to a shared vehicle paradigm where one wheelchair space needs to accommodate many different people using wheelchairs.

Figure 1. Examples of wheelchairs engaged with docking systems mounted to vehicle floor (upper left and right) and example of mating hardware with low ground clearance (lower center).

For people traveling as passengers in modified vehicles or via public transportation, the most common method of securing the wheelchair to the vehicle is a 4-point strap tiedown system. An example is shown in Figure 2. With this tiedown method, four straps are anchored to reinforced points on the vehicle floor, hooked onto the wheelchair, and tightened. This system allows a single WTORS to secure a wide range of wheelchair types and has been shown to be very effective in the field. Although this system is the most common travel scenario for people who remain in their wheelchairs, few wheelchair users can independently secure their own wheelchairs with this technique. This system also usually requires a third party to assist with the application of the seatbelt and its routing around wheelchair features. Often this means that a stranger must enter the wheelchair user's personal space and physically contact them to apply the seatbelt. This can be uncomfortable for wheelchair users. On a public transportation system, the person providing assistance is often the driver of the vehicle, which necessitates a longer dwell time at the stops where the wheelchair user boards and alights from the vehicle, impacting the timeliness of the transit schedule. The added procedures also increase the social stigma for the person in the wheelchair. Because a caregiver or driver may not be present to help in an AV, this approach is not a viable independent solution for securing wheelchairs in AVs.
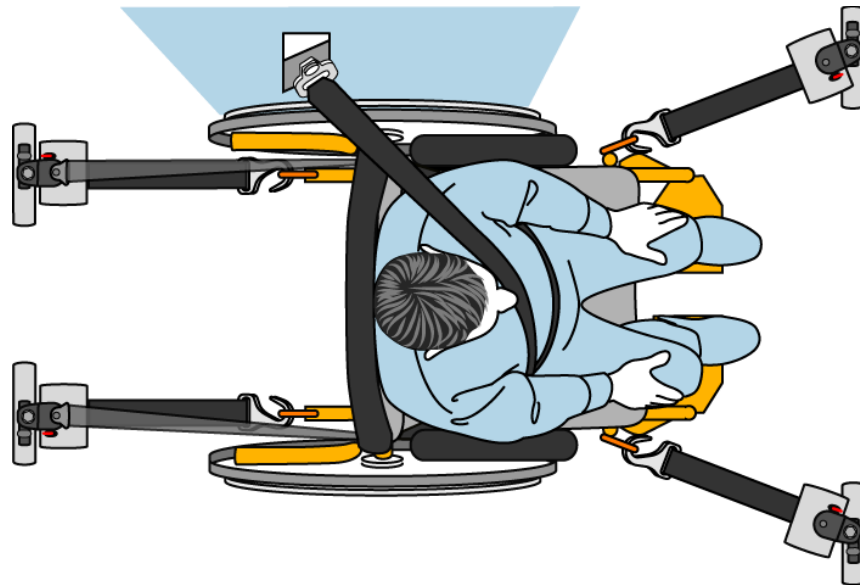
Figure 2. Example of a wheelchair secured by 4-pt strap tiedown system

ADA guidelines allow the use of rear-facing wheelchair passenger stations on large, heavy fixed route vehicles. Examples are shown in Figure 3. These offer a high level of independence on large accessible transit vehicles (LATVs), and provide wheelchair users with a similar level of protection as the other LATV passengers who are not restrained in the bus seats and who are allowed to stand during vehicle travel. However, rear-facing stations are currently not robust enough to meet requirements of voluntary wheelchair tiedown dynamic tests, which are designed for the crash severities expected in lighter, minivan-sized vehicles. Rear-facing wheelchair passenger stations have been deployed since 2005 in some major metropolitan bus systems, while the new Q'Straint Quantum autonomous docking stations (an enhanced version of rear-facing station) have entered the market more recently.

Figure 3. Rear-facing wheelchair passenger station (left) and Q'Straint Quantum automated docking system (right).

LATVs will always have a lower distribution of crash severities compared to passenger vehicles primarily because of their higher mass, but for lighter-weight AVs, both protection in high severity crashes as well as independent use are needed. The operating speed of an AV will influence the overall distribution of crash severities, but even if an AV was unlikely to cause, it could still experience a high severity crash because other vehicles could strike it at high speed.

The Universal Docking Interface Geometry (UDIG), shown in Figure 4 and Figure 5 (Hobson and van Roosmalen, 2007), is one proposed solution for making docking stations that can work in a public transportation setting where one wheelchair station must secure many types of wheelchair users. UDIG defines an interface geometry and interface location that can be the basis for design of docking stations and dockable wheelchairs. For the wheelchair, as shown in Figure 5, the required UDIG elements are two 22-mm diameter, 75-mm long, vertical tube-shaped features located on the lower rear of the wheelchair that are spaced 222 to 333 mm apart. These are located on the wheelchair so that the bottom of the tubes is 203 mm above the floor surface. If needed to control rotation performance during impact, the UDIG can also include a horizontal bar that connects the tops of the two vertical tubes and is 319 mm above the floor. This concept is akin to the standardization of trailer hitches that allow any semi-tractor driver to attach and tow any trailer. Because UDIG attachments are located to the rear of the wheelchair, the design has the advantage of not decreasing ground clearance on equipped wheelchairs. Although this geometry has been defined, prototyped, crash tested, and field tested (Hobson and van Roosmalen, 2007; van Roosmalen et al., 2011; Van Roosmalen et al., 2002; Turkovich et al., 2011), it has not been incorporated into any commercial products to date. However, specifications for UDIG geometry are included in informative and normative annexes of current wheelchair transportation safety standards in the United States and internationally. The key barrier to implementation of the UDIG system is the voluntary nature of wheelchair safety standards; vehicles must be equipped with UDIG docking hardware and wheelchairs must be equipped with UDIG securement hardware before the system is feasible.
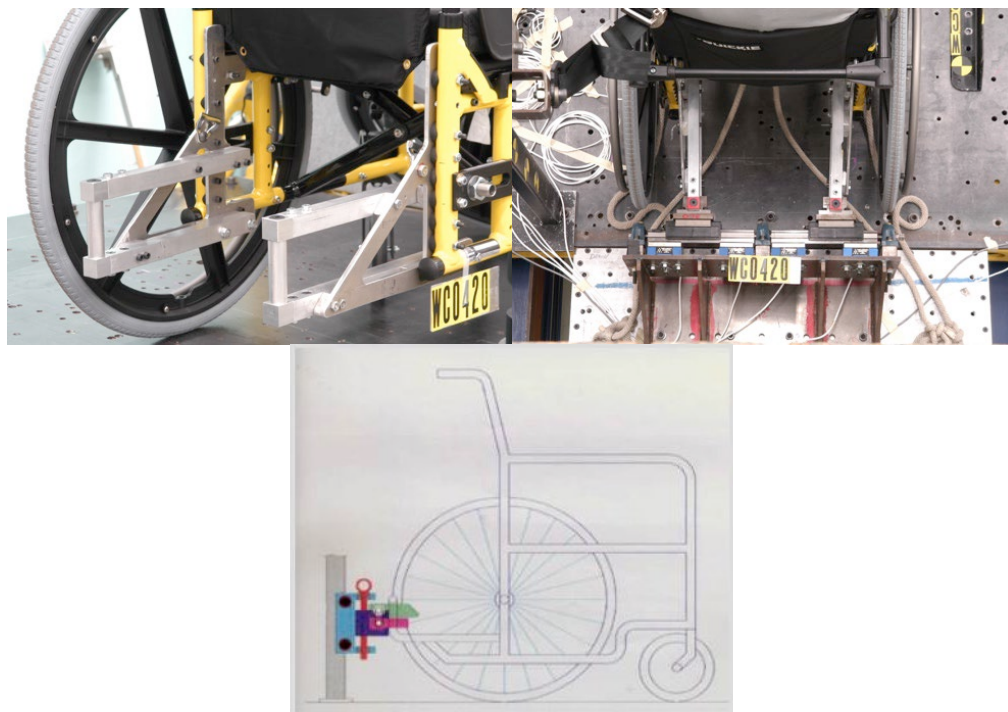
Figure 4. UDIG attachment hardware on wheelchair (upper left), wheelchair engaged with UDIG mounting hardware (upper right), and diagram of UDIG geometry (lower center).

Max. 333
Min. 222
rad. - 0 to 30
75
75
127
11R ± 1
22 ± 1

Rear View

Side View at Section A-A

Dimensions in millimeters
Tolerances: ± 3 mm, unless otherwise noted
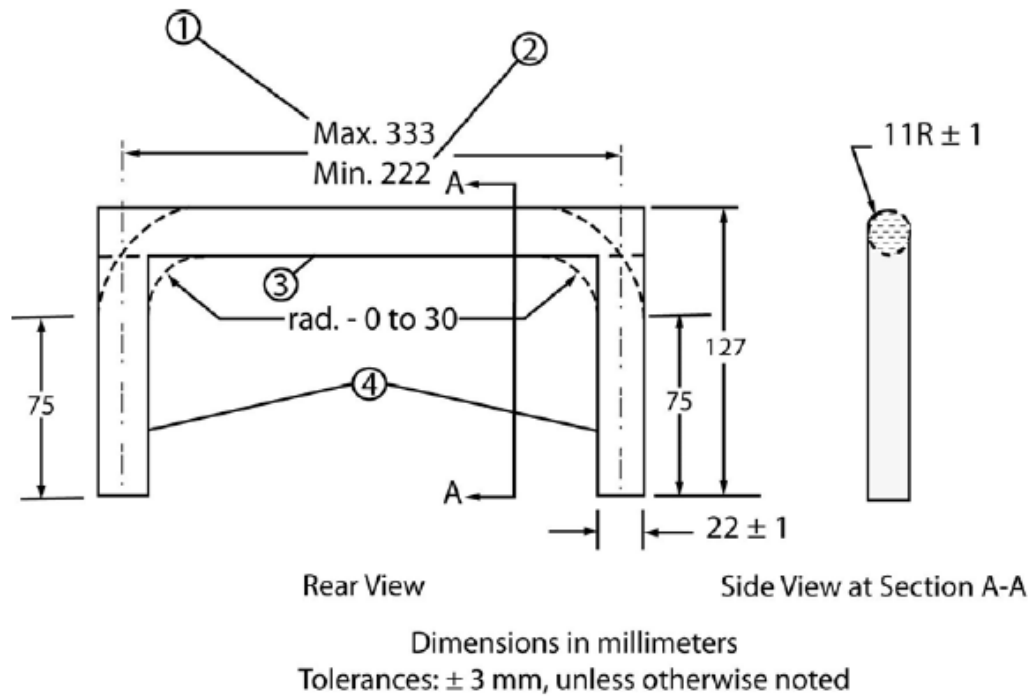
Key
1   maximum UDIG width
2   minimum UDIG width
3   horizontal segment
4   vertical segment

Figure 5. UDIG dimensions.

Hobson and van Roosmalen (Hobson and van Roosmalen 2007) describe the development and testing of an automatic docking device meeting UDIG specifications for public transit vehicles. The system was crash tested at UMTRI using WC18 specifications. An energy-absorbing component was evaluated in one test but did not provide additional benefit. The researchers received input on the system from a focus group of wheelchair users, which led to refinements of the maneuvering area, user controls, driver controls, and emergency release mechanisms for installation on a large transit bus for usability testing. Initial evaluation was performed on a test track with one user evaluating the ride performance of a manual and power wheelchair secured with the docking station. Displacement was monitored during braking and turning maneuvers. The manual wheelchair had more than the 50 mm (2 in) of displacement allowed by ADAAG requirements during turning, but other conditions were acceptable (36 CFR Part 1192, 2017). Because the system was evaluated on a large transit bus, an occupant restraint was not included in the evaluation.

A subsequent study compared usability, comfort, and independent use of 4-point strap tiedown, a rear-facing station, and a UDIG-compatible auto-docking system on a large transit vehicle (van Roosmalen et al., 2011; Turkovich et al., 2011). Twenty subjects who could transfer to the modified wheelchairs took 15-minute bus rides using each device and then completed a survey. Figure 6 shows the three types of wheeled mobility devices used in the study, each equipped with hardware that meets the UDIG specifications. Participants rated the autodocking and rear-facing stations as being faster and easier to use than the 4-point strap tiedown system. Discomfort from riding rear-facing, as well as the inability to see stops, were commonly reported for the rear-facing station. Fourteen occupants preferred the autodocking station for travel, because it allowed secure and independent use. However, they noted that requiring specialized hardware on the wheelchair was a barrier to use. All securement systems met the less than 50 mm displacement requirement established by the ADA. Maximum occupant acceleration during maneuvers was 0.76 g.

Figure 6. A power wheelchair (upper left), manual wheelchair (upper right), and scooter (lower center) equipped with UDIG-compatible hardware.

The effect of UDIG hardware placement on a wheelchair was explored using DYNAMAN models (van Roosmalen et al. 2003). They used a model of a manual wheelchair equipped with a wheelchair-mounted lap belt and a vehicle-mounted shoulder belt. They varied the fore-aft location, lateral spacing, and vertical spacing of the wheelchair-mounted UDIG hardware by 100 mm to evaluate effect on wheelchair and occupant (midsized male ATD) kinematics. They simulated front impact with a 48 km/hr (30 mi/hr)/20 g pulse, and side impact with a 24 km/hr (15 mi/hr)/12 g pulse. The center of gravity (CG) of the wheelchair was varied from 12 in to 17.5 in above the floor. Reported outcomes were frontal or lateral excursions. The lowest excursions in frontal impact occurred when the UDIG was mounted high, wide, and forward, in wheelchairs with a low CG. The lowest excursions in side impact occurred with the widest UDIG mounting configuration.

Table 1 summarizes the different types of existing wheelchair tiedown systems according to their independent use, crashworthiness level, and compatibility between different wheelchairs and vehicles. Currently, only a system meeting UDIG requirements would allow users to independently secure themselves in large and small vehicles using any combination of wheelchair and vehicle equipped with appropriate hardware.

Table 1. Assessment of WTORS by independent use, crashworthiness level, and wheelchair/vehicle compatibility

WTORS type	Independent use	High g and low g crashes	Any combination of wheelchair and vehicle?
4-pt strap tiedown paired with seatbelt	No	Yes	Yes
Docking station paired with seatbelt	Yes	Yes	No
Rear-facing stations	Yes	No	Yes
UDIG docking paired with automatic seatbelt	**Yes**	**Yes**	**Yes**

Belt Restraint Systems Used With Wheelchairs

People who drive while seated in their wheelchairs in private vehicles often use the lap and shoulder belt restraints provided with the vehicles. However, in a modified vehicle, the inboard buckle is often mounted to an aftermarket stalk attached to the floor, as the original vehicle inboard buckle has been removed with the vehicle seat to create the wheelchair station. In addition, active features such as seatbelt pre-tensioner and occupant classification system may be disabled as part of the vehicle modification. If the driver's dexterity will not allow them to buckle a seatbelt, an alternative approach is to drape the pre-buckled lap and shoulder belt onto the steering wheel so that the driver can maneuver into the restraint while seated in the wheelchair. This option often results in a loose belt restraint or poorly placed belts due to interference with the wheelchair armrests and controls. Examples are shown in Figure 7.

Figure 7. Driver using vehicle belt with poor fit (left) and a "drive-in" belt arrangement (right).

An example of a restraint system used for passengers traveling in wheelchairs is shown in Figure 8. Because a wheelchair user who depends on a 4-point strap tiedown system to secure the wheelchair will likely need assistance, the belt restraint systems are also designed to be donned with assistance. They may or may not include retractors.

Figure 8. Passenger belt system

A past project conducted at UMTRI and the University of Pittsburgh included a study of 29 individuals who drove (n=21) adaptive vehicles or traveled in private vehicles while seated in wheelchairs (n=8) (Orton et al., 2019; Ritchie et al., 2009; van Roosmalen et al., 2013). This study evaluated the ease of ingress and egress, wheelchair securement, and seatbelt use as well as the locations of seatbelt anchor points and other vehicle interior features through observation of volunteers and subject surveys. The posture and position of the wheelchair user in their preferred travel position was also quantified. Although recommendations for placing seatbelt anchors to provide optimal protection had been available for some time, and the

process of modifying a vehicle even allows customization for a particular size of person using a wheelchair, almost none of the participants had good seatbelt fit. Many individuals also had trouble using the seatbelt systems. Several subjects needed torso support to maintain a driving position, which led to modifications of the belt restraint system that compromised belt fit. Despite the poor belt fit documented in this study, most of the subjects indicated that they felt safe using their wheelchair tiedowns and occupant restraint systems. Seven of the twenty-one drivers had deactivated steering-wheel airbags.

Wheelchair features, particularly closed-front arm supports and lateral thigh support features, often prevent good fit of the seatbelt system to the rider. The ANSI/RESNA voluntary wheelchair standard for wheelchairs used as seats in motor vehicles, ANSI/RESNA Volume 4: Section 19 (commonly called WC19, ANSI/RESNA 2017d), includes wheelchair performance requirements to eliminate these conflicts. People with decreased dexterity, limited range of motion, and vision deficits often have difficulty buckling, applying, and releasing conventional seatbelt systems.

Poor fit of safety systems for people seated in wheelchairs, along with higher levels of non-use and misuse of seatbelts, have also been documented in analysis of field injury events (Schneider et al., 2010, 2016). In this study, in-depth investigations of 69 incidents involving 74 occupants seated in wheelchairs were reviewed. Most of the incidents were frontal crashes, although three non-crash events were included. 81% of occupants were appropriately using tiedown systems, and only one case had a failure. However, only 29% of the occupants were appropriately restrained by lap-shoulder belts; lack of use and misuse that resulted in poor belt fit were frequent. 62% of occupants in these cases experienced serious injury, with 10 cases resulting in death.

Because of challenges in donning seatbelts, as well as issues with fit, an alternate solution is for the wheelchair to be equipped with a crash-tested belt restraint system. Examples are shown in Figure 9. These belt systems are currently offered on a limited number of wheelchairs and the option must be offered on a WC19-compliant wheelchair. While requirements to include crash tested belt restraint systems on all wheelchairs would simplify use of AVs and likely improve belt fit (thus increasing crash protection) for all occupants, the voluntary nature of wheelchair testing standards coupled with the increased expense of equipping wheelchairs with crash-tested belt restraints has limited their widespread deployment.

Figure 9. Crash-tested wheelchair restraints

Some previous work explored the concept of a self-donning seatbelt. Q'Straint developed the DIOR system shown on the left in Figure 10, but has discontinued its sale. A prototype donning system, shown on the right two pictures of Figure 10 have been developed in a past research project conducted at UMTRI (Weir et al., 2011). The seatbelt deployment system (SBDS) uses the vehicle equipped seatbelt, but with the buckle mounted to a rigid rotating stalk. The length of the stalk can be adjusted for the size of the occupant and wheelchair so the side-view lap-belt angle falls within the recommended 45-to-75-degree range relative to horizontal. The wheelchair user moves into the seating position, then uses a hand control to activate a powered arm that rotates the buckle down to the floor, where it is secured in a floor-mounted anchorage pocket. The SBDS works best with wheelchairs that have an open-front arm support design. The system has successfully been crash tested using WC19 procedures.

Figure 10. Q'Straint DIOR self-donning belt system top) and UMTRI prototype belt donning system (lower left and right).

Relevant Standards

Since current Federal Motor Vehicle Safety Standards (FMVSS) do not address wheelchairs used as vehicle seating (although FMVSS 403 covers wheelchair lifts), groups of stakeholders have used the precedents and crash protection principles of the FMVSS to establish voluntary industry standards for this circumstance. The Rehabilitation Engineering and Assistive Technology Society North America (RESNA) has a suite of standards contained in four volumes that establish ways to measure, define, and test wheelchairs and wheelchair components, including Volume 4 that currently is comprised of four sections: Section 10 *Wheelchair Containment and Occupant Retention Systems for use in LATV, Systems for Rear-Facing Passengers (WC10, ANSI/RESNA, 2017a),* Section 18 *Wheelchair Tiedowns and Occupant Restraint Systems (WC18, ANSI/RESNA, 2017c)*, Section 19 *Wheelchair used as Seats in Motor Vehicles (WC19, ANSI/RESNA, 2017d)*, and Section 20 *Wheelchair Seating (WC20, ANSI/RESNA, 2017b).* A set of similarly intentioned standards exist for global use within the International Organization for Standardization (ISO) that are developed and maintained by international experts in a working group under Technical Committee 173, Subcommittee 1, Working Group 6. These ISO standards overlap significantly with the ANSI/RESNA standards, with standards 10865-1, 10542-1, 7176-19, 16840-4, being international versions of WC10, WC18, WC19, and WC20, respectively. The set of ISO standards also includes 10865-2 that specifically addresses wheelchair spaces in LATVs for forward-facing passengers and places a high emphasis on independent use.

Many of these standards and test procedures were developed at UMTRI and current staff serve as experts on both RESNA and ISO working groups and/or committees that oversee revisions of these standards (Bertocci et al, 2001; Buning et al., 2012; Karg et al., 2009; Manary et al., 2003, 2009; Manary et al., 2010; Ritchie et al., 2009; Ritchie et al., 2006; Schneider et al., 2008; Schneider and Manary 2006). These standards currently include test protocols for frontal and rear impacts only. Numerous tests series were performed at UMTRI to develop these standards as described below. This section provides a brief overview of the four main RESNA standards.

WC10

WC10 (ANSI/RESNA 2017a) provides specifications and test procedures for rear-facing wheelchair passenger stations (RF-WPS) that are intended for use only in large accessible transit vehicles (LATVs). For LATVs that have lower crash rates per mile, as well as lower severity crashes because of their larger mass, providing a passive containment system for wheelchair users is sufficient to provide an equitable level of transportation safety with a higher degree of personal independence. The level of safety is comparable to unrestrained seated passengers or standing passengers who hold onto stanchions or straps to resist movement during travel.

Part 1 of the standard describes the scope, relating to RF-WPS, while part 2 references other RESNA and Federal standards and part 3 provides relevant definitions. Part 4 defines design requirements in terms of the needed geometry and features required for a RF-WPS, which are described in more detail in Annex A of the standard. Performance requirements found in part 5 include testing the static strength of excursion barriers with methods found in Annex C, the

allowable amount of wheelchair excursion for the wheelchair when tested using procedures found in Annex B, and a required coefficient of friction for the flooring material. Part 6 contains information, labeling, and instruction requirements, while Part 7 contains reporting requirements. Annex D defines specifications for a manual surrogate wheelchair (MSWC) and a scooter surrogate wheelchair (SSWC) that can be used to evaluate the RF-WPS. Annex E contains design guidelines for RF-WPS.

WC18

WC18 (ANSI/RESNA, 2017c) applies to WTORS that consist of a system or device for securing wheelchairs, and a system of belts for restraining occupants seated in wheelchairs. This includes both strap-type and docking-type securement systems. The standard is focused on the application of WTORS to passenger vehicles so assumes a more severe crash environment. Part 2 references other RESNA standards and FMVSS; definitions are included in part 3.

Part 4 of WC18 defines design requirements. They define what elements comprise a complete WTORS system, requirements for wheelchair tiedowns and securement devices, specifications for wheelchair tiedowns/securement adaptors, and features and relevant Federal compliance requirements for occupant restraint components.

Part 5 lists performance requirements. WTORS must meet flammability requirements of FMVSS 302, as well as most requirements of FMVSS 209. If the WTORS has a lap-shoulder belt component, crashworthiness in frontal impact is assessed in two tests, one with the lap-shoulder belt anchored to the vehicle, and one that uses the surrogate lap-shoulder belt with a wheelchair-anchored lap belt defined in Annex D of WC19. Options for testing with different combinations of belt restraints are also included. Tests are conducted either with a specific wheelchair model (SWM) or with a surrogate wheelchair pictured in Figure 11 and defined in Annex E. Sled test procedures use a 48 km/hr (30 mi/hr), 20 g acceleration pulse, similar to that used in FMVSS No. 213 for frontal impact testing, although the allowable corridor is wider than the FMVSS No. 213 pulse. Details regarding the test buck, instrumentation, ATD positioning, wheelchair preparation, pre and post-test measurements, and reporting requirements are also included in Annex A. To pass the test, the system must meet wheelchair, head, and knee excursion limits specified for the ATD used in the test. Values are provided for 3YO, 6YO, 10YO, 5th female, 50th male, and 95th male ATDs. In addition, the ATD must be seated in an upright position after the test, the WTORS components should not completely fail, and the wheelchair should remain undamaged if a SWM is used in the test.

Figure 11. Surrogate wheelchair fixture.

WTORS performance requirements also include geometric and adjustability specifications that are evaluated using procedures in Annex B. Annex C includes procedures for assessing the performance of WTORS under partially engaged conditions. WTORS must have less than 25 mm (1 in) of slip when tested under conditions described in Annex D. WC18 has requirements regarding written materials, including product identification and labeling, instructions for installers, advice and warnings for installers, user and maintenance instructions and warnings, in-vehicle placards, and instructions for WTORS components and subassemblies sold separately. The last part provides direction on how to document compliance with the standard. In addition to the annexes that describe test procedures, Annex F provides design and performance recommendations.

WC19

The scope of WC19 (ANSI/RESNA, 2017d) "is to establish design and performance requirements, and associated test methods, for wheelchairs related to their use as seats in vehicles." Part 2 of the standard references multiple FMVSS, as well as related RESNA voluntary standards. Part 3 provides definitions of terms used in the standard. Part 4 specifies design requirements related to seated posture, mass, size, turning radius, and head/back support, reduction of sharp edges, securement points for four-point strap tiedowns, and wheelchair-anchored belt restraints. The design requirements for the securement points specify the geometry and locations of the four securement points and how they should be attached to the wheelchair; Annex G provides recommendations on securement point design. Wheelchair anchored belt restraints should provide a side-view lap belt angle of 30 to 75 degrees (45 to 75

15

is preferred) relative to horizontal as shown in Figure 12, and Annex H provides belt restraint design recommendations. The belt restraint specifications also define a level of adjustability and attachment hardware for connecting to a vehicle-mounted shoulder belt.
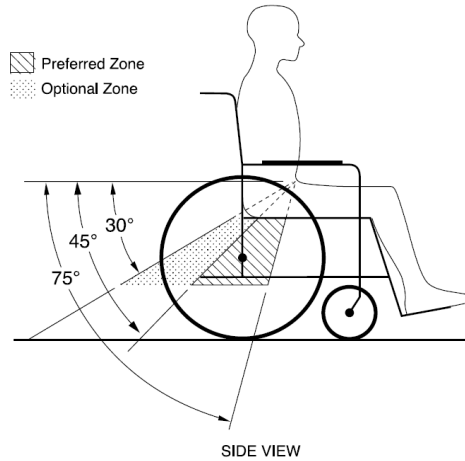
Figure 12. Side view illustration of allowable and preferred lap belt angles.

Part 5 of WC19 describes performance requirements. Tiedown hooks must be able to be engaged to wheelchair securement points with one hand. Seatbelt components must comply with requirements of FMVSS No. 209 and/or FMVSS No. 213. Frontal-impact crashworthiness is assessed with the wheelchair secured by a surrogate four-point strap tiedown system (defined in Annex D and shown in Figure 13), using an adult or pediatric anthropomorphic test device (ATD). To pass the crashworthiness test, wheelchair components must not fail, and the securement points cannot deform to the point where the tiedowns cannot be removed. The wheelchair must be upright and the ATD must be in a seated posture post-test. Maximum wheelchair, knee, and head excursion limits are specified for ATDs ranging from the 3YO to 95th percentile male. Annex A describes the frontal-testing impact procedures, which are essentially the same as the procedures defined in WC18.
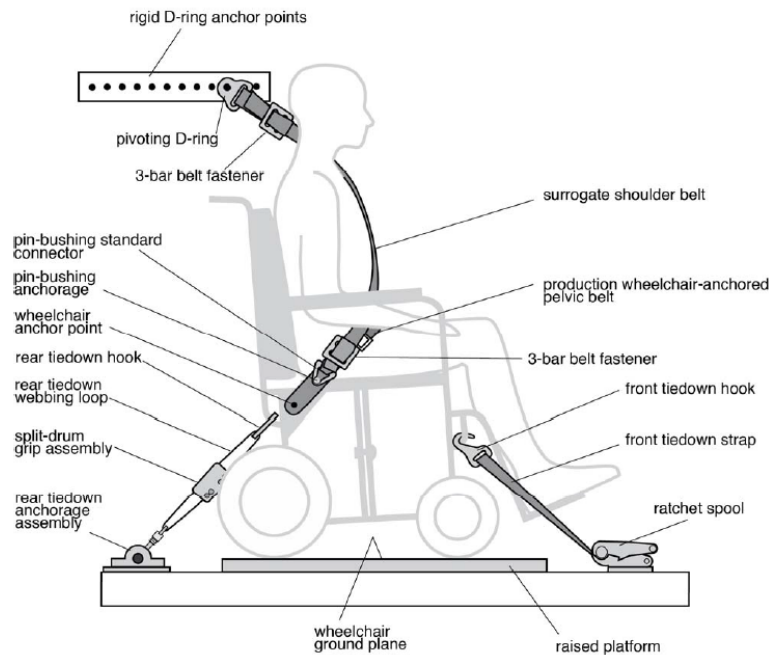
Figure 13. Surrogate WTORS

Additional performance requirements specify that there must be clear paths that are free of sharp edges for the four-point strap tiedowns to reach the securement points. Test procedures for assessing access are provided in Annex B. Lateral stability is assessed with a tilt test described in Annex C. Turning radius must be measured using procedures from RESNA WC:1, Part 5, and included in product literature. Wheelchairs must receive ratings of acceptable or higher regarding accommodation of vehicle-mounted lap-shoulder belt systems, evaluated using procedures in Annex E. The procedures assess ease of achieving proper belt placement on the ATD, lap belt contact and location, shoulder belt contact and location, lap belt angle, lap belt path clear path to anchor points and proximity to sharp edges.

Part 6 of WC19 specifies requirements for product labeling and wheelchair manufacturer literature. Requirements are included for identification and labeling, presale literature, user instructions, and user warnings. Part 7 specifies how to document compliance with the standard.

Annex F of RESNA WC19 provides specifications for the universal docking interface geometry (UDIG), while Annex I provides information about obtaining other standards referenced in Part 2.

WC20

While many wheelchairs are produced as a single piece of equipment made by one manufacturer, for others, a wheelchair base from one manufacturer can be paired with seating systems made by another company to better accommodate the specific needs of the person using the wheelchair. WC20 (ANSI/RESNA 2017b) was developed to allow evaluation of the crash performance of different seating systems independent of the wheelchair frame. Seating systems consist of a seat, back support, and attachment hardware. Part 1 of the standard defines the scope, part 2 incorporates other references, and part 3 defines terminology.

Part 4 describes design requirements related to sharp edges and accommodating vehicle-anchored belt restraints. Part 5 describes performance requirements, which are essentially the same as those required in WC19 for frontal crashworthiness and accommodation of vehicle-mounted belt restraints. However, testing of wheelchair seating systems is performed using a Surrogate Wheelchair Base (SWCB) defined in Annex B and shown in Figure 14. The SWCB allows evaluation of different styles of seating systems independently, and allows lateral adjustability to accommodate smaller and larger wheelchair seating systems.

Figure 14. Surrogate wheelchair and surrogate wheelchair frame.

Parts 6 and 7 describe requirements for written materials and documentation similar to those found in WC19. In WC20, Annex A describes frontal-impact test procedures, Annex B specifies the SWCB fixture, Annex C contains method for evaluating accommodation of belt restraints,

and Annex D contains methods for performing quasi-static tests of wheelchair seating systems (which are recommended before performing dynamic testing but are not required.) Annex E provides sources for relevant information.

Wheelchairs and Side Impact

Since many wheelchairs are designed to fold along the centerline to facilitate storage, some wheelchairs that pass frontal impact testing standards may not demonstrate the same integrity during side impact crashes.

As part of the research funded by a National Institute on Disability, Independent Living, and Rehabilitation Research (NIDILRR) Rehabilitation Engineering Research Center, side impact performance of occupied wheelchairs was explored. The work evaluated the current level of side impact crash protection afforded to wheelchair users seated in wheelchairs that comply with WC19 and that are secured with WTORS that comply with WC18. Since injury protection in nearside crashes is primarily addressed with vehicle features (padding, airbags, sidewall features), the work focused on farside crash protection, where features of the wheelchair and occupant restraint can improve occupant protection. The work considered three crash severities that were precedents in side impact protection at that time: an FMVSS 214 pulse for a van [24.5 km/hr (14 mi/hr)/16 *g*], the EuroNCAP small vehicle pulse that is also used as a side impact pulse for CRS testing [25 km/hr (15.5 mi/hr)/13 *g*] and the proposed pulse for CRS side impact testing included in the ANPRM [23.3 km/hr (14.5 mi/hr)/20.6 *g* and 33.8 km/hr (21 mi/hr)/26 *g*]]. Manary et al. (2005) reported on the first phase of testing three side impact tests performed with the midsized male Hybrid III ATD in commercial wheelchairs secured with a 4-point strap tiedown systems. Test severities ranged from 23 km/h (14.3 mi/hr), 16.4 *g* to 30 km/h (18.5 mi/hr), 15.8 *g*. Two tests were performed with the shoulder belt in a far-side configuration, while the third test evaluated a near-side configuration without intrusion. The tiedown system was effective at limiting wheelchair movement to no more than 254 mm of excursion, and there was minimal deformation of the three wheelchairs that met WC19 requirements for frontal testing. The ATD moved out of the belt in the two far-side conditions, with excursions approximately double the excursions measured in the nearside condition, where the shoulder belt prevented the ATD from moving excessively laterally. The work continued with six more tests of manual, power, and stroller type wheelchairs, including one secured using UDIG. The wheelchair frames were well-secured by the WC18-compliant WTORS, including UDIG. However, the ATD was not well restrained from excursion when the upper shoulder anchor point was opposite the impact directions. In these cases, the lateral features of the wheelchair were heavily loaded by the ATD and the ATD was not contained in a seated position. Wheelchairs equipped with fabric seating that hammocks the occupant did a better job of limited lateral motion than those with planar seating. In total, UMTRI has conducted 14 additional side impact sled tests of wheelchairs under a variety of configurations.

Vehicle Modifications

Information about modifying personal vehicles (typically vans) can be found on the National Mobility Equipment Dealers Association (NMEDA) national website as well as those from individual NMEDA dealers.

Under the topic of safety, the NMEDA website states "Having the right type of equipment installed in a wheelchair accessible vehicle can not only transform your life with added mobility and independence, it can also prevent serious injuries caused by standard highway equipment." This statement reflects the typical practice to disable airbags when modifying a vehicle for use by a driver seated in a wheelchair; current guidelines allow, but do not require this practice (NMEDA, 2019). While this recommendation was reasonable when airbags were first introduced and had a higher potential for inducing injury to occupants sitting too close to the steering wheel, this practice may no longer be warranted with newer designs. Vehicle safety system engineers now design less aggressive airbags to work in an integrated manner with seatbelts that can include advanced features such as load limiters and pre-tensioners. Disabling the airbag in an adaptive vehicle may also disable the sensing systems used to activate the seatbelt features, reducing protection even further for these occupants. Sensors needed to control safety features may also be removed when vehicle seats are replaced with wheelchair docking stations.

The first section of NMEDA guidelines (2019) provides instruction to modifiers on how to document compliance with the Exemption to the Make Inoperative Prohibition (49 CFR 595.7). Modifications relative to occupant protection that are spelled out in this document include the following:

- FMVSS 201u: Exemption if the roof is raised or the floor is lowered; pillars and roof rails around a ramp/lift are exempt if the floor and roof are not modified
- FMVSS 202a: Person in a wheelchair is allowed to travel without rear head restraints
- FMVSS 203: exempt because control devices often attached to steering wheel
- FMVSS 204: exempt from displacement requirements in case modifications to the column are needed to install alternate controls
- FMVSS 208: Can remove/deactivate all airbags for front seating positions if a Type 2 or 2A seatbelt is installed in that position
- FMVSS 207, 214: can remove vehicle seat and exempt from side impact protection

We summarize the remaining topics covered by NMEDA guidelines (2019) below, listing titles for each section and selected excerpts related to occupant protection. Of the forty different sections in the guidelines, only section 26 addresses wheelchair and scooter securement and occupant restraint.

2) Consumer Documentation
3) General Best Practice. 3.18 specifies that "All mobility dealer installed lap belts will cross the occupant at the H-point."
4) Service Practice (related to training and customer service). This section refers to fitting of seat belts and tiedowns as follows: "Of special note for drivers using adaptive

equipment, a mid-conversion and final fitting with the end user or client present is expected to occur at the dealer location to fine tune equipment adjustments, determine tie-down locations, torso belt dimensions, etc."

5) Vehicle Weight Ratings (how to calculate after the modifications are made)
6) General Electrical Specifications
7) High Tech and Low Tech Adaptive Equipment Definitions
8) Accelerator, Brake, and Clutch Pedal Modifications
9) Automotive Wheelchair Roof Carriers/Loaders
10) Driver Training Brake (installed for use when a driver seated in a wheelchair is first learning how to operate the vehicle).
11) Electrically Powered Seat Bases, where a vehicle seat is replaced by another seat with greater maneuverability that would allow a person to transfer from a wheelchair docked in an adjacent seating position.
12) Extended doors
13) Exterior Door and Lift Controls
14) Floor lowering. This section states "When installed in the driving position, the seat shall be located so as to allow the driver to use the OEM seat and shoulder safety belt system."
15) Left foot accelerator control
16) Mechanical Hand Controls
17) Parking Brake
18) Power Door Openers
19) Raised Roof. This section includes a statement regarding strength of upper belt anchorages. "If a NMEDA raised roof F/CMVSS 210 manual exists for the vehicle make and model year to be modified, the manufacturing instructions must be followed or the modifier must document their pathway to F/CMVSS compliance with a prototype vehicle test report for the upper seat belt anchorages under F/CMVSS 210."
20) Seats. This section states: "Seat belt geometry must be maintained within OEM specifications."
21) Steering Column Extension
22) Steering Wheel Devices. This section states: "If interference with operation of the airbag cannot be avoided the airbag should be deactivated while the steering device is in use."
23) Transfer Aids. This section states: "Transfer aids shall not be installed to interfere with the function of the vehicle's airbag systems."
24) Vehicle Steering Column Mounted Accessory Controls
25) Unoccupied Lifts
26) **Wheelchair and Scooter Securement**
27) Wheelchair Flooring
28) Power Elevating Platform for Wheelchair Driver. This section includes specifications for seat belt installation as follows: "There shall be a three-point seat belt provided for the wheelchair occupant. If the seat belt is anchored to the elevating platform, it shall be tested as per F/CMVSS 210 in conjunction with the requirements of section 28.7. If the

seat belt is anchored to the vehicle floor, it shall be tested as per F/CMVSS 210 independently of the load requirements of section 28.7."

29)Backup Braking System
30) Reduced Effort Hydraulic Steering System and Backup Hydraulic Steering System
31) Electronic Vehicle Interface
32) Gear Shifter Operation
33) Horizontal Steering System
34) Power and Gas Brake System
35) Reduced Effort Braking System
36) Reduced Effort Electronic Power Steering System and Electronic Power Steering Backup System
37) Remote Steering Systems
38) Secondary Control/Systems. This section states: "Installation of the controls shall assure the greatest possible retention of OEM driver and occupant protection features including collapsible steering column, knee bolsters and airbags."
39) Interlocks
40) Off-Site Installation and Service Policy
41) Hybrid/Electric Vehicles
Appendix A: Summary Descriptions of FMVSS/CMVSS
Appendix B: Out of Service Area Agreement for NMEDA Dealers
Appendix C: Adaptive Equipment Transportation Industry Terminology
Appendix D: Labels and Descriptions

Recent computational modeling studies performed by UMTRI researchers under sponsorship from the National Highway Traffic Safety Administration (NHTSA) demonstrate that modern airbags are more likely to improve protection than cause injury in frontal crashes (Hu et al., 2020; Schneider et al., 2016).

When vehicles are modified to accommodate drivers or passengers using a wheelchair, the entire floor is removed and replaced with a lower reinforced floor. This is necessary to allow sufficient clearance for the occupant to enter the vehicle while seated in a wheelchair, which typically has a higher seating height than vehicle seats. In addition, rear passenger locations are often placed in the center of the vehicle, to allow greater room for the occupants to enter and maneuver their wheelchairs into position relative to the tiedown locations. As a result, the rear occupants are not usually situated to benefit from deployment of side curtain airbags.

Computational Modeling
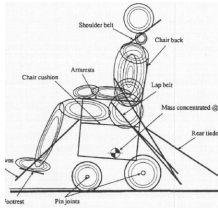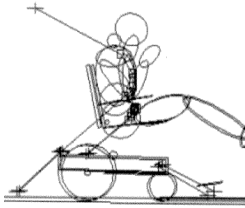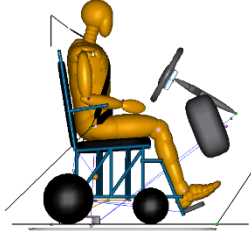
Few studies of computational modeling for WTORS, wheelchairs, and wheelchair users have been published. Table 2 summarizes details of previous computational models related to wheelchair occupant protection. One of the first computational models of wheelchairs under frontal impact loading used DYNAMAN to model the surrogate wheelchair with a Hybrid III midsized male ATD (Kang and Pilkey, 1998). Parameter studies with this model investigated effects of tiedown stiffness, height of tiedown attachment point on the wheelchair, wheel stiffness, and crash pulse severity at the lower and higher ends of the ISO corridor. Other early

studies used DYNAMAN to model a commercial power wheelchair, and then to estimate how variations in seat and seatback stiffness and angle affect kinematics during frontal impacts. (Bertocci et al., 1999; Bertocci et al., 2000). Subsequent studies developed a MADYMO model of a commercial manual wheelchair (Invacare Compass Allegro) validated against tests using the surrogate WTORS and a Hybrid III midsized male ATD (Dsouza and Bertocci, 2010). Other researchers performed additional simulations using this wheelchair model with small female, midsized male, and large male occupants seated to evaluate different lap belt angles (Cabrolier et al., 2013; McDonnell et al., 2012). They recommend a range of 45 to 60 degrees as best for accommodating a range of occupant sizes using wheelchairs as seating. This model was also validated under rear impact conditions (Salipur and Bertocci, 2010).

More recently, UMTRI has developed a full set of MADYMO models, including a surrogate wheelchair, docking or 4-point tie-down system, 3-point seatbelt, knee bolster, steering wheel, and driver airbag, to investigate restraint system designs on protection for wheelchair users (Schneider et al., 2016). These models have been validated against multiple sled tests with varied ATD sizes, belt fit, and airbag conditions. The parametric simulation results clearly demonstrate that wheelchair-seated occupants without a seatbelt or a seatbelt with poor belt fit experience higher injury risks in frontal crashes. The simulation studies also demonstrated that a properly deployed driver airbag can provide important safety benefits for occupants with a wide range of sizes who are seated in wheelchairs in frontal crashes. Therefore, optimizing the seatbelt system for wheelchair users should consider a restraint system for frontal impact that includes airbags. No models of wheelchairs in side impact conditions have been developed.

NHTSA performed crash testing in two vehicles equipped with wheelchairs in the driving position (Wiacek et al., 2017) to validate modeling performed at UMTRI (Schneider et al., 2016). Tests were performed with modified 2015 Dodge Caravans, with Q'Straint QLK-150 docking stations securing Quantum Q6 2.0 wheelchairs. A mid-sized male ATD was positioned to represent the average posture documented in the UMTRI/Pitt study of wheelchair users (Orton et al., 2019). One test was run with the driver airbag, and one without. Comparison of Injury Assessment Reference Values between the two tests showed that the airbag reduced injury risk to head and chest, while it remained the same for the neck, and showed an increase for femur loads (though they remained below critical levels). The back of the wheelchair failed from inertial loading.

Table 2. Summary of previous modeling work related to wheelchair occupant protection

Model	UVa Model	U. of Pittsburgh Model	U. of Louisville Model	UMTRI Model
References	Kang and Pilkey 1998	Bertocci et al., 1999; Bertocci et al., 2000	Dsouza and Bertocci, 2010; Salipur and Bertocci 2010; McDonnell et al., 2012; Cabrolier et al., 2013	Schneider et al., 2016
Figure				
Software	DYNAMAN	DYNAMAN	MADYMO	MADYMO
Wheelchair	Surrogate wheelchair	Commercial Power WC	Commercial manual wheelchair	Surrogate wheelchair
Securement System	4-point strap tie-downs	4-point strap tie-downs	4-point strap tie-downs	4-point strap and docking tie-downs
Occupant	H-III 50th Male	H-III 50th Male	H-III 50th Male, 5th Female, 95th Male	H-III 50th Male H-III 5th Female
Restraint	3-point belt	3-point belt	3-point belt	3-point belt Driver airbag
Validation	Frontal crash	Frontal crash	Frontal crash Rear impact	Frontal crash
Applications	Tie-down stiffness Tie-down position Wheel stiffness Sled pulse	Surface stiffness seatback angle	Belt angle	Unbelted and belt misuse Airbag effect Oblique impact

Advanced Restraint System Features

Conventional automotive seatbelts include safety features that are not yet found in the seatbelt systems of commercial WTORS. Belt pre-tensioners remove slack from the seatbelt system when a crash is imminent. Load limiters moderate the restraint forces in the shoulder belt by allowing a limited amount of additional excursion upon reaching a predetermined load, reducing risk of chest injury. Belt pre-tensioners and load limiters have been available in outboard front seating positions of passenger vehicles in the United States since 2008, although they are not required by regulation. The presence of both a pre-tensioner and load limiter was associated with a 12.8% decrease in fatality risk (Kahane, 2013). Motorized retractors that reversibly reduce slack before the crash event have been available since 2011. Some upscale production vehicles have a buckle anchor that shifts between an initial position for easier access to another one that provides a more protective lap belt angle.

Inflatable restraints, such as driver airbag, are typically de-activated in vehicles modified for wheelchair users. However, many of those inflatable restraints are expected to be highly beneficial for wheelchair occupant protection in a frontal crash. Inflatable seatbelts introduced in 2009 have airbags built-in to the shoulder belt portion of the webbing that deploy during a crash. They reduce occupant injury risk by spreading the crash forces, limiting forward movement of the head, and cushioning the head during forward flexion (Sundararajan, 2011). Another innovative airbag design is the Self Conforming Rear seat Air Bag (SCaRAB), which provides supplemental crash protection to rear occupants of various sizes (Hu et al., 2017). The SCaRAB is in a rainbow shape originally designed to deploy from the front seat back, conforming to the space between the occupant and front seat back. A knee airbag is another type of airbag that could be beneficial for wheelchair users. Specifically, wheelchair users typically do not have the same level of lower extremity restraints as able-bodied occupants due to the poor lap belt fit and seat cushion with different contours than a vehicle seat. Consequently, a knee airbag can potentially provide an additional energy loading path to the lower extremities, and in turn reduce both lower extremity and chest injury risks.

To improve protection for occupants seated in wheelchairs in rear impacts, a deployable head and back restraint, which is hinged to fold back for storage, can swing out and lock into place when deployed once the wheelchair occupant is in position. This strategy might be used to deploy interior components to improve protection once the wheelchair is in the seating position.

Design Space

The Americans with Disabilities Act Accessibility Guidelines (ADAAG) for Transportation Vehicles (36 CFR Part 1192, 2017) specifies that a floor space measuring 760 mm (30 in) wide and 1,220 mm (48 in) long is required to accommodate a wheelchair, based on common wheelchair dimensions found in the 1970s. The ADA requirements also specify that vehicle door heights should be at least 1422 mm (56 in). A detailed study of combined occupant and wheelchair dimensions was published in 2010 to quantify the space needed to accommodate a greater variety of wheelchair and occupant sizes (D'Souza et al., 2010; Steinfeld et al., 2010). In this

study, they measured 276 people using manual wheelchairs, 189 using power wheelchairs, and 30 using scooters.

Statistical data on the range of occupied heights from this study is shown in Table 3. Occupied height is defined as the distance from the floor to the highest point on the person's head. The mean value of power chair users is 25 mm higher than the mean value of manual chair users, while the mean value of scooter users is 47 mm higher than those of power users. The current ADA requirement for vehicle door height is 1422 mm (56 in), which would accommodate 95% of manual and power chair users, but not the upper range of scooter users.

Table 3. Occupied height for different types of wheeled mobility devices (from Steinfeld et al. 2010).

Type	Sample size	Mean (SD)	Min	5%ile	10%ile	Median	90%ile	95%ile	Max
Manual	276	1249 (77)	1020	1123	1144	1253	1347	1376	1459
Power chair	189	1274 (81)	1000	1140	1153	1281	1373	1392	1492
Scooter	30	1321 (71)	1218	1220	1242	1316	1434	1477	1513
All	495	1263 (80)	1000	1130	1152	1267	1360	1385	1513

The Steinfeld study evaluated knee clearance of people using wheelchairs, with a suggested value of 700 mm (28 in) as suitable for accommodating 95% of occupants using wheelchairs. Their overall results in Figure 15 showing the percentile distribution of knee profiles across their range of subjects will provide guidance when designing knee bolsters or knee airbags. In addition, although they do not report the variation in wheelchair seat heights, we can infer the range of locations where the lap belts should be placed across the range of occupants from this figure.

Knee Clearance
Design Guidelines for People Using Manual Wheelchairs

CLEARANCE AS MEASURED FROM ANTERIOR-MOST POINT
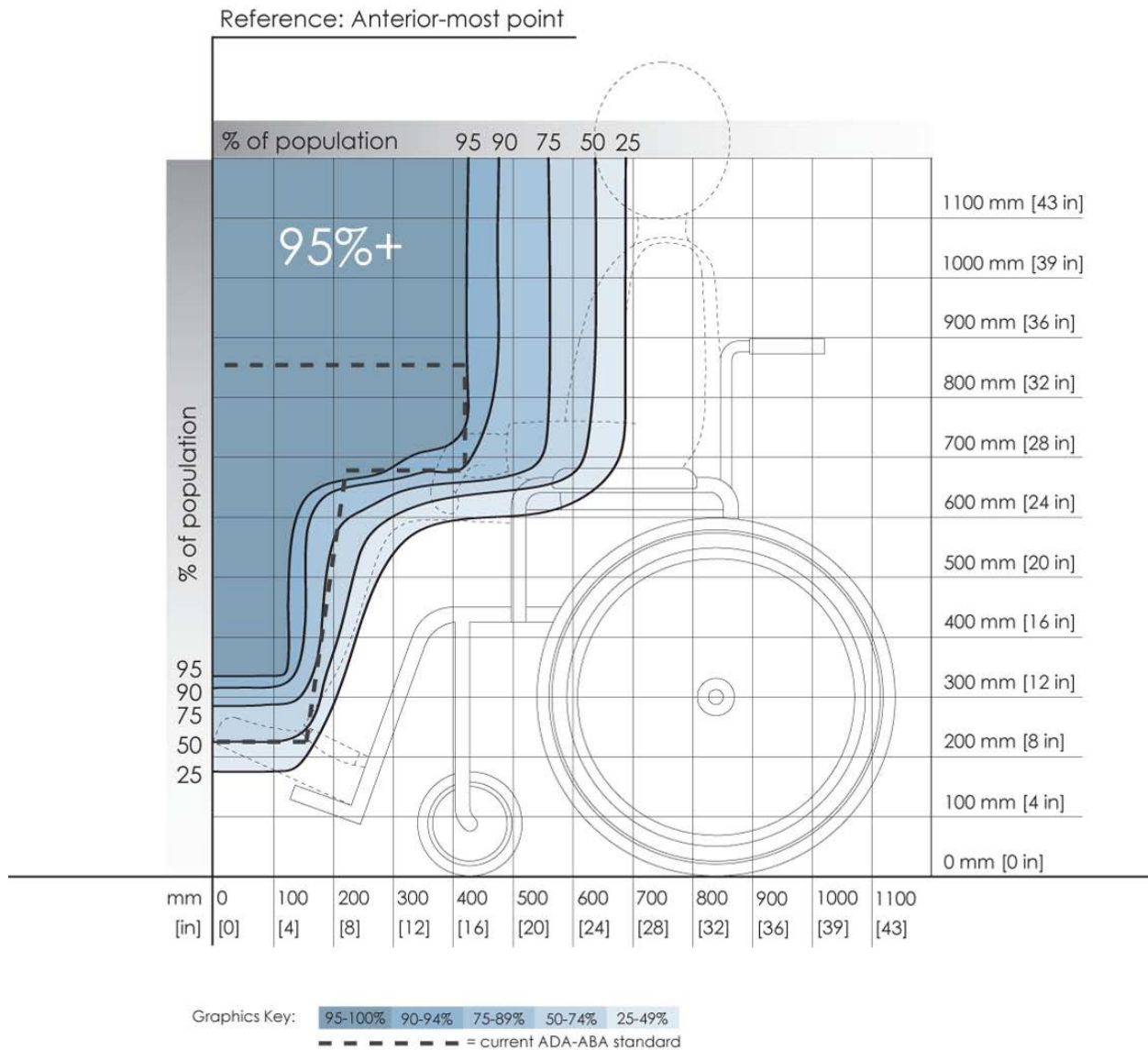
MANUAL

Figure 15. Distribution of knee clearance.

Accessibility and Automated Vehicles

The previous sections of the chapter focus on literature related to providing wheelchair users the opportunity to use automated vehicles safely, easily, and independently by developing an automated wheelchair tiedown and occupant restraint system. Several organizations have recently addressed broader needs of people with disabilities related to using automated vehicles, and a short summary of their efforts is reported in this section.

The Auto Alliance organized a 3-workshop series to address automated vehicles and accessibility, including legal and policy issues (Auto Alliance, 2019). To ensure that AVs are accessible for people with disabilities, collaboration will be needed among users, vehicle manufacturers, AV designers, wheelchair manufacturers, assistive device manufacturers, and government agencies. They provide a summary of inclusive design considerations that could be a starting point for best practice guidelines for AV design, and recommend that people with disabilities be consulted throughout the design process. Additional regulatory guidance beyond that provided by the ADA and Access board would be useful. As seen earlier in Table 1, no current production wheelchair tiedown systems are suitable for independent use in AVs, and additional research is needed to develop a feasible automated WTORS. Wider use of crashworthy wheelchairs is limited by current policies regarding insurance reimbursement of transit features on wheelchairs.

Part of the Public Listening Summit on Automated Vehicles hosted by the U.S. Department of Transportation (John A. Volpe National Transportation Systems Center, 2018) addressed disability and accessibility concerns. According to the report, clearer guidance on accessibility requirements for AVs are needed. They pointed out that different types of disabilities (vision, hearing, cognitive, or mobility) may require different accommodations. They noted that standardization of auxiliary mobility aides, such as wheelchair lifts or accessible displays, would facilitate use of vehicles where a human driver is not present.

The Intelligent Transportation Society of America published a report, *Driverless Cars and Accessibility: Designing the Future of Transportation for People with Disabilities* (Bayless and Davidson 2019). As summarized in the report, fully automated vehicles offer people with disabilities new opportunities for independent access to employment, health care, and education. Deployment of AVs could potentially increase annual vehicle miles traveled substantially, as AARP estimates that up to one-third of people in the United States do not currently drive. AVs would be beneficial to people with temporary disabilities and may allow older people to remain in their homes longer. While technologies are available that would allow people with different types of disabilities use an AV, standards and best practice recommendations would be welcome. Strategies for dealing with emergency situations is a key issue, as well as other non-driving tasks typically handled by a driver (ingress/egress, passenger monitoring.) Additional infrastructure is needed to accommodate people before and after they travel in an AV. Deployment of AVs may change the transportation system, reducing private vehicle ownership and increasing ride-sharing opportunities. Collaboration among a wide range of stakeholders will be needed to ensure that future transportation options are available to everyone.

A white paper discussing the impact that self-driving cars could have on the lives of people with disabilities (Claypool et al., 2017) indicates that approximately 6 million Americans with disabilities have trouble accessing the transportation they need. Limited transportation options can result in reduced economic opportunities, isolation, and diminished quality of life. Improving transportation options for people with disabilities could lead to greater employment and substantial savings from fewer missed medical appointments. As automated vehicles are introduced to the fleet, service providers and manufacturers need to ensure that the needs of people with disabilities are considered in their design.

Design Concept and Approach

The goal of this project is to develop an AWTORS that could be used safely and independently in an AV by people who remain seated in their wheelchairs while traveling. The design concepts and approaches build upon past research conducted at UMTRI and other institutions, incorporate features specified in voluntary standards for wheelchair transportation safety, and address issues noted by advocacy groups related to the use of AVs by people with disabilities.

Wheelchair Selection

Surrogate fixtures

This project tested and evaluate concepts using production wheelchairs and surrogate wheelchairs. For the modeling efforts and initial dynamic testing, we used the surrogate wheelchair base specified in WC20 (ANSI/RESNA 2017b) and shown in Figure 14 for evaluating specialized seating systems that may be prescribed for a wheelchair user that can be used with different commercial wheelchair bases. The SWCB allows lateral adjustment of the width to accommodate different wheelchair seating systems, which allowed us to examine the effect of wheelchair width on dynamic performance during side impacts. An aluminum seat pan and back support were used with the SWCB as needed to create a complete wheelchair.

Production wheelchairs

In addition to evaluations performed with the SWCB, we assessed the AWTORS designs with volunteers who use wheelchairs. Because the surrogate test fixtures are designed for dynamic testing, they are not suitable for self-propelled navigation in a vehicle mockup to evaluate ease of use of tiedown or restraint system use. For this reason, we purchased a production manual wheelchair and a production power wheelchair to be used in the volunteer portion of the study. In addition, these wheelchair models were tested dynamically in front and side impact conditions.

When choosing wheelchairs to be used in this study, we reviewed available options that met the following criteria:

- Meets requirements specified in WC19 for wheelchairs used as seats in motor vehicles
- Different manufacturers for each wheelchair
- Typical wheelchair features
- Wheelchair structure receives excellent ratings with respect to allowing good vehicle-anchored, lap-shoulder belt placement on the occupant
- Rear wheelchair structure is suitable for placing attachment hardware for use with the AWTORS concepts being evaluated.

Using these criteria, we identified four candidate products of each type for use with volunteer evaluation. A positive outcome of this review is that there were relatively few products where the rear geometry of the wheelchair would prevent installation of UDIG hardware components. Because the features of any of these candidates did not favor any particular model for use in our study, we purchased two wheelchairs commonly used by the University of Michigan

Wheelchair Seating Clinic to take advantage of their bulk purchase discount. The manual wheelchair was the Ki Mobility Catalyst 5 (Figure 16, left), while the power wheelchair was the Quantum Rehab Q6 Edge 2.0 (Figure 16, right). The manual wheelchair weighs 20.6 kg (45.5 lb), while the power wheelchair weighs 144 kg (317.5 lb).

Figure 16. Manual wheelchair model (Ki Mobility Catalyst 5, left) and power wheelchair model (Quantum rehab Q6 Edge 2.0).

Design Space

Vehicle Geometry

While future AVs may have substantially different geometry, we used a modified Dodge Caravan as the baseline design space for this project for several reasons. First, we believe it is conservative to try to develop a safe, feasible, wheelchair seating station incorporating AWTORS using a realistic vehicle geometry. If it is not possible, we can identify the barriers to doing so that will be helpful for future designs of AVs.

Second, we have available for use the following items:

- Loan of a 2017 Dodge Caravan SE modified for use by occupants seated in wheelchairs (Figure 17)
- A body-in-white (BIW)[2] of a Chrysler Town and Country (sister vehicle to Dodge Caravan) that can be used for component development and volunteer testing (Figure 18)

---

[2] The term "body-in-white" refers to automobile manufacturing stage where a car body's frame has been joined together, before painting and before the motor, chassis sub-assemblies, or trim (glass, door locks/handles, seats, upholstery, electronics, etc.) have been added.

- A validated finite element model of a 2007 Dodge Caravan from the NHTSA website (Figure 19)

Figure 17. 2017 Dodge Caravan modified for use by wheelchair users.

Figure 18. Body-in-white of a Chrysler Town and Country.

Figure 19. FEM of a 2007 Dodge Caravan available from NHTSA.

Occupant and Wheelchair Sizes

The scope of this project focused on developing an AWTORS that works for an occupant the size of the midsized male ATD. However, for due diligence, we thought about how the system might be used by a range of occupant sizes and considered options that might make the system more usable for a wider range of occupant sizes. As an example, computer modeling might indicate that the optimal lateral spacing of lap belt anchors for a midsize male is 762 mm (30 in) apart. However, mounting anchors at this distance may prevent someone with a wider wheelchair from using the wheelchair seating station. If a wider spacing is acceptable (if not optimal) for a midsize male occupant, we might modify the design to accommodate larger occupants and wheelchairs. We would also check to see how the wider spacing works for a small female occupant. If acceptable performance is not achievable for a range of occupant sizes using a fixed lateral spacing of anchorages, we would note issues and possible solutions that may be pertinent for future vehicle design, while keeping the project focused on accommodating occupants the size of a midsized male.

Ideally, an AV fleet that includes automated wheelchair seating positions should be able to accommodate the majority of wheelchair users. The data collected on the range of wheelchair sizes and occupant sizes (D'Souza et al., 2010; Steinfeld et al., 2010) provide information on what spacing requirements would be needed to accomplish this.

The ADA requires that wheelchair seating stations in vehicles provide a space 760 mm (30 in) wide and 1,220 mm (48 in) long to accommodate those using wheelchairs as seating. The data from the Steinfeld study indicate that a space 838 mm (33 in) wide and 1422 mm (56 in) long would be needed to accommodate 95% of wheelchairs and scooters from their study.

The ADA minimum height requirement for vehicle door openings is 1422 mm (56 in). According to the Steinfeld study, this would accommodate 95% of manual and power wheelchair users

(but not the tallest ones), but less than 90% of scooter users. However, people who use scooters may be more likely to be able to transfer to a vehicle seat than those who use wheelchairs.

The median eye height of occupants seated in wheelchairs is 1152 mm, with a 95% value of 1269 mm and a maximum value of 1387 mm. For comparison, the Z-coordinate of the centroid of the SAE eyellipse in the modified Dodge Caravan is 936 mm.

The vertical locations of wheelchair armrests are also documented in the Steinfeld study. The mean among all types of wheeled mobility devices is 716 mm, with a minimum value of 568 mm, maximum value of 876 mm, 5th percentile value of 645 mm, and 95th percentile value of 801 mm. The location of armrests may be particularly important in design of occupant protection systems for side impact, as well as evaluating how the automatic belt donning system may interact with a variety of armrest heights.

Steinfeld et al. (2010) present knee clearance profiles for occupants seated in manual wheelchairs for the 25%ile through the 95%ile population in their study, defined using different reference points. The plots in the report provide information on the range of expected knee, pelvis, and torso locations to assist in designing airbag components and belt geometries.

The study of functional wheelchair dimensions also includes the amount of space needed to enter and turn in a vehicle. These recommendations were considered when assessing possible locations for wheelchair seating stations within the vehicle.

Seating Positions

For this project, we have considered two seating positions as candidates for a wheelchair station, the first-row-right and second-row-left, as shown in Figure 20. The yellow rectangles represent the current ADA space recommendations for a wheelchair seating station, while the green rectangles represent the space suggestions from the Steinfeld study.
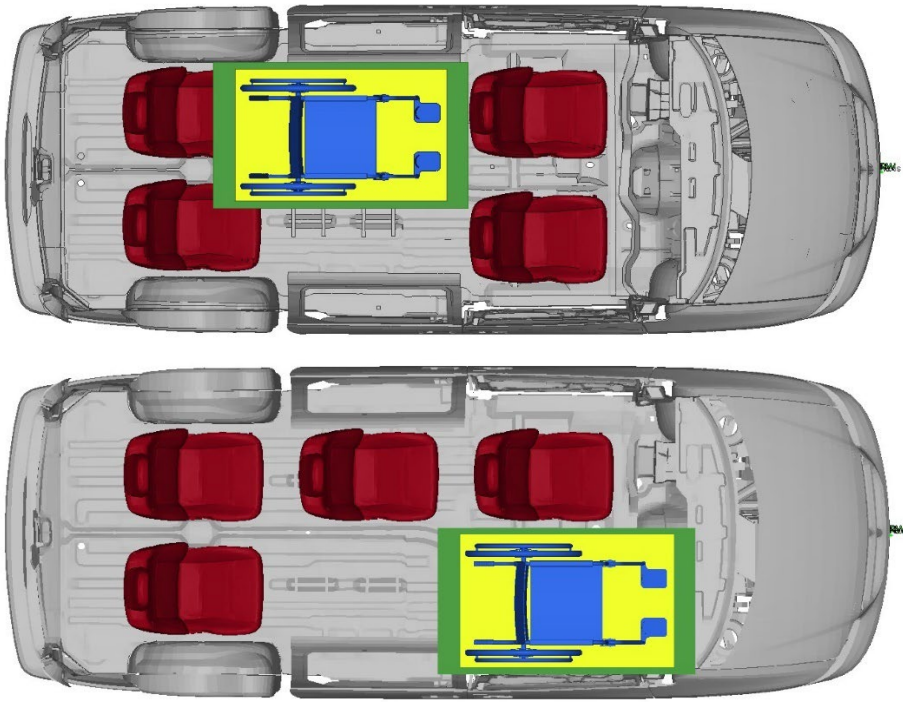
Figure 20. Candidate locations for wheelchair seating position.

These two seating positions would be most feasible in a future shared AV model for several reasons. First, while wheelchair ramps can be mounted at the side or rear of a vehicle, it would be more inclusive to have a side entry for wheelchairs, because side entry is already common in many production vehicles. In addition, side entry from a sidewalk would likely be easier to manage than rear entry, where the AV would need to position itself to allow adequate space for a person to navigate in through the back of the vehicle from the street. The first-row right and second-row left positions offer the most maneuverable solutions when entering from a right-side door via ramp, as they would have the clear space available in the second-row right area to enter from the ramp. The third-row right might also be navigable. However, we did not consider this position because there would be no forward structure to provide a mounting and reaction surface for an airbag. The front-row left and third-row left would be harder to reach from the right side because of other seating positions.

Second, we did not consider a rear seating position in the center of the vehicle, though this location is commonly used now in paratransit vehicles. A center seating position allows the person securing the wheelchair access to attach 4-point strap tiedowns; this space would not be needed by a wheelchair user using an independent securement method. Placing a wheelchair in a center position situates occupants so they cannot be well protected by side curtain airbags. While a center seating position places the occupant further from lateral intrusion, the benefits of side airbags in medium severity crashes and vehicle energy-absorbing structures in low severity impacts were hypothesized to outweigh the benefits of center seating in more severe crashes, which should be less frequent because of the advanced crash avoidance technologies needed in an AV. In addition, if the most likely scenario for AV

35

deployment is through shared ride-hailing services, we anticipate that service providers would prefer to maximize available seating positions, which would be hampered by center placement of a wheelchair seating station.

Third, both of these seating positions offer potential reaction surfaces for deployment of frontal-impact airbags. Airbags could be mounted in the instrument panel, or in the front row left seat. The second row left position would have the wheelchair user backing into the space but could allow UDIG hardware to remain in place during ingress and egress. The front-right position allows the rider to roll forward into the space but would need the UDIG hardware to be stowed and then deployed so as not to block entry.

Wheelchair Securement to Vehicle

The automatic wheelchair tiedown portion of our AWTORS was designed to meet the specifications of the UDIG. The specifications for the geometry have been included in an annex of WC18 and WC19 (ANSI/RESNA, 2017c and 2017d) since 2009. Any wheelchair with attachment hardware meeting the specification should be able to connect with any vehicle securement hardware meeting the specification.

Wheelchair attachment hardware
Past research at UMTRI and at other institutions have evaluated many styles of UDIG attachments for wheelchairs. A selection of past hardware designs is shown in Figure 6, and other concepts are shown in Figure 21. As noted in the literature review, van Roosmalen et al. (2003) performed computational modeling to evaluate the effect of different UDIG geometries (that all still fell within the specification) on ATD kinematics. They found that UDIG attachment hardware located at the highest and most forward location possible led to the smallest forward excursions. For side impact, the widest spacing between the two attachment points was most favorable. Past prototype development efforts have often used robust structural components, as the main intent was to demonstrate proof of concept. In this project, we tried to minimize the size of components, as this would reduce the weight of components added to a wheelchair, and potentially improve ease of docking.
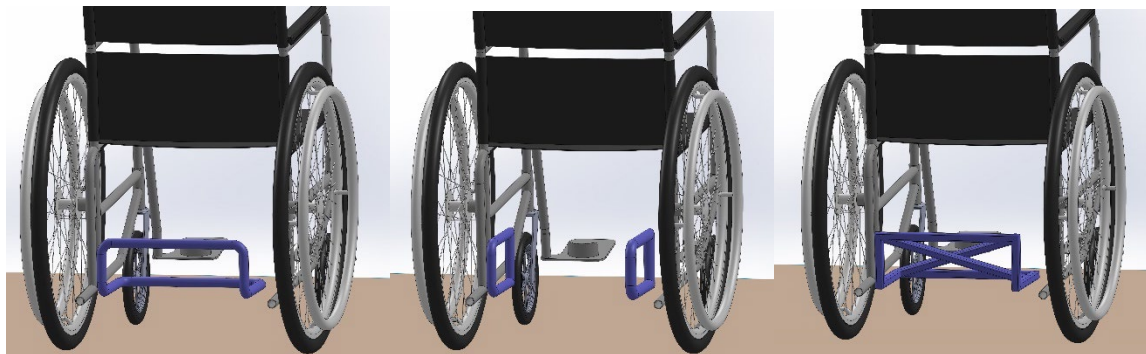
Figure 21. Potential UDIG designs for wheelchair attachment hardware.

Vehicle securement hardware

Consideration for placement of the securement system in the vehicle included examination of the vehicle interior space. This includes location of other vehicle seating, vehicle side structures for upper belt anchor mounting, and location of stored ramp hardware. The position of the wheelchair seating station must allow sufficient floor space to maneuver into the passenger area and engage with the securement system. To facilitate wheelchair docking, mirrors, sensors, or guiding hardware were considered as possible options to assist the user.

Different UDIG vehicle securement system deployment options were considered. One idea was to allow the securement device to be stowed in the floor or under a flip-up seat when not in use, which may allow use of the space for other passenger seating. This may also provide more space for navigating into the wheelchair seating station. One preliminary concept drawing of what this type of vehicle UDIG hardware may look like is shown in Figure 22. Once the person positions their wheelchair, the wheelchair user positions the vehicle UDIG hardware so it rotates up and locks. The user would then deploy an actuator that would shift the hooks so they engage the wheelchair attachments.
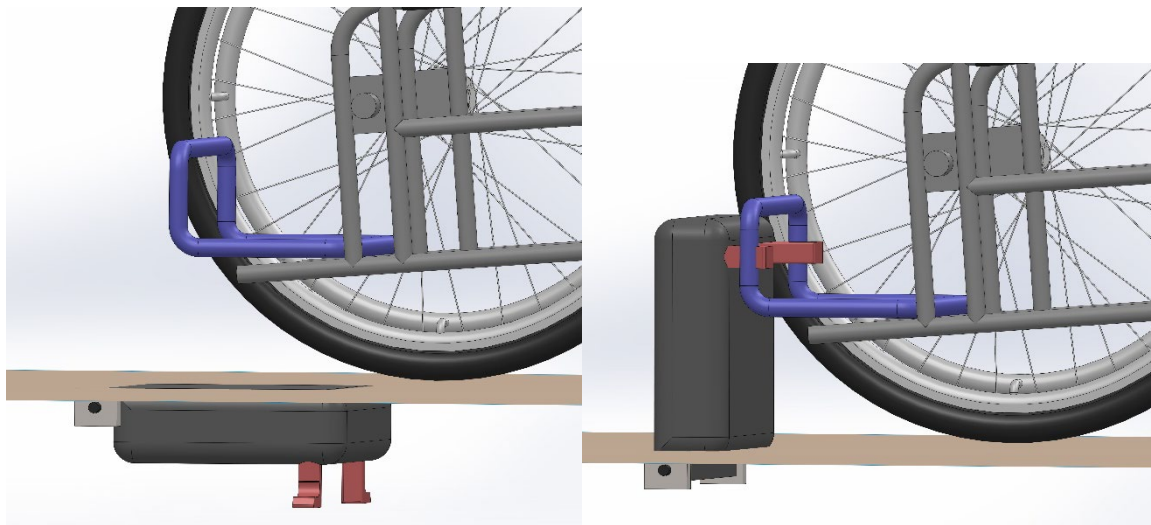
Figure 22. Flip up concept drawing of vehicle UDIG hardware.

Another idea, shown in Figure 23, is to anchor the UDIG securement system onto a pivoting structure that can swing away when not in use, and swing into place upon push of a button. To explore this idea, a latching mechanism would be needed to support the portion of the securement system farthest from the pivot point to provide sufficient strength during impact loads. Actual implementation of stowable UDIG securement components in an AV may be limited by under-floor structures and available interior compartment space.
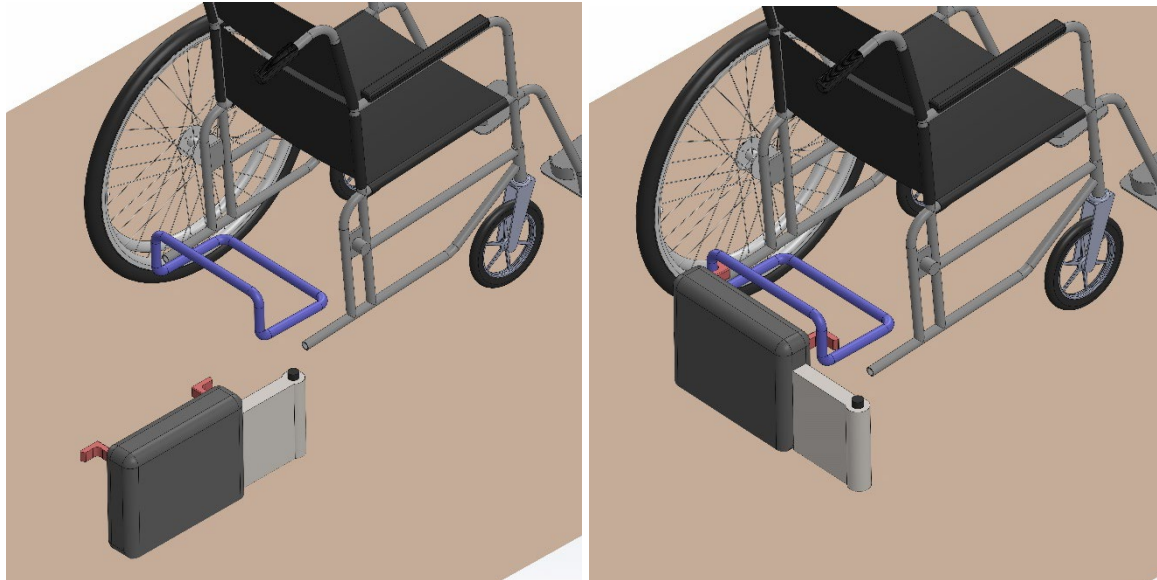
Figure 23. Swinging concept drawing of vehicle UDIG hardware.

Occupant Restraint System

Seatbelt components

A previous UMTRI project developed an automated belt donning system shown in Figure 24. With this system, the belt runs from the retractor at the D-ring through a sliding latchplate attached to a rotating rod that initially holds the belt up and forward near the instrument panel. The user navigates forward into the seating position, then activates the belt donning control manually. The rod rotates the belt down to the floor, allowing the buckle receptacle webbing to pay out, placing the buckle near the occupant's hip and the lap belt low on the occupant's lap. A latch mechanism at the end of the rotating rod anchors into a recessed pocket in the floor. This system requires minimal upper body and hand dexterity while placing the belts in a good position on the body. The system was successfully crash tested using WC18 procedures.
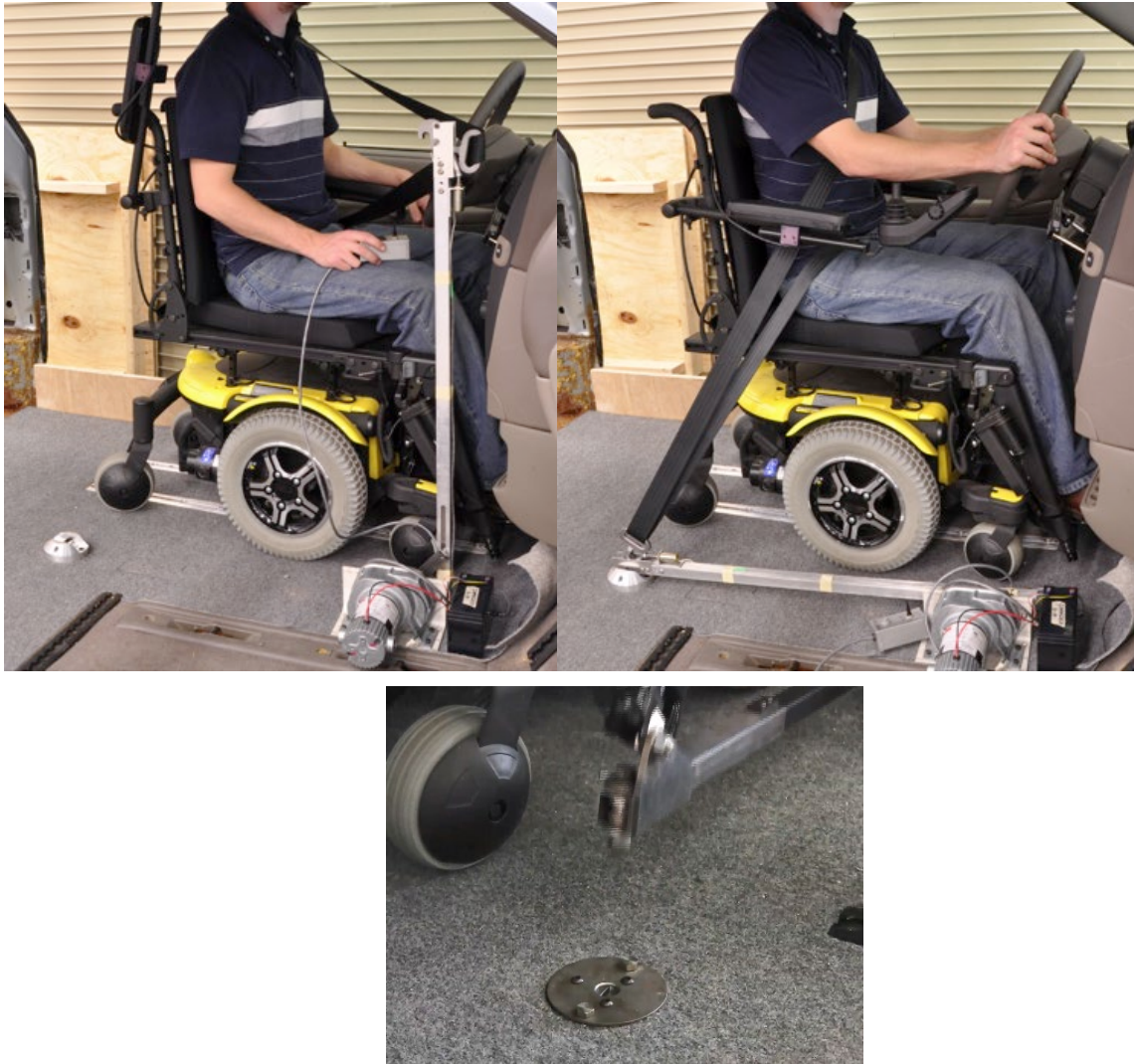
Figure 24. Prototype UMTRI belt-donning system before (left) and after (right) deployment; recessed floor pocket (bottom).

While the previous project achieved the goals of automatic belt donning and providing good belt fit, other options for belt protection of occupants in wheelchairs were also considered. One concept shown in Figure 25 utilized a harness to restrain the upper torso that was anchored to the roof and to the floor of the vehicle. This harness was paired with a knee bolster that would contact the occupant's knees after pulling the wheelchair into the riding position, since it was assumed that leg movement would not be necessary. The knee bolster would provide restraint to the pelvis and lower extremities. A main limitation of the harness and knee blocker combination is that the positioning of the harness and knee bolster would need to be customized to the individual, which may not work well with a variety of users and wheelchair seating geometries. Another design concept (Figure 26) incorporated a vehicle-mounted head and back support with anchor points for the shoulder straps of a vehicle-mounted harness. This concept is limited by the dexterity and reach required to clip the shoulder straps onto the back support once it is deployed into place.
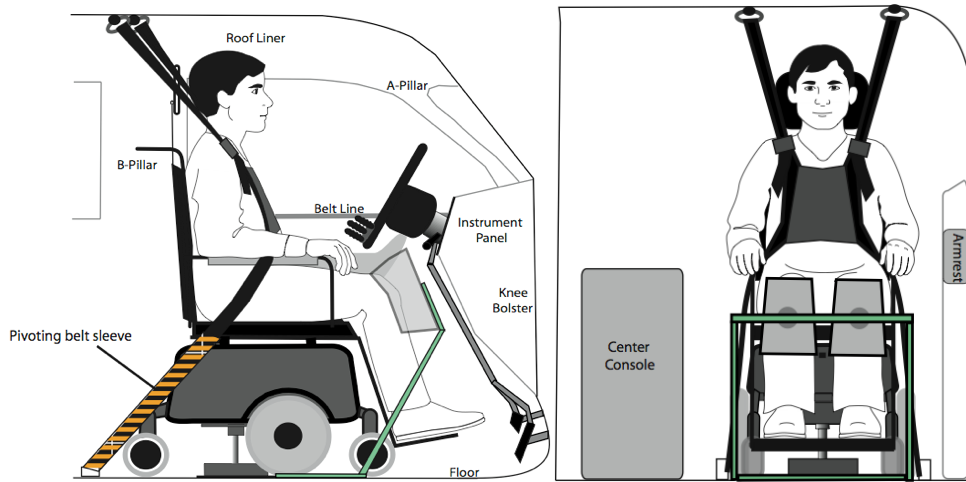
Figure 25. Drive-in harness and knee bolster concept.
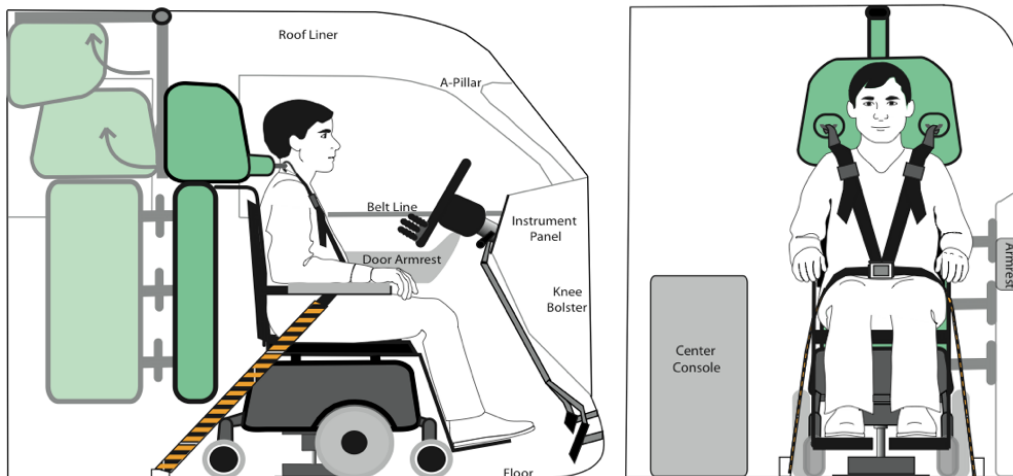
Figure 26. Swing-out back support harness concept.

While we reconsidered some of these ideas for this project, the main design concept we will be pursuing will build on the automatic belt donning system shown in Figure 24 and Figure 27. One planned modification (right side of Figure 27) is to add a structure to the rod that would place the lap belt anchor point closer to the occupant's hip; previous modeling work has shown that lap-belt systems with less webbing that are anchored closer to the occupant are more effective. This would also make the rotating arm shorter, as achieving the target angle will be accomplished by raising the anchor point. We designed the geometry of the system so it provides a side view lap belt angle from 45 to 60 degrees for a range of occupant sizes.
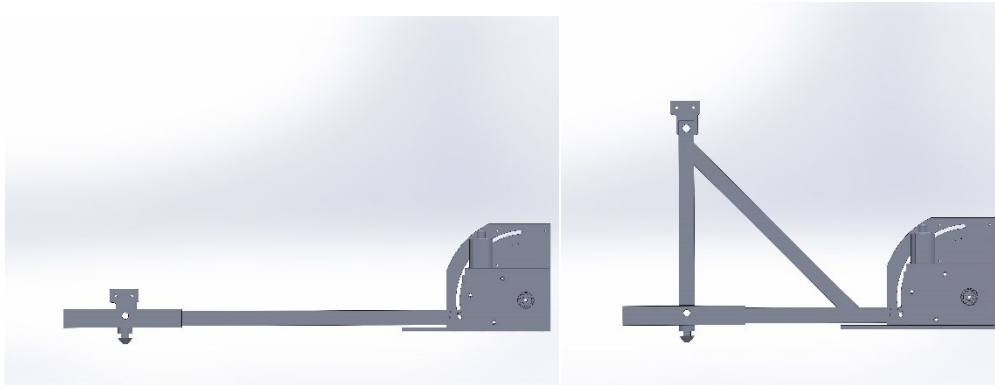
Figure 27. Original (left) and planned (right) modification to previous automatic belt-donning system to place inboard anchor closer to occupant and reduce amount of webbing in the system.

Design Optimization With Airbags and Other Components

Currently, it is common practice to disable driver airbags for occupants seated in wheelchairs, and to place rear passenger docking stations in the center of vehicles where the occupant is positioned away from curtain airbags and energy-absorbing interior structures. We used computational modeling to identify whether placing an occupant seated in a wheelchair closer to the side of the vehicle would allow them to benefit from standard vehicle airbags, as well as how to incorporate additional airbag systems (such as a SCaRaB airbag that deploys from the IP or front seatback) that may provide additional benefit in a crash. In addition, the project used computational models to optimize belt geometry and characteristics.

Frontal Crashes

In this study, the restraint design optimization in frontal crashes was conducted using an integrated MADYMO model by combining the surrogate wheelchair model, the Hybrid III midsize male ATD model, the model representing the UDIG design, a three-point seat belt system model, and airbag models (Figure 28).

Because our previous study has demonstrated that airbags play an important role in occupant protection for wheelchair users, we evaluated two airbags in the design optimization in frontal crashes. The Self Conforming Rearseat Air Bag (SCaRAB), originally designed for rear-seat occupant protection (Hu et al., 2015, 2017) was used in this study for head and neck protection. SCaRAB (Figure 29) is a rainbow shaped airbag that allows it to conform to the space between the occupant and the interior in front of the occupant. There are several major advantages of using the SCaRAB for wheelchair users over a traditional passenger airbag. First, SCaRAB can adapt to the space between the occupant and the instrument panel or front seatback (Figure 29), which might vary depending on the wheelchair. Second, the volume of SCaRAB is relatively small compared to a typical passenger airbag, which may reduce the size of the inflator for easy packaging and potentially reduce the risk of airbag-induced injuries (although such injury risk has been minimized by introducing dual-stage airbag inflations). Third, SCaRAB moves laterally with the occupant thus minimizing head rotation in an oblique impact. Because the lower

extremities are less restrained for wheelchair users, a knee airbag was also considered to provide an additional loading path to absorb energy during frontal crashes. All the seatbelt and airbag models to be used in this study were provided by ZF (sub-contractor of this project) and were validated extensively at the component level and the system level.
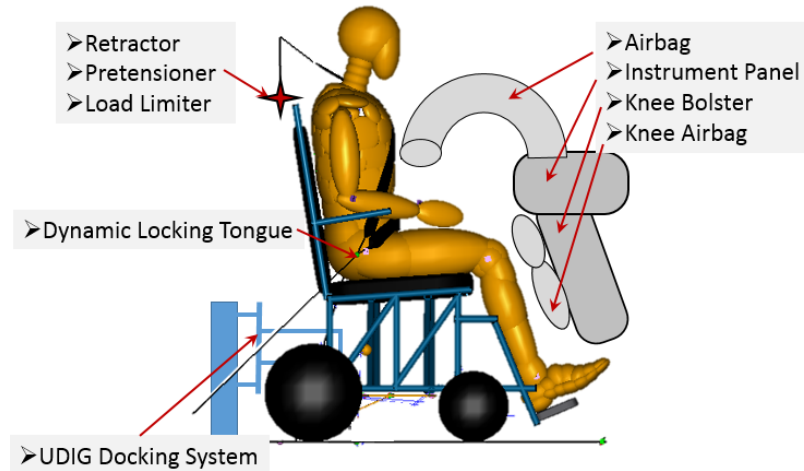
Figure 28. Illustrated MADYMO model for restraint optimization in frontal crashes

Figure 29. SCaRAB Design adapting to varied occupant space

A generic frontal crash pulse corresponding to a 48 km/h (30 mi/hr) full barrier vehicle frontal crash (that also meets the RESNA test specifications) was used for restraint optimization. Design parameters to be considered included belt anchorage locations, shoulder belt load limit, the presence of dynamic locking tongue (DLT), the presence of SCaRAB and the associated design parameters (size, inflation, venting, etc.), the presence of knee airbag, and knee bolster fore-aft location.

The injury measures, injury assessment reference values (IARVs), and the associated injury risk curves followed those used in FMVSS 208 and U.S.-NCAP frontal crashes. Injury risks for the head, neck, chest, and femur were calculated based on the injury risk curves used in U.S.-NCAP. A single joint probability of injury (Eq 1) combining all four injury risks was also calculated as the main output, which is used for assigning the star rating in the NCAP tests. In addition to the injury risks, the chest acceleration was monitored in each simulation.

$$P_{joint}=1- (1-P_{head}) \times (1-P_{neck}) \times (1-P_{chest}) \times (1-P_{femur}) \quad (1)$$

Optimizing the restraint system began with sensitivity analyses. In the sensitivity analyses, 6N (with N being the number of design parameters) simulations were sampled using the Uniform Latin Hypercube Sampling (ULHS) method based on a study on building metamodels for crash simulations (Hu et al., 2013). This method allows a uniform distribution of restraint conditions in the design space. In the sensitivity analyses, the statistical significance and the effect size of every design parameter on each output variable will be calculated following the UMTRI procedure reported previously (Yang et al., 2005). To calculate the effect size of input parameter A on output variable B, values of parameter *A* will be first split into two equal sub-ranges, namely a lower range and an upper range. The mean of the values of variable *B* corresponding to the lower range of *A* will be calculated as *B-*. Similarly, the mean of the values of variable *B* corresponding to the upper range of *A* will be calculated as *B+*. The effect of the variable *A* on variable *B* is calculated as the difference between *B+* and *B-*, and a student *t*-test will be performed between *B+* and *B-* to calculate the significance level. The effect size of *A* on *B* serves as a good indicator of the influence of a design parameter on an output variable; the sign of the effect described the nature of influence (positive or negative) and the magnitude of effect described the level of influence. A ranking of all input parameters on each output variable can be achieved based on the effect size, providing an objective evaluation of the relative importance of each design parameter on each output variable over the range investigated.

Once the simulations in the sensitivity analysis are completed, several response surface methods (RSM), will be used to develop statistical surrogate models of the ATD responses with respect to the crash restraint conditions for each ATD/crash condition. The purpose of the surrogate model is to set up the relationship between restraint system design parameters and the occupant injury risks. These surrogate models will be used for the following optimizations to save computational time. To test the quality of the surrogate models, another set of computational simulations other than the simulated conditions in the sensitivity analyses will be conducted and compared to the surrogate model predictions. High correlation (e.g., $R^2>0.8$) and low root mean square error (RMSE) need to be achieved for each occupant injury measure; otherwise, additional simulations will be conducted to rebuild the surrogate model and in turn increase the accuracy. The correlation and RMSE will also be used to compare the accuracy of different RSMs, so that the best models can be selected.

After the accuracy of the RSM models is validated, restraint design optimizations will be conducted. The Pjoint of the HIII ATD will be considered as the objective function, and the injury criterion to the head, neck, chest, and lower extremities in the FMVSS 208 will be considered as the constraints. Since only one objective function will be used, the design with the lowest Pjoint and without violation of the injury criteria will be selected as the optimal design.

Side Impacts

In the design optimization for side impacts, a generic near-side impact crash pulse consistent with the FMVSS 214 moving deformable barrier tests will be used. A set of MADYMO models

similar to those used in frontal crashes will be used for side impact simulations, except that ES-2re ATD will replace the HIII ATD, and side door and curtain airbag models will be added (Figure 30). Design parameters will include, but not be limited to, belt anchorage locations, shoulder belt load limit, the presence of DLT, the presence of curtain airbag and the associated design parameters (size, inflation, etc.), the Y distance between the two UDIG anchors/attachments, and the lateral distance between the wheelchair and the side structure.
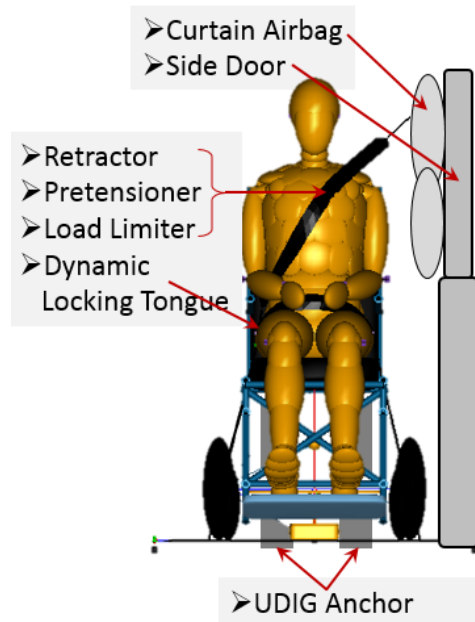
Figure 30. Illustrated MADYMO model for restraint optimization in side impacts

The design optimization process for side impacts was the same as that used for frontal crashes, except that the injury measures, injury criteria, and injury risk curves were based on the FMVSS 214 and U.S.-NCAP side impact tests. More specifically, the head, chest, abdomen, and pelvis injury measures and risks were evaluated in the side impact conditions. The combined injury risks will be used as the sole objective function in the design optimization, while other injury criteria in FMVSS 214 will be used as design optimization constraints.

Because the UMTRI wheelchair model had not been validated in side impact testing before this project began, preliminary sled tests were run using the SWCB. These tests used the proposed FMVSS 213 side impact pulse, orientation that includes a 10-degree offset from pure lateral, and the ES2-RE ATD. Validation tests (described in more detail under Computational Modeling) evaluated 4-point strap tiedowns vs. UDIG, varied wheelchair seating width, examined effect of armrests, and compared near and farside kinematics.

Design Balance between Frontal and Side Impacts

Since the initial design optimizations were conducted separately between the frontal and side impacts, the optimal restraint conditions, especially the optimal seatbelt design parameters, may not be consistent between the frontal and side impacts. If this occurs, we will re-evaluate

the sensitivity of those inconsistent design parameters. If it turns out that some of the design parameters are sensitive in both crash conditions, a new design optimization will be conducted by considering the Pjoint values in both the frontal and side impacts as the objective functions. A set of parietal optimal designs will be achieved, and a comprehensive decision will be made to ensure the safety in both frontal and side impacts at the same time.

Volunteer Assessment

In addition to securing the wheelchair and protecting the occupant, the AWTORS must be usable unassisted by people seated in wheelchairs for travel. We performed usability testing of the proposed AWTORS with 8 volunteers.

Test Fixtures

The AWTORS were installed in a body-in-white shown in Figure 18 available at UMTRI that has been previously used to evaluate WTORS. This body-in-white is from a Chrysler Town and Country minivan, so it is compatible with the vehicle interior geometry being used in the modeling design phase. The van includes a lowered floor, so there is adequate headroom for people seated in wheelchairs. The van also includes ramps that allow side or rear access to the vehicle. The AWTORS were also installed in the modified Braun van shown in Figure 17 to allow assessment of multiple configurations. Both fixed and deployable UDIG-compatible vehicle anchors were evaluated with volunteers.

As mentioned previously, the surrogate wheelchairs are not viable options for conducting volunteer testing, as they do not include swivels or features that allow steering by an occupant seated in the wheelchair. Instead, the wheelchair models shown in Figure 16 were used for volunteer testing.

Test Protocol

Volunteer testing protocols and data collection tools were developed and approved by the University of Michigan Institutional Review Board. The main participant criteria were that participants must be regular users of wheelchairs but can transfer to our test wheelchairs that are equipped with the UDIG hardware. Test sessions will last up to 2 hours, and subjects will be paid $40 to participate.

Original test plans for volunteer evaluation needed modification to ensure safety of participants and experimenters relative to COVID-19, which required limiting contact less than 1.8 m (6 feet) to 15 minutes or less during the test session. This involved switching from our typical measurement procedures (using a FARO arm 3D coordinate measurement arm) to extracting anthropometry and belt fit measures from scans, photos, and videos. After reviewing the consent form, the subject will transfer to each of the test wheelchairs in turn and perform the study tasks in the test fixture. We will direct each volunteer to enter the vehicle using a wheelchair ramp, maneuver to the wheelchair space, secure the wheelchair using the automated docking station, and don the automated seat belt. Then the subjects will resume the process by doffing the belt, disengaging the wheelchair from the docking station, and exiting the vehicle via the side ramp.

Each subject will perform these tasks with the manual and power wheelchairs, while entering the vehicle from curbside, and to first-row right and second-row left seating positions. At least two different belt geometries will be evaluated, as well as the two different styles of UDIG anchor deployment. A fractional factorial design will be constructed so each subject will evaluate eight different configurations of wheelchair type, seating position, UDIG deployment, and belt geometry. If time permits, we will repeat conditions to identify if the process improves with user experience.

In addition to objective measures of docking efficiency and effectiveness, subjective feedback will be gathered using questionnaires. Subjects will answer questionnaires after each trial that will ask questions such as "Is the shoulder belt comfortable?", "Is the lap belt comfortable?" and "Do you feel safer in this seatbelt than in what you usually use?" These questions provide subjective measures of belt fit that can be compared to quantitative measures of belt fit and provide guidance on what range of belt fit may be most acceptable to occupants. Past studies of belt fit show that occupants may choose not to use the seatbelt, or may wear it incorrectly, if it is uncomfortable.

Assessment will include length of time between entry and being docked and restrained for travel as well as the number of attempts needed to dock and apply the seatbelt. Measures of shoulder belt and lap belt fit will be quantified and compared to the range of seatbelt fits measured in previous studies for production vehicles (Reed et al., 2013, Park et al., 2016). A comparison will be made between the quantitative measures of belt fit and subjects' perception of belt fit.

Dynamic Testing

Test Conditions

Evaluation of the AWTORS included dynamic testing AWTORS to determine hardware response, occupant kinematics, and occupant protection levels. The UMTRI sled impact test facility, depicted in Figure 31, was used to simulate both frontal and lateral impacts by orienting the hardware to be tested appropriately and tuning the pulse to achieve the desire combination of change in velocity and deceleration level.
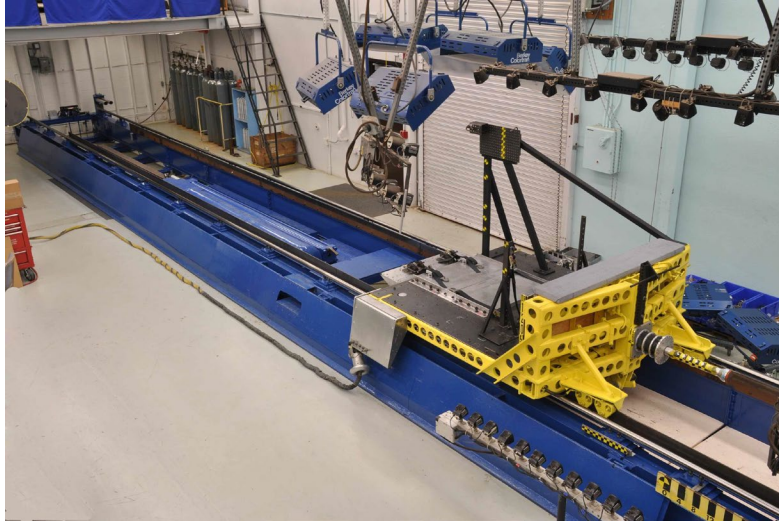
Figure 31. UMTRI sled test facility with wheelchair testing buck installed.

The first phase of dynamic testing involved use of the surrogate wheelchair base using midsized males ATDs. The SWCB was used rather than the SWC because it allows for testing variable widths and armrest designs. UDIG anchorage hardware will be mounted to the simulated vehicle floor and used to secure the wheelchair. The wheelchair will be loaded with the Hybrid III midsized male for frontal impacts and midsized male ES-2re ATD for side impacts. The ATDs will be instrumented with head, chest, pelvis and/or abdomen instrumentation to allow calculation of relevant injury criteria and to allow for comparisons with the findings from the modeling portion of the study. The sled platform is also instrumented with three accelerometers to measure the sled deceleration-time history during each test for comparison with the specified target corridors used for the model development phase. Belt load cells will be placed on the occupant restraints to record load-time histories. High-speed digital video recorded at 1000 frames per second will be captured using side, overhead and oblique camera angles to document ATD excursions, occupant motion, and close up views of the dynamic hardware responses. Sets of pre- and post-test photographs will document the hardware before and after each test run. A FARO Arm 3-D coordinate measurement system will be used to document the position of the wheelchair, ATD, and belt system prior to each test.

For frontal impact testing, we plan to use the pulse included in WC18 (ANSI/RESNA, 2017c_ shown in thick lines in Figure 32, which specifies procedures for dynamic testing of WTORS. As indicated by the dashed lines, the pulse should reach 15 g for at least 40 ms and 20 g for at least 15 ms. This pulse is intended to be similar to the pulse used for frontal FMVSS 213 testing, shown in red dots for comparison.
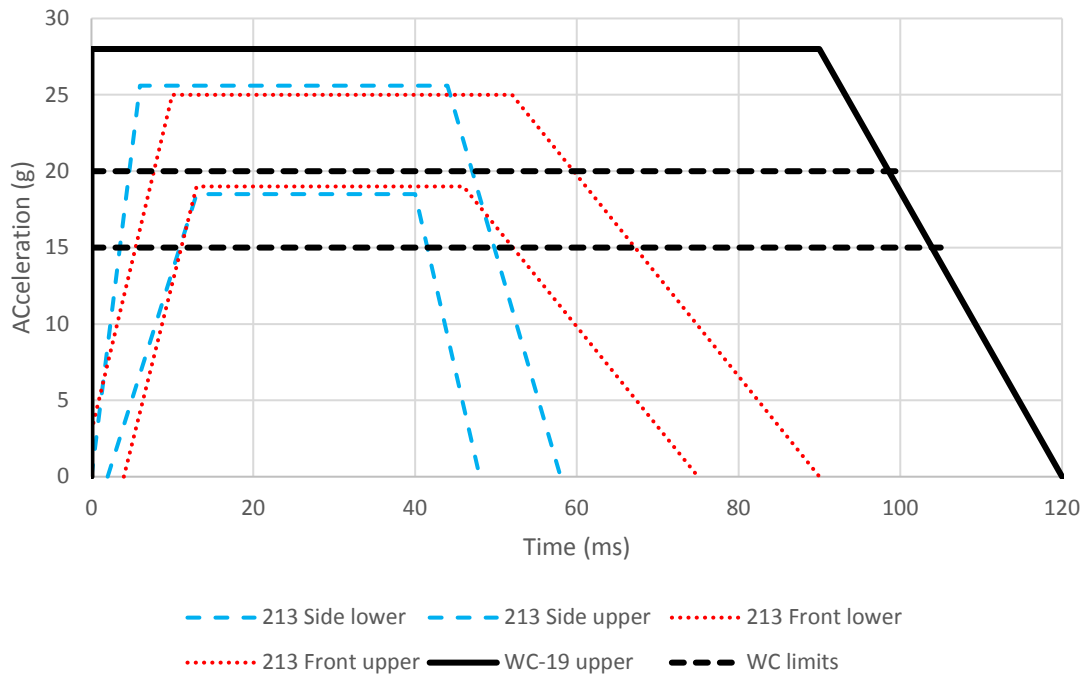
Figure 32. WC-19 sled pulse, FMVSS 213 frontal pulse, and proposed FMVSS 213 side impact pulse

There are currently no side impact testing standards for WTORS, and no FMVSS currently include a pulse to simulate typical side impact loading with a sled test. However, we propose to use a pulse based on the 2014 NPRM proposing side impact testing of child restraints, which is shown in thin blue dashes in Figure 32. This NPRM proposed a pulse that would have a peak acceleration of 20 *g* (range 16 to 25 *g*) and a velocity change of 26 to 29 km/hr (16 to 18 mi/hr), based on the average right rear sill accelerations of ten small vehicles in side impact (79 FR 4569, 2014).

Preliminary Test Matrix

We proposed running an initial set of twelve sled tests, with the matrix shown in Table 2. As described later in the Dynamic Testing chapter, the matrix was modified based on results of computational modeling and volunteer testing, as well as input from NHTSA collaborators on the project. The first series uses the surrogate wheelchair fixture and tests with a midsize male ATD. The benefit of performing the first set of tests with the SWCB is that the same wheelchair structure can be used in each test, saving the expense of purchasing a wheelchair for each test. For the first series, we planned two frontal tests each with belt only and belt plus airbag. Our past work modeling wheelchairs and restraint systems demonstrated the benefit of using an airbag in conjunction with a belt, as well as poor kinematics that could result from bad belt fit. These four tests could be used to demonstrate the benefit of airbag compared to belt alone. We would either do repeated tests, or different belt geometries or wheelchair spacing layouts for each paired comparison.

For the six side impact tests in the first series, we also wanted to demonstrate the value of airbags compared to belt alone. In addition, because minimal testing has been performed on wheelchairs in side impact, we hypothesized that varying the seat width of the surrogate wheelchair frame could play a role in lateral kinematics. As a result, we proposed performing three pairs of tests with and without airbag, which varied the wheelchair seat width to 406, 457, and 508 (16, 18, and 20 in) wide.

Table 4. Preliminary matrix for initial dynamic testing with SWCB

Direction	ATD	Wheelchair	Restraint system
Frontal	Midsize male	Surrogate	Belt only
Frontal	Midsize male	Surrogate	Belt only
Frontal	Midsize male	Surrogate	Belt & AB
Frontal	Midsize male	Surrogate	Belt & AB
Side	Midsize male	Surrogate	Belt only
Side	Midsize male	Surrogate	Belt & AB
Side	Midsize male	Frame-Narrow	Belt only
Side	Midsize male	Frame-Narrow	Belt & AB
Side	Midsize male	Frame-wide	Belt only
Side	Midsize male	Frame-wide	Belt & AB

The second set of dynamic tests would use manual and power commercial wheelchairs retrofitted with the AWTORS as shown in Table 3. Again, the matrix was revised based on modeling, volunteer testing results, and input from NHTSA and is detailed in the Dynamic Testing chapter. These tests would provide a more realistic demonstration of how the AWTORS work with production wheelchairs and identify possible issues under side impact loading conditions for which minimal research has been conducted. However, a new wheelchair would need to be used in each test. To economize, the power wheelchair purchased for volunteer testing would be used for one of the tests, while a second one would be purchased for the sled testing series. In addition, while the project focus is on occupants the size of a midsize male, it would be beneficial to run some tests with a small-female ATD to demonstrate how well the restraint system design optimized for midsized males can protect another size of occupant.

The second series uses the surrogate wheelchair fixture and small female ATD, as well as two tests with a midsize male ATD in a power wheelchair (one frontal and one side), three tests with a midsize male ATD in a manual wheelchair (two frontal and one side) and one frontal test with

a small female ATD in a manual wheelchair. For the second series of tests, we wanted to begin by examining the kinematics of the small female ATD in the surrogate wheelchair using a belt geometry and airbag that was designed with a focus on the midsize male. The remainder of the tests would evaluate performance of WC19- compliant wheelchairs equipped with UDIG-compatible attachments designed and fabricated at UMTRI, using the belt geometries and airbag designs from the first series of sled tests. We planned only two tests with a power wheelchair, one front and one side, because of the higher expense to purchase power wheelchairs (approximately three times the cost of a manual chair.) We planned two frontal tests with a manual chair and a midsize male, to allow testing of either different wheelchair models or different attachment designs. We also planned for one test with the small female ATD in the manual chair, to investigate the same potential size issues we investigated with the surrogate tests with the small female. We also planned one side impact test with a manual chair.

Table 5. Preliminary test plan with midsize male and small female ATDs in production wheelchairs/surrogate wheelchair fixture

Direction	ATD	Wheelchair	Restraint system
Frontal	Small female	Surrogate	Belt only
Frontal	Small female	Surrogate	Belt & AB
Frontal	Midsize male	Manual	Belt & AB
Frontal	Midsize male	Power	Belt & AB
Frontal	Small female	Manual	Belt & AB
Frontal	Midsize male	Manual	Belt & AB
Side	Midsize male	Manual	Belt & AB
Side	Midsize male	Power	Belt & AB

Computational Modeling

Overview

Computational modeling was used to identify the optimal location of the vehicle UDIG securement hardware relative to other interior vehicle components for both front and side crashes. Simulations analyzed how to balance the occupant position relative to belt anchorage locations and airbags, while considering that wheelchair size will vary, whereas a vehicle seat would not. Simulations also considered placement of components relative to recommendations for space to accommodate wheelchairs and the amount of room needed to navigate into the wheelchair seating station.

In this study, the restraint design optimization in frontal crashes was conducted using an integrated MADYMO model by combining the surrogate wheelchair base (SWCB) model, the Hybrid III midsize male ATD model, the model representing the UDIG design, a three-point seat belt system model, and airbag models. In the first phase of modeling work, we focused on identifying the trends and effects from wheelchair location and belt anchorage location. Occupant injury risks with and without baseline airbag designs have also been investigated. Optimizations were conducted for both right-front and second-row-left locations. The results provide a better understanding on how seatbelts may interact with wheelchair-seated occupants in a wide range of UDIG and belt anchorage locations considering the size of the wheelchair with and without airbags.

In the design optimization for side impacts, a set of MADYMO models similar to those used in frontal crashes was be used for side impact simulations, except that ES-2re ATD replaced the HIII ATD and a representation of a side door based on Dodge Caravan geometry was included. Because the UMTRI wheelchair model had not been previously validated in side impact testing, validation tests were conducted before proceeding with simulations to optimize side impact protection. Simulations examined wheelchair station location and belt geometry with and without airbags in near and farside impacts. Alternative belt configuration with an inboard rather than outboard Dring were examined. Optimization results were harmonized with frontal optimizations. Because adequate restraint in farside crashes was not feasible with only belt restraint, modeling was used to design an innovative Center Airbag To Contain Humans (CATCH).

The next modeling task developed MADYMO models representing the manual and power wheelchairs being used in volunteer and dynamic testing. Simulations evaluated the differences in frontal response using the SWCB and the two wheelchair models, using geometry for the wheelchair seating station and seatbelts that was feasible to achieve in the test vehicles. These simulations were used to identify test conditions for dynamic testing.

Frontal Model Validation

The first step in conducting optimization simulations in frontal impacts was to modify previously validated models secured by a 4-point strap tiedown system to incorporate a UDIG-compatible securement instead. Comparison of excursion between simulation and a test from a previous research project is shown in Figure 33, while an overlay of ATD signals is shown in

Figure 34. Results show good agreement. The main difference is a slightly different distribution of load between the lap belt and shoulder belt in the simulation and test.
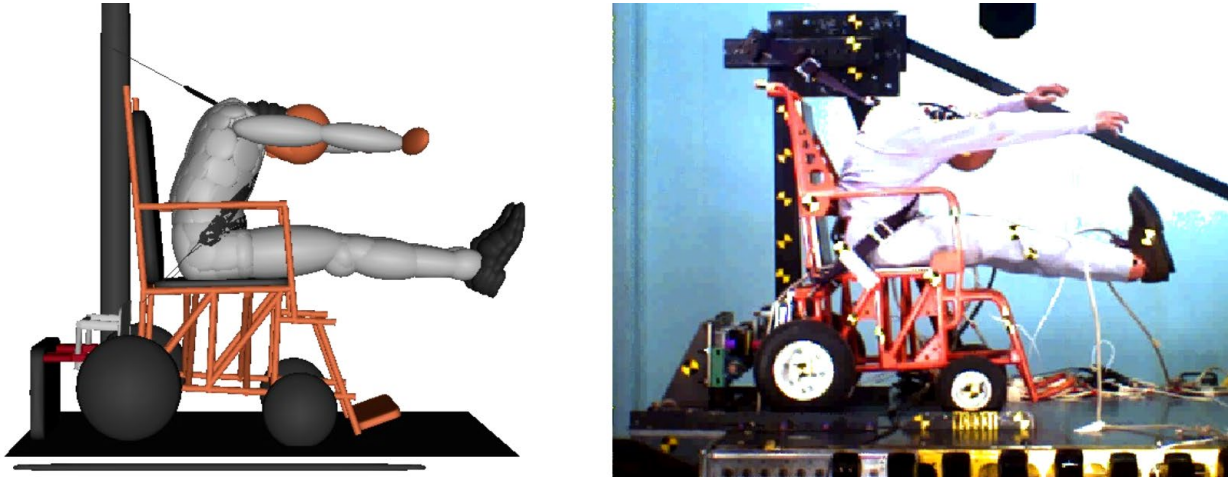
Figure 33. Frontal crash peak excursion comparison between simulation and test.
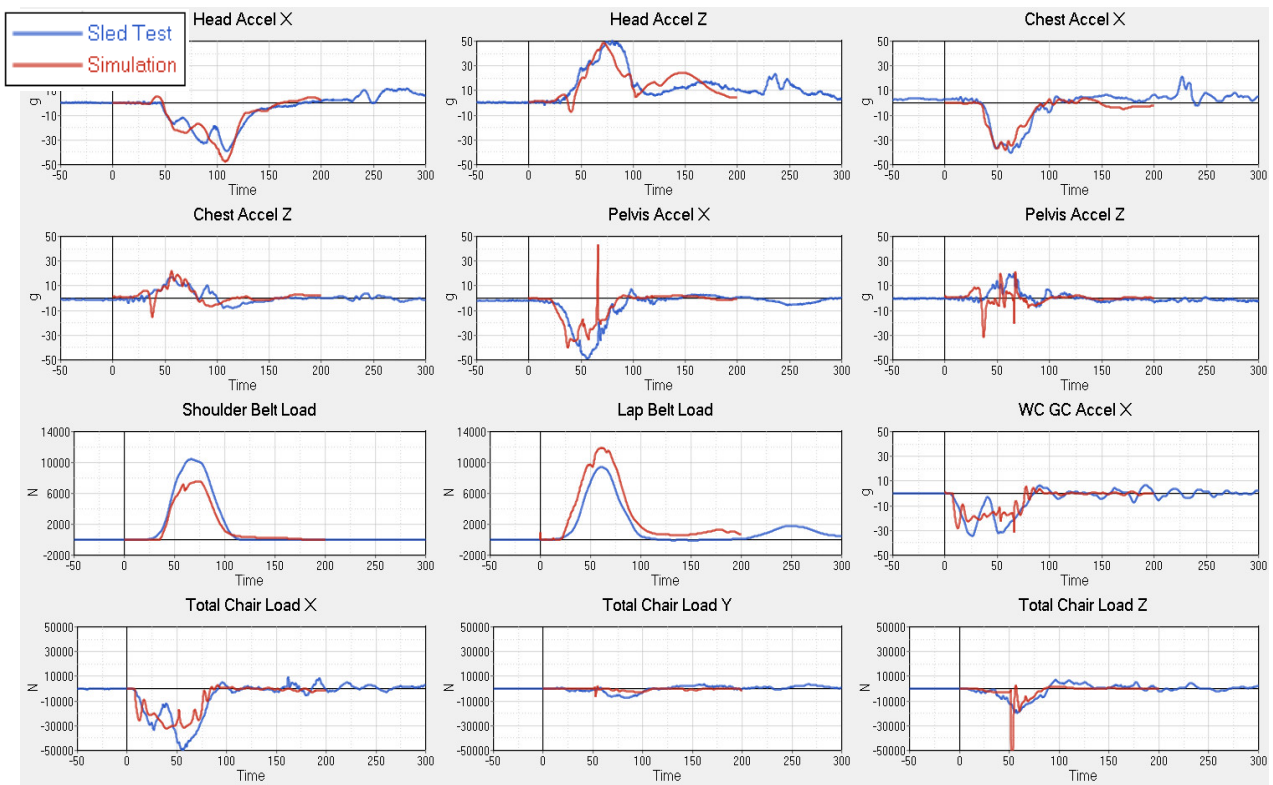
Figure 34. Frontal crash ATD response comparison between model and test with UDIG docking.

Side Impact Validation Tests

Methods

To provide validation data for the current effort a set of sled test was conducted that focused on side impact performance. This sled test series collected data from seven side impact tests to support development of computer modeling tools. The tests explored the effect of wheelchair width, nearside/farside upper shoulder anchor point placement, armrests presence/style, and UDIG/4-point securement on the ATD measures and WC responses. In addition, because no voluntary performance standards exist for wheelchairs under side impact testing conditions, we wanted to collect data on the performance of the SWCB secured with 4-point strap tiedowns. These results could be used as a reference for evaluating performance of UDIG-secured systems in side impact, with the goal of achieving results equal to or better than the test with the typical tiedown condition.

The test series was conducted on the impact sled at UMTRI. The tests were visually documented with pre- and post-test photos along with four views of high-speed digital video at 1000 fps: front, side, overhead, and left oblique. The side view videos were digitized to determine the maximum forward excursion of the leading edge of the ATD head and the most forward excursion of the center of the ATD knee joint. The overhead video was analyzed to measure the maximum rotation of the wheelchair centerline. The sled pulse used was the 30 km/h (18.6 mi/hr), 24 *g* corridor proposed in the 2014 FMVSSS 213 side impact test procedure for CRS and shown in Figure 35.
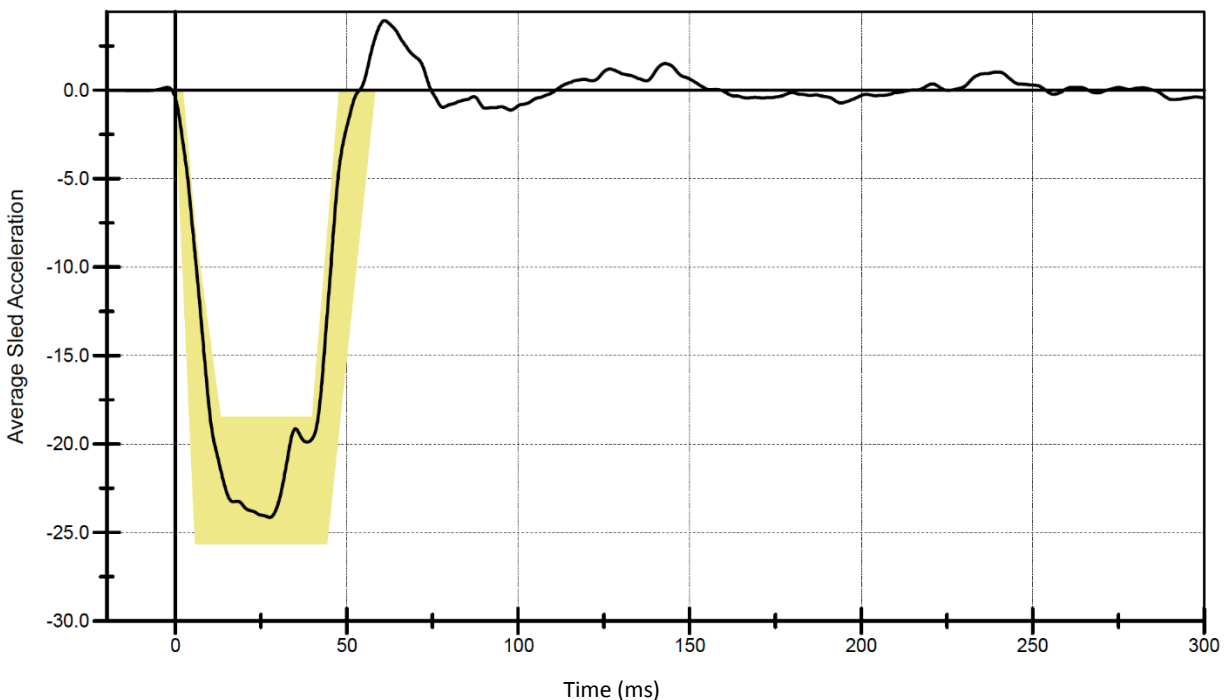
Figure 35. Example side impact pulse and corridor.

The wheelchair station was oriented on the sled plate so the center line of the wheelchair was rotated 80 degrees to the right from the forward-facing orientation (80 degrees counterclockwise rotation if viewed from above) as shown in Figure 36. This orientation was selected to represent a side impact event with a partial frontal impact component that is common in the field and is also the orientation suggested in the FMVSS 213 NPRM for side impact testing of CRS.
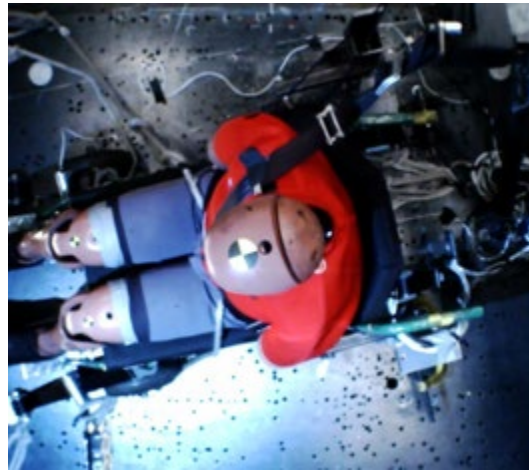
Figure 36. Orientation of wheelchair at 80 degrees.

The wheelchair was secured to the sled using either the crashworthy UDIG or four-point WTORS. Both of these systems were instrumented to capture the load time history data for the securement forces during impact. The UDIG forces were measured with an array of four 3-axis load cells along with 3 orthogonally mounted accelerometers whose outputs can be used to inertially compensate the load cell data. The 4-point SWTORS have strain-gauge load cells in line with the belts.

The ES-2RE crash test dummy was used to represent the wheelchair occupant and was instrumented to measure head acceleration, ribcage deflection, lower spine acceleration, abdominal loads, pubic loads, and pelvis acceleration. Before each test, the position of the ATD and relevant test hardware was documented by digitizing the key landmarks. Special attention was paid to: centering of the ATD torso and pelvis on the wheelchair seat, consistent fore/aft position of the ATD relative to seat, the locations of top and bottom of the lap belt and shoulder belt at the ATD centerline, and the location of seat (four corners of pan and back) relative to the SWCF.

The three-point seat belt was configured to have the lower lap belt anchors close to the ATD H-point. The pelvic belt was tightened to fit snugly over the ATD pelvic region. The shoulder belt was tightened snugly across the ATD chest with a 75-mm block between the belt and ATD inserted at the height of the top ATD rib. The block was removed prior to the test. This slack is used in wheelchair crashworthiness testing to simulate the spoolout of the retractor with a static belt set up.

The SWCB is designed to be width-adjustable by swapping out the center box frame to create different frame widths. It also includes deformable elements, replaced before each test, at the

front casters and at the base of the back canes to simulate the response of a commercial wheelchair frame (Ritchie et al., 2006).

Many wheelchair armrests flip up or rotate out to allow the lateral transfer out of the device. For this test series, we included one style of flip up armrest, one style of rotate out armrest and a no armrest condition. The armrests used are shown in Figure 37.
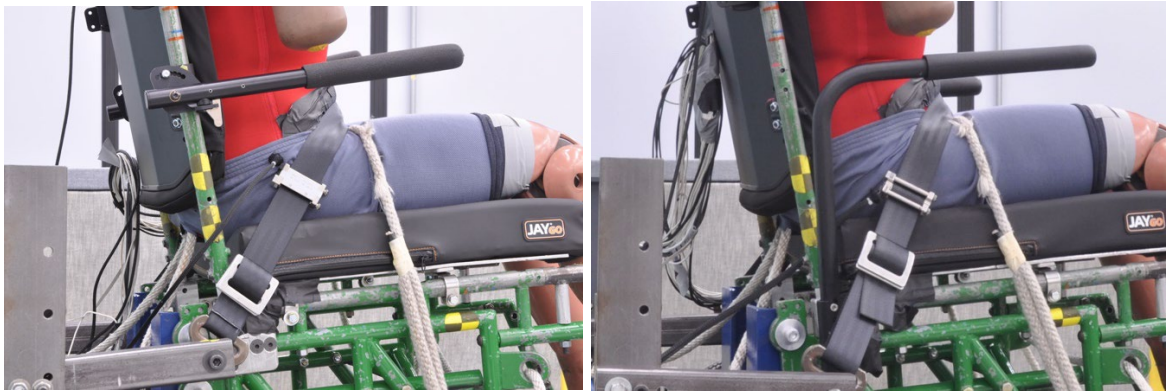
Figure 37. Flip up armrest (left) and rotate out armrest (right).

After tuning the target pulse in tests AW2001 through AW2004, the seven conditions outlined in Table 6 were tested.

Table 6. Test Matrix

Test ID	Purpose	ATD	Anchorage	Direction	Armrest	Restraint System	Fixture	Seatback
AW2001	checkout pulse	H350th	4-pt	Farside	None	WC Anchored Lap belt	SWCB, 18", alum seat	Fabric back, old cushion
AW2002	checkout pulse	ES2-RE	UDIG1	Nearside	None	Veh-Anch 3PB, geom1	SWCB, 18", alum seat	Fabric back, old cushion
AW2003	checkout pulse	ES2-RE	UDIG1	Nearside	None	Veh-Anch 3PB, geom1	SWCB, 18", alum seat	Fabric back, old cushion
AW2004	Check pulse, Anchors	ES2-RE	UDIG1	Nearside	none	Veh-Anch 3PB, geom1	SWCB, 18", alum seat	Fabric back, old cushion
AW2005	near-side	ES2-RE	UDIG1	Nearside	None	Veh-Anch 3PB, geom1	SWCB, 18", alum seat	Jay cushion/ seat
AW2006	armrest 1	ES2-RE	UDIG1	Farside	AR1	Veh-Anch 3PB, geom1	SWCB, 18", alum seat	Jay cushion/ seat
AW2007	armrest 2	ES2-RE	UDIG1	Farside	AR2	Veh-Anch 3PB, geom1	SWCB, 18", alum seat	
AW2008	16" width UDIG	ES2-RE	UDIG1	Farside	None	Veh-Anch 3PB, geom1	SWCB, 16", alum seat	Jay cushion/ seat
AW2009	Baseline UDIG	ES2-RE	UDIG1	Farside	None	Veh-Anch 3PB, geom1	SWCB, 18", alum seat	
AW2010	20" width UDIG	ES2-RE	UDIG1	Farside	None	Veh-Anch 3PB, geom1	SWCB, 20", alum seat	Jay cushion/ seat
AW2011	Baseline 4pt IARV	ES2-RE	4-pt	Farside	None	Veh-Anch 3PB, geom1	SWCB, 18", alum seat	

Results

Table 7 shows the ATD transducer-based measures while Table 8 shows the ATD and WC excursions and WC rotations.

Table 7. ATD Injury Measures

Run #	HIC 15	Peak Upper Rib Deflect	Peak Middle Rib Deflect	Peak Lower Rib Deflect	Peak Result Spine Accel	Peak Abd Front Fy	Peak Abd Middle Fy	Peak Abd Rear Fy	Peak Pubic Fy	Peak Result Pelv Accel
units		Mm	mm	mm	g	N	N	N	N	g
AW2005	331.1	-9	-6.2	6.4	28.7	189.4	-44	-32.9	-1812.1	30.6
AW2006	157.1	3.8	6.0	3.2	28.1	266.4	73.0	270.0	-1822.2	33.9
AW2007	130.2	8.9	4.3	4.8	32.0	276.4	138.3	337.2	-1810.8	34.5
AW2008	233.8	4.8	3.9	4.7	43.3	306.9	311.9	449.0	-3773.5	32.6
AW2009	128.7	6.5	5.5	4.6	27.4	220.4	234.5	402.7	-2543.0	35.3
AW2010	126.1	4.1	4.3	3.9	34.6	467.3	240.5	306.6	-4238.2	32.1
AW2011	237.3	---	8.7	3.7	26.8	196.3	209.5	187.1	-2333.6	34.5

Table 8. Wheelchair and ATD Kinematics

Run #	ATD head ex	ATD knee ex	WC ex	WC rotation
	mm	mm	mm	deg
AW2005	528	414	87	15
AW2006	730	408	82	12.5
AW2007	795	455	90	14
AW2008	806	495	90	14
AW2009	800	417	76	13.5
AW2010	773	441	71	12
AW2011	727	373	147	17

Figure 38 shows the wheelchair excursion and rotation data. Rotation was measured from the overhead digital video and the value reported in the peak rotation about the Z-axis, relative to a 90-degree pure lateral orientation. All the wheelchairs were initial positioned 10 degrees off of full lateral, from that starting angle, the wheelchairs rotated an additional 2-5 degrees toward the impact. In the laboratory coordinate system, wheelchair excursion is the peak forward (X-direction) displacement of the wheelchair seat rails, measured from the side view video. It was calculated by averaging the displacements measured from the right and left end faces of the mounting rails for the wheelchair seating system. As shown in the graph, the test with the 4-point tiedown exhibited the highest rotation and excursion levels. The lowest values for both measures were recorded with the surrogate wheelchair frame adjusted to the widest level tested in this series.
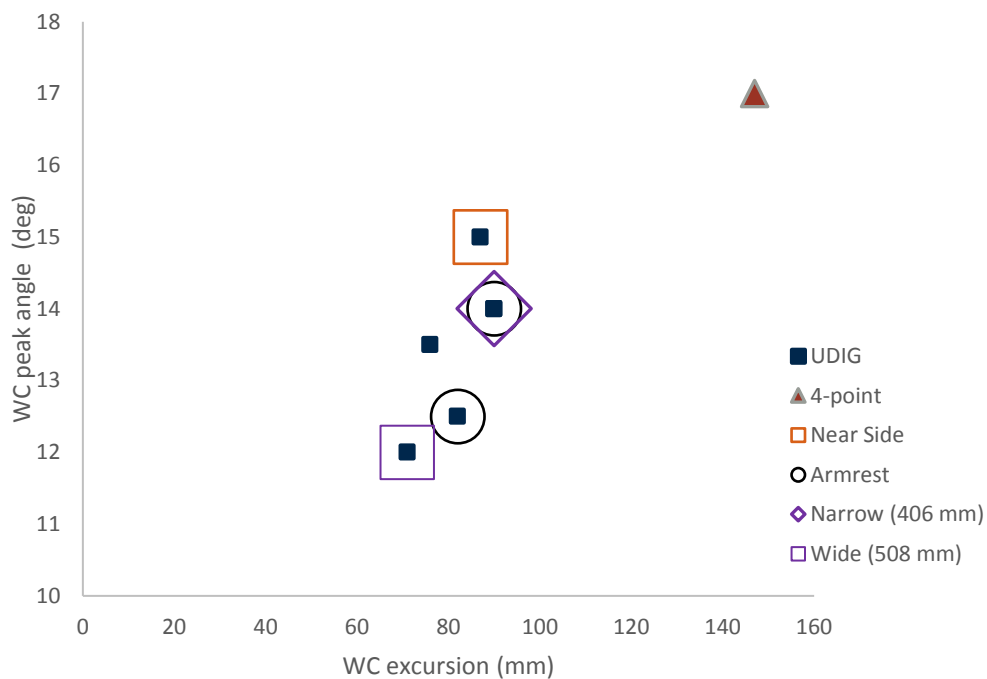
Figure 38. Wheelchair Rotations and Excursions

58

Figure 39 presents the ATD head and knee excursions, measured from the side view video. These are forward displacements from the time zero position for the leading edge of the head and the center of the knee joint. The head excursion is greatly reduced in the nearside seat belt configuration where the shoulder belt is routed to the shoulder closest to impact. The 4-point tiedown had a knee excursion close to, but lower than, the tests where the wheelchair was secured with UDIG. The presence of the armrest in two tests did not systematically reduce dummy excursions. The test with the highest head and knee excursions was the narrow wheelchair condition. The lateral motion of the ATD was not well controlled in any of the farside impact tests, and the ATD did not remain fully seated in the wheelchair for any but the nearside test condition.
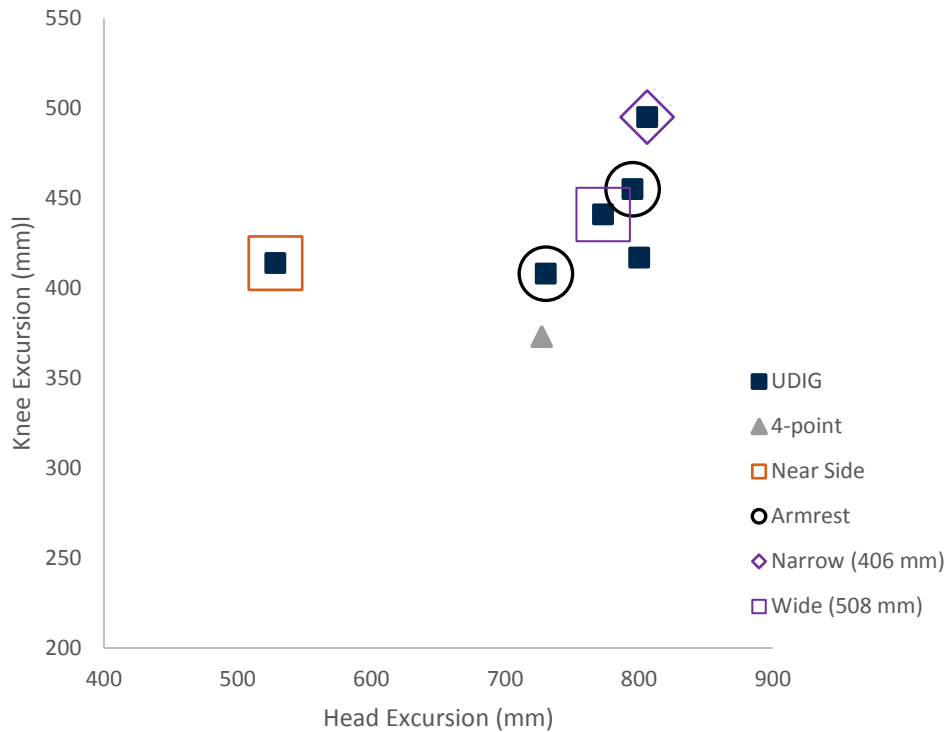
Figure 39. ATD knee excursion vs. head excursion.

Figure 40 plots HIC 15 and spine acceleration. All the HIC values are very low and are generated from non-contact accelerations. The highest spine acceleration was measured with the narrow WC condition. The highest HIC was measured in the nearside seat belt condition because the forward head motion was limited by the shoulder belt, compared with the upper torso rotating freely toward the impact. The data from the remainder of the UDIG runs is clustered together, but the 4-point tiedown data is set apart by a higher HIC value.
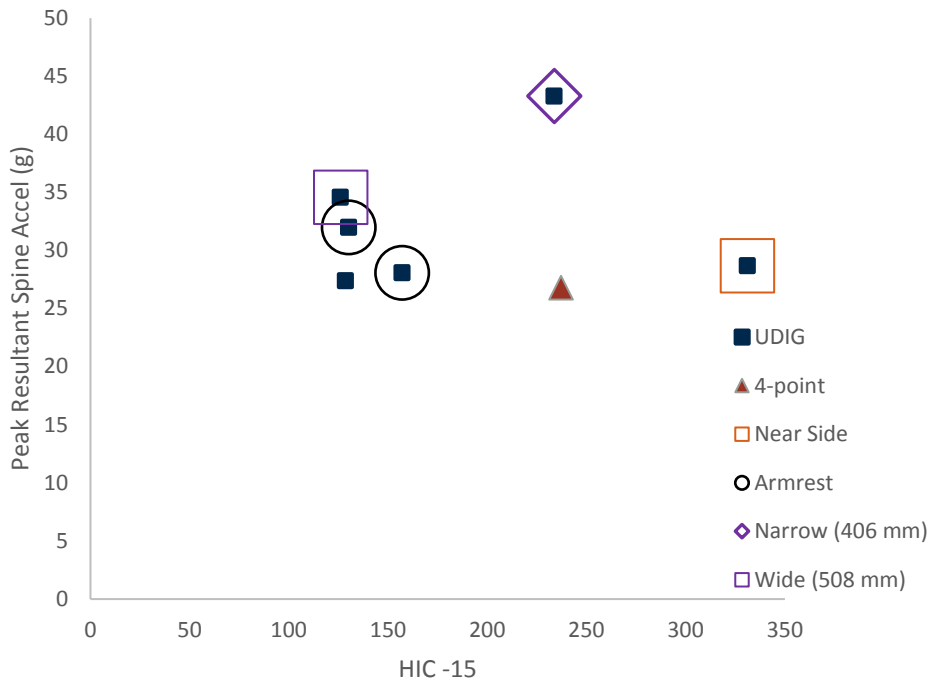
Figure 40. Peak resultant spine acceleration vs. HIC-15.

The ES-2RE was instrumented to measured lateral deflections at the upper, middle, and lower rib levels. These data are shown in Figure 41. All the values measured are below 10 mm of deflection. Due to a transducer wiring fault, the upper rib deflection for the 4-point tiedown test is missing.

Figure 41. Rib Deflections

The abdominal forces and pelvic forces reported in Table 7 and presented in Figure 42 and Figure 43 are all well below the FMVSS 214 levels of 2500 N and 6000 N, respectively. The highest abdominal forces were less than 500 N, and observed in the test with the widest surrogate wheelchair frame condition. The lowest levels of pelvic force were recorded in the narrow configuration and the two tests with armrests.
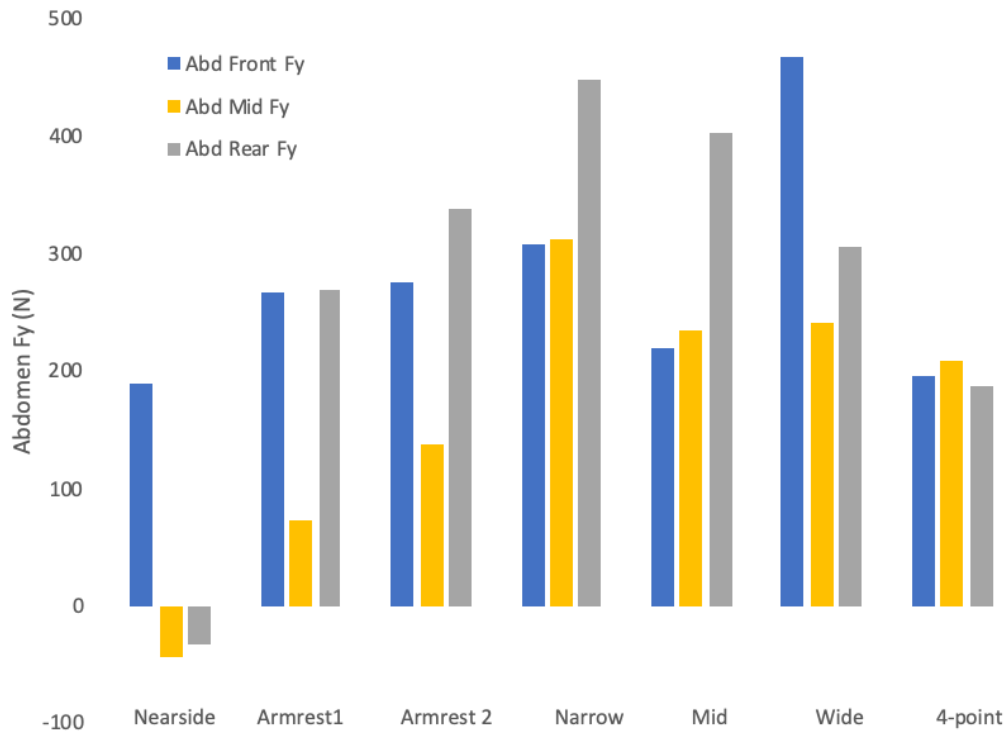
Figure 42. Abdominal loads.
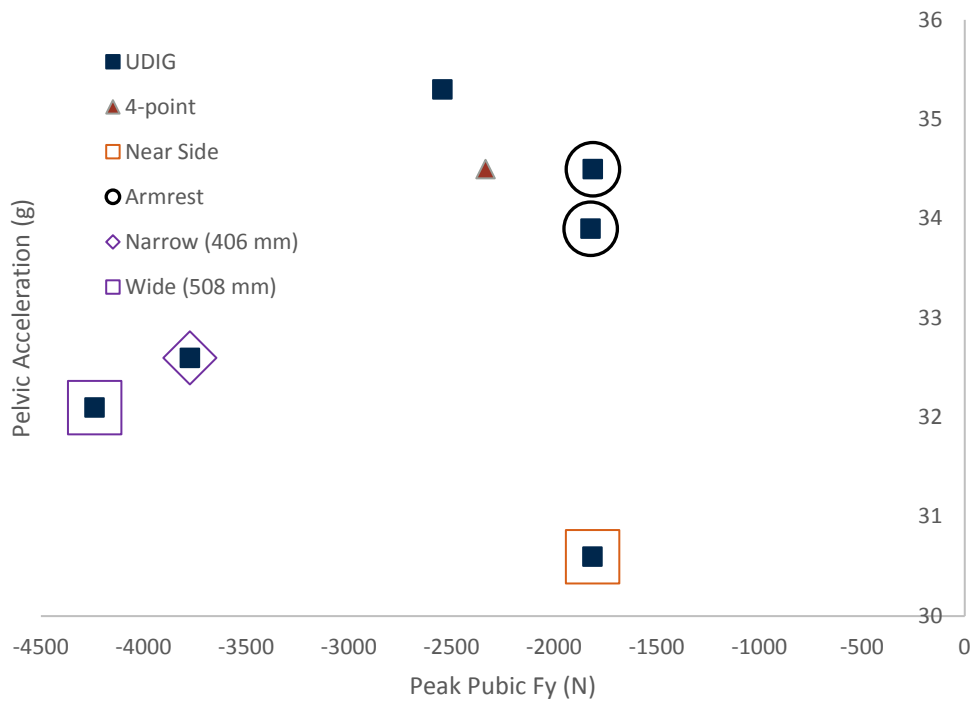
Figure 43. Pelvic loads and accelerations.

Discussion and Summary

The primary goal of this test series was to provide data to validate a side impact wheelchair model and to explore the effects of wheelchair width, nearside/farside seat belt configuration, wheelchair securement method and the presence/absence of an armrest. Although not exhaustive, these data support the following observations:

- Securing the surrogate wheelchair with UDIG instead of a 4-point tiedown reduces wheelchair excursion and rotation, likely because tiedown anchor points are optimized for frontal crashes, and the rigid UDIG attachment deforms less than tiedown straps.
- The nearside seatbelt configuration (shoulder belt routed over the shoulder closest to impact) reduces head excursion but does not show a big effect on limiting lower body excursion.
- In the absence of a vehicle side wall or side airbag and despite a deliberate effort to locate the lap belt anchors near the ATD hips, the ATD was not contained to a seated position in any of the configurations tested.
- The ATD injury metrics did not suggest a high risk of torso, abdominal, or pelvic injury in these configurations.

When deciding which conditions to use as the baseline for side impact modeling, we decided to use the no-armrest condition as the baseline because the ATD interactions with the armrests in tests AW2006 and 7 were chaotic and did not have a measurable effect on ATD lateral motions. Both armrest hardware assemblies were damaged during testing. The flip up armrest twisted around the wheelchair cane at the hardware interface while the fold out armrest hardware fractured.

We also selected the farside seatbelt configuration for baseline because it allowed us to collect data on uninhibited ATD movement that can be used to model the effect of side structures. In addition, the sled fixtures used for creating the nearside seatbelt configuration had potential to interact with the head in an unrealistic way, creating high acceleration head impacts.

Side Model Validation

The side impact model was validated against the baseline condition of test AW2009, which is far-side and no armrest. A comparison of peak head excursions is shown in Figure 44, while an overlay comparison of ATD signals between the test and simulation is shown in Figure 45. Results generally show good agreement, with the largest difference seen in the head z acceleration.
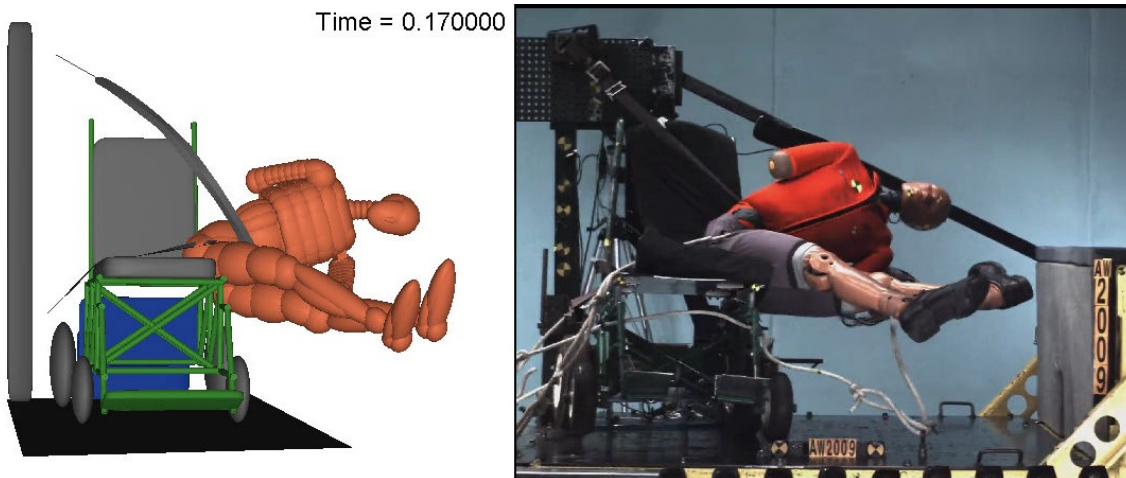
Figure 44. Validation of baseline side impact condition: peak excursion of model and test.
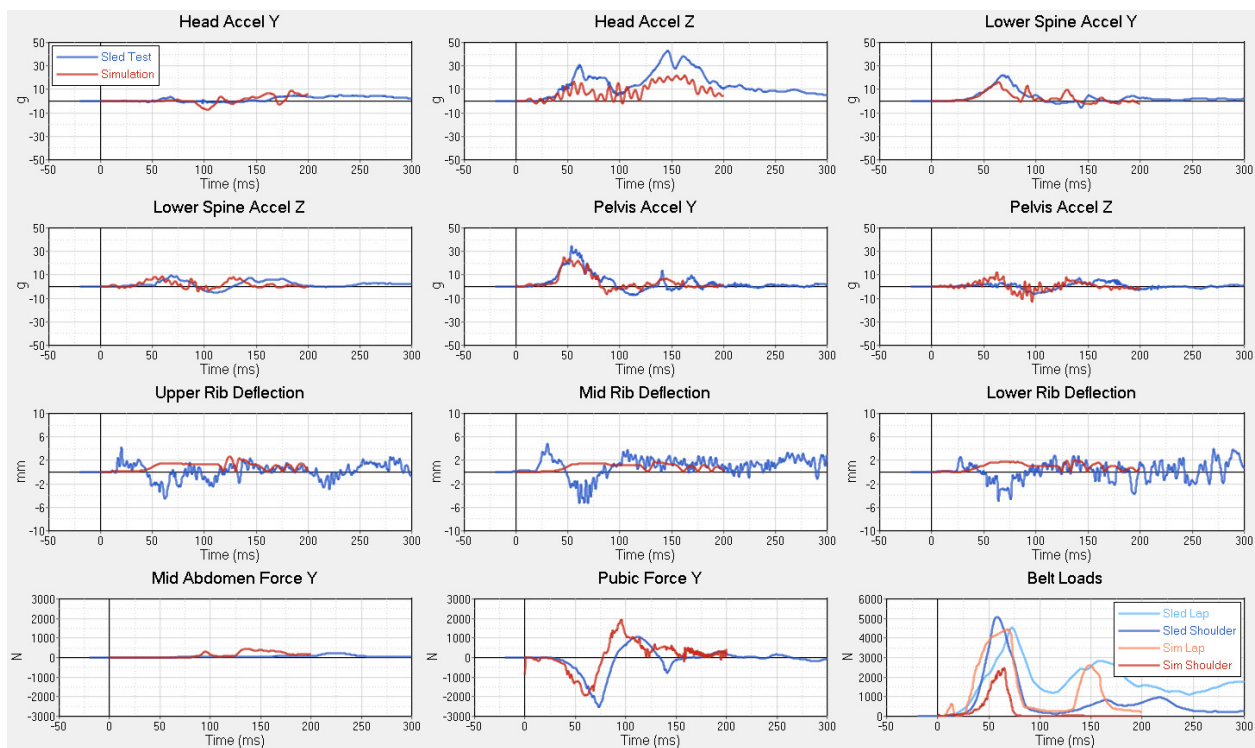
Figure 45. Side impact validation overlay plots of ATD signals for model and test.

Restraint Optimization in Frontal Crashes

Figure 46 shows the MADYMO model being used for the optimizations, as well as the parameters under consideration. Parameters include the fore-aft position of the wheelchair relative to the UDIG anchors, the vertical and fore-aft locations of the buckle, and the fore-aft location of the D-ring. In addition, simulations were run with and without a SCARAB airbag. Simulations monitored a number of injury measures: HIC15, peak resultant head acceleration,

forward head excursion, chest deflection, peak resultant thorax acceleration, pelvis acceleration, and femur forces.
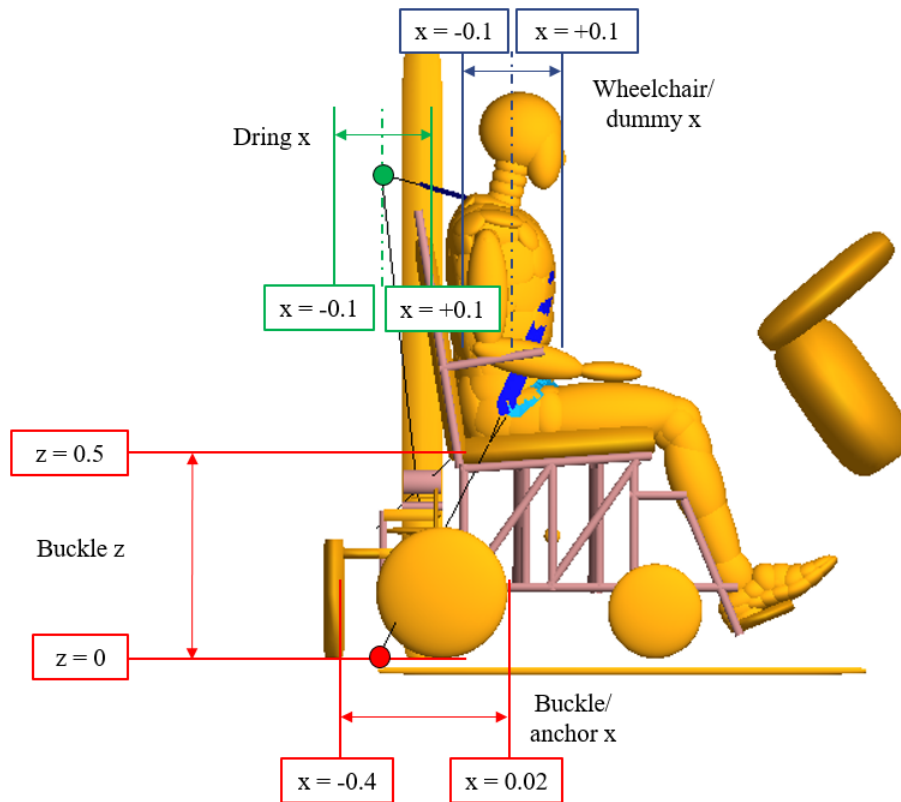
Figure 46. Diagram of parameter ranges considered in frontal optimization. Unit=m

ModeFrontier software was used to implement Design of Experiment (DOE) for the simulations; the workflow is illustrated in Figure 47. The workflow started with defining input variables within the design ranges. Each set of input variables was used to reconfigure the pre-simulation and crash simulation setup. The pre-simulation was specifically used to fit the seatbelt onto the ATD. The fitted seatbelt location results were then passed to the crash simulation. ATD injury measures, such as HIC, Nij, chest deflection and femur force were output from the crash simulation for assessing occupant injury risks. ATD head excursions were also recorded to ensure low probability of a head contact to vehicle interior.
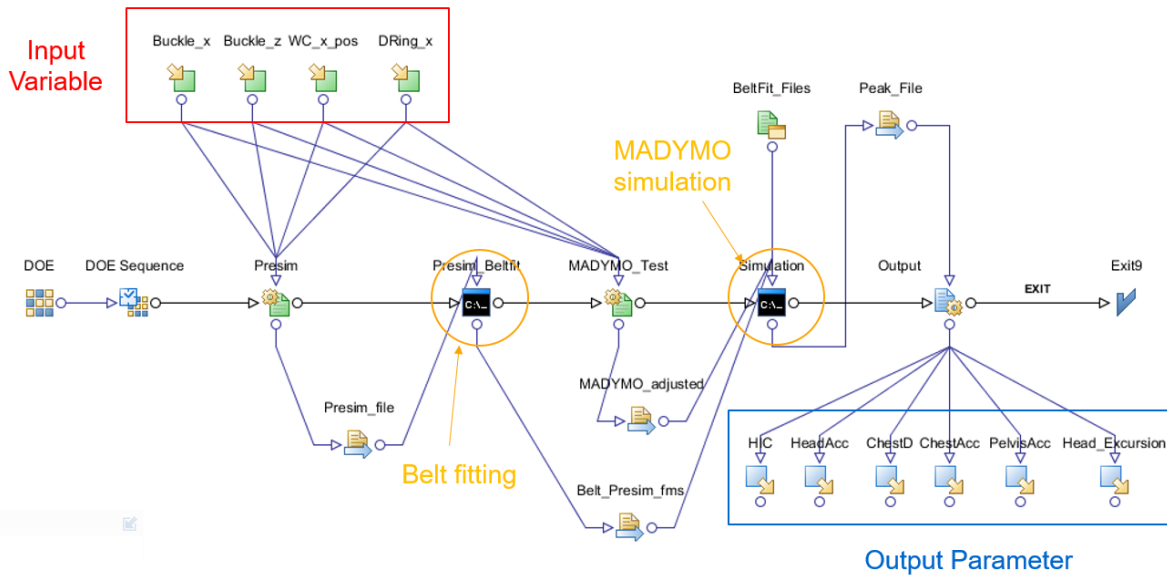
Figure 47. ModeFrontier Workflow diagram for frontal impacts without airbag.

The correlation matrix for simulations without an airbag are shown in Table 9 for the right-front position and 2nd row left seat in Table 10. Blue cells correspond to negative correlations between input and output variables (as input value increases, output value decreases), while red cells correspond to positive correlations (output value increases as input value increases). Darker shades show stronger correlations. There are differences between the two seating positions because the larger space available in the second row provides more room for the occupant to avoid head contact. For this reason, adding an airbag shows a clear benefit for the front seat occupant, but the effects on second row occupants are not as strong. Overall, head excursion is highly sensitive to the wheelchair fore-aft position at both seating locations. The D-ring location primarily affects the chest measures and head excursion in the front seat location, and the head acceleration-based criteria in the second row. The buckle vertical location has the strongest effect on the chest displacement in both positions, while the buckle fore-aft location affects the lower extremity and head excursion measures for the front seating position, but has less influence on injury measures in the second-row seating position.

Table 9. Correlation matrix between input and output variables for front seat wheelchair users without an airbag.

	Pelvis Acc	Chest Acc	Chest D	Head Excursions	Head Acceleration	HIC
WC X position	-0.373	-0.296	-0.347	-0.670	0.543	0.449
D Ring X	0.247	0.492	0.457	0.422	0.235	0.370
Buckle Z	-0.247	0.085	0.427	-0.334	0.282	0.280
Buckle X	0.465	0.255	0.048	0.447	-0.095	-0.311

66

Table 10. Correlation matrix between input and output variables for 2nd row seat wheelchair users with an airbag

	Pelvis Acc	Chest Acc	Chest D	Head Excursions	Head Acceleration	HIC
WC X position	0.472	0.494	-0.218	-0.579	-0.137	-0.289
D Ring X	0.062	0.162	0.162	0.364	0.559	0.499
Buckle Z	0.042	0.136	0.136	-0.384	-0.334	-0.325
Buckle X	-0.112	-0.289	-0.289	0.492	0.208	0.256
airbag	0.354	0.328	0.328	-0.227	-0.069	-0.226

The initial set of parameters led to some belt anchorage locations with high potential for injury risk. Examples are shown in Figure 48, where the combination of parameters led to lap belt angles that were either too shallow or too steep. As a result, we adjusted the range of modeling parameters to avoid these conditions. This reduced the maximum vertical location of the belt anchor to 0.4 m from 0.5 m, and the maximum forward location to -0.1 m from 0.0 m. The range of D-ring locations was also restricted to limit to conditions that produced acceptable shoulder belt placement, as shown in Figure 49, defined by a location on the shoulder that is not touching the neck nor too close to the arm.
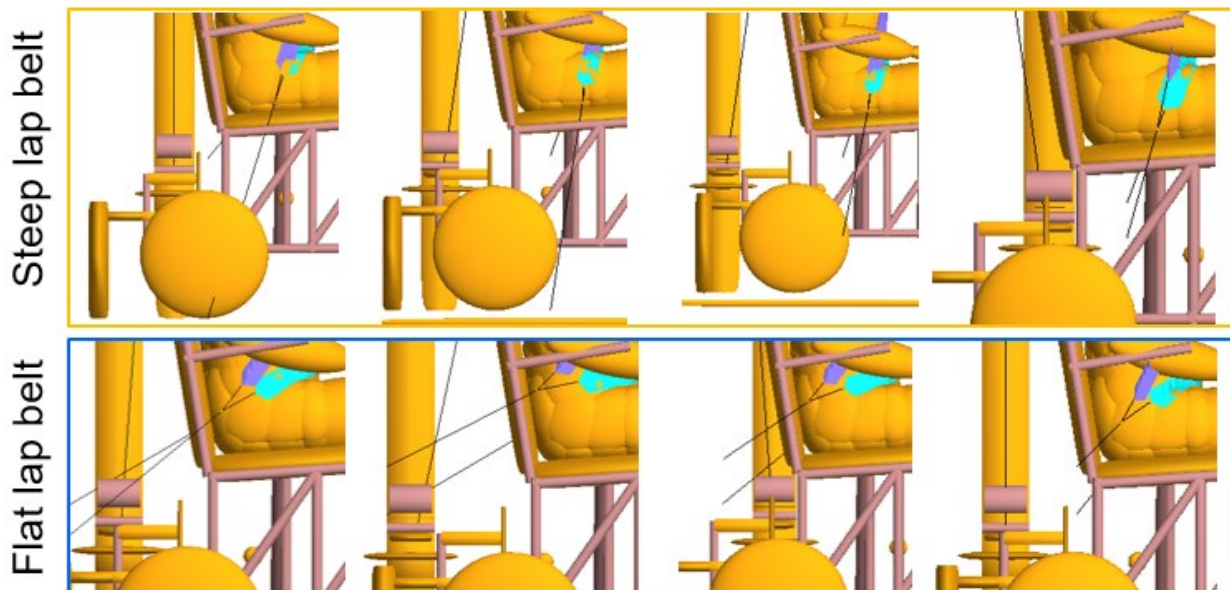
Figure 48. Examples of modeling configurations producing lap belt angles that are too steep or too flat.
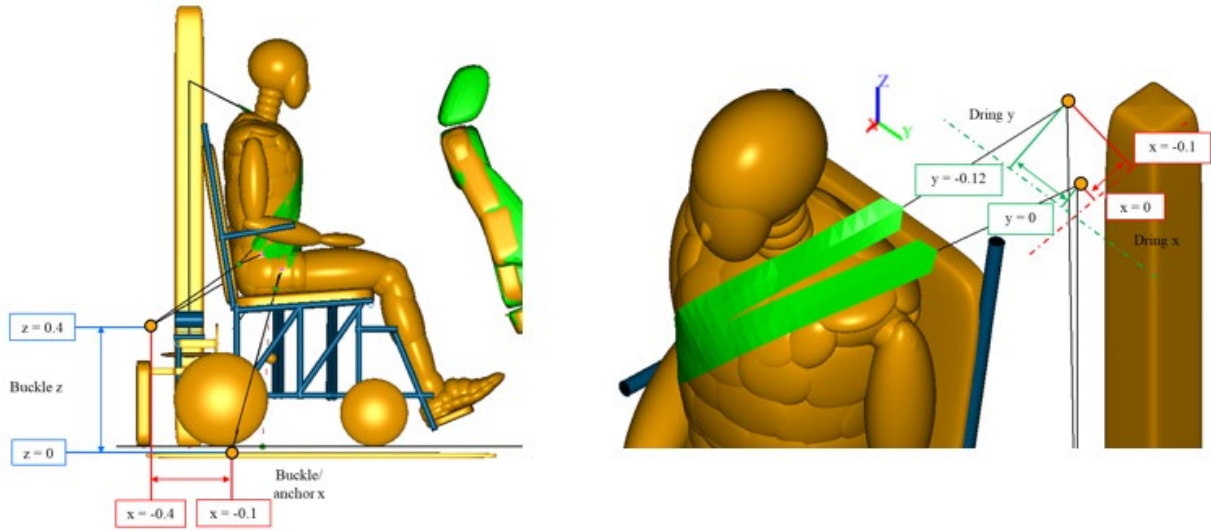
Figure 49. Adjusted ranges of belt anchorages in ULHS

Using the revised parameter range, a Uniform Latin Hypercube Sampling (ULHS) method was used to sample 100 conditions each for simulations of front seat and 2nd row seat positions. Since the goal of these simulations was to find optimal belt anchorage locations, they were conducted without airbags. Results are shown in Figure 50 for the second row seating position and Figure 51 for the front-row seating position. Optimal buckle locations (outlined in red dashes) were selected when simulations simultaneously produced low HIC, low head excursion, and low chest deflection.
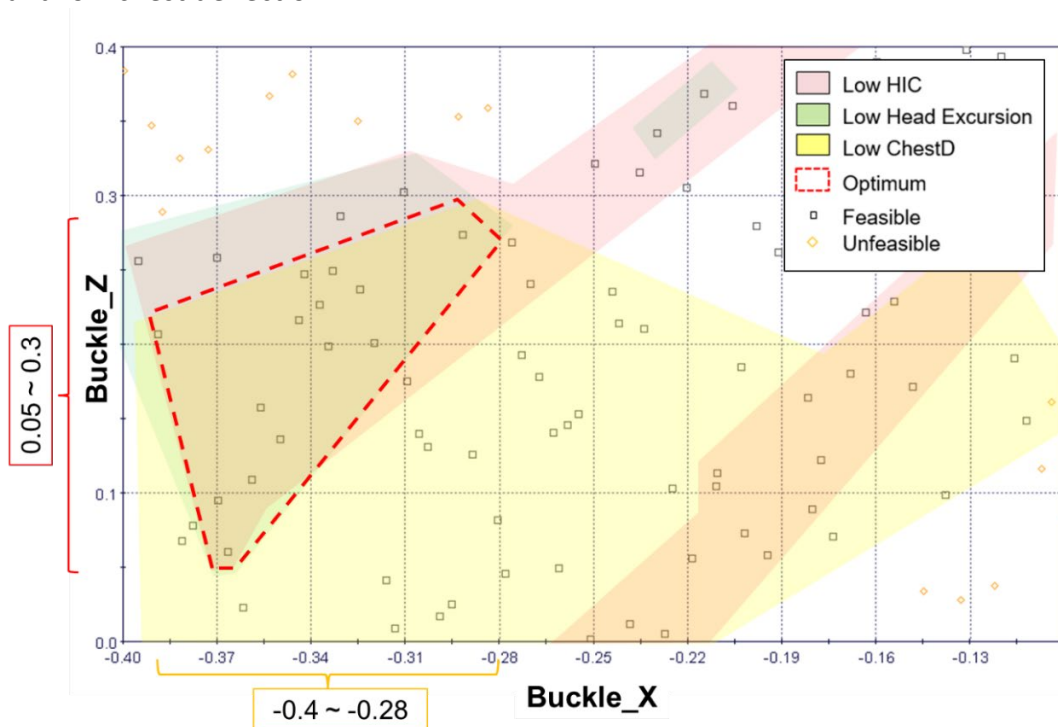
Figure 50. Optimal buckle anchorage locations for the 2nd row wheel-chair users.
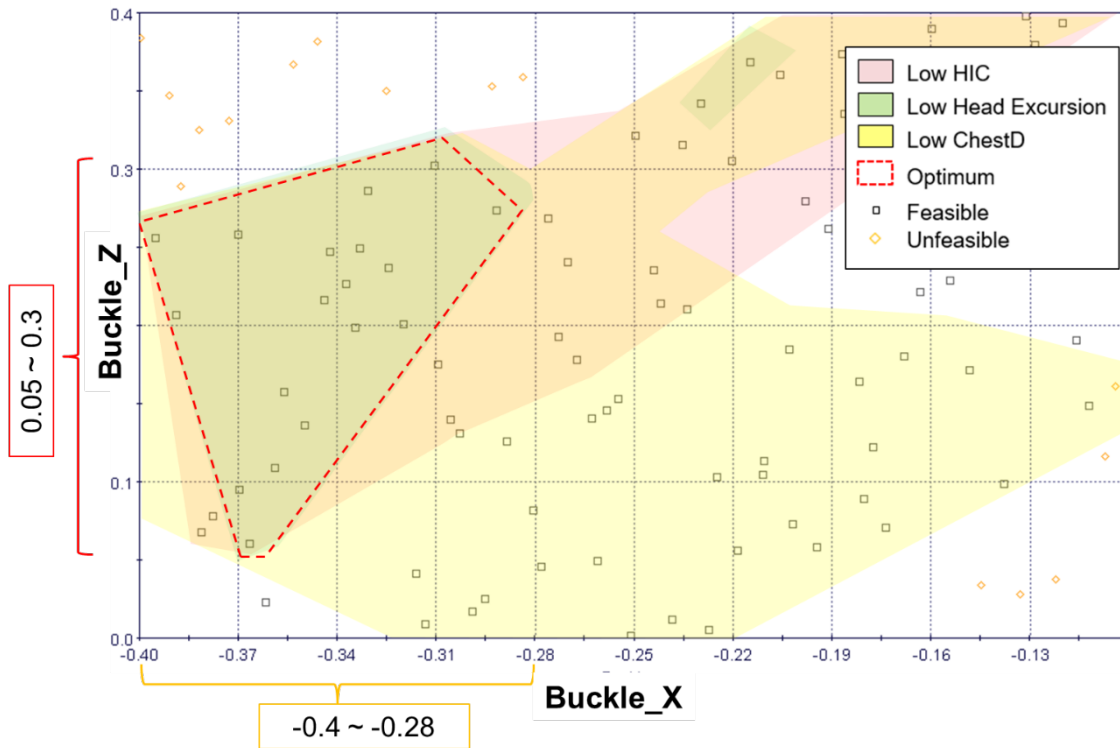
Figure 51. Optimal buckle anchorage locations for the front row wheel-chair users.

After identifying the optimal buckle locations for each seating position, a selection of conditions was rerun with the addition of an airbag. Conditions included five simulations within the optimal zone, as well as five conditions outside the optimal zone. These suboptimal conditions were selected to represent how the belt designed for a mid-sized male might fit on someone of a different size. Results are shown in Table 11 and Table 12 for the second row conditions and Table 13 and Table 14 for the right-front conditions. Overall, the results indicate that the airbag can effectively reduce head and neck injury risks and combined injury risks, but may slightly increase the chest injury risks without belt load limit changes. The airbag is especially beneficial when considering anchorage locations that may result in poor belt fit. Adding an airbag to optimal belt locations in the second row reduces the overall injury risk by 17-19% relative to the no-airbag condition, and 18-23% for suboptimal belt placement. For the front-row, potential reduction in combined injury risk with optimal belt conditions only ranges from 11-14%, but with suboptimal it ranges from 11% to 72%. These results indicate adding an airbag may be useful in compensating for suboptimal belt fit on a wider range of occupant sizes, and would be strongly recommended for a front-row seating position and helpful for a second-row seating position.

Table 11. Airbag benefit at five design locations with good belt fit for second row position.

	P(HIC15)	P(Nij)	P(chest)	P(Lfemur)	P(Rfemur)	P(femur)	Pjoint(AIS 3+)
32-no airbag	0.00000	0.06744	0.00005	0.00311	0.00313	0.00313	0.07000
32-airbag	0.00000	0.05415	0.00006	0.00308	0.00312	0.00312	0.05700
32-difference	-93%	-20%	8%	-0.8%	-0.4%	-0.4%	-19%
34-no airbag	0.00000	0.06697	0.00005	0.00311	0.00311	0.00311	0.07000
34-airbag	0.00000	0.05454	0.00006	0.00308	0.00313	0.00313	0.05800
34-difference	-93%	-19%	9%	-1.2%	0.6%	0.5%	-17%
41-no airbag	0.00001	0.06856	0.00005	0.00305	0.00313	0.00313	0.07200
41-airbag	0.00000	0.05540	0.00006	0.00306	0.00313	0.00313	0.05800
41-difference	-98%	-19%	9%	0.3%	-0.1%	-0.1%	-19%
66-no airbag	0.00000	0.06815	0.00005	0.00310	0.00313	0.00313	0.07100
66-airbag	0.00000	0.05517	0.00006	0.00308	0.00313	0.00313	0.05800
66-difference	-98%	-19%	8%	-0.6%	-0.3%	-0.3%	-18%
87-no airbag	0.00001	0.06951	0.00005	0.00311	0.00313	0.00313	0.07200
87-airbag	0.00000	0.05515	0.00006	0.00308	0.00313	0.00313	0.05800
87-difference	-98%	-21%	7%	-1%	0%	0%	-19%

Table 12. Airbag benefit at five design locations with poor belt fit for second row position.

	P(HIC15)	P(Nij)	P(chest)	P(Lfemur)	P(Rfemur)	P(femur)	Pjoint(AIS 3+)
0-no airbag	0.00007	0.07404	0.00006	0.00307	0.00321	0.00321	0.07700
0-airbag	0.00000	0.05983	0.00006	0.00309	0.00312	0.00312	0.06300
0-difference	-98%	-19%	9.3%	0.7%	-2.9%	-2.9%	-18%
10-no airbag	0.00007	0.07562	0.00006	0.00312	0.00317	0.00317	0.07900
10-airbag	0.00000	0.05815	0.00006	0.00310	0.00312	0.00312	0.06100
10-difference	-99%	-23%	8.4%	-0.5%	-1.3%	-1.3%	-23%
19-no airbag	0.00006	0.07387	0.00006	0.00322	0.00315	0.00322	0.07700
19-airbag	0.00000	0.05724	0.00006	0.00307	0.00307	0.00307	0.06000
19-difference	-99%	-23%	8.0%	-4.9%	-2.3%	-4.6%	-22%
29-no airbag	0.00011	0.07569	0.00006	0.00314	0.00322	0.00322	0.07900
29-airbag	0.00000	0.05883	0.00006	0.00309	0.00313	0.00313	0.06200
29-difference	-99%	-22%	8.6%	-1.5%	-2.6%	-2.6%	-22%
79-no airbag	0.00007	0.07507	0.00005	0.00318	0.00314	0.00318	0.07800
79-airbag	0.00000	0.05733	0.00006	0.00310	0.00311	0.00311	0.06000
79-difference	-100%	-24%	8.6%	-2.6%	-0.8%	-2.2%	-23%

Table 13. Airbag benefit at five design locations with good belt fit for front row position.

	P(HIC15)	P(Nij)	P(chest)	P(Lfemur)	P(Rfemur)	P(femur)	Pjoint(AIS 3+)
57-no airbag	0.00013	0.08143	0.00005	0.00332	0.00333	0.00333	0.08500
57-airbag	0.00000	0.06868	0.00005	0.00408	0.00491	0.00491	0.07300
57-difference	-100%	-16%	0%	23.0%	47.3%	47.3%	-14%
60-no airbag	0.00002	0.07480	0.00005	0.00318	0.00317	0.00318	0.07800
60-airbag	0.00000	0.06495	0.00005	0.00350	0.00328	0.00350	0.06800
60-difference	-100%	-13%	2%	10.0%	3.5%	10.0%	-13%
76-no airbag	0.00002	0.07380	0.00005	0.00314	0.00315	0.00315	0.07700
76-airbag	0.00000	0.06504	0.00005	0.00343	0.00335	0.00343	0.06800
76-difference	-99%	-12%	2%	9.3%	6.1%	8.9%	-12%
81-no airbag	0.00005	0.07964	0.00005	0.00319	0.00345	0.00345	0.08300
81-airbag	0.00000	0.06710	0.00005	0.00513	0.00330	0.00513	0.07200
81-difference	-100%	-16%	2%	61.1%	-4.4%	48.9%	-13%
83-no airbag	0.00002	0.07519	0.00005	0.00313	0.00325	0.00325	0.07800
83-airbag	0.00000	0.06493	0.00005	0.00350	0.00338	0.00350	0.06800
83-difference	-100%	-14%	2%	12%	4.2%	7.8%	-13%

Table 14. Airbag benefit at five design locations with poor belt fit for front row position.

	P(HIC15)	P(Nij)	P(chest)	P(Lfemur)	P(Rfemur)	P(femur)	Pjoint(AIS 3+)
0-no airbag	0.04532	0.06913	0.00006	0.00305	0.00336	0.00336	0.11400
0-airbag	0.00000	0.07330	0.00006	0.00404	0.00431	0.00431	0.07700
0-difference	-100%	6%	-1.2%	32.4%	28.4%	28.4%	-32%
3-no airbag	0.17599	0.07742	0.00005	0.00323	0.00358	0.00358	0.24300
3-airbag	0.00000	0.07498	0.00005	0.00383	0.00451	0.00451	0.07900
3-difference	-100%	-3%	0.4%	18.6%	26.0%	26.0%	-67%
26-no airbag	0.20235	0.08969	0.00005	0.00325	0.00415	0.00415	0.27700
26-airbag	0.00000	0.07350	0.00005	0.00355	0.00381	0.00381	0.07700
26-difference	-100%	-18%	0.7%	9.3%	-8.2%	-8.2%	-72%
29-no airbag	0.01791	0.06736	0.00006	0.00308	0.00334	0.00334	0.08700
29-airbag	0.00000	0.07280	0.00006	0.00347	0.00428	0.00428	0.07700
29-difference	-100%	8%	-1.0%	12.9%	28.4%	28.4%	-11%
70-no airbag	0.14637	0.08606	0.00005	0.00347	0.00359	0.00359	0.22300
70-airbag	0.00000	0.07419	0.00005	0.00441	0.00397	0.00441	0.07800
70-difference	-100%	-14%	0.3%	27.1%	10.7%	23.0%	-65%

Compared to the lap belt anchorage locations, the D-ring locations are less sensitive to the injury measures, as long as the shoulder belt is on the shoulder without falling off. Although simulation results indicated that the optimal D-ring location is the most inboard location, such location may cause shoulder belt to touch occupant's neck, leading to discomfort. Therefore,

the optimal D-ring locations should be the ones resulting in the shoulder belt in the middle of the clavicle.

Side Impact Modeling and Optimization

For side impact modeling, parameters that were considered are shown in Figure 52. The wheelchair lateral and fore-aft position relative to vehicle interior, the presence of an outboard curtain airbag, the D-ring lateral location, and the buckle vertical and horizontal placement were varied in simulations of nearside and farside impacts. For the simulations to optimize location of the lap belt anchors, we added constraints to ensure that the range of locations evaluated are feasible to produce physically with the intended seat-belt donning system and the two commercial wheelchairs purchased for volunteer testing. In addition, we had hypothesized that if a wheelchair seating station was placed optimally relative to the vehicle interior, the standard curtain airbag might provide adequate nearside impact protection even if the D-ring was located inboard rather than outboard. In addition, we hoped that an inboard D-ring location might prevent the occupant seated in a wheelchair from falling out of the wheelchair during a farside impact. In addition to the factors listed previously, the general D-ring location was also modeled as inboard and outboard for farside and nearside impacts as shown in Figure 53. Injury measures included lateral rib displacement, abdomen force, upper neck loads, pubic symphysis force, lateral head excursion, head acceleration, and HIC.
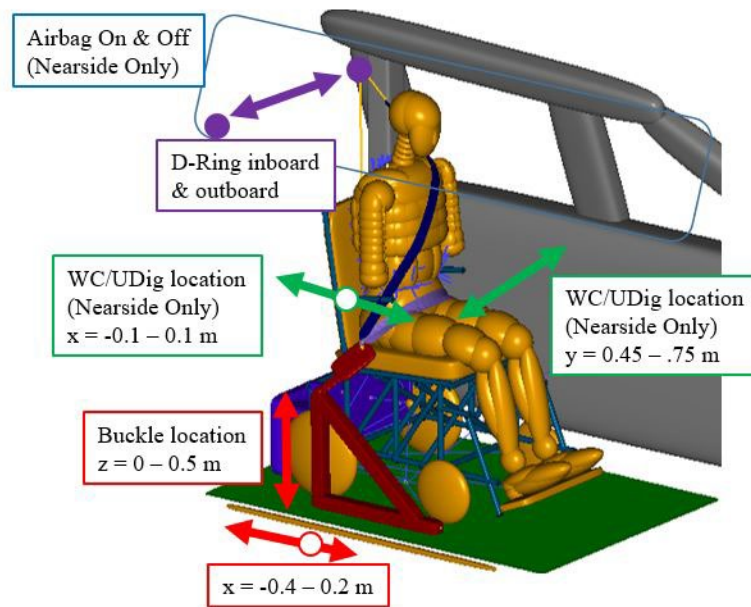

Figure 52. Parameters to consider in optimization of wheelchair seating station geometry for side impact.
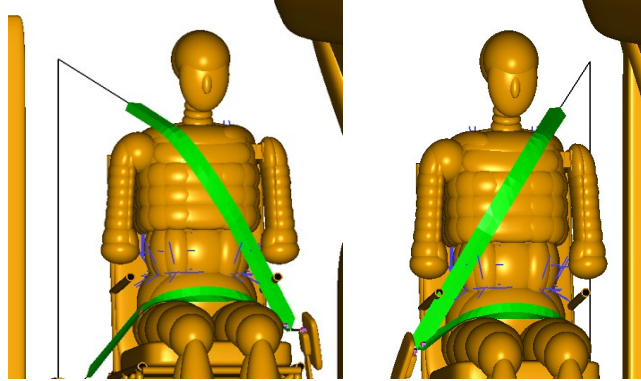
Figure 53. Inboard and outboard D-ring locations for nearside and farside impact conditions.

For the near-side conditions, we included a baseline curtain airbag design, working with collaborators at ZF to determine which of their available products would be suitable for installation in a vehicle matching the Chrysler Town and Country dimensions. They provided specifications for defining airbag characteristics in our MADYMO model.

Unlike the frontal impact conditions, where there are voluntary standards that specify performance criteria for testing, there are no established criteria or injury reference values for side impact testing of wheelchairs. Our goal in developing the side impact occupant protection system was to ensure that ATD measures are better than in a baseline test of a wheelchair secured by a 4-point strap tiedown system (test AW2011 in our validation series.)

Table 15 shows the correlations between input parameters and injury measures for nearside simulations performed without a curtain airbag. D-ring location (inboard vs. outboard) has the strongest impact on multiple injury measures, followed by the occupant-to-door distance. Other parameters are not as significant. Subsequent simulations added a curtain airbag. Overall, nearside impact simulations showed that moving the occupant further away from the door generally reduced most injury measures, with the exception of lateral head excursion and pubic symphysis force, which increased. When comparing nearside results with a curtain airbag while varying the D-ring location, the inboard location substantially increased the HIC, lateral head excursion, and abdomen force, although it lowered the neck force compared to the outboard D-ring location. Illustrations of the differences in nearside kinematics with and without a curtain airbag and with inboard and outboard D-ring locations are shown in Figure 54. In addition, Table 16 summarizes the injury metrics for these four nearside impact conditions. In general, the outboard D-ring with or without a curtain airbag resulted in acceptable injury risk values, and switching the D-ring inboard was detrimental for injury outcomes. Adding the curtain airbag is beneficial.

Table 15. Correlation table for nearside simulations without curtain airbag.

|	PevA	AbdF	RibD	PSF	NKUT	NKUS	HeadEX	HeadAcc	HIC36	Xpos	DRing	Side Y	BucklZ
AbdF	-0.24												
RibD	0.10	-0.06											
PSF	0.36	0.13	-0.38										
NKUT	0.16	-0.43	-0.19	0.12									
NKUS	0.23	-0.66	-0.41	0.27	0.45								
HdEX	-0.03	0.62	-0.15	0.12	-0.13	-0.59							
HdA	-0.03	0.53	0.50	-0.18	-0.16	-0.82	0.60						
HIC36	-0.04	0.46	0.49	-0.20	-0.19	-0.78	0.61	0.97					
Xpos	-0.13	-0.18	0.05	-0.05	0.19	-0.01	0.03	0.10	0.09				
DRing	-0.23	0.65	0.39	-0.28	-0.31	-0.91	0.67	0.89	0.88	0.00			
SideY	0.08	0.14	-0.59	0.46	0.16	0.13	0.55	-0.15	-0.10	-0.02	-0.05		
BklZ	-0.08	0.40	-0.20	0.03	-0.32	-0.15	0.07	-0.07	-0.09	0.00	0.02	0.00	
BklX	-0.53	0.00	-0.18	-0.14	0.19	0.02	-0.13	-0.07	-0.09	0.00	0.07	0.00	0.00
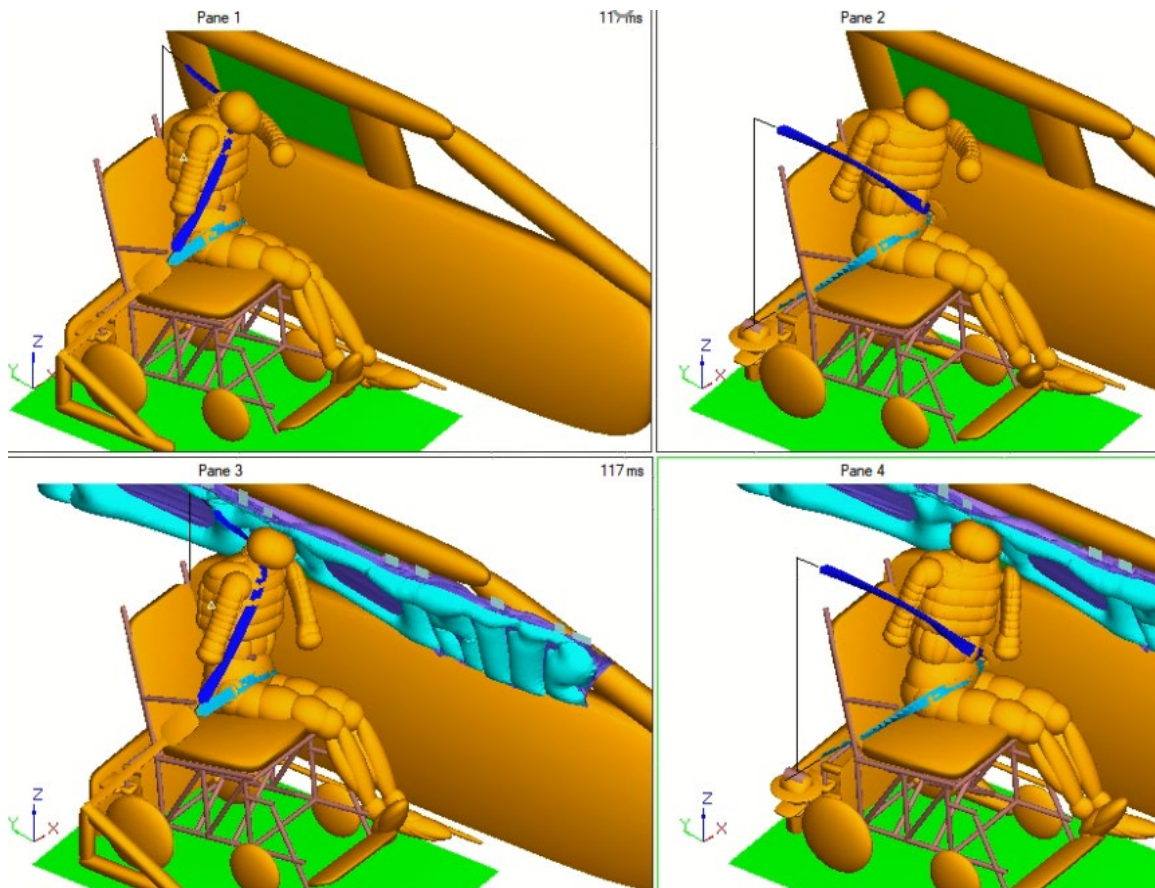
Figure 54. Illustration of nearside occupant kinematics with and without a curtain airbag and with inboard and outboard D-ring location.

Table 16. Injury metrics for nearside impact with and without curtain airbag and with inboard and outboard D-ring location.

	P(HIC36)	P(Chest)	P(abdomen)	P(pelvis)	Pjoint (AIS3+)
Outboard Dring, no airbag	0.000	0.077	0.013	0.047	0.132
Outboard Dring, CAB	0.000	0.080	0.014	0.028	0.119
Inboard Dring, no airbag	0.679	0.042	0.080	0.001	0.718
Inboard Dring, CAB	0.079	0.045	0.038	0.003	0.156
Difference: OB with vs. OB without airbag	-68%	4%	9%	-39%	-10%
Difference: inboard vs. outboard no airbag	178800%	-45%	513%	-98%	444%
Difference: inboard vs. outboard with airbag	20595%	-42%	190%	-93%	18%

Relationships between input and output variables for the farside simulations are shown in Table 17. Similar to the results of nearside impact simulations, D-ring location has the most significant effects on injury measures. However, in the majority of the simulations, the seatbelt alone cannot prevent the occupant from falling off of the wheelchair. In the few simulations in which the occupant stayed on the wheelchair, there was always excessive neck loading.

Table 17. Correlation table for farside simulations without curtain airbag.

	PevA	AbdF	RibD	PSF	NKUT	NKUS	HdEX	HdA	HIC36	DRing	BklZ
AbdF	-0.283										
RibD	-0.063	-0.05									
PSF	0.34	-0.306	0.339								
NKUT	0.144	0.138	-0.085	-0.087							
NKUS	0.08	-0.226	0.22	0.602	0.125						
HdEX	0.004	0.571	-0.407	-0.653	0.162	-0.769					
HdA	0.271	0.021	-0.05	0.065	0.959	0.249	0.057				
HIC36	0.049	0.506	-0.267	-0.058	0.648	0.069	0.358	0.623			
DRing	-0.192	0.732	-0.286	-0.695	0.133	-0.717	0.946	-0.012	0.345		
BklZ	-0.092	0.412	0.188	0.242	-0.065	0.34	-0.14	-0.03	0.128	-0.028	
BklX	-0.521	-0.05	0.139	-0.271	-0.119	0.117	-0.186	-0.208	-0.238	0.005	-0.005

Multiple belt geometries were further modeled in an attempt to find a belt anchorage geometry that could keep the occupant in the wheelchair without excessive neck loading. Figure 55 shows exemplar simulated kinematics from many unsuccessful examples.
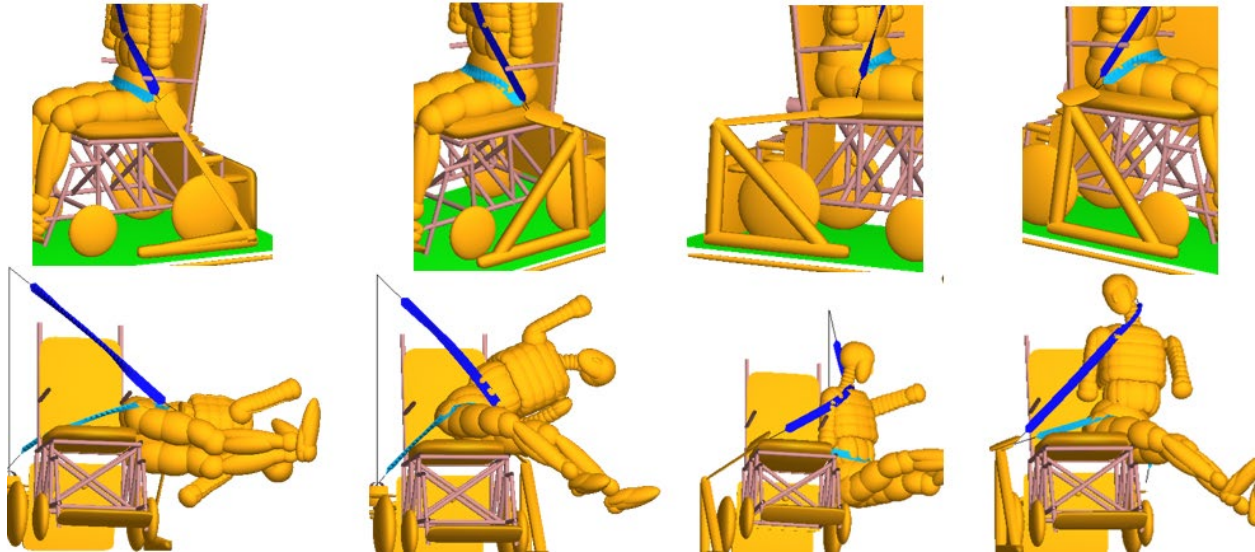
Figure 55. Illustration of seat belt inability to retain farside occupant within wheelchair.

The results shown in Figure 54 and Table 16 indicate that occupant protection decreases in nearside impact with an inboard D-ring compared to an outboard D-ring, despite the presence of a curtain airbag. In addition, as shown in Figure 55, the inboard D-ring location was not effective at keeping the occupant in the wheelchair during farside impact without excessive neck loading. As a result, we asked our collaborators at ZF to consider a design for a curtain airbag mounted to the center of the roof that might help control farside kinematics for an occupant in a wheelchair. They came up with two designs for a Center Airbag To Contain Humans (CATCH), which involves innovative tethering to restrain the occupant. Figure 56 contains illustrations of how the CATCH designs improve kinematics compared to a baseline condition. The second CATCH design contains a "window" that was intended to reduce neck loading. As seen by preliminary simulations with the two designs, they seem to achieve the design goal of keeping occupants in their wheelchairs. Prototype versions of these airbag designs were manufactured by ZF and evaluated in farside sled tests described under Dynamic Testing.

Belt Only
Time = 0.000000 : Frame 1

Roof Airbag 1
Time = 0.000000 : Frame 1

Roof Airbag 2
Time = 0.000000 : Frame 1

Belt Only
Time = 0.035000 : Frame 36

Roof Airbag 1
Time = 0.035000 : Frame 36

Roof Airbag 2
Time = 0.035000 : Frame 36

Belt Only
Time = 0.071000 : Frame 72

Roof Airbag 1
Time = 0.071000 : Frame 72

Roof Airbag 2
Time = 0.071000 : Frame 72

Belt Only
Time = 0.135000 : Frame 136

Roof Airbag 1
Time = 0.135000 : Frame 136

Roof Airbag 2
Time = 0.135000 : Frame 136

Figure 56. Comparison of kinematics in farside impact for belt only (left), CATCH 1 design (middle), and CATCH 2 design (right).

Models of manual and power chairs

The initial simulations performed to optimize restraint system geometry used a MADYMO model of the surrogate wheelchair base, a test fixture (without armrests) that can be used to evaluate the dynamic performance of different seating systems. To improve understanding of how different belt geometries would interact with wheelchairs of different sizes, we developed simplified MADYMO models of the two wheelchairs being used for volunteer testing. A Sense scanner was used to create a detailed 3-dimensional representation of the wheelchair geometry, shown in gray and blue for the manual wheelchair in Figure 57 and for the power wheelchair in Figure 58. The detailed scan was simplified to focus on capturing overall geometry and features while eliminating detailed components that would not be critical for modeling interactions with the occupants, tiedowns, and restraint systems. Rigid body MADYMO representations (shown in red) were then used to capture the key components for modeling.
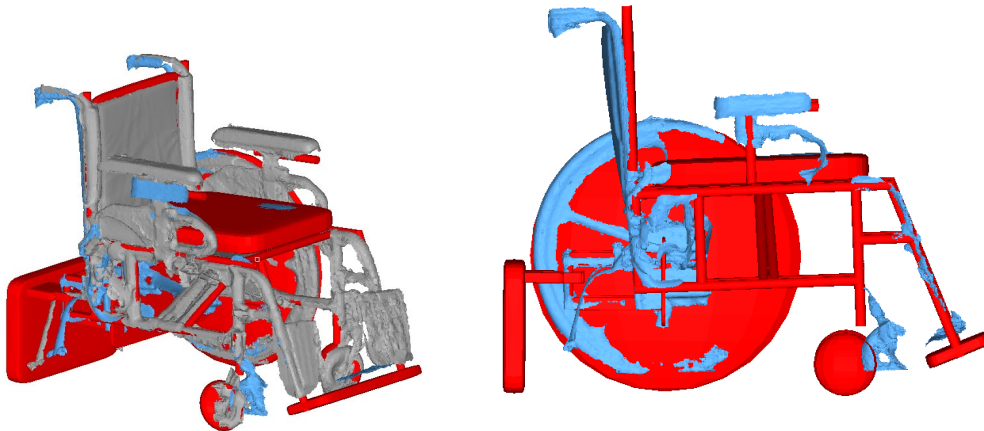

Figure 57. Detailed scan (gray), simplified scan (blue), and MADYMO model (red) of manual wheelchair.
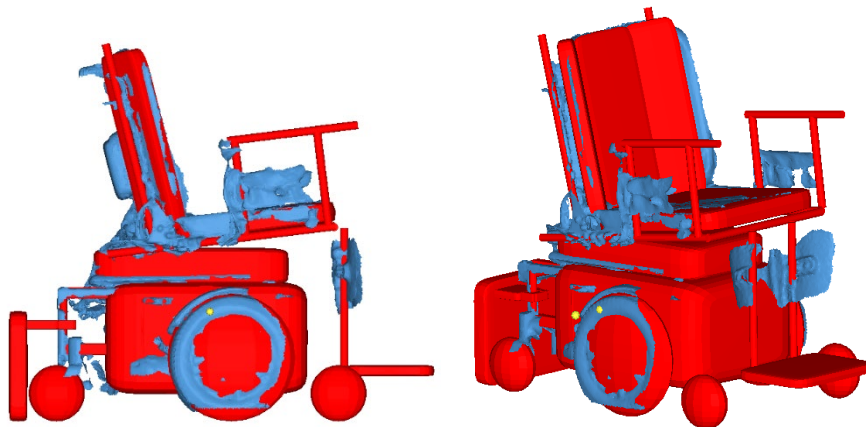

Figure 58. Detailed scan (gray), simplified scan (blue), and MADYMO model (red) of manual wheelchair.

Preliminary validations of the models were performed using tests from the UMTRI wheelchair database that had been run previously using these wheelchair models. The initial validations were performed using 4-point strap tiedowns to match the test conditions in the database. The models were then revised to incorporate UDIG attachments with geometry matching the prototype attachments made for volunteer testing. Each wheelchair showed similar kinematics with both types of securement.

Simulations of Feasible Geometry

The original research plan intended to use computational models to optimize placement of UDIG anchorages, belt geometry, and airbags through simulations of frontal, nearside, and farside impacts. Fixtures to be used for volunteer testing would then be constructed to incorporate the optimal geometry. Feedback on belt fit and usability from the volunteer testing would be used as input to perform further simulations to refine the restraint system characteristics that would then be used during sled testing.

The plan was revised as we attempted to create test fixtures matching the optimal belt geometry prescribed by the models for use in volunteer testing. Vehicle constraints and the dimensions of the two wheelchairs being used prevented us from implementing the optimal geometry; more details are provided in the Design and Prototype section. As an example, models showed that placing the lap belt anchors laterally as close as possible to the occupant's hip would provide the best restraint. However, because the manual wheelchair was 762 mm (30 in) wide, the lap belt anchors had to be placed slightly further apart than this dimension to allow space for the occupant to maneuver the manual wheelchair into the seating station.

As a result, the second phase of modeling was used to compare the kinematics and injury measures when two different belt geometries used for volunteer testing were implemented in the model. One geometry was closer to the initial modeling recommendations (B, light blue), while the second was a more "practical" geometry that approximated the conditions seen when an existing D-ring location on the C-pillar is used (D, dark green). In addition, simulations were performed using the surrogate wheelchair base, the manual wheelchair, and the power wheelchair models, to examine the differences in kinematics and injury measures associated with differences in wheelchair geometry. This optimization effort was also used to fine tune the characteristics of the SCaRAB airbag (vent size and fore-aft location) and seatbelt load limiter that would work the best with the two belt geometries. Table 18 shows the range of values considered for each parameter, while Figure 59 shows the minimum and maximum spacings of the front seat/airbag location. A total of 625 simulations were planned, and 591 were run to normal completion.

Table 18. Range of parameter values for second phase of frontal restraint optimization.

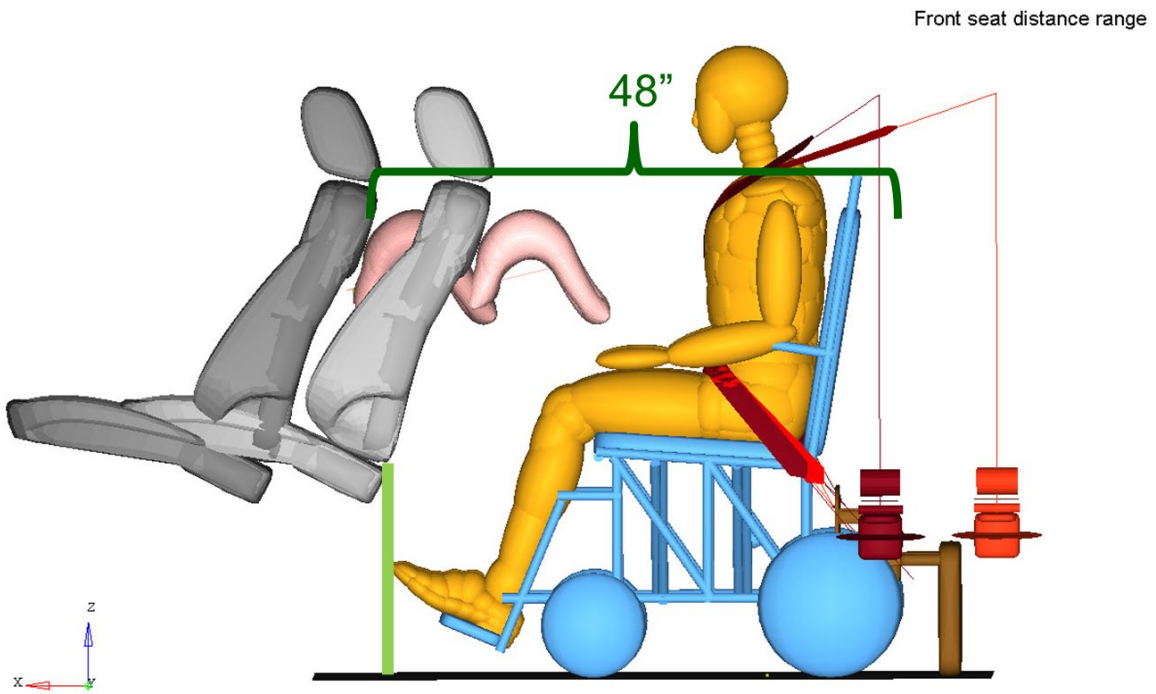| Parameter	Conditions
SCaRAB	0: No airbag
	1: Airbag
Front seat/ airbag location	0, 50, 100, 150, 200, 250 mm
Belt anchor locations	1: Braun light blue condition
	2: Braun dark green condition
Retractor torsion bar/ load limiter	8, 9, 10 mm diameter
Airbag vent size	2x20, 2x25, 2x30 mm
Wheelchair	1: Surrogate wheelchair base
	2: Manual wheelchair
	3: Power wheelchair

Figure 59. Illustration of minimum and maximum front seat/airbag location.

Figure 60 shows the differences between the two belt geometries for the simulations. The light red is geometry 1, while the dark red is geometry 2. Figure 61 shows an overlay of the initial starting positions for the surrogate wheelchair (blue), manual wheelchair (red), and the power wheelchair (green).
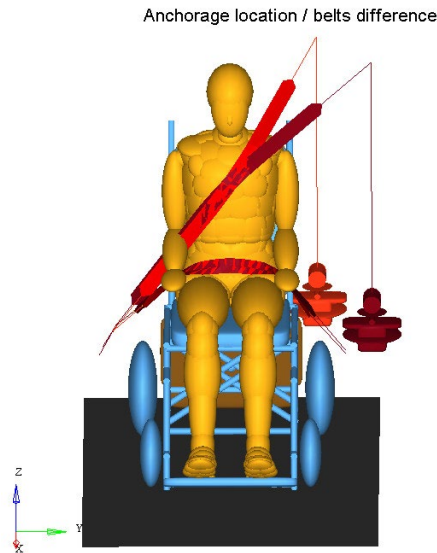

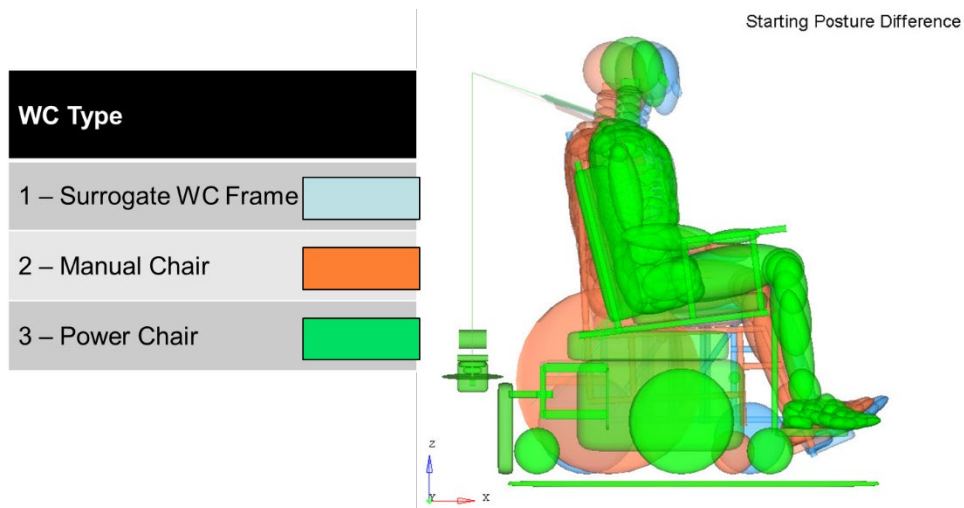Figure 60. Illustration of differences between two belt geometries.

Figure 61. Differences in starting occupant position because of differences in wheelchair geometry.

Figure 62 to Figure 65 show exemplar occupant kinematics with varied restraint and wheelchair conditions with and without SCaRAB at the time of peak excursion. Simulation results showing the associations between injury measures and input conditions are shown in Table 19. The chest injury measure dominates the combined injury risk, and is most closely associated with the different anchor locations and the seatbelt load limit. The injury measures do not vary much with the airbag characteristics. A reassuring result is that the injury measures do not vary

substantially with the type of wheelchair used, suggesting that restraint systems designed with the surrogate wheelchair should provide good designs for other midsize wheelchairs.
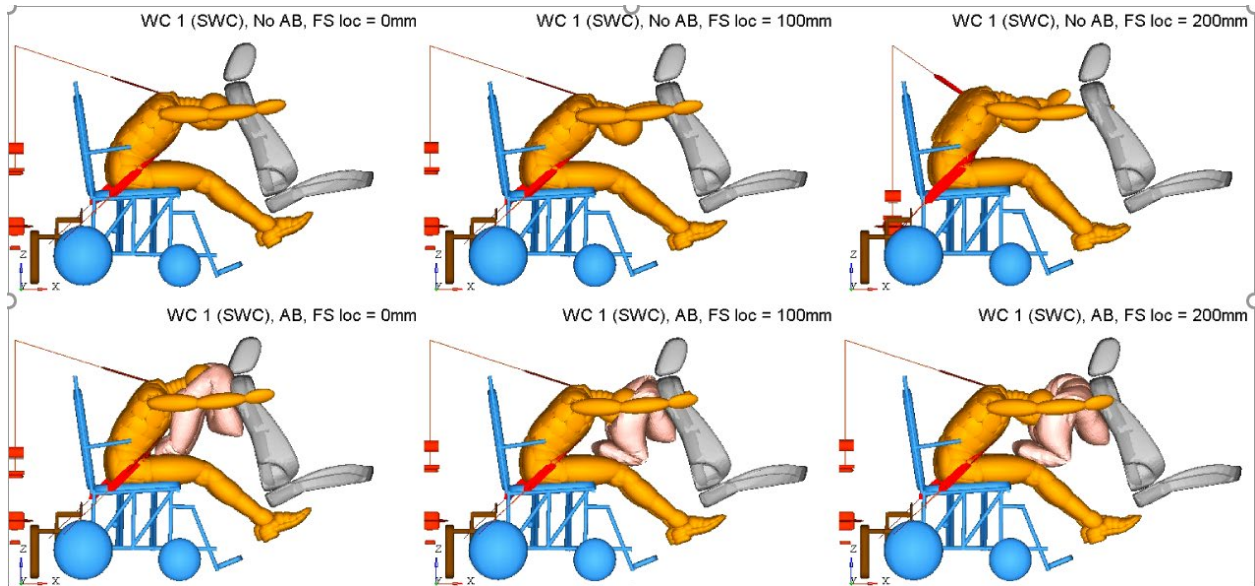

Figure 62. Simulated occupant kinematics with three different forward spacings, with and without SCaRAB, using the surrogate wheelchair base.
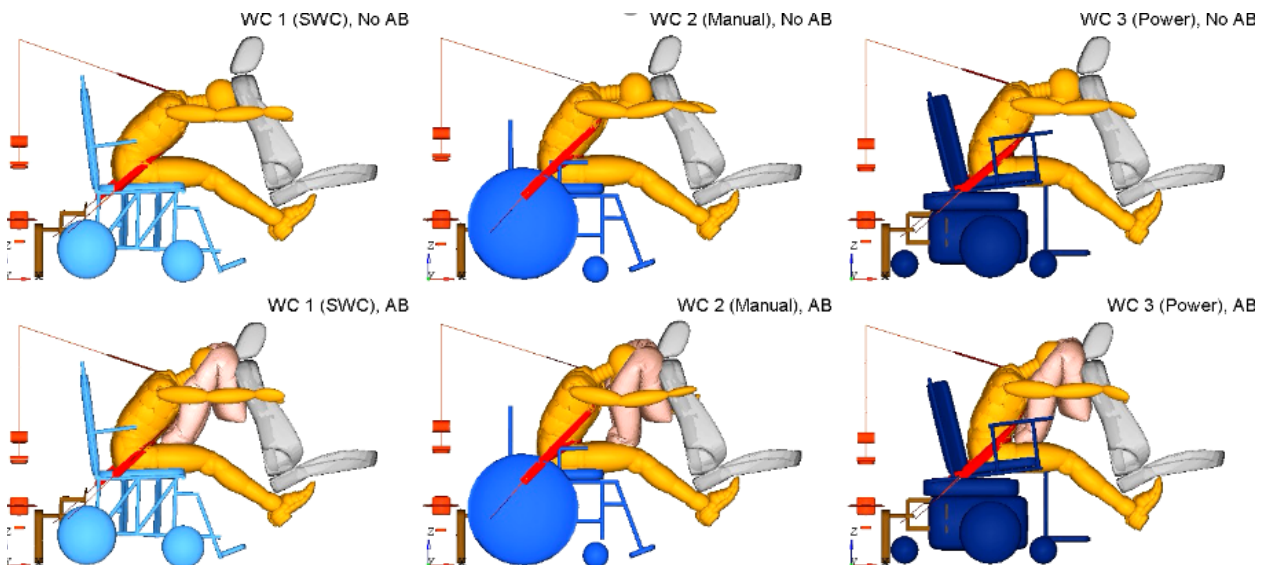

Figure 63. Simulated occupant kinematics with SWCB, manual chair, and power chair with and without an airbag.
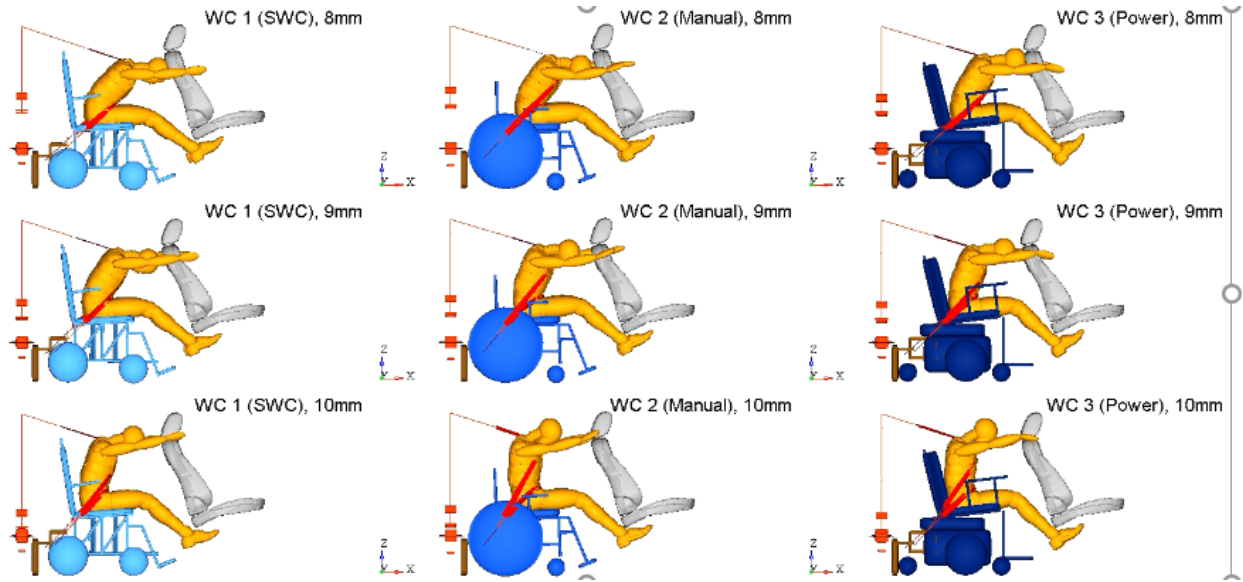
Figure 64. Simulated occupant kinematics with SWCB, manual chair, and power chair and three belt load limits (Top: low, Middle: mid, Bottom: high)
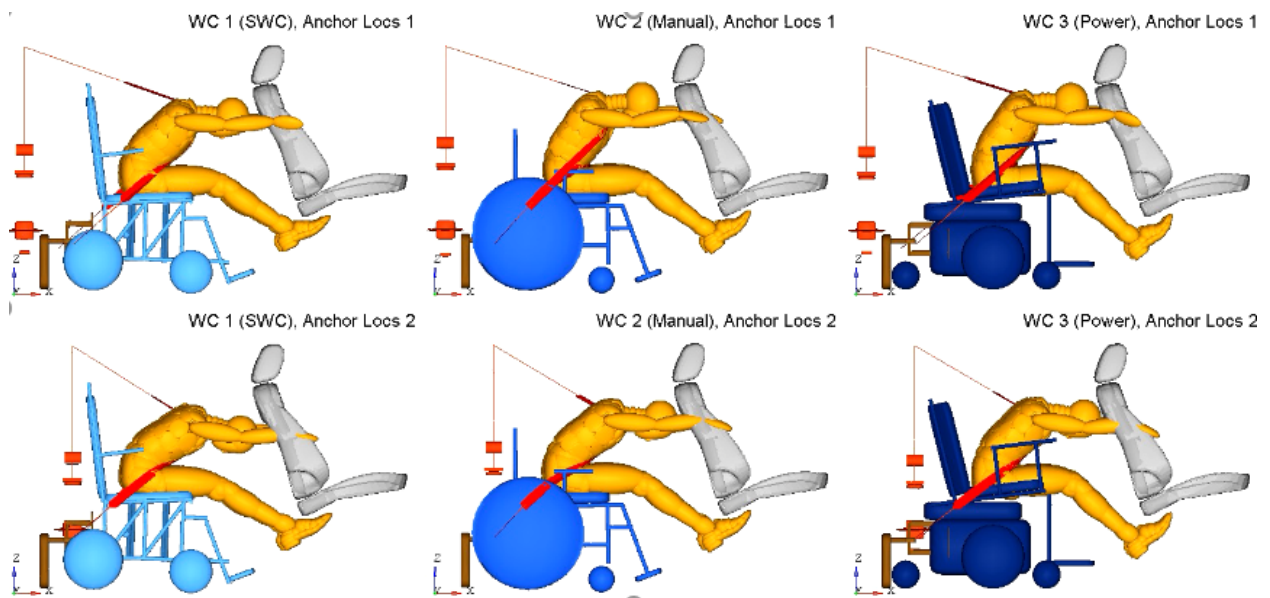

Figure 65. Simulated occupant kinematics with SWCB, manual chair, and power chair and varied belt anchor locations (Top: good belt fit, Bottom: suboptimal belt fit)

Table 19. Correlation table between design parameters and injury measures.

	WC	PJoint	PKTH	PChest	PNeck	PHead	WC	PAB_vntD	Load_limit	Anchor_locs	AB_loc
PJoint	-0.068										
PKTH	-0.017	0.135									
PChest	-0.119	0.988	0.100								
PNeck	0.313	0.266	0.230	0.116							
PHead	0.083	0.069	0.188	-0.036	0.607						
WC	1.000	-0.068	-0.017	-0.119	0.313	0.083					
PAB_vntD	0.046	0.014	-0.005	-0.006	0.137	0.062	-0.003				
Load_limit	-0.371	0.421	-0.146	0.496	-0.379	-0.260	0.005	-0.005			
Anchor_locs	0.245	0.662	0.172	0.602	0.486	0.359	-0.020	0.015	-0.008		
AB_loc	-0.436	-0.044	0.295	-0.055	0.046	0.162	-0.026	-0.010	-0.006	-0.074	
AB	-0.111	-0.079	-0.086	-0.015	-0.433	-0.282	0.009	-0.002	0.000	-0.039	-0.045

These simulations confirm previous results demonstrating that the presence of a SCaRAB reduces injury risk particularly to the head and neck, by reducing the risk of contact with forward structures. Because results did not vary widely with airbag vent size, but the lowest head and neck measures occurred with the smaller vent hole sizes, a SCaRAB design with 20 mm diameter vent holes was selected for use in dynamic testing.

The relationship between belt geometry, torsion bar stiffness, and fore-aft spacing is more complicated and different combinations of acceptable conditions are summarized in Table 20. In condition I, using the better belt geometry (1), the lowest torsion bar stiffness (and lowest load limit) and a SCaRAB prevents injurious contact at even the closest forward seat position. If the SCaRAB isn't present (condition II), the front seat needs to be placed at least 150 mm further forward to prevent head contact. This much space is also required for condition III, where a SCaRAB is present but the less optimal geometry (2) is used. If no SCaRAB is used with geometry 2, the front seat needs to be at least 200 mm further forward. Alternatives to preventing head contact with the suboptimal belt geometry are shown in conditions V and VI. These conditions require less forward space, but use of a stiffer torsion bar increases chest injury probability.

Table 20. Different combinations of simulation conditions to prevent head contact.

Model	Anchorage	SCaRAB	Torsion bar stiffness (mm)	0 mm	50 mm	100 mm	150 mm	200 mm	250 mm
I	1	Yes	8	Yes	Yes	Yes	Yes	Yes	Yes
II	1	No	8	No	No	No	Yes	Yes	Yes
III	2	Yes	8	No	No	No	Yes	Yes	Yes
IV	2	No	8	No	No	No	No	Yes	Yes
V	2	Yes	9	No	No	Yes	Yes	Yes	Yes
VI	2	Yes	10	Yes	Yes	Yes	Yes	Yes	Yes

These simulations led us to choose the restraint characteristics for sled testing that will help illustrate the differences expected from using the two belt geometries with and without airbags. Conditions used a 9 mm torsion bar and a forward seat location of 100 mm.

Design and Prototype

UDIG attachments for manual wheelchair

The manual wheelchair selected for volunteer testing is a Ki Mobility Catalyst 5, shown in Figure 66. The wheelchair has two anti-tip legs at the rear of the chair that can be adjusted to provide more or less rearward rotation. The wheelchair has multiple levels of adjustability to better accommodate different sizes of people. In its most compact configuration shown in Figure 66, the large propelling wheel of the chair would interfere with achieving good lap belt fit. However, we were able adjust the seating surface so it is higher, reducing the potential for interference.

Figure 66. Manual wheelchair purchased for volunteer testing.

When designing the location of the attachments, we needed to balance creating hardware that met the UDIG specifications while avoiding interference with the rear wheels and rear anti-tip legs on the wheelchair. Modeling demonstrated that locating the attachments closer to the wheelchair/occupant center of gravity provided the best dynamic performance, so this was a goal we tried to achieve. The manual wheelchair has a structural component on each side with multiple holes that allows vertical adjustment of the seat, as shown in Figure 67. These structures also have the two rear 4-point strap securement brackets attached to them, indicating that they are strong enough to sustain crash loads. We designed the UDIG attachments so they can be attached at these locations, while providing clearance around the 4-point securement brackets so that they are still accessible.

Figure 67. Location on manual wheelchair (pictured upside down) to attach UDIG-compliant attachments.

A wooden mockup of the prototype hardware for the manual wheelchair is shown in Figure 68. The attachments meet the UDIG specifications and would not interfere with attachment using a 4-point strap tiedown. The bottom of the attachments is about 12 cm above the floor.

Figure 68. Mockup of UDIG attachments for manual wheelchair.

Figure 69 shows the UDIG attachments for the manual wheelchair. The attachments are constructed of aluminum tubing components, connected via aluminum plates to the wheelchair structure near the crash-tested rear tiedown hooks. Total mass of the attachments is 9 lb. Per the UDIG specifications contained in WC19, the attachments do not extend past the rearmost point of the rear wheels or increase the wheelchair footprint. The attachments also do not interfere with use of the anti-tipper wheels that prevent rearward tipping.

Figure 69. UDIG attachments for manual wheelchair.

UDIG attachments for power wheelchair

The power wheelchair purchased for volunteer testing is the Quantum Rehab Q6 Edge 2.0 with Synergy Seating, shown in Figure 70. Because the default armrests that came with the chair would not work with the belt donning system, we replaced them with a cantilever style armrest that was also used in some of the sled validation tests.

Figure 70. Power wheelchair purchased for volunteer testing.

The power wheelchair has an adjustable seat that can rotate rearward to provide a reclined posture for the occupant if needed. A challenge for designing the UDIG attachments for the power wheelchair is that while there is structure suitable for attaching the UDIG hardware, rotation of the seat has potential to cause interference. As shown in Figure 68, the wheelchair has components below the seat that have two threaded holes on each side, which we used as an upper location for connecting the attachments. Because these threaded holes are located near the rear 4-point strap securement hardware, this area of the wheelchair should be strong

enough to sustain load in a crash without failure. The wooden mockup prototype of the wheelchair attachments for the power wheelchair is shown in Figure 72. The structure was designed to avoid interference with the rear wheels and allow the 4-point securement brackets to remain accessible. In addition to the upper bolts, the attachment is also connected to a rigid point on the wheelchair using a threaded rod near the bottom for added strength and stability.

Figure 71. Connecting UDIG attachments near tiedown securement point on power wheelchair.
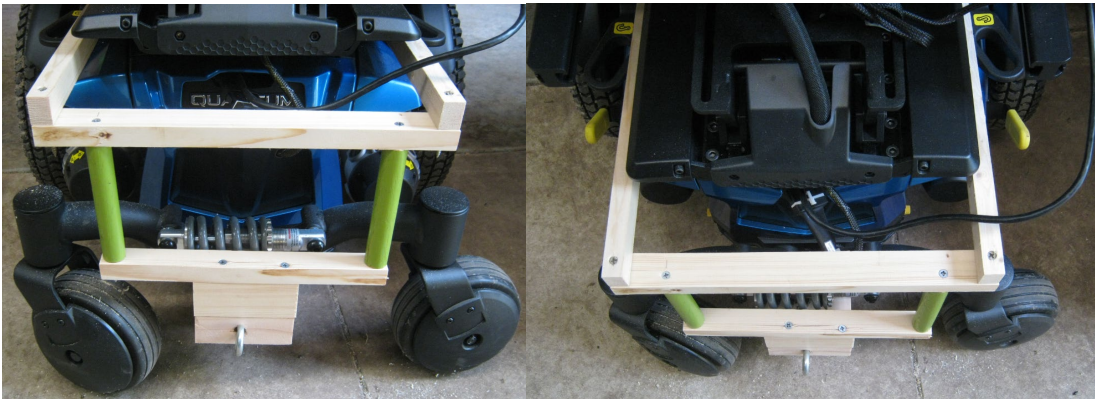
Figure 72. Mockup of UDIG-compatible attachments for power wheelchair.

The actual attachments for the power wheelchair are shown in Figure 73. These attachments were also mainly constructed of aluminum tubing components and bolted to the wheelchair near the crash-tested rear tiedown securement points. The attachments were also secured to a third point between the rear caster wheels for increased stability because of a conveniently located structure on the wheelchair. The attachments do not extend past the rear casters when they are aligned for forward travel.
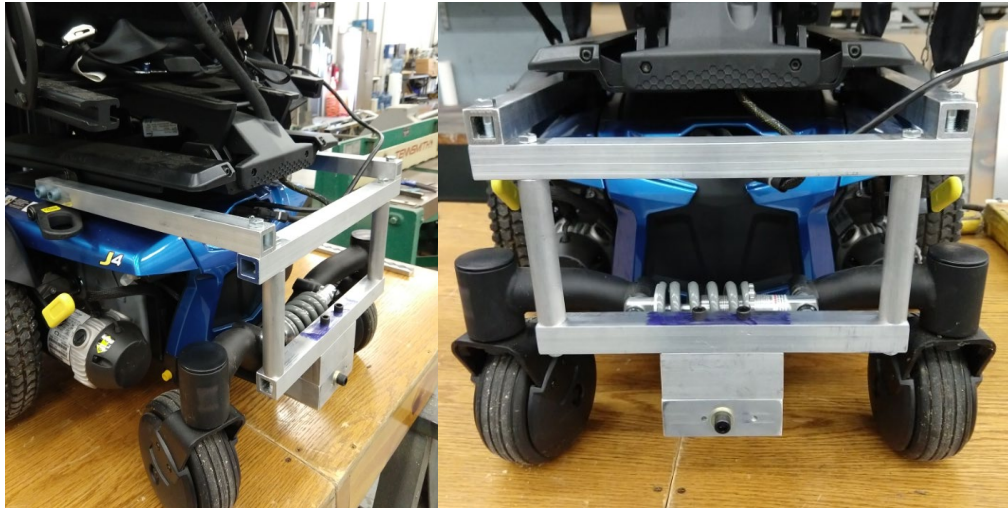
Figure 73. UDIG attachments for power wheelchair.

UDIG vehicle anchorages

The UDIG docking station used on the sled during the validation testing was designed to demonstrate proof of concept in an earlier research program. The main design criteria were to meet the UDIG specifications and make it robust enough to withstand repeated dynamic tests. During our side impact validation tests, review of the video indicated that the UDIG anchorage hardware exhibited no visible deflections during the side impact testing. Post-testing review of components showed residual deformation in the SWCB, as well as the UDIG attachment structures built for it, but no deformation in the UDIG anchorages.

For UDIG docking station to be installed in the vehicle test fixture for use with volunteers, the design criteria are different. While the main criteria of meeting the UDIG specifications is the same, we are also tried to make the UDIG anchorages as compact and as lightweight as possible. This should make them either 1) easier for the user to maneuver around or 2) require less force to deploy if stowed. Permanent deformation of the anchorages would be allowable (as anchorages would be replaced after a crash) if simulations/testing with the hardware could demonstrate that it still allowed the secured wheelchair to meet intended dynamic performance criteria.

The UDIG anchorages need to have a mechanism to deploy the anchoring hooks outward once the wheelchair attachments are in position. Initial designs considered commercially available actuators, as shown in Figure 74. An advantage of using these actuators is that there is a built-in contact feedback that could be used to indicate to the user that the system is engaged. However, the smallest available actuators that provided the required amount of stroke were large and did not lend themselves to a compact installation.
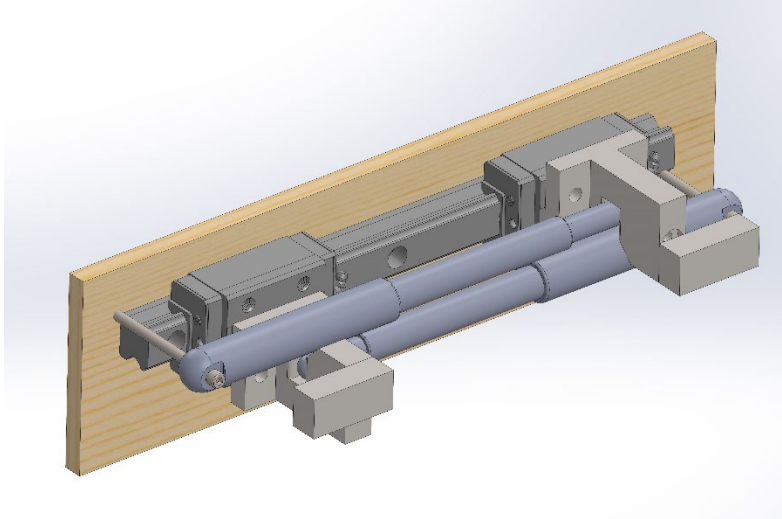
Figure 74. Initial design of UDIG anchorages with commercial actuators.

The mechanism used on the sled fixture to deploy the anchoring hooks used a small motor to drive a screw mechanism that moved them outward. This design is more compact, but would require additional sensors to be installed to notify the passenger when the hooks are deployed.
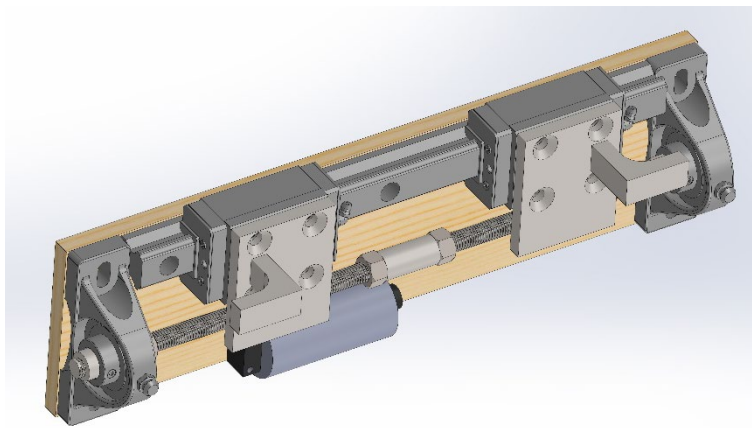

Figure 75. UDIG anchorage design incorporating screw mechanism.

Further consideration of using the design shown in Figure 75 led us to change it to include two drive mechanisms shown in Figure 76, so the hooks can be moved independently. The single-drive system used on the sled needs to have the wheelchair position centered between the hooks so they engage evenly. While this is fairly easy to do during lab setup, it would be challenging for occupants to do when maneuvering their own wheelchairs. Allowing each engagement hook to move independently would likely be an easier-to-use option.
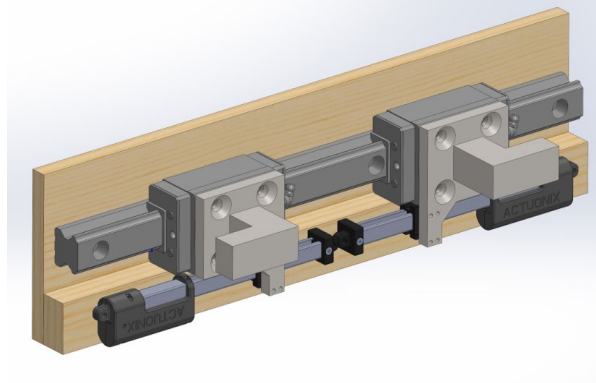
Figure 76. Revised design with two smaller actuators to allow independent movement of anchors for non-centered conditions.

An initial mockup of the prototype anchoring system is shown in Figure 77, while Figure 78 shows overhead views of the hooks before and after engaging with the attachments on the manual wheelchair. Implementation of the design led us to realize that the mechanisms should be separated from the occupant by a surface to avoid unintended interactions and possible damage. Adding a surface and providing a slot along which the hooks can travel when powered by the actuators seemed to be a feasible way of controlling the anchorages. Drawings shown in Figure 79 indicate what this might look like.

Figure 77. Mockup of UDIG-compatible vehicle anchorages.
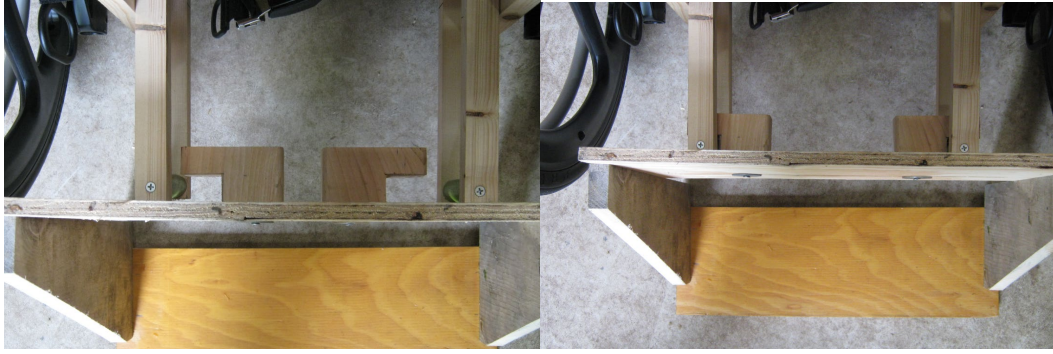
Figure 78. Mockup of UDIG anchorages before (left) and after (right) engaging UDIG attachments on manual wheelchair.
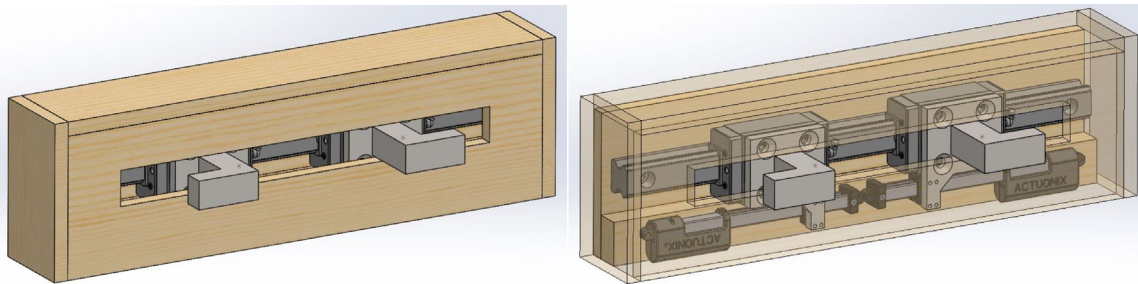
Figure 79. Revised design of UDIG anchorages to enclose the mechanisms.

The vehicle UDIG anchorages are shown in Figure 80. The anchorages consist of two hooks that are initially positioned near the center of the fixture (left) and then powered by two separate actuators to move outward (right) until they engage with the UDIG attachments on the wheelchair. The actuators stop automatically when they engage with the attachments. The wheelchair user backs into the station until their attachments contact the front "bumper" (structure with top edge marked in green) that prevents them from damaging the actuators. Future iterations of the anchorages would likely cover the upper part of the attachments as well, leaving just an open slot through which the anchorage hooks could travel. For the preliminary evaluation, we left it open to facilitate potential troubleshooting. The actuators are powered by a dedicated wheelchair battery (similar to a vehicle battery) stowed beneath the vehicle for testing. While we mounted the anchorages on an L-shape structure that can be bolted to the vehicle floor, it would also be possible to mount the UDIG anchorages to a rear vertical wall. Figure 81 shows examples of how the manual and power wheelchairs engage with the anchorages.
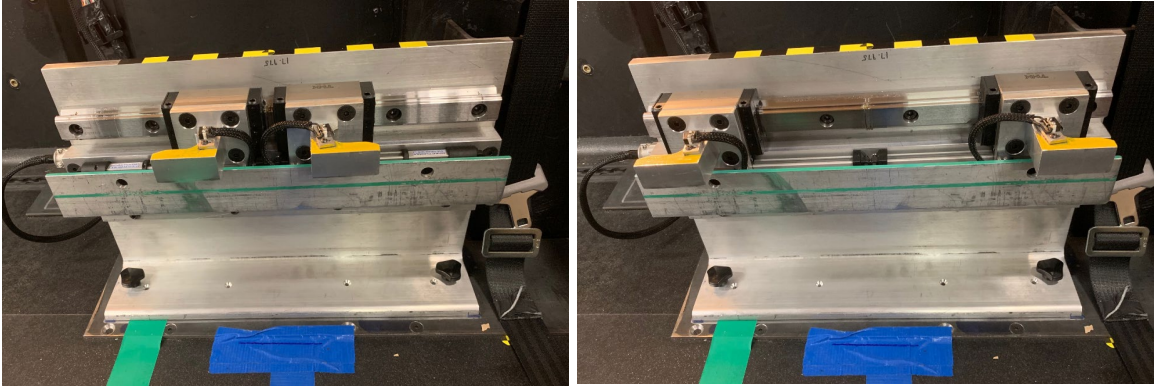
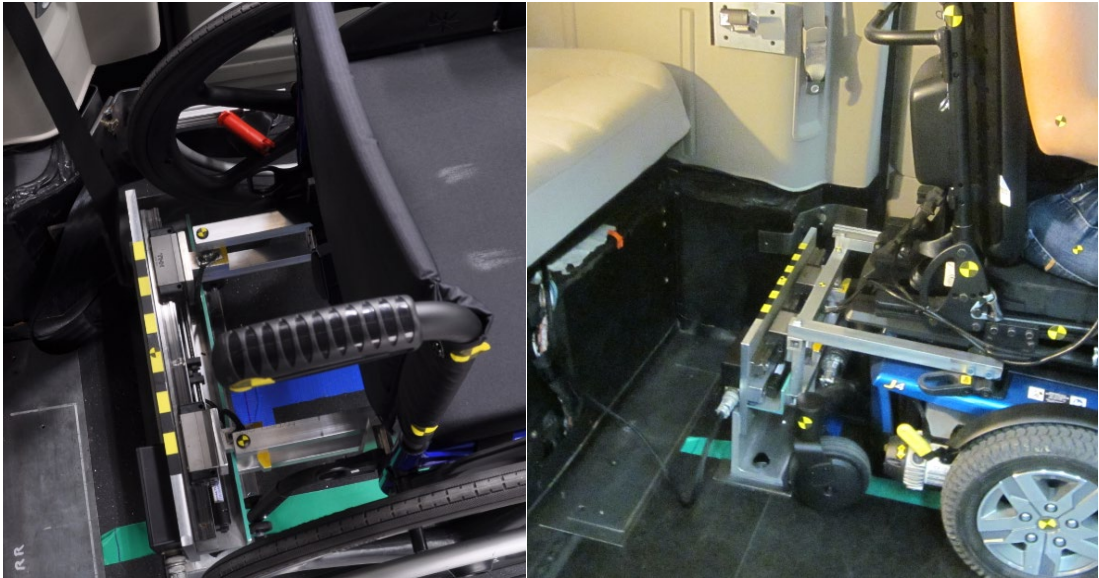Figure 80. UDIG vehicle anchorages in initial (left) and extended (right) conditions.

Figure 81. Manual (left) and power (right) wheelchairs engaged with the vehicle UDIG anchorages.

Automated Occupant Restraint System

Belt Geometry

The side impact sled tests run to validate the models showed that the ATD had substantial lateral excursions in the side impact configuration. Because of this, we wanted to evaluate the feasibility using a non-traditional belt arrangement, where the D-ring is mounted inboard, with the hardware attached to the vehicle roof as shown in Figure 82. We hypothesized that side impact protection in near-side crashes could primarily rely on airbags, with the seatbelt providing the main restraint during far-side crashes. This arrangement might also improve maneuverability, as the donning system hardware could be located against the interior structure rather than the center of the vehicle. (Subsequent modeling efforts performed after the volunteer testing setup began demonstrated that the inboard belt location was insufficient

to provide adequate restraint in farside impact, and increased injury risk for nearside crashes; this led us to pursue the CATCH concept.)
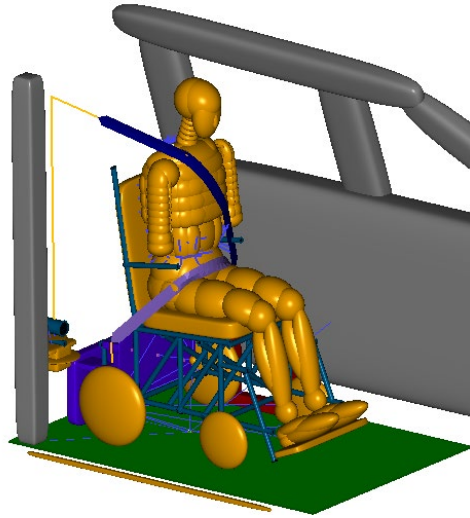

Figure 82. Wheelchair seating station with D-ring mounted inboard.

To identify target locations for belt geometry in our test fixtures, the initial modeling results to identify optimal location of lap belt anchors were overlaid with photos of the two wheelchairs being used in the study as shown in Figure 83. The blue corresponds to optimal location for the manual wheelchair relative to the seat H-point, while the purple corresponds to the location for the power wheelchair. The small area of overlap where occupants in both chairs could achieve optimal belt location defined by the models was the initial target for locating lap belt anchors in the vehicle fixtures.

Figure 83. Overlap of optimal lap belt anchor zones for sample power and manual wheelchairs.

Automated Donning Arm

A prototype of the automated belt donning system had been developed as part of a previous research project (Figure 24) for a driver wheelchair station. The buckle end of the seatbelt was attached to the end of a rotating arm. The arm would initially be positioned upright, holding the seatbelt out of the way as the driver drove forward into the seating station. When the driver deployed the donning arm, it would rotate down to the floor, placing the lap and shoulder belts across the driver's body. The arm would be secured via a pin to a reinforced slot in the floor. The system was demonstrated to be crashworthy using WC19 crash protocols. A requirement is that the wheelchair must have armrests that allow a space between the seatback and armrest.

For the current project, we iterated on this design (Figure 84, left) so the buckle end of the seatbelt is now attached to an extended structure on the rotating arm (Figure 84, right), such that it places the belt anchor closer to the occupant's hip. This allows an acceptable geometry with a shorter arm length and improves protection because less webbing is used to secure the occupant.
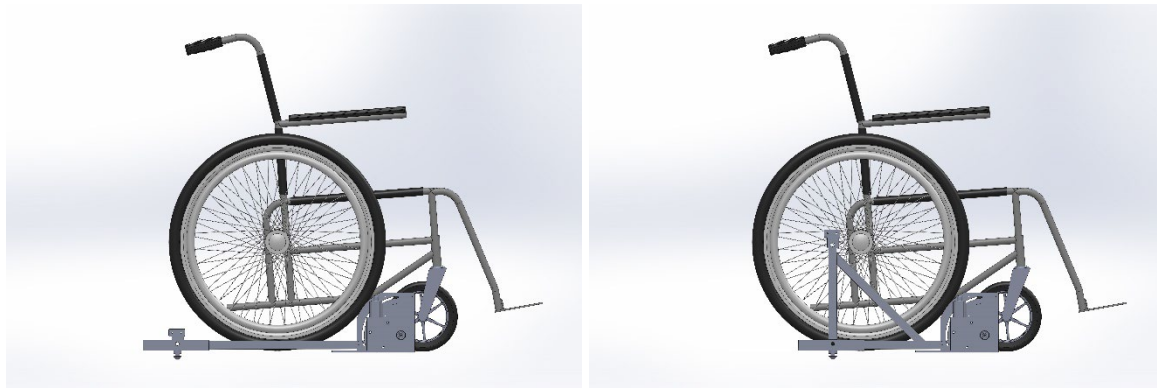
Figure 84. Original (left) and revised (right) designs of the seatbelt-donning system.

For the current study, we wanted to evaluate how different donning arm configurations affected usability. Thus, the donning arm assemblies constructed for volunteer testing prioritized adjustability rather than crashworthiness. The geometry can be adjusted three ways, as illustrated in Figure 85. Geometry of donning arm can be adjusted by shifting the vertical mount fore-and-aft on the arm, by shifting the belt attachment up-and-down on the vertical component, and by relocating the anchorage plate where the hinge and controlling actuator are connected.

Figure 85. Adjustability of donning arm geometry.

Compared to the original version of the donning arm, most of our volunteer configurations involve backing into the UDIG docking station instead of driving forward into the seating station. For the Braun van fixture (Figure 86, left), we used a donning arm that was fairly similar in concept to the original with one degree of freedom rotation about the lateral vehicle axis. However, for the body-in-white fixture (Figure 86, right), we added a second degree of freedom (about the vehicle longitudinal axis) to determine if moving the seatbelt further out of the way improved usability. Because of time constraints, the BIW arm was operated manually by the experimenter, but an actual implementation would involve automation.

As described in more detail in the following section, locating the donning arm near the side structure of the vehicle, on the opposite side of the entry, actually caused a problem for maneuverability because the seatbelt would block the occupant's path to the seating station. A possible solution was evaluated in one test condition in the body-in-white. For the light purple condition, where the D-ring was located close to the entrance, the donning arm was initially in the down position, with the belts positioned behind the seating station, because an upright position would block the seating station with the shoulder belt. After the participant docked the wheelchair, the experimenter would rotate the arm and belt above the person's head to a forward location, then rotate it back down so the arm placed the belt in position in front of the occupant.

Figure 86. Belt-donning device in Braun van (left) and body-in-white (right).

Implementing Wheelchair Seating Stations in Test Fixtures

A finding from the frontal modeling effort was that the second-row left position may be preferable to the right-front position for two reasons. The first is that there may be sufficient space to locate the wheelchair seating station relative to the left-front vehicle seat such that an airbag may not be required to protect the occupant in frontal impacts. Simulations with the wheelchair located in the right-front position indicate that with the space currently available in a minivan-type configuration, an airbag would be required to provide adequate protection in a frontal impact, because the geometry does not allow sufficient space to position the wheelchair as far rearward relative to the dashboard to avoid head contact, particularly if the occupant may have suboptimal belt fit because they differ in size from a mid-size male occupant. The second reason is that the second-row-left position allows placement of the wheelchair seating station more favorably relative to the C-pillar (for mounting belt and UDIG anchorages) than the front-right does relative to the B-pillar. Because future AVs may not have these size restrictions, the volunteer testing matrix still included the right-front seating position, to see if it offered advantages in terms of accessing the vehicle through a side door.

Initial simulations to locate the wheelchair seating station were performed with an interior scan of the Braun minivan vehicle rather than the body-in-white, because it includes more realistic interior surfaces. As shown in Figure 87, when locating the second-row left seating position, we tried to locate the UDIG anchoring hardware under the third-row seating, with the idea that the third row could be used by an occupant if no occupant seated in a wheelchair was present. The lateral position of the wheelchair relative to the left interior structure is limited by the location of the rear wheel well. Figure 88 shows photos of the interior of the Braun van, with the mockup anchors resting on the floor and the manual wheelchair in position. There seems to be adequate room to maneuver, and room for the occupant's knees and feet behind the left-front seat.
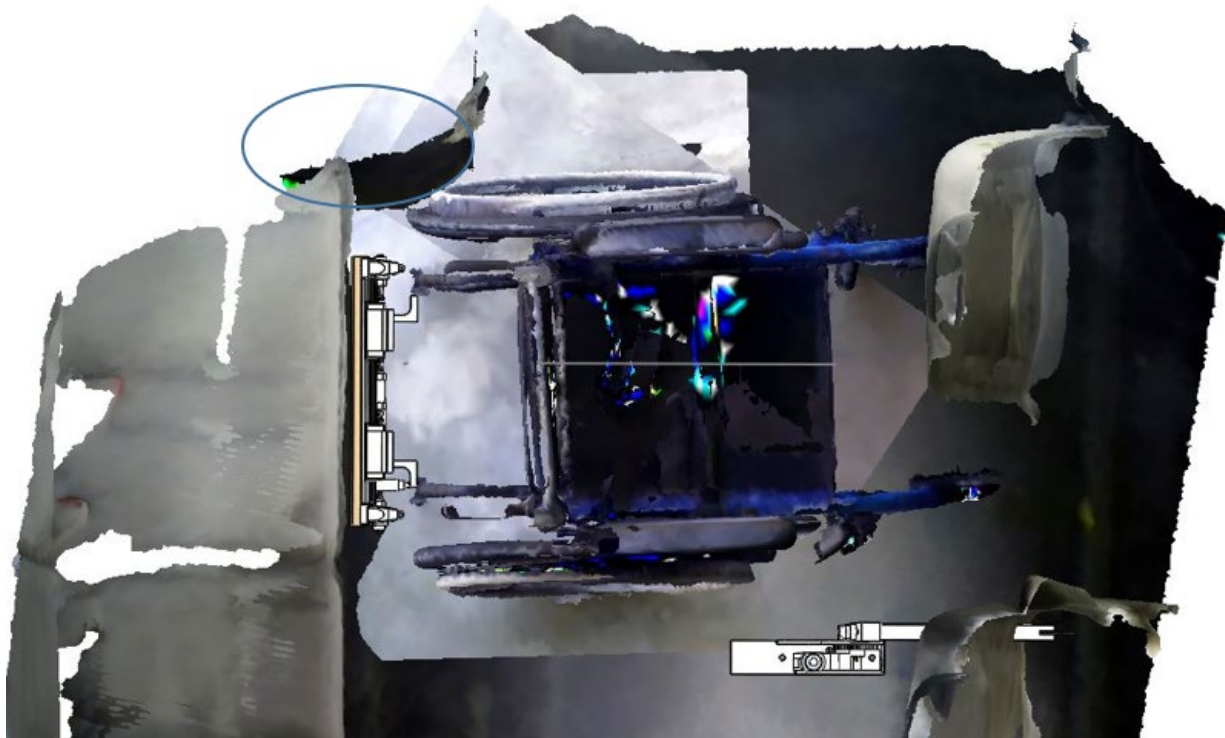
Figure 87. Overlay of manual wheelchair placed in Braun van, with vehicle docking hardware located beneath the third row of seating. Lateral position of the wheelchair is limited by the location of the circled rear wheel well.

Figure 88. Manual wheelchair and UDIG anchorages in Braun vehicle; lateral location limited by wheel well.

The first round of computational modeling provided targets for optimal location of belt geometry relative to the location of UDIG anchorages placed in the vehicle. As we worked to implement anchorage locations, we quickly learned that it would not be possible to achieve the optimal locations for all anchors because of constraints from existing vehicle structures and the need to provide sufficient space and maneuvering room for the two different sizes of wheelchairs. However, the process of implementing the wheelchair seating stations in the two

fixtures proved to be extremely informative regarding the challenges of balancing safety and usability when designing a wheelchair seating station.

For the volunteer testing, we wanted to set up two different UDIG anchorage locations in each fixture, each with two sets of belt geometry. Because the Braun vehicle includes finished interior components (which we wanted to minimize damaging) that limit the range of options more than the BIW, we first set up the four Braun conditions, and then set up the BIW conditions.

The simulations showed that placing lap belt anchors as close as possible to the occupant in the lateral direction provided the best restraint. The dimension used for the models with the surrogate wheelchair base was 508 mm (20 in). However, the requirement to have 762 mm (30 in) of clear lateral space to accommodate the width of most wheelchairs prevented us from implementing an optimal lateral position. Instead, we placed lap belt anchors just outside the 762 mm (30-in) window for all conditions.

Figure 89 shows how the two locations for the UDIG in the Braun vehicle were selected. The process of lowering the floor to allow sufficient height for occupants seated in wheelchairs exposes the interior surface of the wheel wells. For the rearward (blue) conditions, we placed the UDIG anchorages as far rearward as space allowed, with the centerline located ~380 mm (15 in) inboard relative to the most prominent surface of the wheel well. This would allow the minimum 762 mm (30 in) width for the seating station required by ADA, which was needed to accommodate the width of our manual wheelchair. For the outboard (green) condition, the UDIG anchorage was placed directly in front of the wheel well, as close as possible to the left interior wall while still allowing room for the 762 mm (30 in) wide minimum seating space.
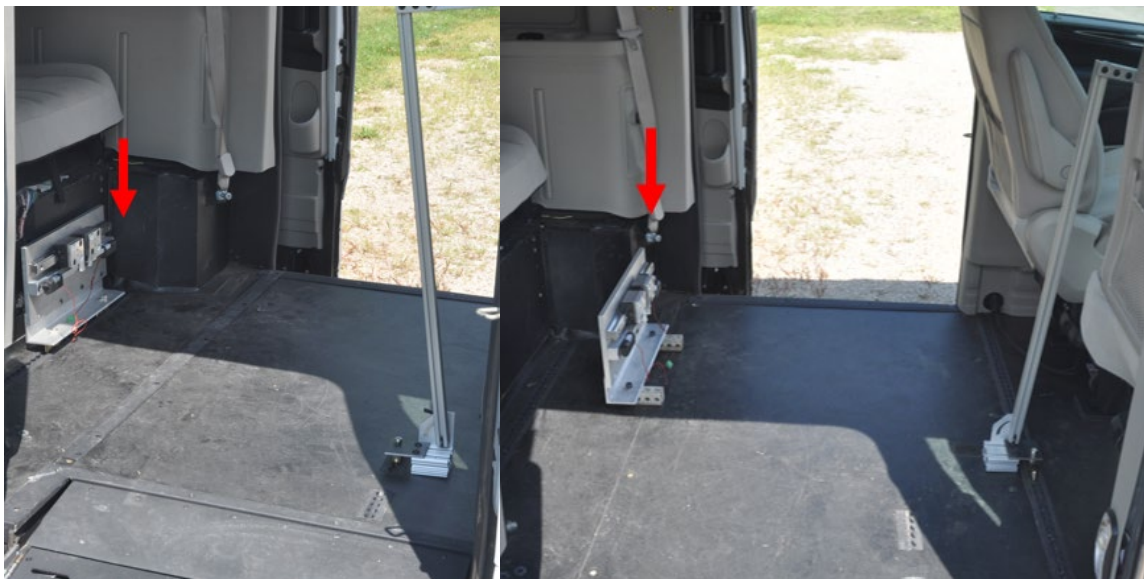
Figure 89. Two locations of the UDIG anchorages in the Braun vehicle: inboard of the left rear wheel well (left) and forward of the left rear wheel well (right).

The presence of the wheel well did not allow us to locate the outboard seatbelt anchor in the optimal location suggested by the simulations. Some quick additional simulations were

performed to determine if it would be better to have an optimal inboard anchor and suboptimal outboard, or symmetric suboptimal anchors. The asymmetric anchor condition led to excessive rotation of the ATD that increased the risk of head contact with forward structures. As a result, we placed the outboard anchor where it was feasible, and adjusted the donning arm geometry to place the inboard anchor in a matching location.

While we could maneuver the manual chair into the seating station reasonably well with the driver seat present, it was not possible to do so with the power chair and the outboard condition. Instead, to gain an understanding of how much space volunteers would use to maneuver if it was unrestricted, we removed the driver's seat and placed strips of green, orange, and blue colored duct tape on the floor at locations 123, 137, and 152 cm (48, 54, and 60 in), respectively, forward of the UDIG anchorage hooks (Figure 90). During testing, the experimenter observed and recorded how far forward the volunteers drive the wheelchair as they back it into the station.

Figure 90. Duct tape used to mark centerlines and space 123, 137, and 152 cm (48, 54, and 60 in) forward of the UDIG anchorages.

Even when the driver and right-front passenger seat were present, it was possible to operate the donning arm when its base plate was mounted so the lateral position provided a 30+" width for both the green and blue conditions. However, both front seats were removed to allow more distanced experimenter scanning of volunteer posture and belt fit.

For the blue conditions, we chose feasible lap belt anchor locations that provided an approximately 45-degree sideview lap belt angle for each of the two wheelchairs. Because the power wheelchair is longer than the manual chair, this resulted in a lap belt anchor position (dark blue) that was approximately 90 mm forward of the lap belt anchor position based on the manual chair (light blue). For the green condition, the wheel well made it difficult to vary belt anchor without compromising maneuverability, so the same lap belt anchor was used for both

the dark and light green conditions. Figure 91 shows the fixture attached that allows shifting the anchor location between subject trials.
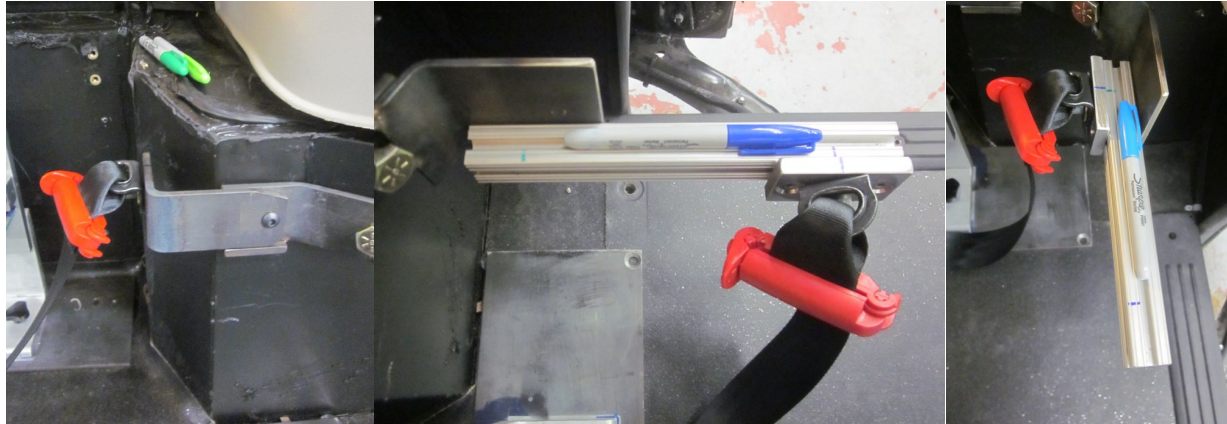
Figure 91. Fixture used to locate hardware for green, dark blue, and light blue outboard anchor in Braun.

Figure 92 shows the fixture installed in the Braun van that allows adjustment of the D-ring laterally, vertically, and fore-aft. For the blue conditions, we placed the D-ring close to the optimal locations in the X and Y directions. Vertically, we located the D-ring above the optimal location for the dark blue condition and below optimal location for the light blue condition. For the light green condition, we placed the D-ring in the optimal location. For the dark green condition, we placed the D-ring in a "practical" location that simulates using the existing D-ring location located on the C-pillar.

Figure 92. Fixture to allow vertical, lateral, and fore-aft adjustment of D-ring location.

For the BIW, we first set the conditions for the right-front position. As shown in Figure 93, with the current vehicle geometry we are working with, allowing enough space for a 762 x 1219 mm (30 x 48 in) seating station (required by ADA) means that the UDIG anchorages need to be placed well rearward of the B-pillar. While we intended for this seating position to represent a scenario where the UDIG anchorages would be stowed in the floor or alongside the vehicle wall and deploy after the occupant pulls into the wheelchair station, it illustrates the additional

complication of blocking access to the ramp once they are deployed. The location of the B-pillar relative to the occupant also shows that D-rings mounted to the B-pillar would the route belt forward of the occupant's shoulder, which is undesirable. Placing lap and shoulder belt anchors in the optimal positions would interfere with the entrance. Instead, for the outboard anchor, we placed a mount at a higher location than used in the Braun, and ended up securing the lap belt to the rearmost location possible without blocking the entry. For the inboard anchor, we set the angle to 45 degrees for either the power (dark orange) or manual chair (light orange). For the D-ring, we mounted a track to the roof and evaluated the belt fit using forward and rearward conditions. Even this placement caused some interference with the door opening.

Figure 93. For current vehicle configurations, a right-front position that allows the required 122 cm (48 in) long space for a wheelchair places the UDIG well behind the B-pillar.
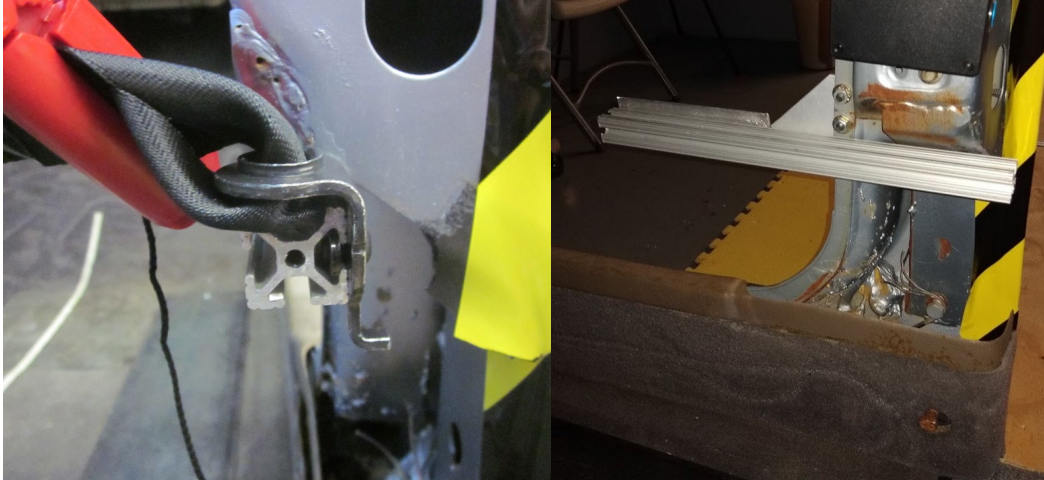
Figure 94. Outboard lap belt anchorage mounts in first-row right position of BIW.

For the purple conditions in the BIW second row, we wanted to compare the accessibility when the shoulder belt was located either inboard or outboard. (At the time of fixture setup, we had not yet abandoned the use of an inboard shoulder belt as a countermeasure to keep the occupant in place during farside impact.) We aimed for optimal belt anchorage placement, with the light based on manual and dark based on power. Both purple conditions used the same D-ring geometry, except the Y-location was inboard in the dark purple and outboard in light purple.

Table 21 summarizes the qualitative differences between each test condition, while Figure 95, Figure 96, and Figure 97 show the differences in belt geometry when all are set to have an origin at the top center of the UDIG anchorage fixture. In addition, Figure 98 shows how belt fit varies for one pilot participant in each condition with the power and manual wheelchairs. Figure 99 and Figure 100 show the available space in the BIW and Braun, respectively.

Table 21. Summary of UDIG and anchor locations.

Condition	UDIG Location	Lap belt anchors	D-ring location
A	Braun, 2nd row, rearward	Fixed, best possible	Optimal
B	Braun, 2nd row, outboard	45 degrees with manual	Above optimal
C	Braun, 2nd row, outboard	45 degrees with power	Below optimal
D	Braun, 2nd row, rearward	Fixed, best possible	Practical (C-pillar)
E	BIW, 2nd row, right	45 degrees with power	Optimal Inboard
F	BIW, front row, right	45 degrees with power (IB) Practical, higher (OB)	Forward
G	BIW, front row, right	45 degrees with manual (IB) Practical, higher (OB)	Rearward
H	BIW, 2nd row, right	45 degrees with manual	Optimal Outboard
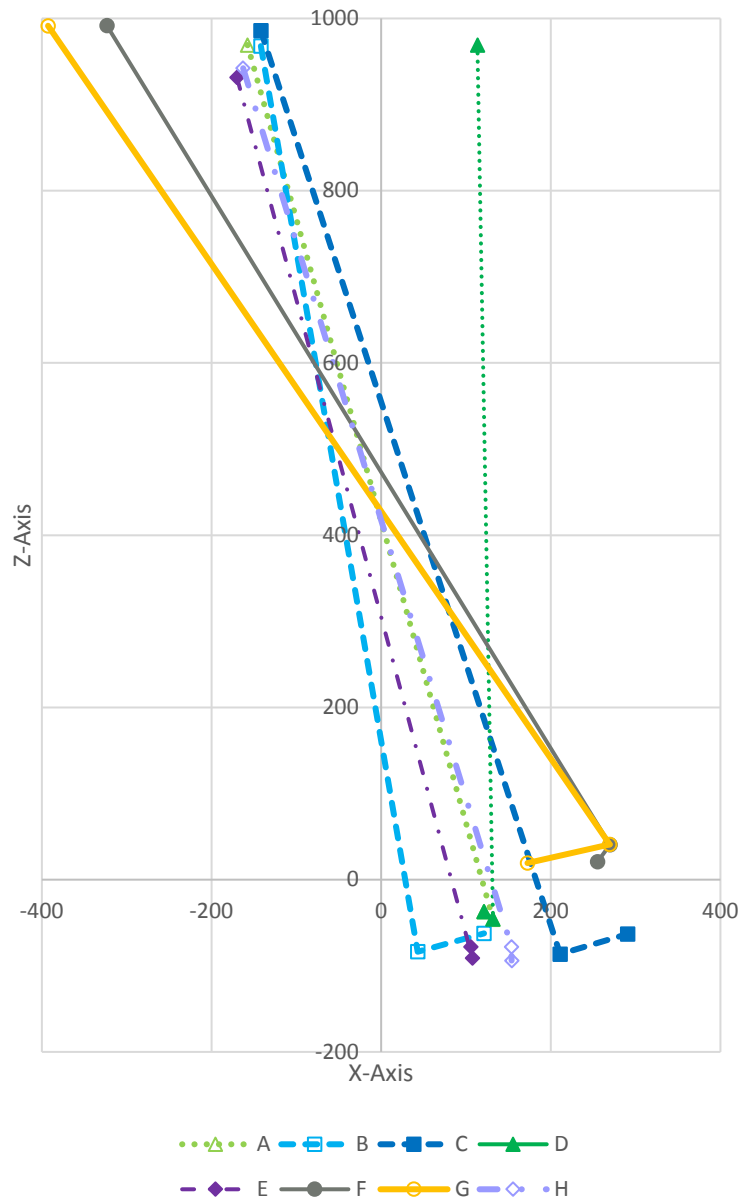
Figure 95. Belt geometry in X-Z plane (right side view).
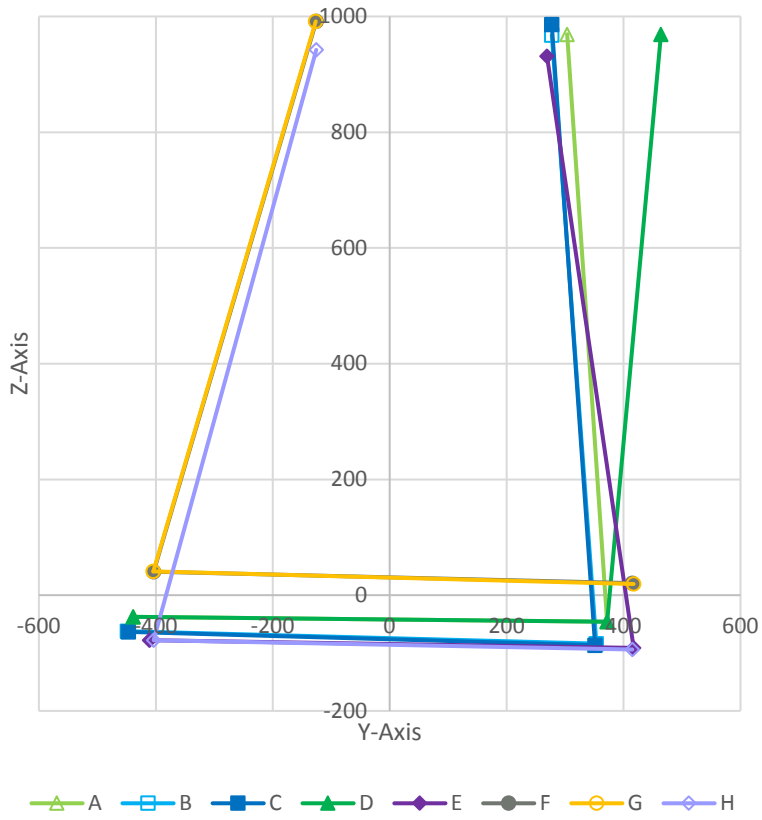
Figure 96. Belt geometry in Y-Z plane (front view).
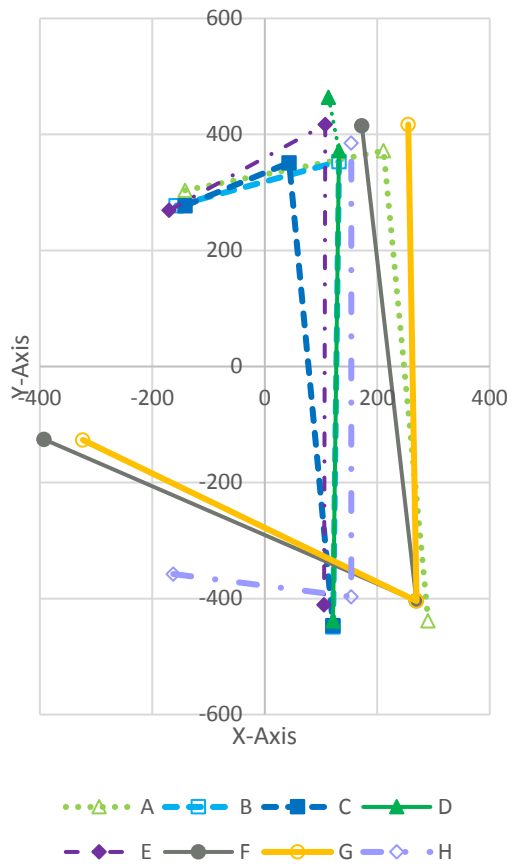
Figure 97. Belt geometry in X-Y plane (plan view).

Figure 98. Examples of belt geometry in each condition in manual and power wheelchairs.

Condition A-D	A	D	B	C
Manual photo				
Power photo				
Condition E-G	E	H	F	G
Manual photo				
Power photo				

Figure 99. Figures illustrating space to maneuver in BIW.

Figure 100. Photos showing space to maneuver in Braun van.

When setting up the test fixtures, ZF provided us with the longest typical seatbelts they had available. Unfortunately, this was not long enough to allow the seatbelts to be held out of the way by the donning system and allow the participant to maneuver the wheelchair into position. We spliced approximately 18" more length onto each seatbelt to address the issue. However, a retractor spring strength is tuned to the length of the belt, and adding length means that it had more webbing on the spool, and as it retracted, it was not able to snug the belt around the participant as it normally would. As a result, we instructed participants to snug the belts around themselves during testing. This problem could be addressed in an actual installation by using a stronger retractor spring, adding an additional retractor to the lap belt, or using a smart retractor that snugs the belt around the participant prior to the vehicle moving.

Volunteer Assessment

Methods

COVID Adjustments

The COVID-19 pandemic began roughly 6 months after this project began, and all testing with volunteers was paused. The UM Office of Research developed new criteria for determining whether testing could resume. A key item was whether contact of less than 1.8 m (6 feet) could be limited to 15 minutes or less. Our normal procedure for measuring belt fit and posture uses the FARO arm to collect three-dimensional coordinates from body landmarks, but this would require close contact for more than 15 minutes. As a result, we developed an alternative procedure of using a sense scanner to document the participant's posture as shown in Figure 101. This method requires the experimenters to stay further away from the volunteers, and takes approximately 1 minute to complete the scan in each trial. Posture and belt fit were also documented through a series of photos shown in Figure 102. In addition, rather than taking direct measurements of volunteer anthropometry, we took photos of them seated in each wheelchair in front of a grid on the wall, as shown in Figure 103.

Figure 101. Measuring volunteer belt fit with remote scanner instead of FARO arm.

Figure 102. Examples of photos used to document belt fit and wheelchair position relative to UDIG.

WC	Right	Oblique	Front	Left	UDIG
Manual					
Power					
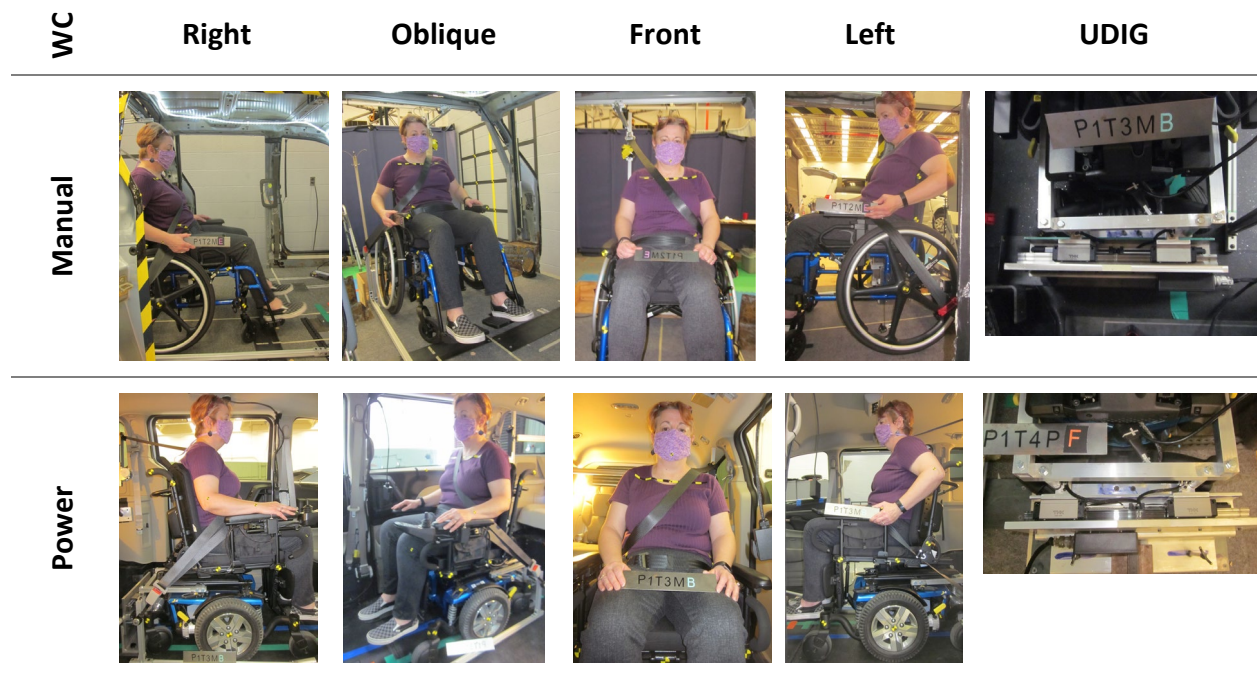
Figure 103. Photos in front of grid used to estimate anthropometric measures.

Several other changes to procedures were made to allow testing of participants. The participant wore a mask throughout the test session; experimenters wore masks and face shields. Because participants aged 65 and older were deemed higher risk, we restricted volunteer age to be 19 to 64 years. Volunteers filled out the same health screening required by all people entering the building, and they entered the building through a door close to the lab to minimize their presence in the rest of the building. Each lab has a cleaning checklist that is performed at the beginning and the end of each day, as well as in between participants if there is more than one in a day. Each experimenter was assigned to lead testing in one vehicle to minimize their interaction with each other. Participant test sessions were recorded on a common calendar to coordinate COVID-related lab capacities and allow for contract tracing if needed.

Subject requirements and recruitment

The main screening criteria for the volunteers was that they regularly used a wheelchair in the past year, but would be able to transfer to and operate the two wheelchairs purchased for the study. Beyond that, we attempted to recruit subjects divided among these stature ranges: $\leq$ 63", 64"-69", $\geq$70". The main method of recruiting subjects involved posting the study at umhealthresearch.org. In addition, flyers were also distributed by the Ann Arbor Center for Independent Living and were posted at the University of Michigan Wheelchair Seating Clinic. When potential subjects responded, they were interviewed by phone or email using the screening questions included in Appendix A.

Test protocol

To allow contact tracing, experimenters scan into each lab used for testing, and check that the power wheelchair is in the nominal setting of a seatpan angle of 5 degrees and seatback angle at 10 degrees. The experimenters clean the fixtures, tools, and equipment with sanitizing wipes and record the effort on a checklist.

One experimenter prepares the paperwork, which involves two consent forms, an ethnicity form, a test matrix for each experimenter, and a checklist. The second experimenter sets up the area where the participant self-applies reference targets, ensuring there are sufficient stickers and tape available, and placing a mirror on the participant table. Experimenter Two also prepares the scanner and laptop and places it in position for use in the first test vehicle. To minimize interaction, Experimenter 1 works in the Braun vehicle, while Experimenter 2 works in the BIW. Each experimenter prepares the fixture for testing. Steps include:

- Check that tools are available and stowed
- Turn on lighting
- Set up first configuration
    - Check that actuators are working
    - Check connections if needed
- Mount GoPro on side panel (Braun only)
    - Mount iPad to steering wheel
    - Check that connection is working

- Set up video camera in correct spot
  - Check battery / plugged in
  - Check video card
  - Check camera angle / view
- Check battery and place still camera on prep table
- Prep test labels for video/photos
- Move mirror to BIW after participant uses it for sticker placement

Participants were asked to pull up to the front of the building upon arrival and were met by an experimenter. The experimenter checked their health screening status and directed them to drive around the building to the high bay area. An experimenter then met them outside the high bay door and escorted the participant into the testing area.

The experimenter read the introduction script to the participant and gave them consent and demographic forms to fill out. After consent was complete, the participant was shown a short video showing them what docking in the vehicle looks like. The participant then transferred to the first wheelchair and applied target stickers with the help of a diagram, verbal instructions, and a mirror. Next, a diagram of good belt fit was explained, and participants were informed that they could adjust the seatbelt if it got caught during application or request help if necessary. After the participant transferred into one of the testing wheelchairs, front and side photos were taken of the participant in front of a grid on the wall and then they began the trials.

Participants used a ramp to enter the vehicle mockups and then maneuvered their wheelchair into the docking stations. Tape on the vehicle floor, mirrors, and a camera were used to help participants line up with the docking station located behind them. When the wheelchair was in position, the participant pressed a button to activate the UDIG hooks to latch onto the wheelchair hardware.

In the Braun van, once the wheelchair was locked in place, the participant pressed a button to activate the seatbelt to lower into position over their body. Another button was pressed to raise the seatbelt out of the way and another to unhook the UDIG hardware from the wheelchair when the participant was ready to exit the vehicle mockup. In the BIW, an investigator moved the seatbelt into position after the UDIG was engaged. After measurements were taken, the investigator moved the seatbelt back to its stowed position and then the participant disengaged the UDIG and exited the vehicle.

Each trial was video recorded during ingress and belt application. Photos of each participant were taken to record their position and belt fit for each condition, and then the participant was scanned with a handheld scanner. The participant began a survey (Appendix A) while belted in the vehicle, and then completed the survey after exiting the vehicle. The survey includes questions about ease of docking and belt application, as well as belt comfort. Video was also collected during belt removal and egress.

There were four trials in each vehicle mockup in two different wheelchairs for a total of eight trials. The test matrix used a fractional factorial design. Participants alternated between

vehicles for each trial, completing two trials in the first wheelchair before transferring to the second wheelchair, and then switching back to the first wheelchair for the last two trials. After transferring to the second wheelchair, front and side photos were again taken in front of a grid on the wall.

After all trials were complete, participants were given a Volunteer Questionnaire to fill out (Appendix A) that includes questions about their personal travel experiences while using a wheelchair. They transferred back to their personal wheelchair and front and side photos were taken in front of a grid on the wall. They were given a payment form to fill out and paid for their participation. Then they were escorted back to their vehicle.

The post-session lab protocol involves downloading video and photos for each subject. All electronic equipment was moved to the charging area. Experimenters repeat the laboratory cleaning checklist after each participant.

Results

Participant Characteristics

Table 22 shows the characteristics of the study participants. Two volunteers were considered to have short stature, two tall, and four intermediate. Participant age ranged from 39 to 63.

Table 22. Participant characteristics.

ID	Age	Gender	Stature (cm)	Disability	Normal wheelchair
AW01	39	F	160	Spinal cord injury	Manual
AW02	48	F	142	Spina bifida	Manual
AW04	63	F	168	Multiple sclerosis	Power
AW05	39	M	175	Spinal cord injury	Power
AW06	53	M	168	Post COVID, fatigue	Manual (not full time)
AW07	48	F	168	Scoliosis, fused spine	Manual or power
AW08	54	M	188	Spinal cord injury	Manual
AW09	58	M	188	Parkinson's	Manual

Test Matrix

The executed test matrix is shown in Table 23. The initial plan for testing was that each participant should have 8 trials, one in each condition. Odd-numbered participants had their first two trials in the manual wheelchair, followed by four in the power wheelchair, followed by the last two trials in the manual wheelchair. Even-numbered participants reversed this wheelchair order. Trial orders were randomized for each participant. If a volunteer was not able to independently operate the manual wheelchair, all trials were conducted in the power wheelchair.

Table 23. Order of trials completed by each participant using each wheelchair.

	A	B	C	D	E	F	G	H
AW01	1M	3P	5P	7M	2M	4P	6P	8M
AW02	2P	6M	4M	8P	7P	3M	5M	1P
AW04	4M	6M	8P	2P	5M	1P	7P	3M
AW05	5P	3P	1P	7P	6P	2P	8P	4P
AW06	6M	8P	2P	4M	1P	5M	7P	3M
AW07	7M	5P	1M	3P	2M	8M	4P	6P
AW08	8P	6M	2P	4M	1P	7P	3M	5M
AW09	4P			2M	3M		1M	
# Power	4	4	5	4	4	4	5	3
# Manual	4	3	2	4	4	3	3	4

Overall, there were 27 completed trials in the manual wheelchair, and 32 completed trials in the power wheelchair.

Belt Fit

Because of COVID-motivated protocols to reduce close proximity measurements, we assessed belt fit three ways for redundancy: still photos of participants, 3-D scan data, and participant videos. Shoulder belt score was calculated from the scan data, measuring the horizontal distance from the manubrium to the inboard point on the seatbelt. Figure 101 shows examples of the range of belt fit scores. For lap belt fit, a qualitative assessment of belt fit was made from the photos using the categories illustrated in Figure 102. Categories include touching thighs (no examples available), below ASIS, over ASIS, above ASIS, and on abdomen.

Figure 104. Examples of range of shoulder belt fit scores (mm).

Fit	Against neck	Inboard	Inboard	Centered	Outboard
Photo					
Score	-66	-27	0	30	89

Figure 105. Examples of qualitative lap belt fits.

Fit	Below ASIS	Over ASIS	Above ASIS	On Abdomen
Photo				
Score	2	3	4	5

Appendix B contains photos of belt fit for all participant trials, while Figure 103 compares fit across all participants for condition B and Figure 104 does so for condition D. Condition B has the D-ring slightly below optimal (defined by simulations) and lap belt angle set at 45 degrees with the manual wheelchair, while condition D has the D-ring approximating using the vehicle D-ring location on the C-pillar and the most feasible location for the lap belt. For condition B, the shoulder belt is centered on the shoulder only for participants 4, 5, and 8, while it touches the neck for the remaining participants. In addition, the shoulder belt seems to route too close to the participant's arm (rather than their hips) for four of seven participants. Lap belt fit looks reasonable only for participants 1, 4, and 6, with the lap belt above the ASIS or on the abdomen for other participants.

For condition D (representing a practical belt geometry often used in van conversions, with the D-ring on the C-pillar), the lap belt was centered on the shoulder of the two shortest participants (1 and 2), but was too close to the arm for remaining participants. Three participants (2, 6, 7) had the lower end of the shoulder belt routed closer to the arm than the hip. Lap belt fit was acceptable only for participants 1, 4, and 6.

For participants 2, 6, and 7, their visibly higher BMI seems to affect their belt fit. However, for several other participants, their disabilities affect their posture and belt fit. Participant 4 had the best belt fit across all conditions, partly because she was able to achieve an upright and symmetric posture. Participant 1 sits asymmetrically and the belt routes higher over her right hip compared to her left fairly consistently across all conditions. Participant 2 sits with her head quite close to her chest, and has a very short stature; these contribute to the belt routing close to her neck in most conditions. All trials with Participant 5 used the power wheelchair because his disability prevented him from operating the manual wheelchair. He was able to maintain an upright torso posture, and had reasonable shoulder belt fit in most test conditions, but his lower body slouches somewhat. It was challenging for him to adjust the belt fit, and his lap belt is too high in many conditions. For Participant 6, he was able to sit upright, but his higher BMI tended to route the shoulder belt closer to his arm than his hip, which also caused the belt to be closer to his neck than desired in most conditions. He was able to achieve reasonable lap belt fit across conditions. For Participant 7, she usually shifted her lap belt higher (despite being instructed that good belt placement was low), leading to poor fit across all conditions, as well as the belt routing too close to her neck in most conditions. For Participant 8, his disability led to a slouched seated posture with splayed lower extremities. This led to the lap belt routing over the abdomen in most cases. The shoulder belt routed over the shoulder in a reasonable position for most conditions, but slack is visible in most trials, and it would probably be closer to the neck if the slack was removed.

Figure 106. Belt fit of all participants in condition B.

Figure 107. Belt fit of all participants in condition D.

Ingress, Docking, Donning, Egress Analysis

The following items were coded from the video from each trial and participant:

Ingress:

> Approach direction on ramp
>
> Any problems maneuvering around seatbelt on entry?

Docking:

> Number of times they moved forward to align
>
> Was realignment needed after first engagement attempt?
>
> Time from entry to complete docking

Donning:

> Did seatbelt catch on any wheelchair structure during donning?
>
> Time from start to completion of donning
>
> How did participant adjust belt?
>
> Shoulder belt fit
>
> Lap belt fit

Doffing:

> Did seatbelt catch on any wheelchair structure during doffing?
>
> Did participant move belt during doffing?
>
> Time from start to completion of doffing

Egress:

> Number of times they moved backwards to exit station
>
> Any problems on maneuvering around seatbelt on exit?
>
> Time from unbelting to exit

Figure 105 shows the mean entry time for each configuration, across all conditions, for the power and manual conditions, and the minimum time across conditions. The times are divided into docking time (from activating the actuator control to being fully docked), donning time (from reaching for the belt control to finishing adjusting the seatbelt), and positioning time (remaining time from leaving the ramp to being ready to go.) The average mean entry time was just over 2 minutes, and there were minimal differences between the power and manual conditions. Condition C had the highest mean entry time, that seems to be happening because it was easy to bump into the outboard lap belt anchor position. The minimum times for each task across all trials was 35 seconds. The maximum times (not shown to allow better

comparison for other conditions) was 32 s for docking, 102 s for donning and 202 s for positioning.
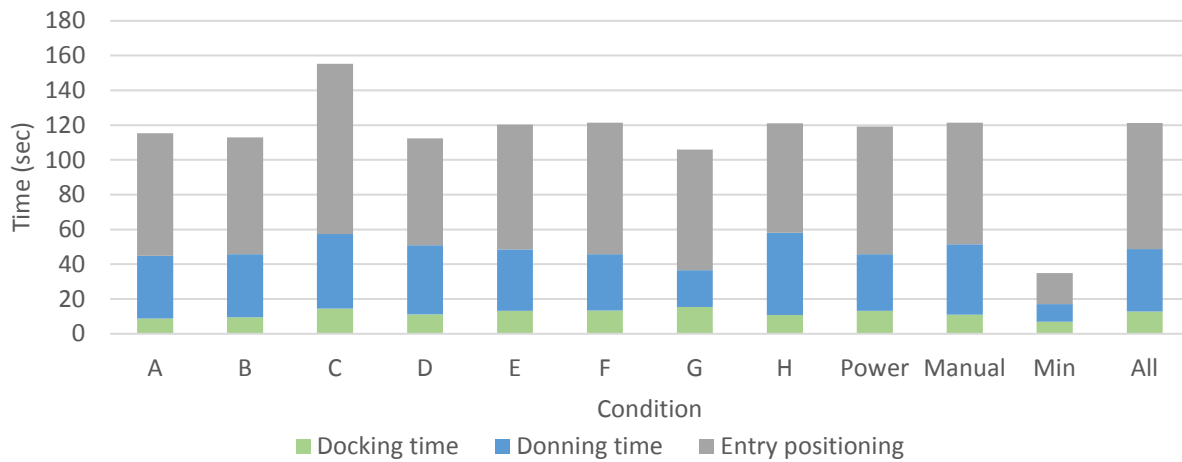
Figure 108. Mean entry time for each condition and type of wheelchair, divided by entry positioning, docking time, and donning time.

The same data are shown in Figure 106 for exiting. The mean total exit time was just over a minute. Total exit time for most conditions was less than a minute, except for conditions F and G where the participant needed to back out of the front row wheelchair seating station. The average power wheelchair exit time was slightly longer than the manual exit time, with most of the difference in positioning. The maximum exit times (not shown to allow better comparison of other conditions) were 66 s for doffing, 18 s for undocking, and 140 s for exit positioning. For consistency, these times do not include the time to deploy or remove the anchors behind the station in conditions F and G; mean times for this task (which would be done by a mechanism in a real implementation) were 53 s for deploying and 35 s for removing. We would expect a mechanism to be faster than these times.
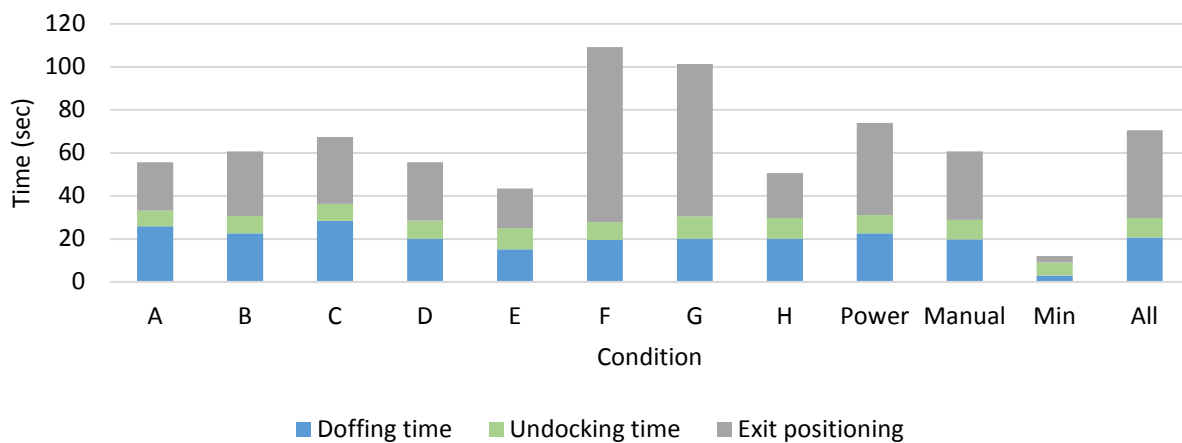
Figure 109. Mean exit time for each condition and type of wheelchair, divided by doffing time, undocking time, and exit positioning.

122

Table 24 lists several factors that were assessed in the video analysis, by the percentage of trials where they occurred. In the majority of trials (95%), the participant traveled on the ramp facing forward. Only 8% had problems maneuvering around the seatbelt while positioning the wheelchair in front of the anchorages; about half placed the belt on their laps as part of maneuvering. In 20% of trials, participants moved forward and backed up 3 or more times to align the wheelchair in position in front of the UDIG anchorages. In 28% of trials, participants had to move the wheelchair again after the first engagement attempt to allow full engagement of both hooks. For exiting, participants were able to directly move out of the station onto the ramp without changing direction in 72% of trials. In 15% of trials participants had some issues maneuvering around the seatbelt on exit.

Table 24. Ingress, docking, and egress characteristics

Metric	% all trials
Traveled in forward position during entry	95%
Problems maneuvering around seatbelt during positioning	8%
Took 3 or more attempts to align	20%
Realignment required after first engagement attempt	28%
Steered directly out of station on exit without changing direction	72%
Problems maneuvering around seatbelt on exit	15%

In addition to the items observed on video, the experimenter recorded the most forward location the participant maneuvered the wheelchair. As shown in Table 25, in most trials, the participants used as much space as was available. However, in a few trials, the participant maneuvered within the minimum required space of 48", even in the power wheelchair.

Table 25. Space used to maneuver in each trial.

	Manual trials	Power trials
Green (48 in)	9%	6%
Orange (54 in)	20%	16%
Blue (60 in)	71%	78%

Questionnaire Responses

After each trial, the participant answered a series of questions regarding ease of use and comfort, often comparing the test experience to their regular travel experience. Figure 107 shows responses to the question rating the difficulty maneuvering the test wheelchair in the vehicle compared to their personal wheelchair. For the manual wheelchair, just over half of responses were extremely easy or moderately easy, while only about one-third of responses for trials involving the power wheelchair were in these categories. This could be related to the shorter length of the manual wheelchair compared to the power wheelchair, or more participants regularly using a manual wheelchair personally.
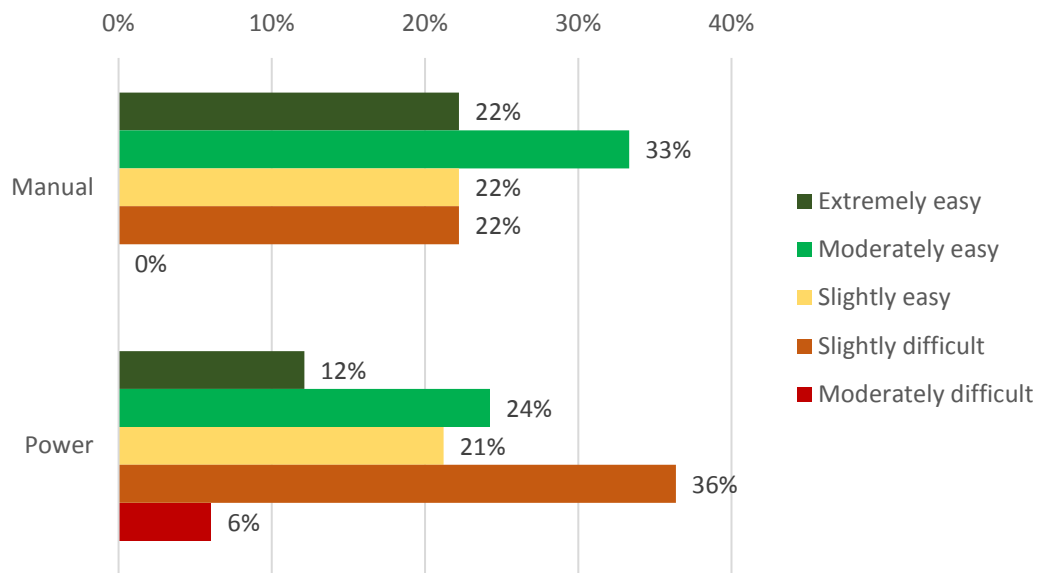
Figure 110. Level of difficulty maneuvering the test wheelchair compared to their personal wheelchair.

Answers to the question regarding ease of lining up the wheelchair with the UDIG anchorages are shown in Figure 108. Condition B had the most positive responses, followed by H and C. Conditions A and D were similar, as were E and F (front row conditions), which had the fewest positive responses. When asked about their feeling of security once docked, participants rated security excellent in 44% of manual trials and 27% of power trials. The remaining manual trials were rated good, while 67% of the power trials were rated good, and one was rated "could be better."
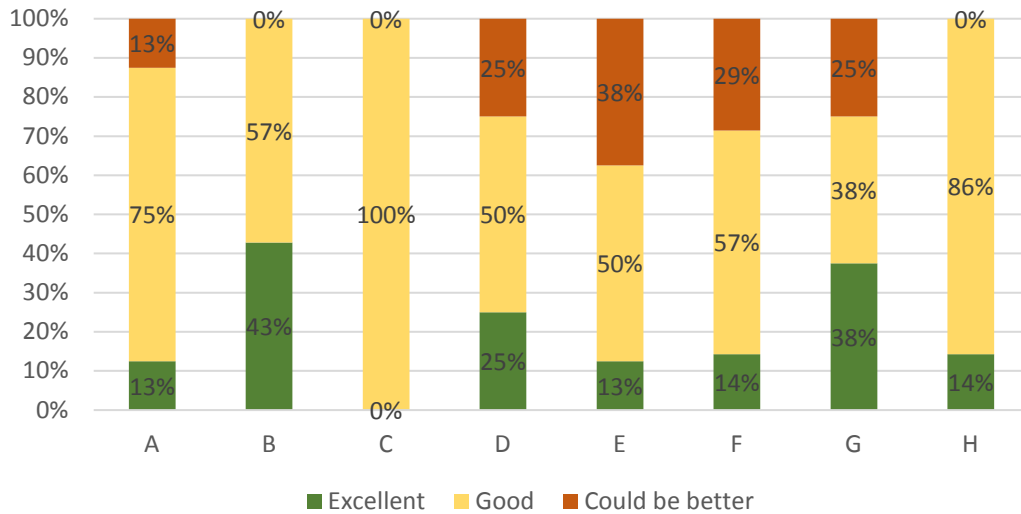
Figure 111. Ease of use of lining up wheelchair with UDIG anchors.

Participant rating of their ability to use the system independently is shown for the seatbelt system on the left side of Figure 109 and the docking system on the right side of Figure 109. About 25% of responses were poor/could be better for both systems, while the rest were good or excellent.
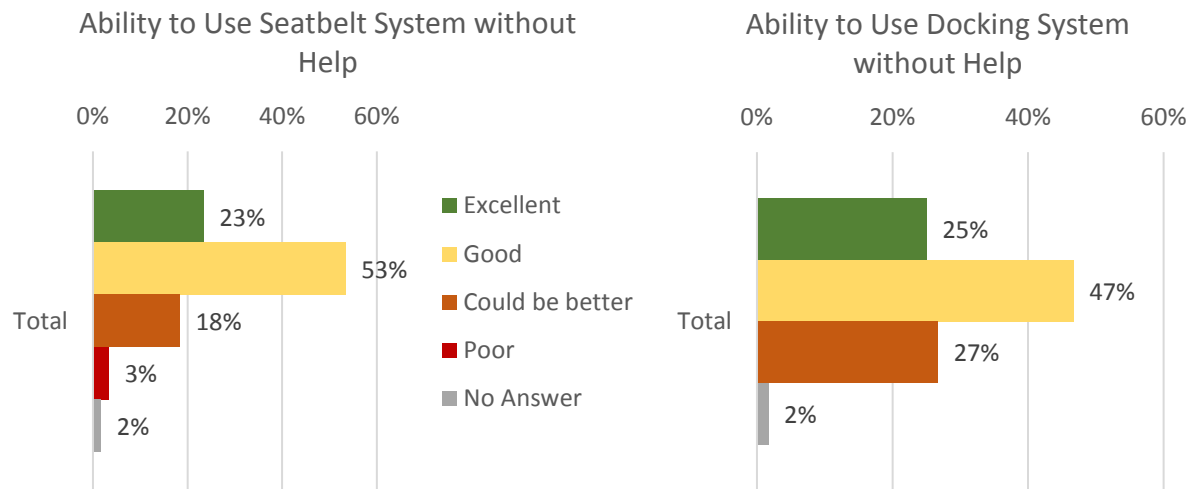
Figure 112. Rating of using the seatbelt system (left) and docking system (right) without help.

Figure 110 shows the distribution of responses to whether the participant would recommend the seatbelt system and the docking system in the configuration that was just tested. Over 72% of answers were rated 7 or higher, including about 20% giving a rating of 10.
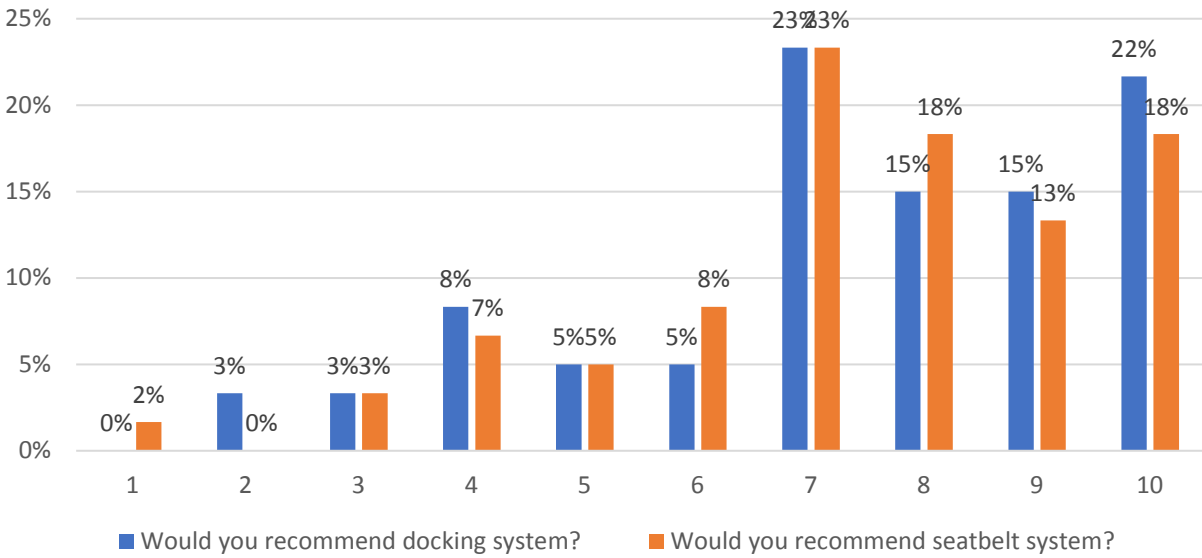
Figure 113. Participants' answers to whether or not they would recommend the seatbelt system and the docking system.

Qualitative Feedback

- Two participants had limited manual dexterity and were unable to operate the actuator controls that came with the actuator (Figure 111).

Figure 114. Photo of actuator controls.

- A test volunteer and spouse planning to purchase a modified van indicated that they would prefer to travel seated together in the front row, even knowing that belt fit may be suboptimal.

- More than one participant expressed concern about the safety of how the seatbelt was routed over the top of the manual wheelchair's rear wheels.
- More than one participant expressed concern about the lack of a head restraint for rear impacts.

Dynamic Testing

Methods

Test Plan Revision

To begin the dynamic testing effort, the original sled test plan was reassessed relative to lessons learned from computational modeling and volunteer testing. The original plan included tests to evaluate the effect of wheelchair seat width in side impact. However, in the sled tests performed in March 2020 to provide validation data for side impact models, we conducted tests with the surrogate wheelchair frame fixture, with the frame width varied to be 16, 18, and 20". Results showed less effect of wheelchair width than anticipated, so assessment of wheelchair width effects in side impacts was considered a reduced priority. In addition, validation tests were also performed with two different armrest styles; both were damaged due to interaction when impacted by ATD but had minimal effect on ATD kinematics or injury measures. This suggested that the presence of armrest and its design were not of significant consequence to side impact outcomes.

For a wheelchair station in the front row of a traditional van/minivan sized vehicle, it is common practice to mount the seatbelt D-ring and outboard lap belt anchor on the vehicle B-pillar. While this practice can produce acceptable belt fit for a rider seated in a manual chair, this practice places the upper shoulder belt anchor too far forward to engage well with the shoulder of a person seated in a power chair that has a longer fore/aft footprint. In addition, the lap belt anchorages are in a location where it is not feasible to achieve a sideview lap belt angle near the target of 45 to 70 degrees for the power chair user. If the shoulder belt D-ring is mounted on the vehicle roof instead, it could potentially cause clearance issues for the right-side door opening. These concerns led us to the conclusion that a rear-seat location for the wheelchair station may be preferred to achieve belt geometry closer to optimal, assuming that the dimensions of future AVs might have a similar distance between A-pillar and B-pillar. However, one test volunteer and spouse planning to purchase a modified van indicated that they would prefer to travel seated together in the front row, even knowing that belt fit may be suboptimal. This led us to consider tests that assessed the effect of a more forward shoulder belt location that reflects a realistic scenario used in modified vehicles.

The computer model demonstrated that lap belt anchors close to the occupant's hip provided the best protection in front and side impact. Initial simulations used a lateral spacing of ~50 cm (~20 in) between the lap belt anchors. While this spacing is feasible for our selected power wheelchair, the manual wheelchair is 76 cm (30 in) wide because the propel wheels are mounted outside of the seat structure, so achieving optimal lateral width will not be possible when accommodating manual wheelchairs. As a result, most of the volunteer test configurations have lateral spacing of ~80 cm (31.5 in), and thus the sled test lateral impact belt locations used the wider spacing needed for accessibility.

Initial installations of belt hardware in the volunteer test fixtures based on available mounting locations led us to consider nonsymmetric configuration for inboard and outboard lap belt anchorages. However, modeling these scenarios showed that they result in excessive lateral

rotation of the occupant compared to the optimized geometry, and led to greater potential for head contact with the vehicle structure. As a result, we prioritized having symmetrical lap belt geometry for the volunteer testing and dynamic testing, even if this required shifting out of the optimal predicted anchor zone.

As described in the modeling section, the original intent for modeling was to identify optimal belt locations, implement them in test fixtures for volunteer testing, and then use results from volunteer testing to determine needed adjustments to improve belt fit. Because vehicle structures and accessibility concerns prevented us from implementing the optimal belt geometry locations in vehicles, the modeling efforts took an alternate path. After initial optimizations, we tried to implement these geometries in the vehicle fixtures. Subsequent simulations then examined the two different feasible belt geometries, using models of the surrogate wheelchair base, the manual wheelchair, and the power wheelchair. These simulations were used to define seatbelt, airbag, and spacing conditions for sled testing.

For the side impact testing, we prioritized farside impact conditions because our modeling has shown that in nearside conditions without simulated intrusion, the combination of good belt geometry, a typical curtain airbag, and placement of the wheelchair seating station away from the struck side (needed to allow maneuvering into the seating station) provides reasonable protection. In addition, the nearside response depends on interior door characteristics, and a standardized method of simulating such side impacts on a sled is not currently available.

For side impact, we had hypothesized that if a wheelchair seating station was placed optimally relative to the vehicle interior, that the standard curtain airbag might provide adequate nearside impact protection even if the D-ring was located inboard rather than outboard. In addition, we hoped that an inboard D-ring location might prevent the occupant seated in a wheelchair from falling out of the wheelchair during a farside impact. Modeling did not confirm the hypotheses. As shown in Table 16, the nearside occupant had lower injury metrics when the curtain airbag was paired with an outboard D-ring. In addition, as shown in Figure 55, the inboard D-ring location was not effective at keeping the occupant in the wheelchair during farside impact without excessive neck loading. As a result, we asked our collaborators at ZF to consider a design for a curtain airbag mounted to the center of the roof that might help control farside kinematics for an occupant in a wheelchair. They developed two initial designs for a Center Airbag To Contain Humans (CATCH), which involves innovative airbag tethering to restrain the occupant. Figure 56 contains illustrations of how the CATCH designs improve kinematics compared to a baseline condition. The second CATCH design includes a "window" that aimed to reduce neck loading. As seen by preliminary simulations with the two designs, they appear to achieve the design goal of keeping occupants in their wheelchairs. As a result, the focus of side impact testing was revised to evaluate injury mitigation potential of the CATCH designs.

For side impact, our initial revised plan included conditions without airbag and with different belt geometries. Instead, the first few tests with the two CATCH designs showed minimal effect of shoulder belt location in the farside condition, so varying belt geometry was removed as a priority. In addition, evaluation of the first CATCH tests showed opportunities for improved

performance with changes of tether location and construction, so the matrix was revised to allow these assessments.

In addition to evaluating restraint system performance with the SWCB, we wanted to evaluate UDIG performance with production wheelchairs and to evaluate the strength of UDIG-compatible attachments designed for the manual and power wheelchairs. Because initial feedback from members of a disability advocacy group indicated that our first attachment design for the manual chair was too heavy, we also designed and tested a lower mass version of the manual attachments. While most of our test conditions used a heavy duty UDIG anchorage system designed for repeated testing, we also evaluated the crashworthiness of the lighter UDIG anchorage system used for volunteer testing. Finally, because the first test to evaluate the strength of attachments with the power wheelchair failed, the test originally intended to test the attachments in side impact was repurposed to test redesigned attachments in frontal impact.

Along with running tests to demonstrate the effect of airbag use and belt geometry with the midsize male, we also wanted to run tests using a smaller ATD to evaluate response using restraint conditions optimized for a larger size of occupant. As a result, we ran frontal impact tests with the Hybrid III small female ATD and farside tests with the SID-IIs.

Table 26 and Table 27 list the dynamic test conditions that were evaluated in front and side impacts, respectively. In addition to the test conditions, the table also lists the goal of each test.

Table 26. Summary of Frontal Test Matrix

Test ID	ATD	WC	Seatbelt	Airbag	Goal
AW2101	H350	SWCB	B	SCaRAB	Airbag benefit
AW2102	H350	SWCB	B	None	Baseline B
AW2103	H350	SWCB	D	SCaRAB	Airbag benefit
AW2104	H350	SWCB	D	None	Baseline D
AW2105	H35F	SWCB	B	SCaRAB	Airbag benefit for small occupant
AW2106	H35F	SWCB	B	None	Small occupant size with baseline B
AW2111	H350	Manual, att M1	D	SCaRAB	Check M1 strength
AW2112	H350	Manual, att M1, light anchors	D	SCaRAB	Check light anchor strength
AW2113	H350	Manual, att M2	D	SCaRAB	Check M2 strength
AW2114	H350	Power, att P1	D	SCaRAB	Check P1 strength
AW2115	H350	Power, att P2	D	SCaRAB	Check P2 strength

Table 27. Summary of Side Impact Test Matrix

Test ID	ATD	WC	Seatbelt	Airbag	Goal: Evaluate
AW2107	ES2RE	SWCB	B	CATCH-V, tether location 1	CATCH-V
AW2108	ES2RE	SWCB	B	CATCH-H, tether location 1	CATCH-V
AW2110	ES2RE	SWCB	B*	CATCH-V, tether location 2	Different tether locations
AW2116	ES2RE	SWCB	B	CATCH-V', tether location 2	Modified tether design
AW2117	ES2RE	SWCB	B	CATCH-V*	Modified CATCH design
AW2118	ES2RE	Manual	B	CATCH-V'	Attachments in side impact
AW2119	SID-IIS	SWCB	B	CATCH-V'	Performance with smaller occupant

*fixed belts without retractor

ATDs and Instrumentation

All signals generated by accelerometers and load cells used were digitized in real time using a dedicated data-acquisition system (DAS) mounted to the sled. The signals collected were processed and digitally filtered according to the requirements of SAE J211. The polarities of all signals will be adjusted to conform to the sign convention of SAE J1733. Data from ATD head and chest accelerometers were processed through standard algorithms to determine peak head resultant acceleration, head injury criterion (HIC), and the 3-ms clipped resultant chest (i.e., thoracic spine) acceleration. Time history graphs of the individual transducer signals, as well as calculated resultants (e.g., result head acceleration), were generated, along with peak values for head and chest accelerations, and the calculated value of HIC, neck loads and Nij, chest deflections, along with any other needed metrics. In addition to ATD instrumentation, the heavy duty UDIG hardware was instrumented with four, 3 axis load cells to collect time-force histories and a triax accelerometer to allow for inertial compensation of these measures.

Restraints

Restraint conditions for the frontal sled tests were chosen based on simulation results. The seatbelts used during tests were supplied by ZF, and included a 9-mm torsion bar which corresponds to a load limit of around 3kN. The anchorage locations of seatbelts B and D match the conditions set up in their respective volunteer test setup. The frontal impacts with airbags all used a SCaRAB with a 20-mm vent, also based on simulations. The simulated dashboard for mounting the frontal airbags was located at a spacing of 100 mm relative to the closest feasible condition.

Results

Frontal testing

Appendix C shows time-sequenced photos of the frontal tests from the right side and overhead cameras. Table 28 shows key injury measures from the frontal test series, while Table 29 shows the probability of injury to each body region and overall. Probability of head injury is consistently low across test conditions. Neck injury risk is below 10% for all conditions, and highest for the two tests run with the small female ATD. (Because the neck injury risks are low and some of the signals noisy, confidence on significant variations between test conditions is low; inspection of signals indicates that neck injury risk may be lower for AW2101 compared to AW2012, and AW2105 compared to AW2106.) Thorax injury risk is higher with the suboptimal geometry conditions compared to optimal, and highest for the last two tests run with the power wheelchair. Excursion measures are in Table 30. All tests met the WC19 requirements for head, knee, and wheelchair excursion, except AW2114 where the original power wheelchair attachments failed.

Table 28. Peak injury measures from frontal sled tests.

Run #	HIC 15	HIC 36	Chest 3 ms (g)	Chest Deflect (mm)	Upper Neck Res F(N)	Upper Neck Res M (Nm)	Lower Neck Res F (N)	Lower Neck Res M (Nm)
units			g	mm	N	Nm	N	Nm
AW2101	77	133	28.4	22.0	1150*	94	1300*	330
AW2102	122	273	28.7	19.6	1550	118	2041	452
AW2103	85	151	25.7	33.2	1350*	71	1425	150
AW2104	400	479	26.4	33.4	2940	136	3421	447*
AW2105	106	199	31.1	23.9	1300*	29	-	-
AW2106	177	294	28.9	23.7	1325	29	-	-
AW2111	78	171	35.1	34.2	1364	89	1603	403
AW2112	86	175	35.6	33.7	1338	71	1699	376
AW2113	172	309	36.1	31.8	1921	97	1595	540*
AW2114	292	434	42.5	39.8	1977	155	4480	--
AW2115	231	294	40.7	41.6	1525	31	1562	46

*estimated from noisy or compromised signal data.

Table 29. Injury probabilities for frontal tests.

Test ID	P(HIC15)	P(Nij)	P(chest)	Pjoint without femur	
AW2101	0.0%	6.2%	1.8%	7.9%	-
AW2102	0.0%	5.8%	1.3%	7.0%	
AW2103	0.0%	5.6%	6.5%	11.7%	
AW2104	2.4%	8.3%	6.7%	16.5%	
AW2105	0.0%	9.1%	2.3%	11.2%	
AW2106	0.1%	6.8%	2.2%	9.0%	
AW2111	0.0%	5.2%	7.2%	12.0%	
AW2112	0.0%	5.6%	6.9%	12.1%	
AW2113	0.1%	5.9%	5.7%	11.3%	
AW2114	0.8%	6.3%	12.2%	18.5%	
AW2115	0.3%	6.4%	14.3%	20.0%	

Table 30. Maximum excursion measures from frontal sled tests.

Test	ATD	WC	Restraint	Head ex (mm)	Knee ex (mm)	WC ex (mm)	Front wheel	Rear wheel
AW2101	50M	SWCB	Optimal + AB	459	243	68	8	8
AW2102	50M	SWCB	Optimal	495	237	60	1	5
AW2103	50M	SWCB	Suboptimal + AB	543	220	63	8	11
AW2104	50M	SWCB	Suboptimal	595	219	62	5	13
AW2105	5F	SWCB	Optimal + AB	309	156	55	5	9
AW2106	5F	SWCB	Optimal	348	150	52	8	11
AW2111	50M	M att1	Suboptimal + AB	513	313	32	-45	24
AW2112	50M	M att2	Suboptimal + AB	532	302	26	-71	11
AW2113	50M	M att1*	Suboptimal + AB	577	322	23	-65	18
AW2114	50M	P att1	Suboptimal + AB	587	508	598	692	599
AW2115	50M	P att2	Suboptimal + AB	510	189	107	25	29
WC19 Limits				650	375	200		

*lighter UDIG anchors

Frames of peak excursion are shown in Figure 115 for the first six tests. The images from the first four tests with the mid-size male illustrate the differences when using optimally positioned belts, and realistic belt position from the volunteer tests representing a D-ring mounted on the C-pillar. Injury risk was lower with the optimal belt geometry, but was acceptable for the realistic condition as well. The fourth and fifth test of the series were run with the small female ATD to examine response of a smaller occupant using belt geometry optimized for the midsized male. Response was acceptable; the smaller stature naturally led to reduced forward excursions.

The first six tests illustrate the benefits of using the SCaRAB as a supplemental restraint. For the three sets of paired tests, head excursion ranged from 40 to 50 mm less with the SCaRAB. The airbag made a bigger difference in reducing excursion with the realistic geometry compared to the optimal geometry predicted from the simulations. For the two conditions with the optimal geometry, the overall injury risk was 11 to 20% higher with the airbag, likely because of the relatively low injury risk among all the tests and calculations based on some noisy signals. For the realistic geometry conditions, the overall injury risk was 40% lower with the airbag.

The next three tests were run with the same model of manual wheelchair used in the volunteer tests. A new wheelchair was used in each test. These three tests demonstrated the frontal crashworthiness of the original attachment design, a lighter attachment design, and the lighter anchorage design. These tests also demonstrated how a restraint system designed using the

SWCB worked with a commercial product. Overall injury risks were similar among the three docking conditions. One difference is that the ATD interacted differently with the SCaRAB in AW2113. Review of video indicates that the airbag just deployed slightly to the left rather than straight ahead when first filling. As a result, head and neck injury measures were slightly higher for this test compared to the previous two. However, the kinematics during the test show that the SCaRAB still provided protection when the ATD head missed the first part of the airbag but contacted the second part located closer to the dashboard.
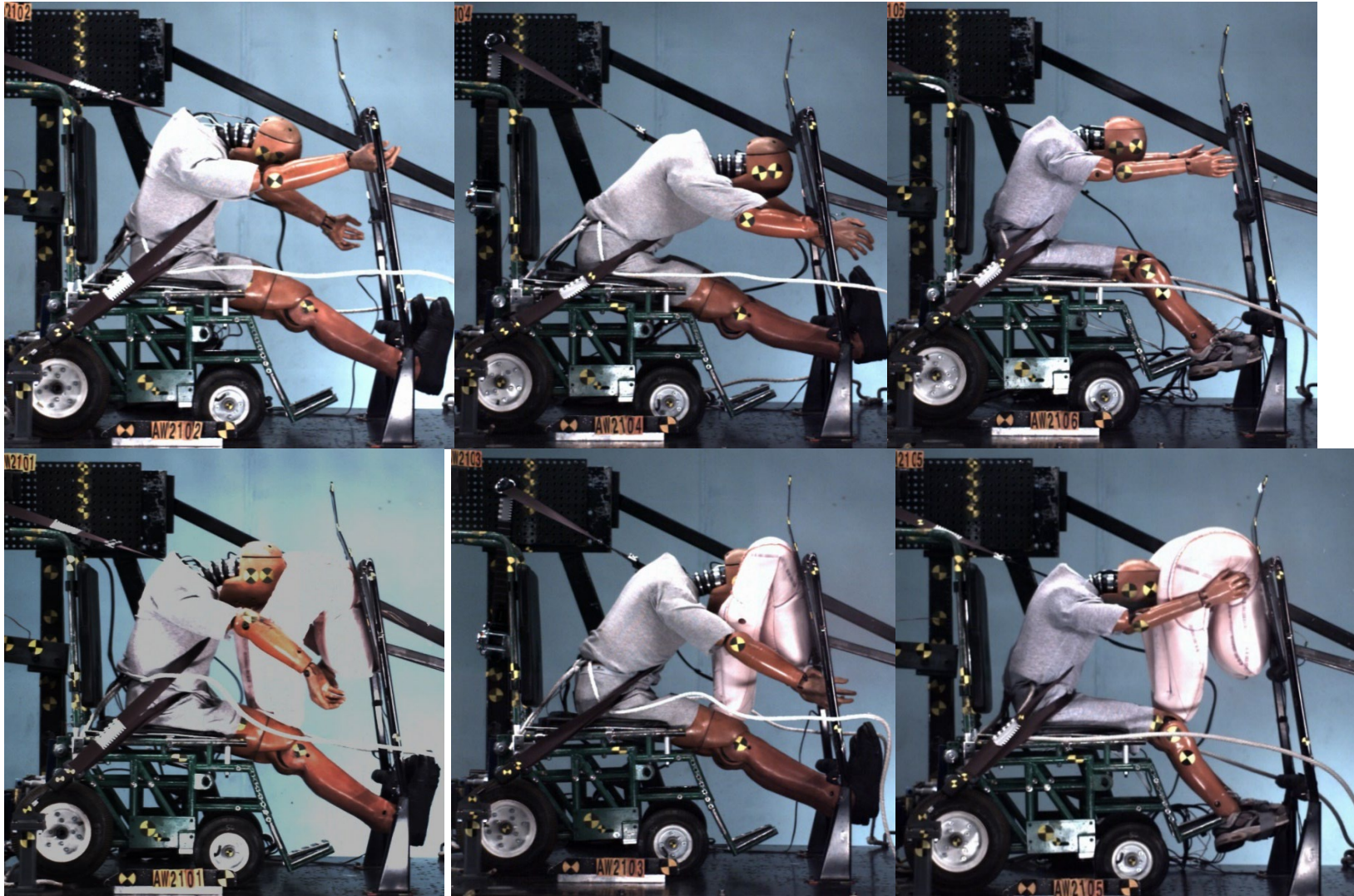
Figure 115. Peak excursion for first six frontal tests. Top row: no airbag. Bottom row: with airbag. Left column: 50th male ATD, optimal geometry. Middle column: 50th male ATD, suboptimal geometry. Right column: 5th female ATD, optimal geometry.
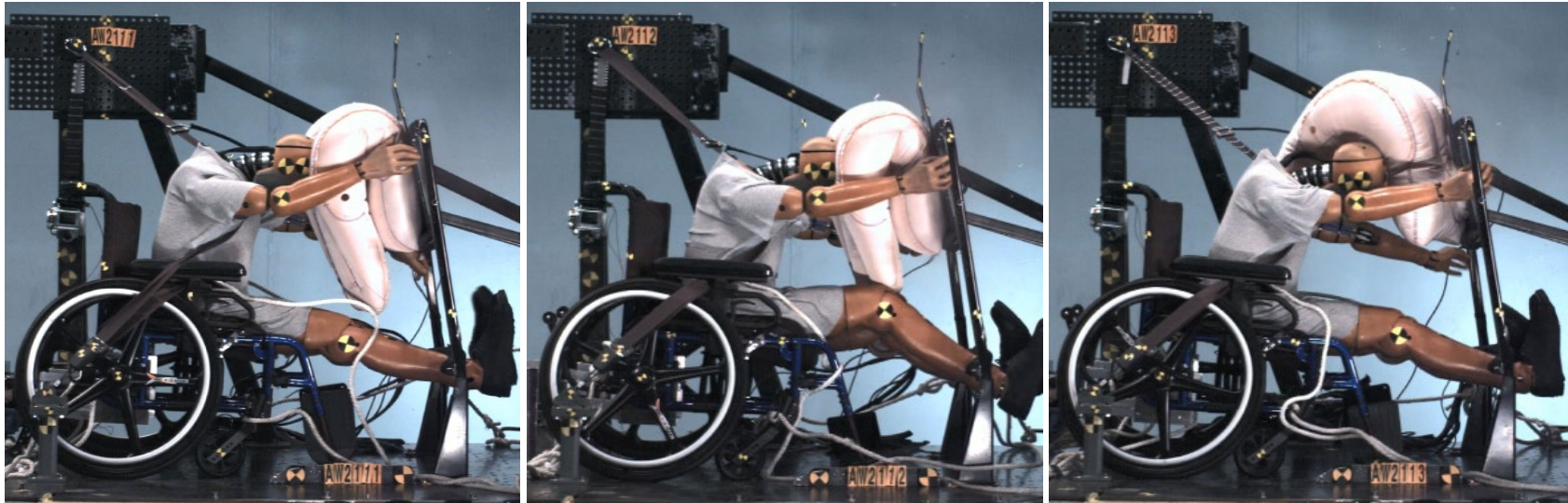
Figure 116. Illustration of peak excursion with the manual wheelchair and 50th male ATD when wheelchair is secured by original attachments (left), lighter attachments (center), and lighter anchors (right).

The final two frontal tests evaluated the attachments for the commercial power wheelchair. In the first test, the attachments failed, shearing the top two bolts that connected the vertical and deforming the horizontal components as shown in Figure 117. Because the power wheelchair sustained no significant visible damage, stronger attachments were constructed for the second test and performed as desired. Figure 118 shows the differences between the two designs. In the first test, 3/8"-16 grade 5 bolts (rated at 4422 lbf shear strength) failed. The second test used 3/8"-16 grade 8 bolts (rated at 6296 lbf shear strength) worked. (Because the vertical rod components of the UDIG attachments are 7/8" diameter, larger bolts were not used because of concerns about weakening the rod.) In addition, many of the aluminum components were replaced with steel.
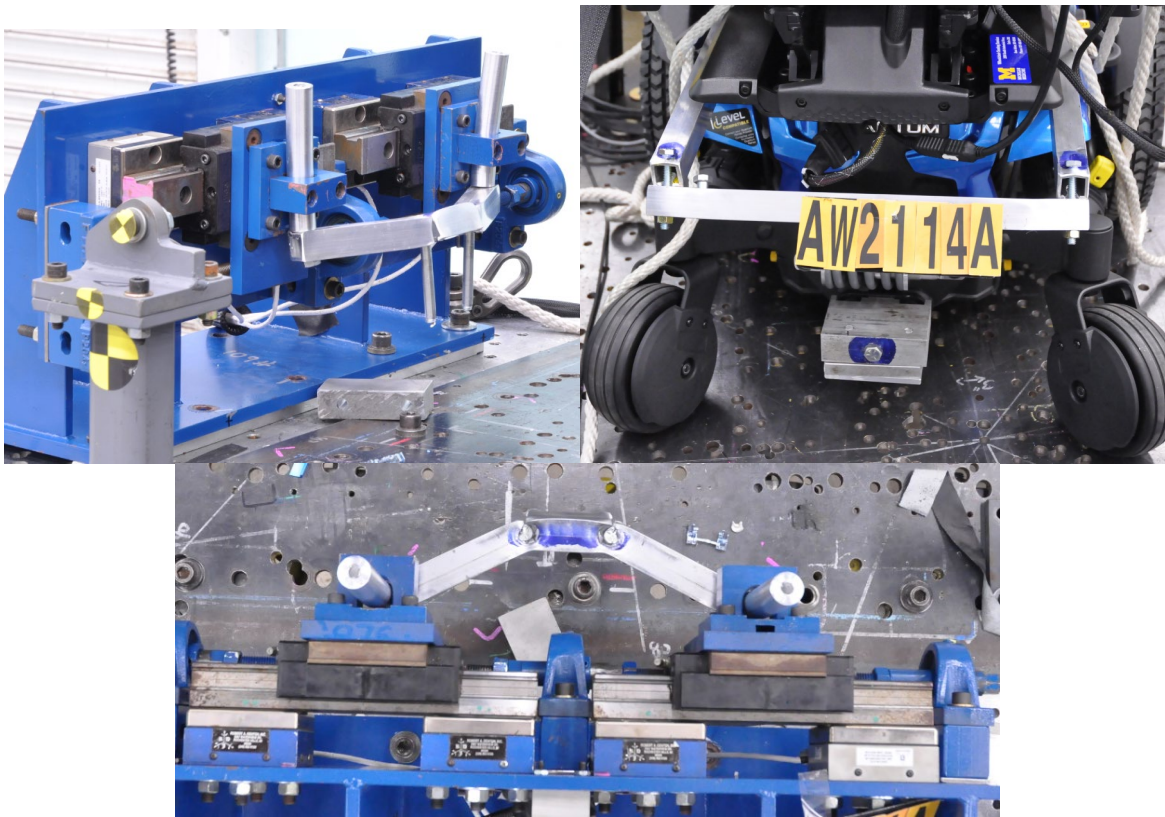
Figure 117. Damaged wheelchair attachments from test AW2114.
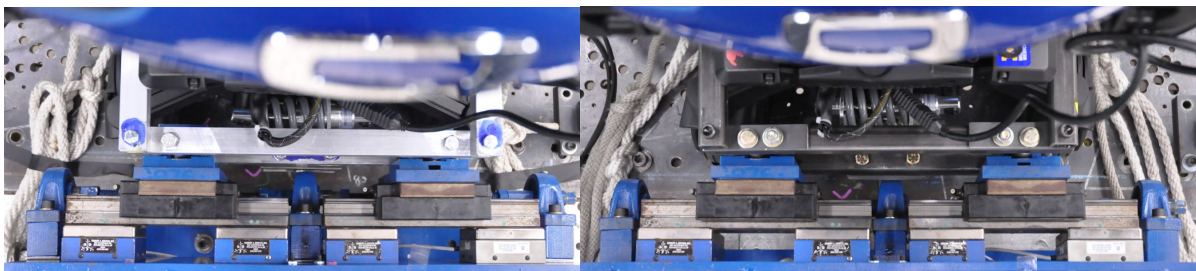
Figure 118. Comparison of original (left) and stronger (right) attachments for power wheelchair.
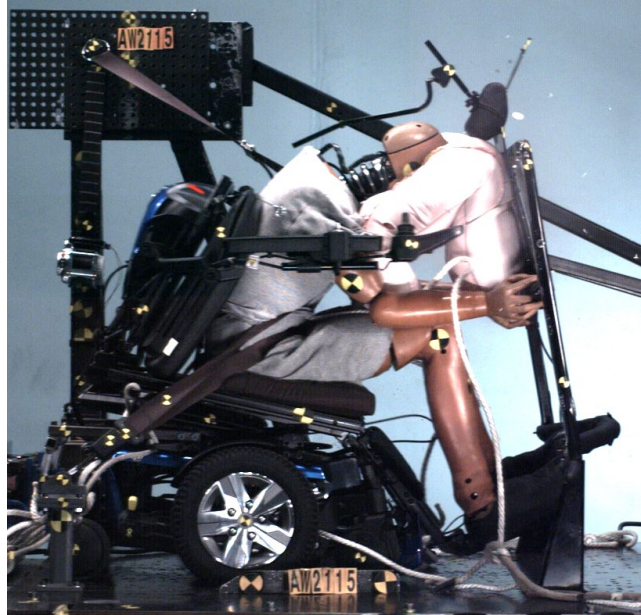
Figure 119. Peak excursion of 50th male ATD in power wheelchair.

The UDIG anchorage loads, measured at four locations, are shown in Figure 120 for tests with the manual wheelchair and the two tests with the power wheelchair, with and without failure. To design attachments for other products, multiplying the mass of the wheelchair by the sled deceleration will estimate the total attachment force. After multiplying by a safety factor of 2, divide the total force by four, assuming equal loading over the four bolts in the attachment, and use the resultant forces as the design targets for selecting hardware. This process should ensure attachments strong enough to meet WC19 test conditions.
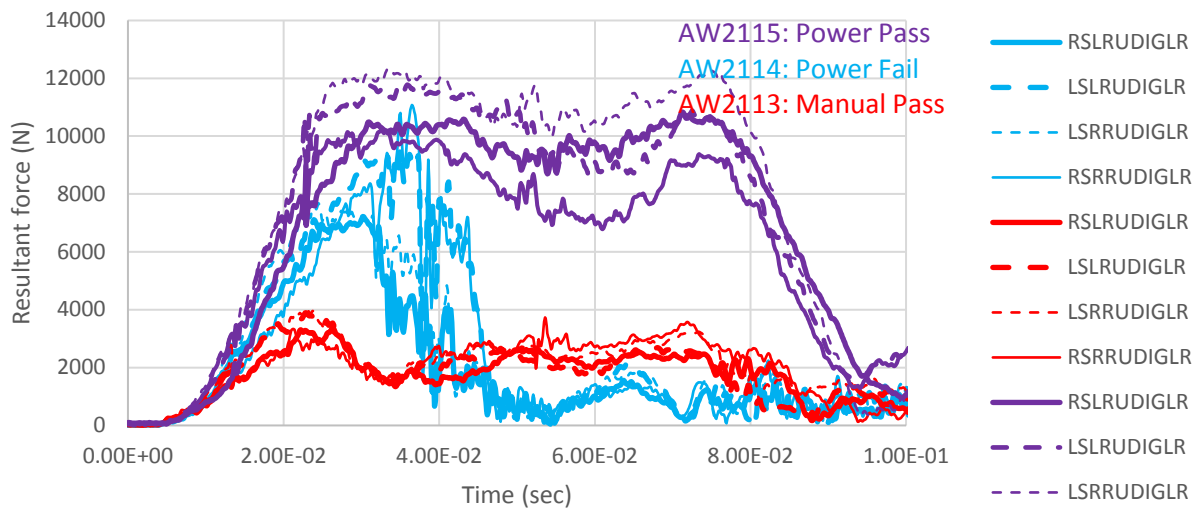
Figure 120. Comparison of UDIG resultant loads for tests with manual wheelchair and power wheelchair, with and without failure.

139

Appendix D includes drawings of the wheelchair attachments and lighter UDIG anchors used during sled testing. It also includes drawing for a geometry of a wheelchair seating station using the optimal geometry (B) used in testing, with the D-ring as an origin. This should provide guidance for locating a wheelchair seating station incorporating a UDIG anchor relative to a vehicle-mounted D-ring.

Side Impact Testing

Table 31 contains key injury measures from the side impact tests, while Table 32 shows the injury probabilities by body region and overall. Neck loads were not collected in the first three tests. Injury risk calculations used rib deflection rather than rib acceleration because of available instrumentation. Test AW2119 was performed with the SID-IIs rather than the ES2-RE, so had slightly different instrumentation. All injury risks were close to zero across all test conditions.

Excursion measures are shown in Table 33. Wheelchair excursions were similar in all tests with the SWCB, but substantially larger with the manual wheelchair. Head excursions were highest in the test performed with the CATCH-H design, followed by the CATCH-V*.

Table 31. Key measures from side impact sled tests.

Measure	2107:V	2108: H	2110: V+	2116: V'	2117: V*	2118: V'	2119: V'
Peak Sled accel (g)	24.1	24.1	24.6	22.8	23.6	23.2	22.6
Delta V (km/hr)	19.0	19.0	18.6	18.3	18.6	18.9	18.6
Peak Head R (g)	36.4	50.1	40	32	32.4	33.6	40
HIC 15	87	230	125	76	57	83	54
HIC 36	134	309	217	131	114	111	79
Upper Neck Fr (N)				712.5	666.4	420.2	676.8
Upper Neck M R (Nm)				329.5	68	60.7	26.1
Upper rib D (mm)	3.8	5.3	5	7.2	9.1	5.2	8.3
Middle rib D (mm)	4	5	4.3	2.7	7.2	-10.3	10.2
Lower rib D (mm)	4	3	3.7	5.6	7.4	6	10.2
Lower spine R (g)	16.1	16.6	22	16.2	16.3	28	34
Front Ab Fy (N)	77.5	55.8	77.5	54.8	41.6	379.2	6
Middle Ab Fy (N)	-30	-30.1	-45.7	-24.6	-28.8	97	7.9
Rear Ab Fy (N)	-26	-24.6	-34	105.7	127.5	147.1	
Pubic force min (N)	-1211	-1363	-1635	-1035	-1507	-1390	
Pubic force max (N)	1042	1023	1301	922	743	171	
Pev R (g)	25.6	26.5	32.8	25.4	27.7	37.1	24.9
UDIG Left Res (N)	20916	22392	22394	19683	24057	3032	23460
UDIG Left C Res (N)	4451	4500	5765	5253	6271	7626	6126
UDIG Rt C Res (N)	7793	8366	11172	13728	10517	2820	10869
UDIG Rt Res (N)	17768	19032	11635	14067	15213	2899	15324
Lumbar Fr R (N)							1172.3
Lumbar Mo R (Nm)							51
Left Iliac Wing Fy (N)							597.5
Left Acetabulum Fy (N)							885.2

Table 32. Injury probabilities from side impact sled tests.

	2107:V	2108: H	2110: V+	2116: V'	2117: V*	2118: V'	2119: V'
ATD	ES2-RE	ES2-RE	ES2-RE	ES2-RE	ES2-RE	ES2-RE	SID-IIS
WC	SWCB	SWCB	SWCB	SWCB	SWCB	Manual, att 1	SWCB
P(HIC36)	0.000	0.010	0.003	0.000	0.000	0.000	0.000
P(chest)*	0.000	0.000	0.000	0.000	0.000	0.000	0.000
P(abdominal)	0.003	0.003	0.003	0.003	0.003	0.006	0.000
P(pelvic)	0.002	0.002	0.002	0.001	0.001	0.001	0.007
Pjoint(AIS 3+)	0.005	0.014	0.007	0.005	0.004	0.006	0.008

Table 33. Excursion measures from side impact sled tests.

Test	ATD	WC	Restraint	WC ex (mm)	Head ex (mm)	Shld ex (mm)	Hip ex (mm)	Knee ex (mm)
AW2107	ES2-RE	SWCB	CATCH-V	77	443	497	572	581
AW2108	ES2-RE	SWCB	CATCH-H	93	602	533	709	556
AW2110	ES2-RE	SWCB	CATCH-V	81	413	365	391	529
AW2116	ES2-RE	SWCB	CATCH-V'	96	458	419	512	583
AW2117	ES2-RE	SWCB	CATCH-V*	82	517	451	622	541
AW2118	ES2-RE	Manual, att 1	CATCH-V'	228	440	304	288	627
AW2119	SID-IIS	SWCB	CATCH-V'	90	400	304	417	418

The first two side impact tests evaluated two versions of the CATCH bag. As shown in Figure 112, one design (V) had vertical inflation channels, while the other (H) had horizontal inflation channels and a sewn window section. When reviewing the kinematics (including times of peak excursion in Figure 113 and Figure 114), the horizontal channels allowed more flexing of the lower part of the airbag. From the overhead view, the vertical channels appear provide more resistance to lateral ATD motion, consistent with the measured excursions.

Figure 121. Comparison of CATCH-V (left) and CATCH-H (right).
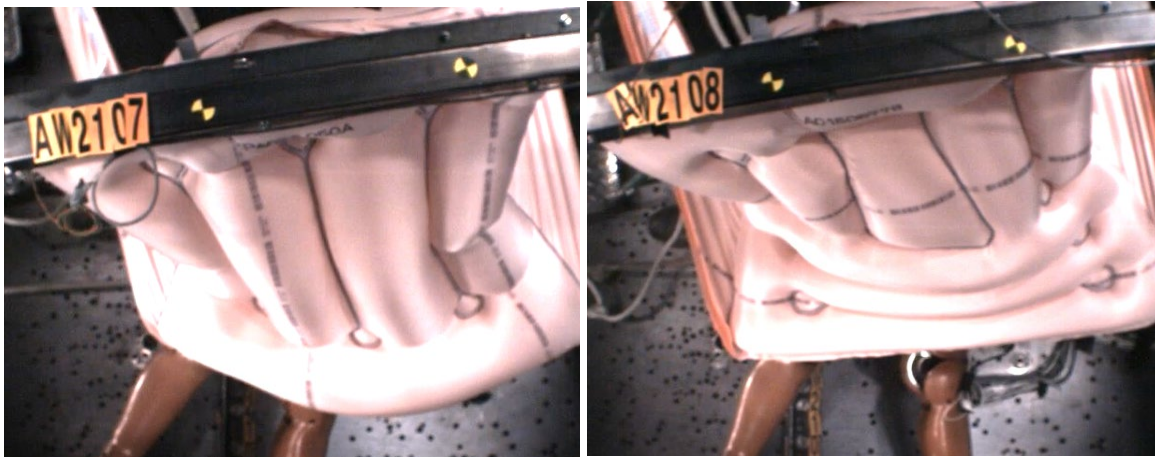
Figure 122. Overhead view at time of peak excursion for test AW2107 with CATCH-V and AW2108 with CATCH-H.
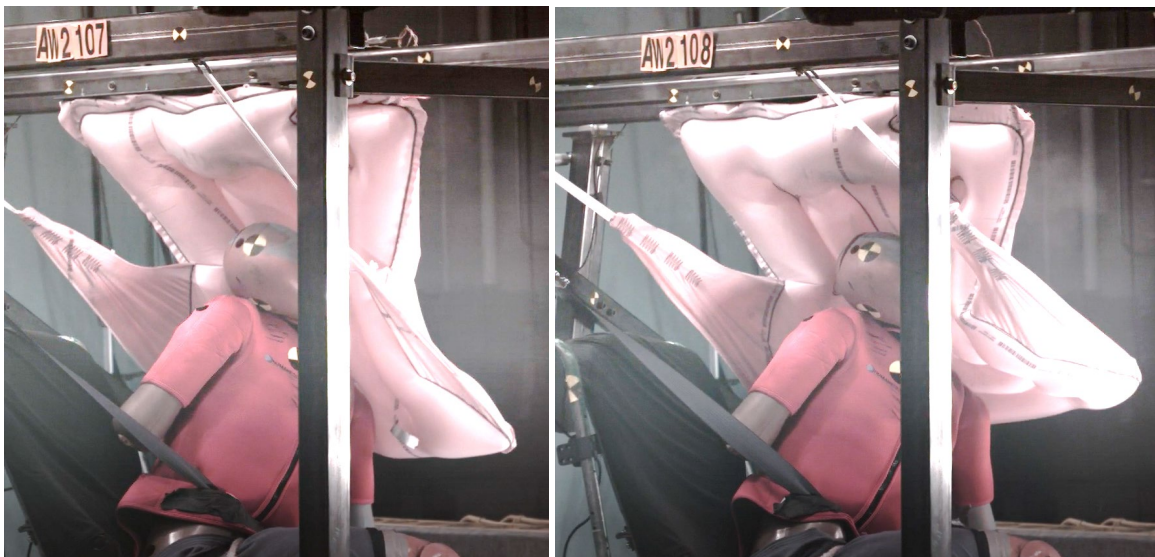
Figure 123. Rear oblique view at time of peak excursion for test AW2107 with CATCH-V and AW2108 with CATCH-H.

After reviewing the first two tests, we realized that shifting the tether locations from the ones used in the model could potentially restrict the CATCH bag to remain in a more vertical position, which could improve its ability to resist ATD lateral motion. Figure 115 shows the differences between the original and shifted positions. Figure 116 shows the difference in peak excursion between the two tests run with CATCH-V bags and the tether locations 1 and 2 (reference lines are aligned with the same chest target in each test).

Figure 124. Static photos of sled buck showing location of CATCH bag when tethers reach the point of no slack with tether location 1 (left) and tether location 2 (right).

Figure 125. Front view at time of peak excursion for test AW2107 (left) and AW2109 (right), showing reduced lateral excursion with tether location 2.

Review of the initial performance of the CATCH bags with our colleagues at ZF led us to choosing the CATCH-V design as potentially more promising for subsequent tests. In addition, they noted that the original tether straps were cut as one piece with the main CATCH fabric, which led to them being cut on the bias. For a revision, they suggested cutting tether straps on the grain and sewing them to slightly different locations on the main part of the CATCH. They also suggested trying a slight modification to the CATCH-V that might achieve what was intended for the CATCH-H to reduce neck loading.

The difference in tether design between CATCH-V and CATCH-V' are shown in Figure 117. Figure 118 compares the time of peak excursion with the original CATCH-V and the CATCH-V' with the different tether design; both used tether location 2. The amount of lateral movement is similar, but the redesigned tethers led to the ATD being more upright at the time of peak excursion as seen by the horizontal reference lines. This leads to the shoulder being more upright and less lateral bending of the neck.

Figure 126. CATCH-V (left) with original tether design and CATCH-V' (right) with alternative tether design.
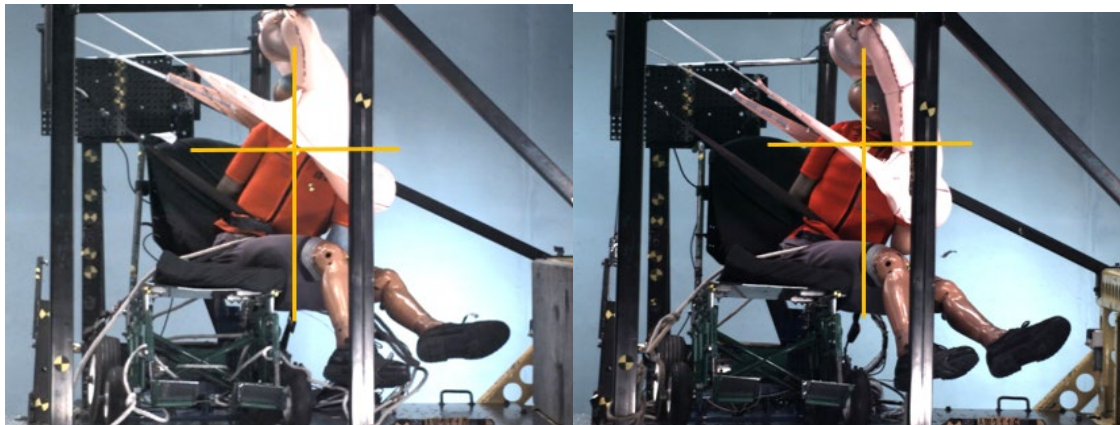
Figure 127. Front view at time of peak excursion for test AW2109 (left) and AW2115 (right), showing more upright posture with alternative tether design.

Figure 119 compares the structural differences between the CATCH-V' and CATCH-V*, while Figure 120 shows the difference in peak excursions in tests run with each. The window in the CATCH-V* allows bending of the airbag, so it does not provide restraint below the upper shoulder as seen with the CATCH-V'. This places the window above the head, higher than intended. As a result, the CATCH-V' seems to do a better job at reducing lateral torso excursion and retaining the ATD in the wheelchair.

Figure 128. Design differences between CATCH-V' (left) and CATCH-V* (right).
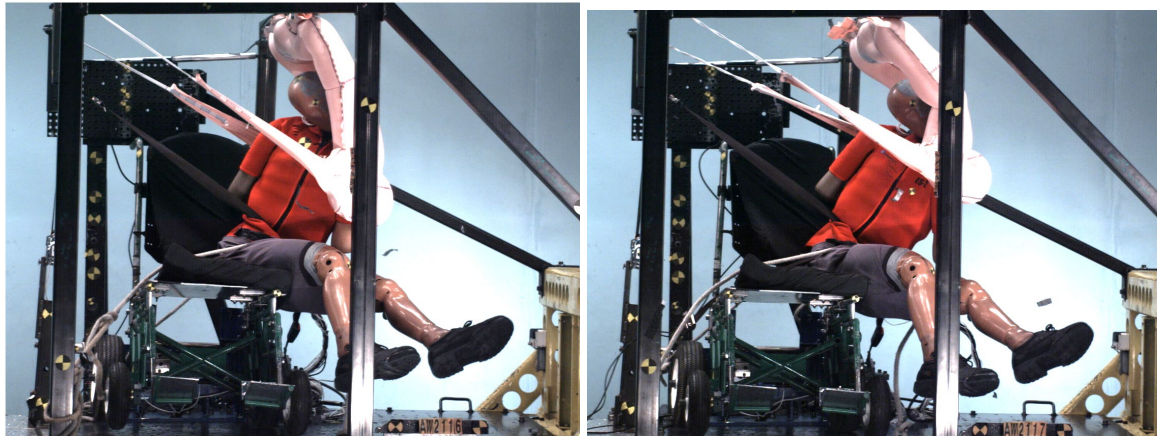
Figure 129. Side view of peak excursion between CATCH-V' (left) and CATCH-V* (right).
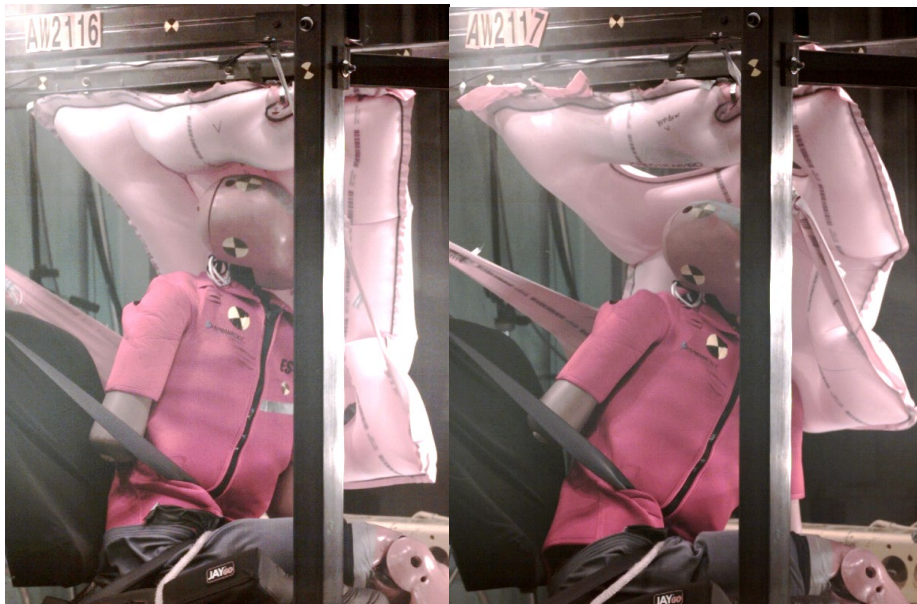
Figure 130. Oblique view of peak excursion between CATCH-V' (left) and CATCH-V* (right).

Figure 122 and Figure 123 shows the differences using the CATCH-V' using the SWCB without armrests and the manual wheelchair with armrests. The UDIG-compatible wheelchair attachments proved to be crashworthy under these farside loading conditions. The armrests on the manual wheelchair helped keep the ATD's pelvis in the seat better. Because the manual wheelchair is less rigid than the SWCB, the whole chair rotated more. In addition, as shown in Figure 133, the right seat rail, cross member, and left frame separated from the right-side frame (with wheels attached) during the test. However, the rotation and component separation of the manual wheelchair, as well as the armrests, allowed the ATD to remain more upright and reduced amount of neck loading.
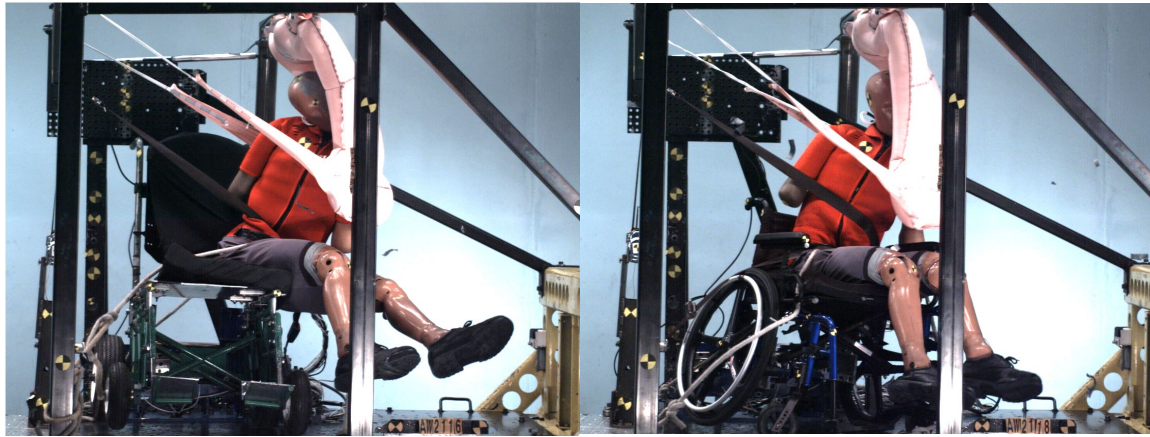
Figure 131. Peak excursion between SWCB (left) and manual wheelchair (right) using CATCH-V'.
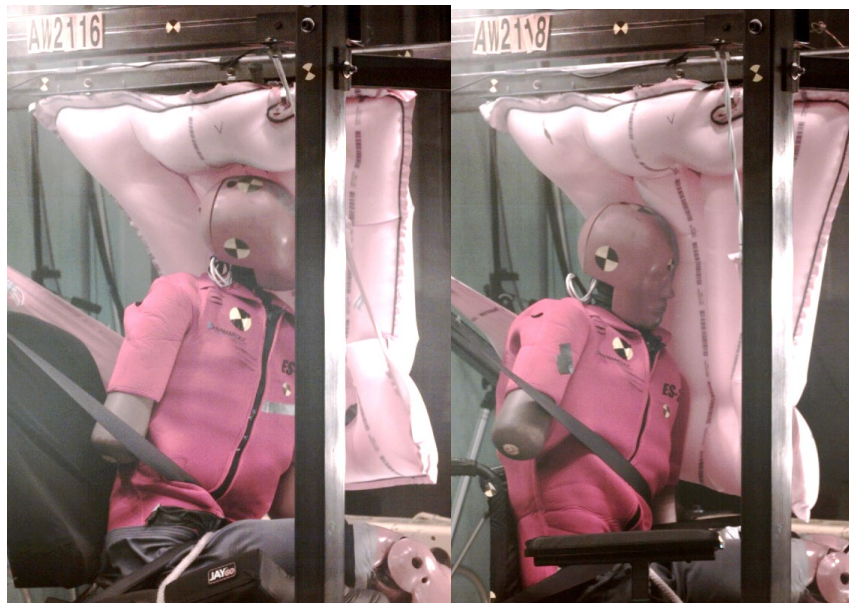
Figure 132. Peak excursion between SWCB (left) and manual wheelchair (right) using CATCH-V'.

Figure 133. Damage to manual wheelchair during test AW2118.

Finally, Figure 124 and Figure 125 show the difference in kinematics with the CATCH-V' between the ES2-RE and the SID-IIS. The belt is more effective at keeping the smaller ATD within the wheelchair space, so the CATCH-V' does not need to provide as much restraint.

Figure 134. Peak excursion between ES2-RE (left) and SID-IIS (right) using CATCH-V' and SWCB.

Figure 135. Peak excursion between ES2-RE (left) and SID-IIS (right) using CATCH-V' and SWCB.

Comparison of Simulations and Tests

Figure 136 and Figure 137 show exemplar comparisons between the model-predicted responses before the tests and actual frontal crash testing results, and Table 34 shows the ATD injury measure comparison between the simulations and the tests. In general, the models provided reasonable estimates of the wheelchair and ATD kinematics, restraint interactions to the ATD, and ATD injury measures.
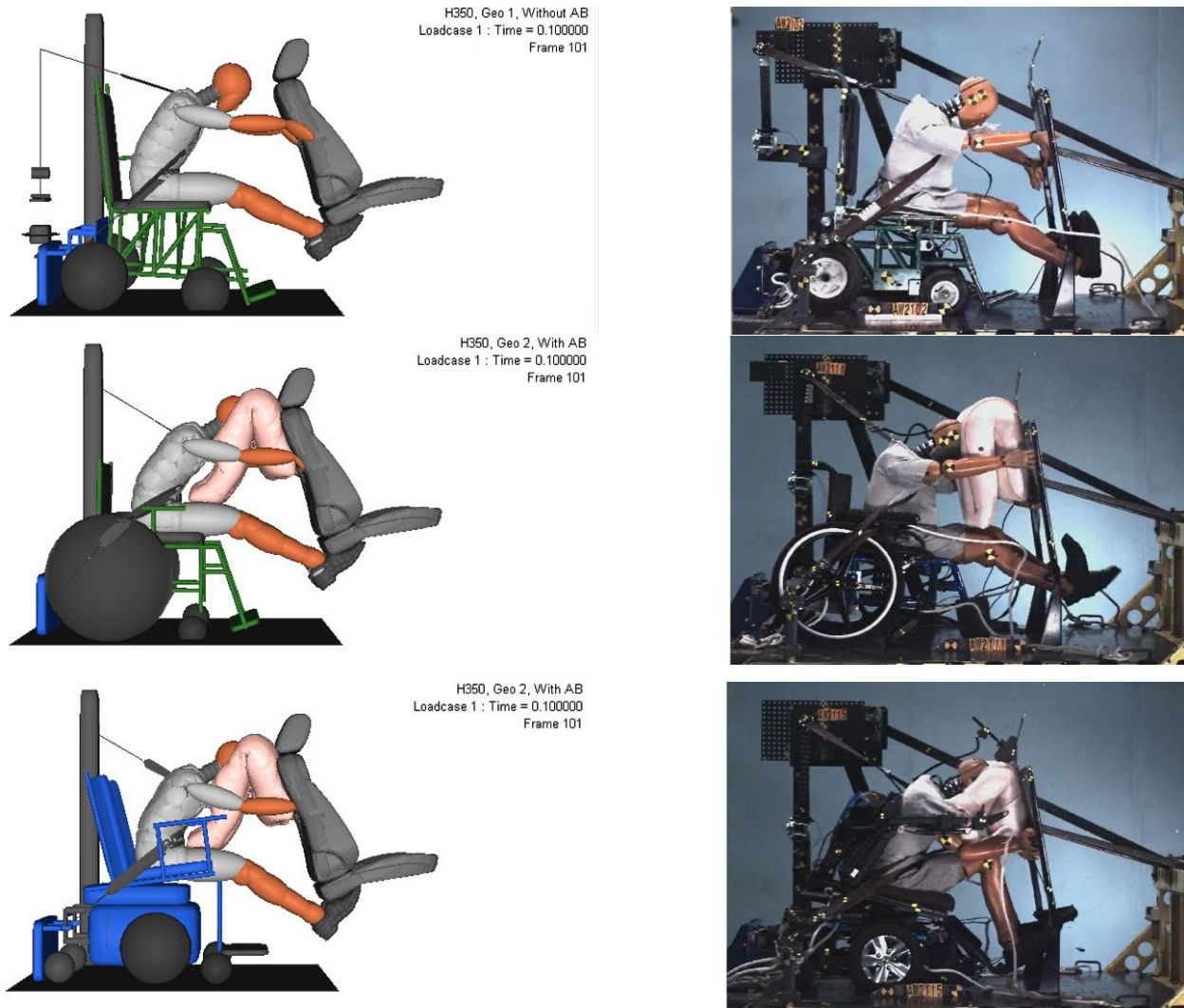
Figure 136. Exemplar comparisons between the model-predicted and tested ATD kinematics in three frontal crash testing conditions (Top: SWCB with no airbag, Middle: Manual chair with SCARaB, Bottom: Power chair with SCARaB)
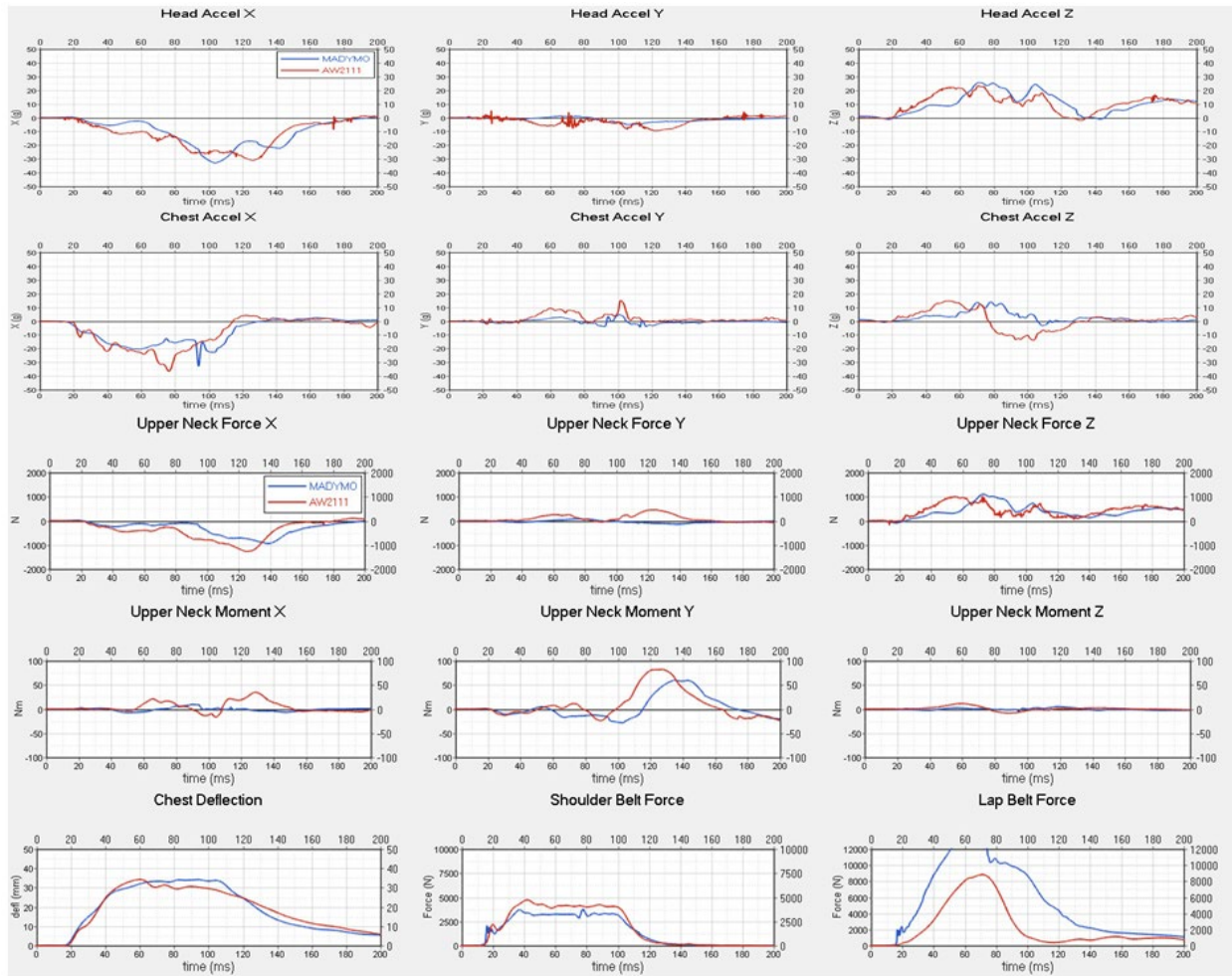
Figure 137. Exemplar comparisons between the model-predicted and tested ATD responses in a frontal crash condition with manual chair and SCARaB.

Table 34. Injury measure comparisons between the simulations and tests in six frontal crash test conditions.

TestID	Type	WC	ATD	HIC15	HIC15 Madymo	NIJ	NIJ Madymo	Chest D (mm)	Chest D Madymo (mm)
AW2101	Frontal	SWC	H350	77	54	0.26	0.24	22.0	19.8
AW2102	Frontal	SWC	H350	122	82	0.22	0.34	19.6	19.6
AW2103	Frontal	SWC	H350	85	63	0.2	0.27	33.2	28.9
AW2104	Frontal	SWC	H350	399	214	0.42	0.43	33.4	28.9
AW2111	Frontal	Manual	H350	79	126	0.16	0.27	34.2	34.2
AW2115	Frontal	Power	H350	230	87	0.28	0.24	41.6	36.9

Discussion

Challenges Implementing UDIG-compatible hardware

We were able to successfully design and install UDIG-compatible attachment hardware for the two wheelchair models purchased for the study. The power wheelchair attachments included horizontal components, while the manual wheelchair attachments did not. The specifications for UDIG on the wheelchair only require the two vertical components shown in Figure 126. An optional horizonal element that spans the width of the two vertical bars is helpful for limiting rearward rotation of the wheelchair during an impact event. The wheelchair manufacturer can choose to include this horizontal feature if extra dynamic rotation control is needed or desired. The vehicle portion of the UDIG docking system should be able to function with wheelchairs that provide either just the vertical bars or the vertical bars and the horizontal element. The work to date shows that for most manual wheelchairs, good performance can be achieved with attachment just to vertical bars because they align well vertically at the typical CG location for the occupied wheelchair. This allows manual wheelchairs to retain a folding feature along the seat centerline for storage of the wheelchair. Some power wheelchairs, particularly those with heavy powered seating units, improve the dynamic crash performance more by including the horizontal bar. The inclusion of a horizontal piece connecting the two members for additional strength and stability may be particularly useful under side impact conditions. Future research could investigate the possibility of adding a crosspiece with a mechanism similar to that used to lock a ladder in its deployed position. This would allow the crosspiece to be compatible with folding wheelchair models.
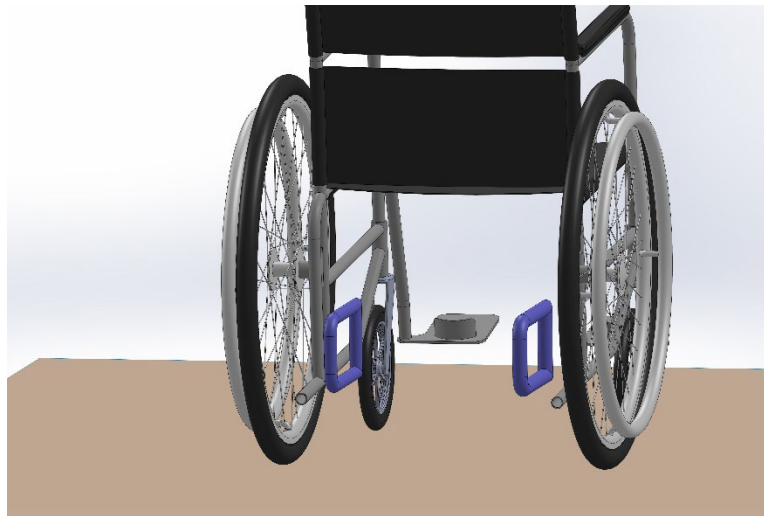
Figure 138. Diagram of required UDIG attachment components in blue.

An unexpected issue during implementation was the allowable tolerance on the vertical locations of the UDIG anchorages and attachments. There is some flexibility in locating the UDIG hardware to allow it to be used with wheelchairs of different sizes. When installing the UDIG anchorages in the BIW, we checked with the manual wheelchair to ensure that the anchorage height would be compatible. However, when pilot testing began, the weight of a

153

participant caused the attachments to shift downward and just missed being able to engage with the hooks. The tolerances in the UDIG specifications should be evaluated to consider how the geometry shifts when an occupant is using the wheelchair, or when tire pressure varies.

Dynamic sled testing showed good results in frontal tests with both the original and redesigned attachments for the manual wheelchair (which addressed advocate concerns about the mass of the original attachments). The data collected from the two frontal tests with the powerchair provide insight on the attachment strength needed to secure a heavier power wheelchair. While the original manual attachments were successfully tested in side impact, future side impact testing to evaluate the strength of the lighter manual attachments and the stronger attachments for the powerchair wheelchair would help demonstrate the viability of automated docking using the UDIG concept.

Our study specifically chose wheelchairs that have been designed to meet the voluntary WC19 standards defining crashworthiness in frontal impacts. Over the course of the project, as we shared preliminary findings, it was disappointing to learn that many advocates for safe travel in wheelchairs were not aware of the "transit" (WC19-compliant) option for their wheelchairs. Even though the RESNA WC19 standard has been in place since 1999, most wheelchairs sold do not comply with the standard. One barrier is lack of awareness of WC19 wheelchairs by clinicians who prescribe and fit wheelchairs, as well as their patients. Even when a prescriber is considering transportation needs, a wheelchair with features that meet the patient medical needs may not also be available in a model that complies with WC19. Particularly in the case of acute trauma, the need or desire of the patient to travel in a motor vehicle is often not considered when the wheelchair is specified and ordered. Many people who were injured note that later in their recovery process when they are trying to return to work, school or to live independently, the lack of a WC19 wheelchair adversely impacts their choices, but because the typical replacement cycle for a wheelchair is every 5 years, they are not able to easily remedy the situation.

Another barrier is wheelchair manufacturers' reluctance to develop and promote WC19 wheelchairs. While some manufacturer test and promote these products widely, it is more common for manufacturers to have concerns related to increased product liability with providing WC19 compliant wheelchairs despite legal professionals noting that their liability is also increased by not making safe provision for a foreseeable use of their products. While there are hundreds of wheelchair makes and models that do comply with the standard, they are often not identified as such and most wheelchair order forms do not prompt the user to consider the option at the time of purchase. (WC19 wheelchairs can be identified by the presence of four attachment points marked with the WC19 symbol.) Instead, prescribers often must specifically seek out compliant products through direct queries to the manufacturer. Additionally, some manufacturers will only sell WC19 wheelchairs if the specific set of supplied features of the wheelchair exactly match that of the models that have been tested, rather than doing more testing or an engineering risk analysis to determine which models can confidently be sold as WC19 compliant hardware based on available test data.

Wheelchairs are expensive pieces of durable medical equipment that are typically paid for by third party payers, namely private insurance companies and Federal insurance/assistance programs such as Medicare and Medicaid. The precedent set by Medicare is to only cover the cost of durable medical equipment that is "medically necessary to maintain daily activities safely in the home." This is commonly referred to as the in-home restriction and has been unsuccessfully challenged in U.S. Congress since its inception. Travel in a motor vehicle happens outside the home and therefore the WC19 option on a wheelchair is often refused for reimbursement. Although outside the Federal system, the in-the-home restriction sets a reimbursement precedent that is usually followed by private insurers. Medicaid will consider covering costs for items used outside the home that reduce need for institutional care. There are also ways for the prescriber to advocate for coverage of the WC19 option, but this requires extra letters of justification and a high level of awareness by the prescriber. The added cost for this option is usually $200 to $400 extra and represents a modest percentage of the total cost of a wheelchair (the price of a wheelchair meant for daily use approximately ranges $2000 to $15,000 and up). Currently, there are no wheelchair manufacturers that allow retrofitting of the WC19 hardware after purchase. There have been CMS codes established for WC19 wheelchair features, in hopes that this would encourage reimbursement, but so far, the effect on available hardware has been minimal. Some notable exceptions to lack of reimbursement for WC19 wheelchairs is the Department for Veterans Affairs healthcare system that in some cases requires wheelchairs purchased for veterans to comply with WC19, and school districts that promote use of crashworthy wheelchairs and are willing to advocate for reimbursement or provide funds to cover WC19 compliant products.

While these issues were not specifically covered through our research project, collaborative efforts among different government agencies that might result in crash-tested wheelchairs being the default rather than the exception would be beneficial for advancing the safety of occupants who use wheelchairs as vehicle seating. The widespread availability of crash-tested wheelchairs with options for UDIG hardware and securement points for 4-point strap tiedowns could advance independent accessibility options for situations other than AVs, including planes and traditional public transportation.

Wheelchairs in Side and Rear Impacts
This project addressed wheelchair occupants in frontal and farside impacts. Prior to this study, limited research had been conducted on wheelchair crashworthiness in side impacts (Manary 2005). When conducting side impact validation tests for the current study, it was challenging to set up a robust D-ring location in the location specified by WC19 that did not lead to unrealistic head contact with non-vehicle-fidelic structures. In addition, there are no standardized methods of simulating a generic interior door contact or striking vehicle intrusion that would be useful for evaluating side impact crashworthiness of wheelchairs and ATD kinematics in a realistic manner.

The farside test conditions and simulations primarily used the SWCB fixture, originally designed and validated for testing aftermarket wheelchair seating systems in frontal impact. The SWCB

structure was damaged and needed repair after the first round of lateral sled tests. Compared to the single test using the manual wheelchair, the SWCB was stiffer under the farside impact conditions. Some of this may have resulted from failure of several components of the manual wheelchair during the side impact test. However, the movement of the commercial manual wheelchair, and presence of armrests, helped the ATD have better interaction with the CATCH airbags compared to the tests with the SWCB. Collecting more data on the side impact performance of production wheelchairs, including assessment of armrest designs, would be beneficial for developing and validating an updated version of the SWCB for use in side impact that is more realistic and durable in this crash mode.

Side impact simulations incorporated planar seat cushion, which is commonly used as the sub surface for wheelchair users who need complex seating. In contrast, flexible fabric seat surfaces are most often appropriate for wheelchairs that are used for short periods of time by people who can more easily transfer out of the wheelchair for travel in motor vehicles. Previous work has shown that the flexible, fabric seat improves occupant retention in side impact. However, given the limited awareness of the availability of wheelchair transportation safety features by consumers and medical practitioners and the medical needs of the target population, this does not seem to be a viable option for improving side impact protection. In addition, some people use custom-molded seat cushions to improve comfort that may not be compatible with seating features that enhance side impact protection.

The scope of this project did not address rear impact safety, but more than one volunteer provided feedback that they had concerns about head restraint in rear impacts. A procedure has been established for testing FF wheelchair in rear-impact scenarios along with a test procedure for vehicle-mounted head and back restraint that enhance rear impact protection once people are positioned in the wheelchair station. Whether provided on the wheelchair or only in the vehicle wheelchair station, the key to good protection in rear impact is back support that extends to the rider's shoulder along with an appropriately positioned head restraint. However, many people, particularly those who use manual wheelchairs, do not need a high backrest or headrest to meet their medical needs and in many cases a high back rest will impede torso turning and sideward/backward reaching tasks that are essential to activities of daily living. In contrast, many people in power wheelchairs do need a high seatback and head rest all the time, so these features could be designed to provide rear impact protection without an adverse impact on occupant range of motion or function. Having rear-impact protection features built into the wheelchair allows for close fit of the back/head supports to the individual. Good fit of a vehicle mounted head and back restraint is much more difficult to achieve because of the range of wheelchair designs and the presence of hardware or accessories on the back of the wheelchair. To optimize occupant protection in rear impacts, it would be ideal if wheelchair users who aren't adversely impacted by a high back/head support have one that also provides rear impact protection, while the vehicle provides head and back support for those who cannot tolerate it on their wheelchair.

An additional complication is that while head restraints designed for vehicle occupant protection and head supports designed for wheelchairs may visually appear similar, very few wheelchair head supports are designed to have the protective characteristics of vehicle head restraints. To protect an occupant in rear impact, a head restraint should have automotive grade padding, be positioned close to the posterior surface of the occupant head, have sufficient height to align with head CG, and be firmly attached to the seating. In some cases, wheelchair head supports will detach during impact and increase injury potential. In many cases, the wheelchair head support does perform some of the functions of a vehicle head restraint. The desirable characteristics for a wheelchair head support that can function as a vehicle head restraint are documented in design guidelines for the rear impact test method included in the voluntary WTS standards.

Belt Fit and Donning System Usability

Qualitatively, the belt fit recorded on the volunteers after they self-donned the belt was disappointing, particularly because the volunteers were instructed on elements of good belt fit at the beginning of the test session. They were also instructed to adjust the belt so it fit well, and ask for help if necessary. In our pilot testing with seven different UMTRI personnel (none were regular wheelchair users), belt fit was reasonable for most people and conditions. Some of this belt fit success for the pilot participants can be attributed to heightened awareness of the importance of good belt fit among auto safety researchers. Some of the regular study participants were physically incapable of adjusting their belt fit, some had posture issues that were not conducive to good belt fit, and some did not wish to adjust their belt fit. Most wore bulkier clothing than the pilot participants. While many of the belt fits were disappointing, we know from other studies of volunteer belt fit that many members of the general public are not aware of how seatbelts are supposed to fit, and we have observed poor belt fit on many volunteers, particularly those with higher BMI. However, typical front-row occupants with poor belt fit have a knee bolster available that can help prevent excessive forward movement from submarining under a poorly positioned lap belt. Providing a similar knee restraint may not be possible while also meeting the space requirements for wheelchair maneuverability.

With only eight participants, we were able to document several challenges to achieving good belt fit for people with disabilities. However, because of our requirement that people be able to transfer to our study wheelchairs, these participants represent relatively low levels of impairment across the spectrum of physical disabilities typical of wheelchair users.

UDIG Dynamic Performance

While this was not a main focus of the validation simulations, we noticed differences in the kinematics of the ATD in wheelchairs secured by UDIG compared to past simulations where the 4-point strap tiedown or a traditional docking system was used to secure the wheelchair. Figure 139 shows a comparison of a wheelchair secured by UDIG docking (left), 4-point strap tiedown

(middle) and traditional docking station (right). In previous work, the higher securement attachment point provided by the 4-point strap tiedown securement limited the ability of the wheelchair to rotate forward (down at the seat front), which decreases risk of submarining. Traditional docking allows users to secure the wheelchair independently, but it also attaches to the bottom of the wheelchair and allows the wheelchair to rotate/pitch forward with the ATD in frontal crashes. These kinematics are undesirable because they may induce submarining. The UDIG system seems to reduce the wheelchair forward pitching motion compared to the traditional docking, and at the same time allows users to secure the wheelchair independently.

Figure 139. Comparison of peak forward excursion in frontal crash simulations with UDIG, 4-point strap tiedown and traditional docking.

Improving Belt System Function

When setting up the test fixtures, ZF provided the longest typical seatbelts they had available. Unfortunately, this was not long enough to allow the seatbelts to be held out of the wheelchair station by the donning system fixture to allow the participant to easily maneuver the wheelchair into position. We spliced approximately 46 cm (18 in) more length onto each seatbelt to address the issue. However, the seatbelt retractor spring strength is tuned to the length of the belt, and adding length means that it had more webbing on the spool, and as it retracted, it was not able to snug the belt around the participant as it normally would. As a result, we instructed participants to snug the belts around themselves during testing. This problem could be addressed in an actual installation by using a stronger retractor spring, adding an additional retractor to the lap belt, or using a smart retractor that snugs the belt around the participant prior to the vehicle moving.

Our previous study of volunteers in their own vehicles customized for use with a wheelchair as seating indicated that many of them used the seatbelt to provide postural stability during normal travel. Our partner ZF has a smart retractor product available, ZF Active Control Retractor (ACR-8) shown in Figure 140 and described Table 35, which is a motorized seatbelt retractor that actively manages seat belt tension. The last two features listed may be particularly useful for an occupant seated in a wheelchair. If the Belt Park Assist function

158

automatically retracts the webbing into the retractor after unbuckling, it may make it easier for the occupant to navigate out of the wheelchair seating station without becoming entangled in the belt system. While many production belt systems just need to be pulled from the retractor one more time to encourage spooling of webbing after unbuckling, this action may be a challenge to someone using a wheelchair. The Slack Removal feature, which slowly applies a low tension to the belt after buckling, would address a problem commonly seen in our past studies, because occupants seated in wheelchairs may lack the dexterity to adjust the belt so it is snug on themselves. Some of the subjects in our past studies have indicated that they also use the seat belt to help stabilize their torso posture while traveling, as they may have less muscular control because of their disability. Extra effort needed to address COVID issues during volunteer testing prevented us from developing a fixture to simulate the retractor functions and evaluate what level of tension is sufficient to provide support while remaining comfortable. Given that the availability of this product shows that it would be feasible to offer variable resting belt tension for occupants in wheelchair seating stations, future research efforts might evaluate the potential benefits for wheelchair users with a fixture to simulate the functions of this retractor for volunteer testing.
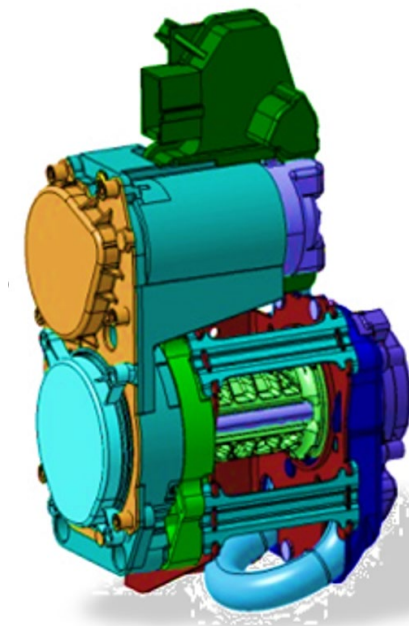
Figure 140. Diagram of the ACR-8

Table 35. Features of the ACR-8

Function Name	Examples of pertinent vehicle conditions	ACR seat belt behavior	Retraction force
Pre-crash	Crash is probable	Highest force and pull-in speed when crash seems unavoidable	>200 N
Full retract, longitudinal	Panic brake or AEB	High force and pull-in speed to prepare for possible impact and position occupants for possible airbag deployment.	~170 N
Full retract lateral	Sliding or skidding	High force and pull-in speed to prepare for possible impact and position occupants for possible airbag deployment.	>200 N
Dynamic support, longitudinal	Heavy braking	Medium force and pull-in speed in highly dynamic driving situations to improve occupant coupling and reduce movement during maneuvers.	~70 N
Dynamic support, lateral	Hard lane changes, over- or understeer situations	Medium force and pull-in speed in highly dynamic driving situations to improve occupant coupling and reduce movement during maneuvers.	~70 N
Haptic warning	Driver not paying attention	Seatbelt vibration alerts driver when ADAS determines that driver attention is needed	~50 N
Slack removal	Buckle up and begin travel	Reduce slack in belt with low force at limited pull-in speed	~20 N
Belt park assist	Stop travel and unbuckle	Helps retract belt webbing into retractor when not in use	~20 N

Wheelchair and Occupant Protection System Compatibility

There are many challenges for vehicle manufacturers trying to develop integrated wheelchair seating stations that provide a level of safety for occupants using their wheelchairs as vehicle seating. Because the range of potential wheelchair dimensions is larger than the adjustability range of a vehicle seat, the space that a wheelchair user can occupy is larger than the space

160

occupied by someone in a vehicle seat. While our study showed minimal differences in belt fit for volunteers seated in the manual and power wheelchairs for a particular belt anchoring geometry (compared to differences between volunteers), both of the wheelchairs selected for this study were sized to fit a midsized male occupant. The range of current production wheelchair sizes is larger, and new products under development often focus on accommodating bariatric patients so may be larger than those reported in the University of Buffalo survey (Steinfeld et al., 2010).

While our simulations showed that having lap belt anchors close to the occupant's hips improved protection, anchors must be located so they do not interfere with the required 762 x 1219 mm (30 x 48 in) of clear space for a wheelchair seating station. WC19 wheelchairs have been tested so they can be equipped with a crash-tested lap belt with anchors located on the wheelchair. This should likely provide better belt fit than vehicle-mounted systems, although the vehicle-mounted 3-point belt would need to be used for torso restraint. However, the limited number of WC19 wheelchairs in use with crash-tested wheelchairs means that this method of restraint cannot be expected very often.

Current ADA regulations state that vehicles providing public transport cannot refuse service to passengers even if they do not have the recommended equipment. This means that AVs will likely have to provide anchors for 4-point strap tiedowns and human assistance for using them, or another means of docking without specialized equipment. Until the policy and insurance issues discussed previously are addressed, vehicle manufacturers should expect that most of their passengers will be using wheelchairs not compliant with WC19. In addition, WC19 wheelchairs do not yet have to meet side impact test requirements, as a voluntary standard for dynamic testing has not yet been established.

While the range of belt fits measured on our volunteers was better than what we had seen in our previous study (van Roosmalen et al., 2013), it was generally not ideal. The range of belt fits among our volunteers was comparable to another study performed at UMTRI where the lap belt fit on some participants, particularly those who were obese, were also positioned too high on the abdomen. As mentioned previously, current vehicles provide some backup restraint to compensate for poor belt fit in the form of knee bolsters or the seating row in front. Providing these options would be more challenging for occupants seated in wheelchairs because of the space maneuverability requirements, although a deployable knee bolster might be an option. Rear-facing wheelchair stations may offer an opportunity for a less severe crash environment, and help compensate for suboptimal belt fit. This would only work half the time in AVs that can travel in either direction. For AVs with a distinct forward mode, an equity issue arises if only the wheelchair seating stations are positioned rearward to the direction of travel.

Current passenger vehicles must meet requirements to provide energy-absorbing structures for locations that may have potential for head contact during a crash. Because private vehicles modified for wheelchair use are exempt from many FMVSS requirements, the wheelchair lifts designed to facilitate ingress/egress (which may be considered for AVs) are not currently subjected to these requirements. In addition, our initial prototype belt-donning system would

also not meet these requirements. The potential for injurious head contact by any passenger in an AV from structures intended to accommodate wheelchair users is another challenge.

Configuring the test fixtures for the volunteer study demonstrated that the current spacing between the A-pillar and B-pillar of a minivan does not provide enough space for the required 762 x 1219 mm (30 x 48 in) wheelchair seating station footprint, unless it extends rearward of the B-pillar. If the seating station is positioned to extend rearward of the B-pillar, the wheelchair will likely block part of the side-door entrance, and using a D-ring mounted to the B-pillar will be located too far forward for optimal protection. Development of nontraditional vehicle structures for AVs should consider this vehicle dimension if a front row wheelchair seating station is of interest.

The child restraint system (CRS) certification process has been suggested as an approach for ensuring people seated in wheelchairs can travel safely in vehicles. With this approach, the wheelchair would need to be treated like a belt-positioning booster secured with lower anchors, relying on the vehicle-mounted lap-shoulder belt to provide the restraint. If the wheelchair has a crash-tested lap belt, testing it simultaneously with a vehicle-mounted lap-shoulder belt may also be useful for evaluating expected real-world use conditions. A sled-based side impact procedure would also need to be developed to evaluate structural integrity and attachment strength under lateral loading; the side impact procedure could also evaluate the injury potential of particular armrest designs. Our current study illustrated the limitations of trying to retain the ATD within the wheelchair with just the seatbelts and wheelchair structures during side impact, so the side impact wheelchair test might just consider structural integrity.

For vehicle manufacturers, evaluation of dynamic performance of CRS in vehicles is not required, although they perform evaluations with a limited number of CRS products for due diligence. The assumption for belt-positioning booster seats is that the booster places a child in a position closer to an adult ATD, so seatbelts and airbags designed for adults in the rear seat should adequately protect children in boosters. For people seated in wheelchairs, the seated location may differ substantially from someone in a vehicle seat. Vehicle manufacturers need tools to design effective occupant protection systems for wheelchair seating stations, as well as to evaluate the strength of floors and docking anchors. The SWC or SWCB found in RESNA standards could be used in crashes and simulations of frontal crashes, but modifications would likely be needed for using the fixtures in side impact (as demonstrated by the damage to the SWCB after our first few side impact tests). In addition, procedures would need to be developed to use the fixtures in full-vehicle crash tests, or when evaluating restraint systems through sled-based testing. It may be desirable to have fixtures representing smaller and larger wheelchairs for use with the small female and large male ATDs to check occupant protection systems for a range of occupant sizes.

This project demonstrated the feasibility of using simulations to develop occupant protection systems. Demonstrating effectiveness of restraints designed for wheelchair seating systems through modeling may be an approach to consider.

References

79 FR 4569 - Federal Motor Vehicle Safety Standards; Child Restraint Systems, Child Restraint Systems-Side Impact Protection, Incorporation by Reference, Issue 18 (January 28, 2014).

American National Standards Institute/Rehabilitation Engineering and Assistive Technology Society of North America [ANSI/RESNA]. (2017a). *ANSI/RESNA WC-4:2017: Volume 4: Wheelchairs and transportation; Section 10 [WC10]: Wheelchair containment and occupant retention systems for use in large accessible transit vehicles: systems for rearward-facing passengers.*

ANSI/RESNA. (2017b). *ANSI/RESNA WC-4:2017, Section 20 [WC20]- Wheelchair seating systems for use in motor vehicles.*

ANSI/RESNA. (2017c). *ANSI/RESNA WC-4:2017, Section 18 [WC18] - Wheelchair tiedown and occupant restraint systems (WTORS) for use in motor vehicles.*

ANSI/RESNA. (2017d). *Wheelchairs: ANSI/RESNA WC-4:2017, Section 19 [WC19] - Wheelchairs used as seats in motor vehicles.*

Americans With Disabilities Act of 1990, 42 U.S.C. ch. 126 § 12101 et seq., July 26, 1990.

Auto Alliance. (2019). *AVs and increased accessibility*.

Bayless, S. H., & Davidson, S. (2019). *Driverless cars and accessibility: Designing the future of transportation for people with disabilities. Transportation Research Board.*.

Bertocci, G. E., Hobson, D. A., & Digges, K. H.. (2000). Development of a wheelchair occupant injury risk assessment method and its application in the investigation of wheelchair securement point influence on frontal crash safety. *IEEE Transactions on Rehabilitation Engineering, 8*(1).

Bertocci, G. E., Szobota, S., Hobson, D. A., & Digges, K. (1999). Computer simulation and sled test validation of a powerbase wheelchair and occupant subjected to frontal crash conditions. *IEEE Transactions on Rehabilitation Engineering, 7*(2):234–44.

Bertocci, G. E., Manary, M. A., & Ha, D. (2001). Wheelchairs used as motor vehicle seats: Seat loading in frontal impact sled testing. *Medical Engineering and Physics, 23*(10).

Brumbaugh, S.. (2018, September). *Travel patterns of American adults with disabilities*. Bureau of Transportation Statistics.

Buning, M. E., Bertocci, G. E., Schneider, L. W., Manary, M. A., Karg., P., Brown, D., & Johnson, S. (2012). RESNA's position on wheelchairs used as seats in motor vehicles. *Assistive Technology, 24*(2).

Cabrolier, L., D'Souza, R., Bertocci, G. E., Tiernan, J., & Simms, C. (2013, September 11-13). *The influence of shoulder and pelvic belt floor anchorage location on wheelchair occupant injury risk: A simulation study*. 2013 IRCOBI Conference, *Gothenburg, Sweden*.

Claypool, H., Bin-nun, A., & Gerlach, J. (2017). *Self-driving cars: The impact on people with disabilities*. Ruderman Family Foundation.

D'Souza, C., Steinfeld, E., Paquet, V., & Feathers, D. (2010). Space requirements for wheeled mobility devices in public transportation. *Transportation Research Record: Journal of the Transportation Research Board*.

Dsouza, R., & Bertocci, G. E.. (2010). Development and validation of a computer crash simulation model of an occupied adult manual wheelchair subjected to a frontal impact. *Medical Engineering and Physics, 32*(3).

Erickson, W., Lee, C., & von Schrader, S. (2018). 20*17 Disability statistics report*. Institute on Employment and Disability, Cornell University.

Frost, K. L., Bertocci, G. E., & Salipur, Z. (2013). Wheelchair securement and occupant restraint system (WTORS) practices in public transit buses. *Assistive Technology, 25*(1).

Hobson, D. A., & van Roosmalen, L.. (2007). Towards the next generation of wheelchair securement— Development of a demonstration UDIG-compatible wheelchair Docking Device. *Assistive Technology, 19*(4):210–22.

Hu, J., Fischer, K., Lange, P., & Adler, A. (2015, April). Effects of crash pulse, impact angle, occupant size, front seat location, & restraint system on rear seat occupant protection. *SAE Technical Papers*.

Hu, J., Orton, N. R., Manary, M. A., Boyle, K. J., & Schneider, L. W.. (2020). Should airbags be deactivated for wheelchair-seated drivers? *Traffic Injury Prevention, 0*(0):1–6.

Hu, J., Reed, M. P., Rupp, J. D., Fischer, K., Lange, P., & Adler, A. (2017). Optimizing seat belt and airbag designs for rear seat occupant protection in frontal crashes. *Stapp Car Crash Journal*.

Hu, J., Wu, J., Reed, M. P., Klinich, K. D., & Cao, L. (2013). Rear seat restraint system optimization for older children in frontal crashes. *Traffic Injury Prevention*.

John A. Volpe National Transportation Systems Center. (2018, July). *U.S. Department of Transportation public listening summit on automated vehicle policy*. U.S. Department of Transportation. www.transportation.gov/sites/dot.gov/files/docs/policy-initiatives/automated-vehicles/314091/usdot-public-listening-summit-automated-vehicle-policy-summary-report.pdf

Kahane, C. J. (2013, November). *Effectiveness of pretensioners and load limiters for enhancing fatality reduction by seat belts* (Report No. DOT HS 811 835). National Highway Traffic Safety Administration. https://crashstats.nhtsa.dot.gov/Api/Public/Publication/811835

Kang, W., & Pilkey, W. D.. (1998). Crash simulations of wheelchair-occupant systems in transport. *Journal of Rehabilitation Research and Development, 35*(1):73–84.

Karg, P., Buning, M. E., Bertocci, G. E., Fuhrman, S., Hobson, D. A., Manary, M. A., Schneider, L. W., & van Roosmalen, L.. (2009). State of the science workshop on wheelchair transportation safety. *Assistive Technology: The Official Journal of RESNA, 21*(3):115–60.

Manary, M. A., Ritchie, N. L., Flannagan, C. A. C., Bertocci, G. E., & Schneider, L. W.. (2009, June 24-27). *The effects of pelvic belt anchoring location on wheelchair seating system loads in frontal impact motor vehicle crashes.* RESNA [Rehabilitation Engineering and Assistive Technology Society of North America] 32nd Annual Conference, New Orleans, LA.

Manary, M. A., Ritchie, N. L., & Schneider, L. W.. (2005, November 8). *Wheelchair and crash dummy response in far-side lateral impacts*. RESNA 28th Annual Conference, Atlanta, GA.

Manary, M. A., Ritchie, N. L., & Schneider, L. W.. (2010). WC19: A wheelchair transportation safety standard-Experience to date and future directions. *Medical Engineering and Physics, 32*(3):263–71.

Manary, M. A., Woodruff, L. M., Bertocci, G. E., & Schneider, L. W.. (2003, June 19-23). Patterns of wheelchair response and seating-system failures in Frontal-Impact sled tests. RESNA 26th International Annual Conference, Atlanta, GA.

McDonnell, G., D'Souza, R., Bertocci, G. E., Tiernan, J., & Simms, C. (2012, October 12-14). *The influence of pelvic-belt angle on wheelchair occupant injury risk: A simulation study*. 2012 IRCOBI Conference, Dublin, Ireland.

National Mobility Equipment Dealers Association. (2019). *NMEDA guidelines*.

Orton, N. R, van Roosmalen, L., & Schneider, L. W.. (2019). *Summary of occupant, wheelchair tiedown and occupant restraint system configuration data for wheelchair-seated drivers and front-row passengers in private vehicles*.

Orton, Nichole R., van Roosmalen, L., & Schneider, L. W.. (2019, November). *Summary of occupant, wheelchair Tiedown and occupant Restraint system configuration data for wheelchair-seated drivers and Front-Row Passengers in Private Vehicles*. Transportation Research Board.

Ritchie, N. L., Manary, M. A., Bertocci, G. E., & Schneider, L. W.. (2006, June 22 - 27). *Validation of a surrogate wheelchair base for evaluation of wheelchair seating system crashworthiness*. RESNA 29th Annual Conference, Atlanta, GA.

Ritchie, N. L., Manary, M. A., van Roosmalen, L., & Schneider, L. W.. (2009, June 24-27). *The role of armrest design in positioning of belt restraints on wheelchair-seated drivers*. 32nd RESNA conference, New Orleans, LA.

Ritchie, N. L, Manary, M. A., van Roosmalen, L., & Schneider, L. W.. (2009, June 24-27). The role of armrest design on positioning of belt restraints on wheelchair-seated drivers. 32nd RESNA conference, New Orleans, LA.

Salipur, Z., & Bertocci, G. (2010). Development and validation of rear impact computer simulation model of an adult manual transit wheelchair with a seated occupant. *Medical Engineering and Physics, 32*(1).

Schneider, L. W., Klinich, K. D., Moore, J. L., & MacWilliams, J. B. (2010, April). Using in-depth investigations to identify transportation safety issues for wheelchair-seated occupants of motor vehicles. *Medical Engineering and Physics, 32*(3).

Schneider, L. W., & Manary, M. A.. (2006). Wheeled mobility tiedown systems and occupant restraints for safety and crash protection. In J. M. Pellerito Jr. (ed.), *Driver Rehabilitation and Community Mobility*. Mosby, Inc.

Schneider, L. W., Manary, M. A., Hobson, D. A., & Bertocci, G. E.. (2008). Transportation safety standards for wheelchair users: A review of voluntary standards for improved safety, usability, and independence of wheelchair-seated travelers. *Assistive Technology, 20*(4).

Schneider, Lawrence W., Manary, M. A., Orton, N. R., Hu, J., Klinich, K. D., Flannagan, C. A. C., & Moore, J. L. (2016, July). *Wheelchair occupant Studies* (UMTRI Report No. UMTRI-2016-8) National Highway Traffic Safety Administration. www.nhtsa.gov/sites/nhtsa.gov/files/umtri-2016-8-wheelchairoccupantstudies.pdf

Steinfeld, E., Paquet, V., D'Souza, C. D., Joseph, C., & Maisel, J. (2010. *Anthropometry of wheeled mobility project*. U.S. Access Board, National Institute for Disability and Rehabilitation Research [U.S. Department of Education].

Turkovich, Michael J., van Roosmalen, L., Hobson, D. A., & Porach, E. A. (2011). The effect of city bus maneuvers on wheelchair movement. *Journal of Public Transportation, 14*(3).

van Roosmalen, L., G. E. Bertocci, Hobson, D. A., & P. Karg. (2002). Preliminary evaluation of wheelchair occupant restraint system usage in motor vehicles. *Journal of Rehabilitation Research and Development, 39*(1).

van Roosmalen, L., Karg., P., Hobson, D. A., Turkovich, M. J., & Porach, E. . (2011). User evaluation of three wheelchair securement systems in large accessible transit vehicles. *The Journal of*

Rehabilitation Research and Development, 48(7):823.

van Roosmalen, L., Orton, N. R., & Schneider, L. W.. (2013). Safety, usability, & independence for wheelchair-seated drivers and front-row Passengers of private vehicles: A qualitative research study. *Journal of Rehabilitation Research and Development, 50*(2):239–52.

van Roosmalen, L., Reeves, S. A., & Hobson, D. A. (2003, June 19-23). *Effect of universal docking interface geometry (UDIG) placement on wheelchair and occupant kinematics*. RESNA 26th Annual Conference, Atlanta, GA.Weir, Q. J. A., Eby, B. J., Manary, M. A., Orton, N. R., & Schneider, L. W.. (208, June 28-30). *A seat belt deployment system for drivers seated in wheelchairs*. RESNA 31st Annual Conference, Arlington, VA.

Wiacek, C., Prasad, A., Weston, D., Orton, N. R., & Schneider, L. W.. (2017, June 5-8). *Assessing the performance of steering wheel air bags for drivers seated*. *25th International Technical Proceedings on the Enhanced Safety of Vehicles (ESV), Detroit, MI*.

Yang, R. J., Wang, N., Tho, C. H., Bobineau. J. P., & Wang, B. P. (2005). Metamodeling development for vehicle frontal impact simulation. *Journal of Mechanical Design, Transactions of the ASME*.

Appendix A: Volunteer Testing Documents

Participant Screening Script

Participant Screening Script

Email to interested participants

Thank you for your interest in our study about traveling in vehicles while seated in a wheelchair. We would like to schedule a time where we can call you to tell you more about our study. Can you please let us know your availability on xx days? And can you confirm that we can call you at xx number?

We prefer to talk to you to answer any questions, but if it would be easier for you to fill out a form instead, please let us know.

Participant Screening Script

Volunteer Participant AWTORS Study

Thank you for volunteering for this study about traveling in vehicles while seated in a wheelchair. I need to ask you several questions to see if you qualify for our study.

How old are you?
> *Reject if less than 19 or older than 65*

Are you pregnant?
> *Reject if pregnant*

Do you use a wheelchair regularly?

> *Reject if they are not a wheelchair user.*

Can you and are you comfortable transferring from your wheelchair into another wheelchair independently or with minimal assistance?
> *Reject if no.*

What is your name, email address and/or contact number?

Let me tell you a little more about the study. You will be coming to our lab on north campus. We will ask you to transfer to a different wheelchair and get in and out of a parked van, dock the wheelchair, and apply a seatbelt. We will take videos and pictures of you throughout the process, as well as some measurements with a handheld scanner. Then we will ask you to complete a survey about your experience. Do you think you will be able to do this several times over the course of two hours?

To keep everyone safe during testing, everyone entering the building needs to go through a health check and temperature screening by our building greeter. We have set up our tests so our researchers will be less than 6 feet from you for less than 15 minutes over the two-hour test session. Our experimenters will be wearing fabric face masks and plastic face shields. We will also give you a fabric mask to wear during testing that you can keep, and ask you to wear

a plastic face shield during testing. We will reschedule testing if you or any of the researchers have any symptoms of illness. We will disinfect our wheelchairs and equipment before and after each test session. Does this sound OK?

Reminder Email

This is a reminder about your appointment to participate in our research study at UMTRI tomorrow at xx. If you have any symptoms of illness, please contact us to reschedule your session. When you arrive at UMTRI, please park in a visitor's spot, and enter through the main doors. Our greeter will perform the health check required for everyone to enter the building. They will also give you a parking pass and a facemask to wear during the study. Please call xx if you have any questions or need to reschedule.

UNIVERSITY OF MICHIGAN
CONSENT TO BE PART OF A RESEARCH STUDY

1. KEY INFORMATION ABOUT THE RESEARCHERS AND THIS STUDY

Study title: Development of an Automated Wheelchair Tiedown and Occupant Restraint System

Principal Investigator: Kathleen D. Klinich, PhD, University of Michigan Transportation Research Institute

Study Sponsor: National Highway Traffic Safety Administration

You are invited to take part in a research study. This form contains information that will help you decide whether to join the study.

1.1 Key Information

Things you should know:

- The purpose of the study is to evaluate new hardware and seatbelt designs that should make it easier and safer to travel in vehicles while seated in a wheelchair.
- If you choose to participate, you will be asked to transfer from your wheelchair to a wheelchair that has special docking attachment hardware. We will then have you try out different wheelchair docking hardware and seatbelt designs in a vehicle mockup. Photos, videos, and scanned measurements will be taken during these trials and a survey will be given following each trial. At the end of all of the trials, a questionnaire will be given regarding your transportation experiences. The test session will take up to two hours.
- Risks or discomforts from this research include frustration when trying out different hardware designs, or discomfort from using a seatbelt that might not fit well. There is a risk of falling from the wheelchair as you maneuver in our test fixture. Breach of confidentiality is also a risk.
- There are no direct benefits for you to participate in this study.

Taking part in this research project is voluntary. You do not have to participate and you can stop at any time. Please take time to read this entire form and ask questions before deciding whether to take part in this research project.

2. PURPOSE OF THIS STUDY

When traveling while seated in a wheelchair, it is important to attach the wheelchair to the vehicle. We are trying to design a way for people to do this without help. We are also designing a seatbelt you can put on by yourself. These designs will be needed to allow safe and independent travel in automated vehicles, where there won't be a driver to help.

3. WHO CAN PARTICIPATE IN THE STUDY

3.1 Who can take part in this study? People 19 to 64 years old who regularly use a wheelchair, but are able to transfer to one of our study wheelchairs, are eligible to participate. You cannot participate if you are pregnant.

4. INFORMATION ABOUT STUDY PARTICIPATION

4.1 What will happen to me in this study?

- Testing will occur in our laboratory at UMTRI.
- We will tell you about the study and obtain your consent.
- We will make sure you can safely transfer to our study wheelchairs, and that you are comfortable using them.
- We will show you where to put stickers on different parts of your body.
- We will take some photos and scans to document your body dimensions.
- We will have you enter the vehicle mockup, and use the hardware to attach the wheelchair and put on the seatbelt. Seatbelt tightness will be varied and we'll ask you about the comfort. Photos and video and will be recorded during this process.
- Then we will document your posture and position using a 3D scanner and photos.
- Then you will remove the seatbelt, undock the wheelchair and exit the mockup. Photos and video and will be recorded during this process. You will fill out a form about the trial.
- We will repeat the trials using at least 8 different configurations, and potentially more if time and comfort allows.
- You will fill out a survey about your personal travel experiences.

4.2 How much of my time will be needed to take part in this study? Up to 2 hours.

5. INFORMATION ABOUT STUDY RISKS AND BENEFITS

5.1 What risks will I face by taking part in the study? What will the researchers do to protect me against these risks?

The highest risk is being frustrated if hardware is difficult to use. There may also be risk of discomfort if our seatbelt system doesn't fit you well. There is also a risk of you falling out of the wheelchair as you drive it in and out of the vehicle mockup. The researchers will try to minimize these risks by padding surfaces and having an experimenter close by to help if needed. You can also choose not to keep the seatbelt on if it is too uncomfortable. You do not have to answer any questions you do not want to answer. Breach of Confidentiality is a risk and the study team will follow data handling procedures and safeguards to minimize this risk.

5.1.1 What happens if I get hurt, become sick, or have other problems because of this research?

The researchers have taken steps to minimize the risks of this study. Please tell the researchers if you have any injuries or problems related to your participation in the study. The University may be able to assist you with obtaining emergency treatment, if appropriate, but you or your insurance company will be responsible for the cost. By signing this form, you do not give up your right to seek payment if you are harmed because of being in this study.

5.2 How could I benefit if I take part in this study? How could others benefit?

You may not receive any personal benefits from being in this study. You might benefit in the future from being in the study. Results from the study will be used to design hardware that should make it easier and safer to travel while seated in a wheelchair.

6. ENDING THE STUDY

6.1 If I want to stop participating in the study, what should I do?

You are free to leave the study at any time. If you leave the study before it is finished, there will be no penalty to you. If you decide to leave the study before it is finished, please tell one of the persons listed in Section 9. "Contact Information". If you choose to tell the researchers why you are leaving the study, your reasons may be kept as part of the study record. The researchers will keep the information collected about you for the research unless you ask us to delete it from our records. If the researchers have already used your information in a research analysis, it will not be possible to remove your information.

If you are unable to use the test wheelchairs safely, we will end your participation in the study.

7. FINANCIAL INFORMATION

7.1 Will I be paid or given anything for taking part in this study? You will receive $40 to for your participation in the study. If you decide to withdraw from the study early, we will pay you $15/hour, rounded to the nearest 15 minutes.

8. PROTECTING AND SHARING RESEARCH INFORMATION

8.1 How will the researchers protect my information?

We will give you a subject code number. All of your data will only be identified with this code. Information with your name on it, such as recruitment and payment forms, will be stored separately you're your data and destroyed after 1 year. All of your data and video recordings will be stored on a password-protected server. If you give consent on this form and we use pictures of you in a report or presentation, we will blur the images whenever possible.

8.2 Who will have access to my research records?

There are reasons why information about you may be used or seen by the researchers or others during or after this study. Examples include:

- University, government officials, study sponsors or funders, auditors, and/or the Institutional Review Board (IRB) may need the information to make sure that the study is done in a safe and proper manner.

8.3 What will happen to the information collected in this study?

We will keep the information we collect about you during the research for future research projects. Datasets that will be made available to the public through archive (using Deep Blue) will include measurements and survey responses but not video or photos where you could be identified. Information, video and photos will be saved locally and will only be shared with collaborators to guide future design improvements if consent has been given by you on this form.

The results of this study could be published in an article or presentation, but will not include any information that would let others know who you are.

8.4 Will my information be used for future research or shared with others?

We may use or share your research information for future research studies. If we share your information with other researchers it will be de-identified, which means that it will not contain your name or other information that can directly identify you. Potentially identifying information, video and photos will only be shared with collaborators to guide future design improvements if consent has been given by you on this form. Future research may be similar to this study or completely different. We will not ask for your additional informed consent for these studies.

Datasets will be made available to the public through the repository Deep Blue and will include measurements and survey responses but not video or photos where you could be identified. The repository contains information about many people. Your information will be labeled with a code, instead of your name or other information that could be used to directly identify you.

9. CONTACT INFORMATION

Who can I contact about this study?

Please contact the researchers listed below to:

- Obtain more information about the study
- Ask a question about the study procedures
- Report an illness, injury, or other problem (you may also need to tell your regular doctors)
- Leave the study before it is finished
- Express a concern about the study

Principal Investigator: Kathleen D. Klinich, PhD

Email: kklinich@umich.edu

Phone: (734) 936-1113

Study Coordinator: Nichole Orton

Email: nritchie@umich.edu

Phone: (734) 936-1107

If you have questions about your rights as a research participant, or wish to obtain information, ask questions or discuss any concerns about this study with someone other than the researcher(s), please contact the following:

University of Michigan

Health Sciences and Behavioral Sciences Institutional Review Board (IRB-HSBS)
2800 Plymouth Road
Building 520, Room 1169Ann Arbor, MI 48109-2800
Telephone: 734-936-0933 or toll free (866) 936-0933 Fax: 734-936-1852

E-mail: irbhsbs@umich.edu

10. YOUR CONSENT

Consent to Participate in the Research Study

By signing this document, you are agreeing to be in this study. Make sure you understand what the study is about before you sign. We will give you a copy of this document for your records and we will keep a copy with the study records. If you have any questions about the study after you sign this document, you can contact the study team using the information in Section 9 provided above.

I understand what the study is about and my questions so far have been answered. I agree to take part in this study.

Print Legal Name: _____

Signature: _____

Date of Signature (mm/dd/yy): _____

Consent to use and/or share your identifiable information for future research

The researchers would like to use your identifiable information (pictures and video) for future research that may be similar to or completely different from this research project. We may also use your pictures and video in reports and presentations. Identifiable means that the data will contain information that can be used to directly identify you, although we will not share your name with anyone. The study team will not contact you for additional consent to this future research. We may also share your identifiable information with other researchers. You can contact us at any time to ask us to stop using your information. However, we will not be able to take back your information from research projects that have already used it.

_____ Yes, I agree to let the researcher(s) use or share my personally identifiable information for future research.

_____ No, I do not agree to let the researcher(s) use or share my personally identifiable information for future research.

Print Legal Name: _____

Signature: _____

Date of Signature (mm/dd/yy): _____

Consent to be Contacted for Participation in Future Research

Researchers may wish to keep your contact information to invite you to be in future research projects that may be similar to or completely different from this research project.

_____ Yes, I agree for the researchers to contact me for future research projects.

_____ No, I do not agree for the researchers to contact me for future research projects.

Appendix B: Photos of Participant Belt Fit

Figure B1: V1
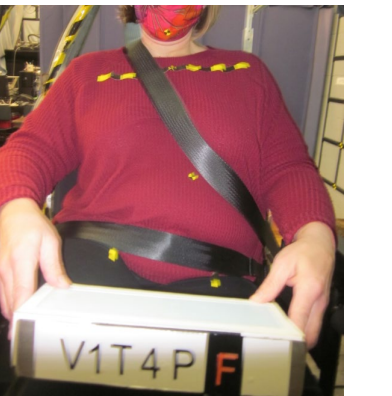
A SBS -37, LBF 4	B SBS -9, LBF 3	C SBS 0, LBF 4	D SBS -20, LBF 3
E SBS -17, LBF 3	F SBS 12, LBF 4	G SBS 21, LBF 4	H SBS 30, LBF 3

Figure B2: V2

A SBS -24, LBF 3	B SBS -39, LBF 4	C SBS -28, LBF 3	D SBS 22, LBF 4
E SBS -100, LBF 3	F SBS -38, LBF 3	G SBS -31, LBF 3	H SBS -24, LBF 4

Figure B3: V4

A SBS 22, LBF 2	B SBS 13, LBF 2	C SBS 15, LBF 3	D SBS 89, LBF 3
V4T4M A	V4T6M B	V4T8P C	V4T2P D
E SBS 0, LBF 3	F SBS 21, LBF 3	G SBS 19, LBF 4	H SBS 0M LBF 2
V4T5M E	V4T1P F	V4T7P G	V4T3M H

Figure B4: V5

A SBS 13, LBF 5	B SBS 17, LBF 5	C SBS 57, LBF 5	D SBS 113, LBF 3
E SBS 27, LBF 4	F SBS 35, LBF 3	G SBS 16, LBF 5	H SBS 101, LBF 5

Figure B5: V6

A SBS -32, LBF 3	B SBS -24, LBF 3	C SBS -24, LBF 4	D SBS 42, LBF 2
V6T6M A	V6T8P B	V6T2P C	V6T4M D
E SBS -27, LBF 3	F SBS -46, LBF 4	G SBS 0, LBF 3	H SBS 11, LBF 3
V6T1P E	V6T5M F	V6T7P G	V6T3M H

Figure B6: V7

A SBS 0, LBF 5	B SBS -66, LBF 5	C SBS -63, LBF 5	D SBS 14, LBF 5
V7T7M A	V7T5P B	V7T1M C	V7T3P D
E SBS -41, LBF 5	F SBS -49, LBF 5	G SBS -27, LBF 5	H SBS -52, LBF 5
V7T2M E	V7T8M F	V7T4P G	V7T6P H

183

Figure B7: V8

A SBS 17, LBF 4	B SBS 0, LBF 5	C SBS 0, LBF 5	D SBS -13, LBF 4
V8T8P A	V8T6M B	V8T2P C	V8T4M D
E SBS -21, LBF 5	F SBS -9, LBF 5	G SBS -16, LBF 5	H SBS 24, LBF 5
V8T1P E	V8T7P F	V8T3M G	V8T5M H

Figure B8: V9

A SBS 0, LBF 3	B	C	D SBS 87, LBF 4

E SBS -11, LBF 3	F	G SBS 16, LBF 4	H

Appendix C: Dynamic Testing

Frontal Sled Tests
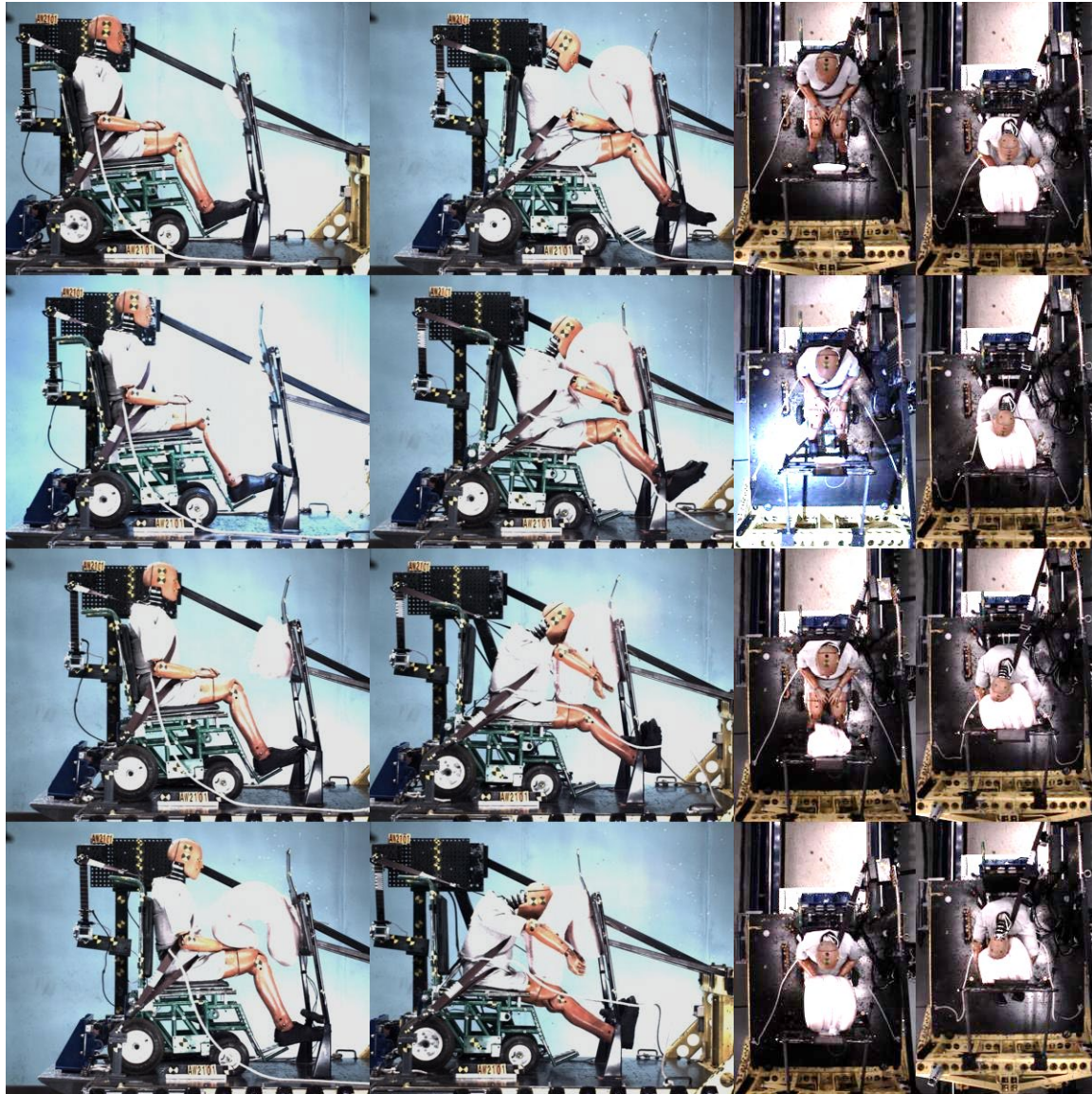
Figure C1. Right side and overhead camera views every 20 ms for test AW2101.
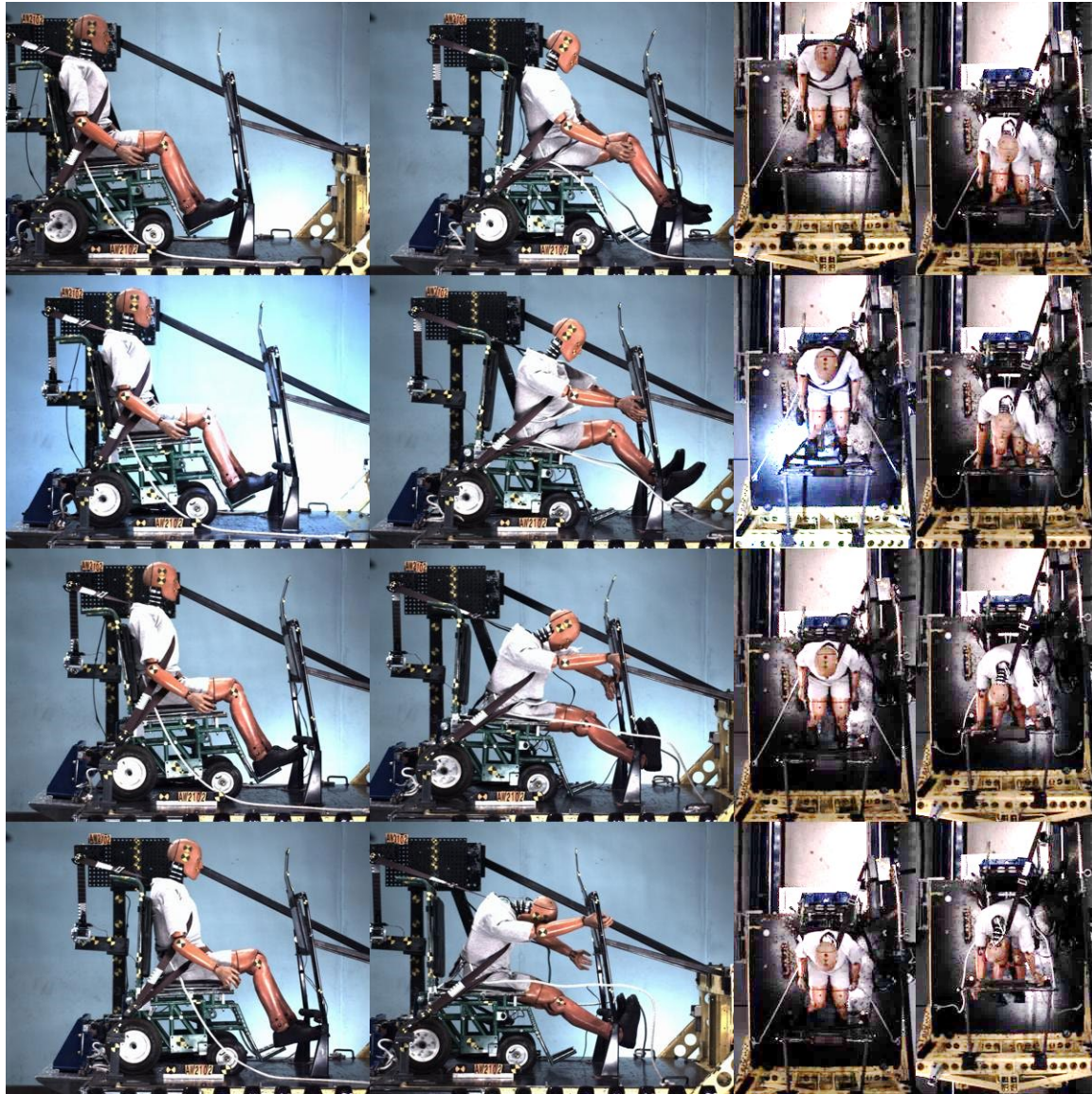
Figure C2. Right side and overhead camera views every 20 ms for test AW2102.
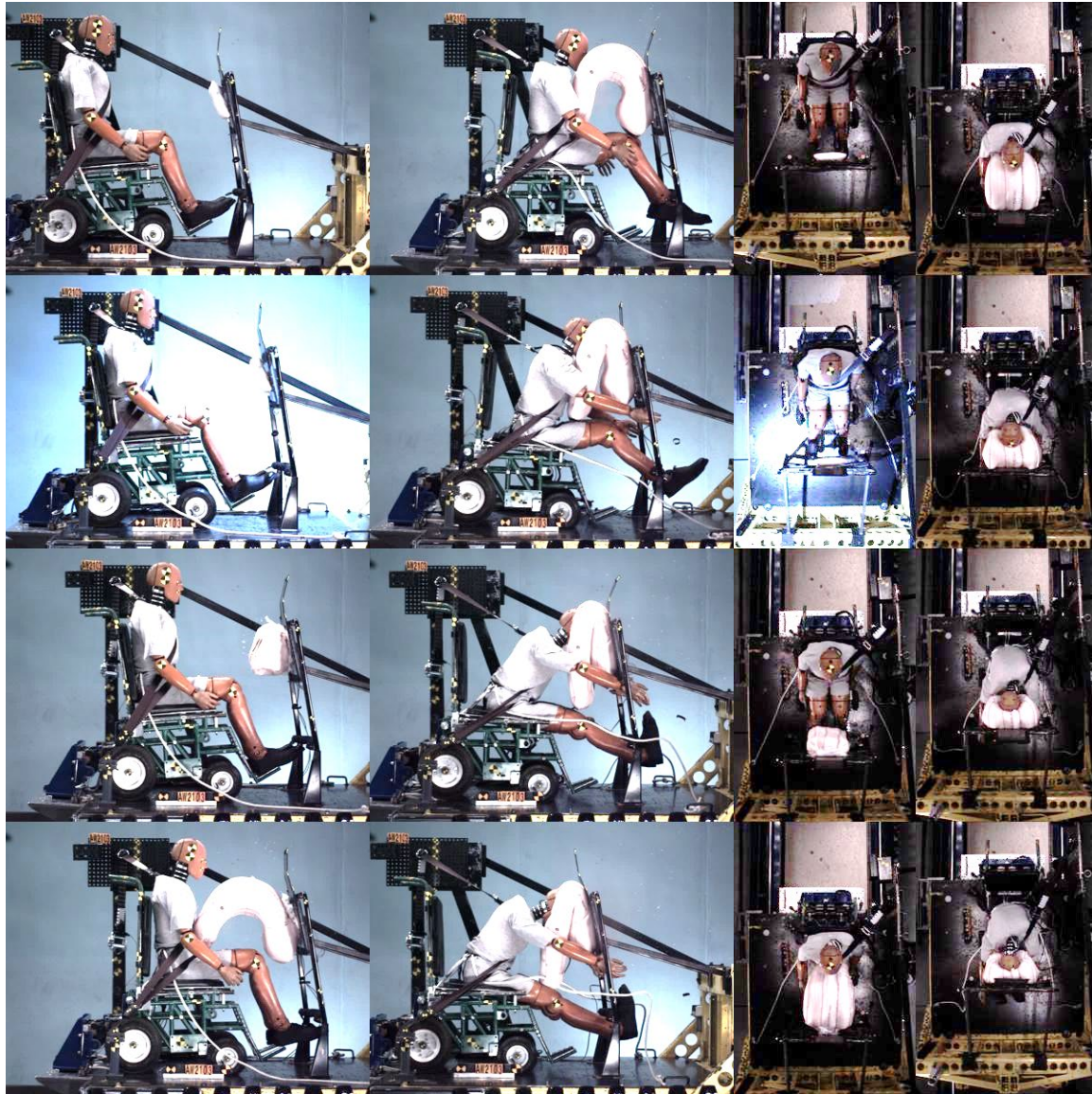
Figure C3. Right side and overhead camera views every 20 ms for test AW2103.
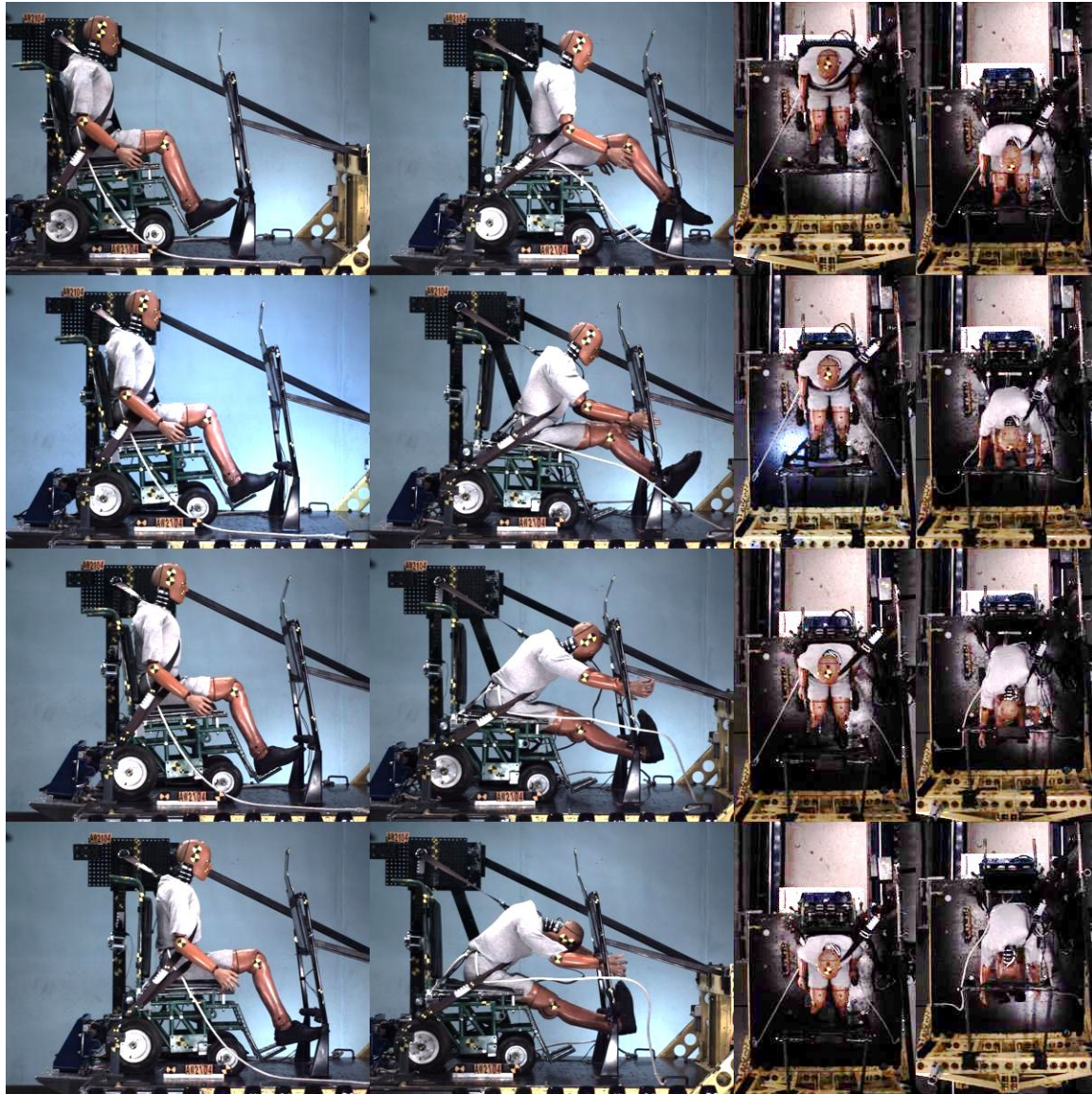
Figure C4. Right side and overhead camera views every 20 ms for test AW2104.
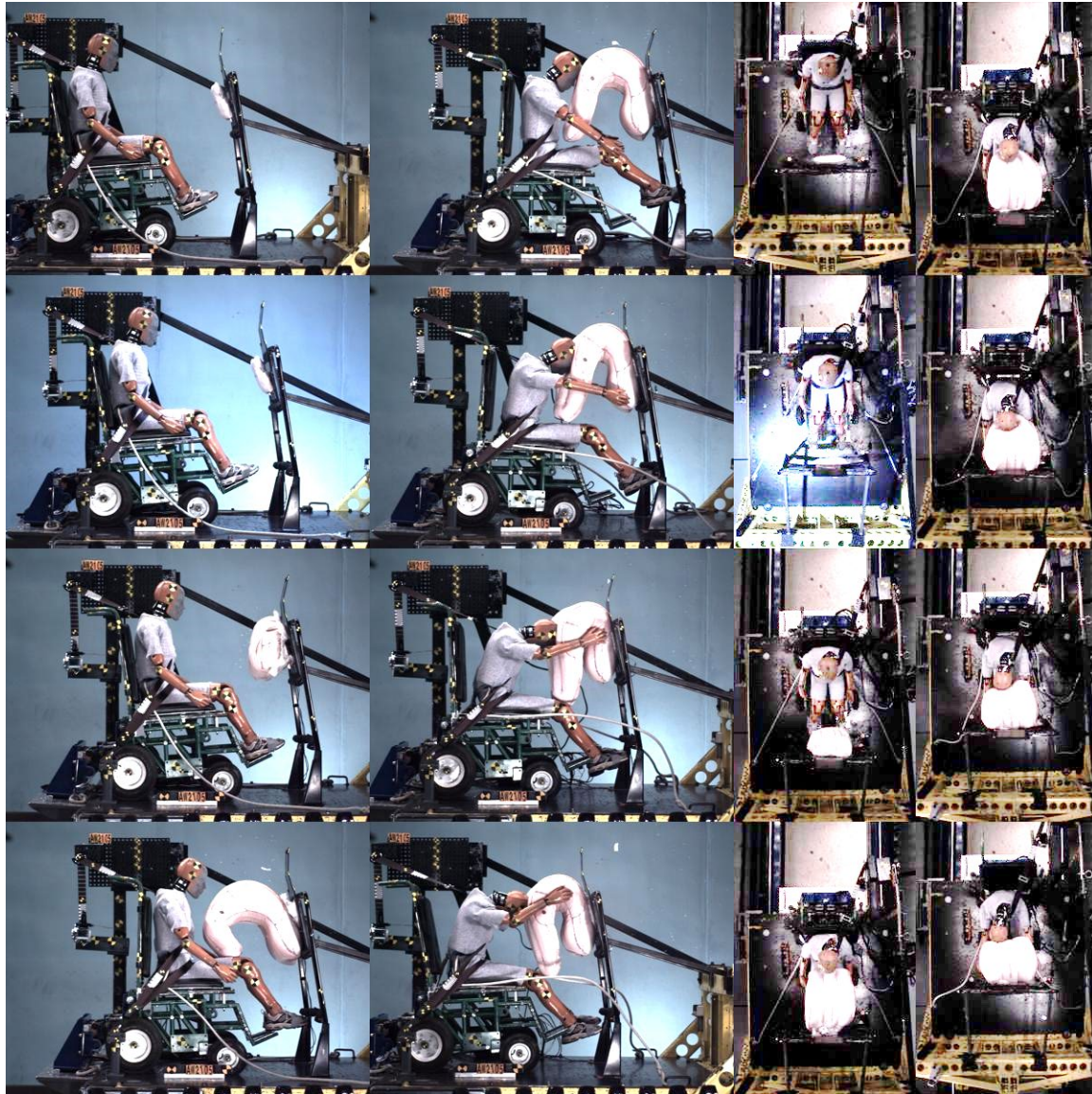
Figure C5. Right side and overhead camera views every 20 ms for test AW2105.
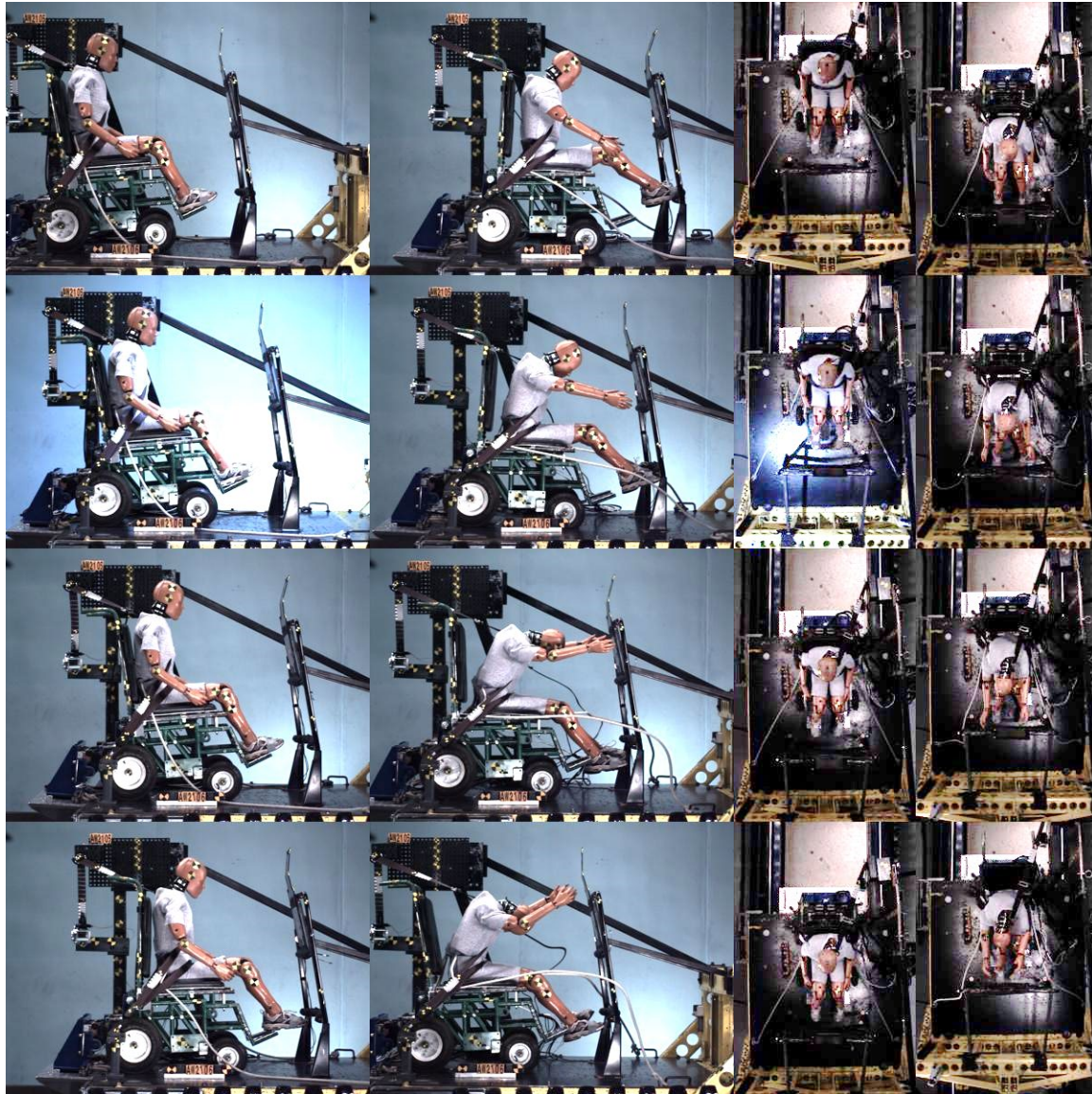
Figure C6. Right side and overhead camera views every 20 ms for test AW2106.
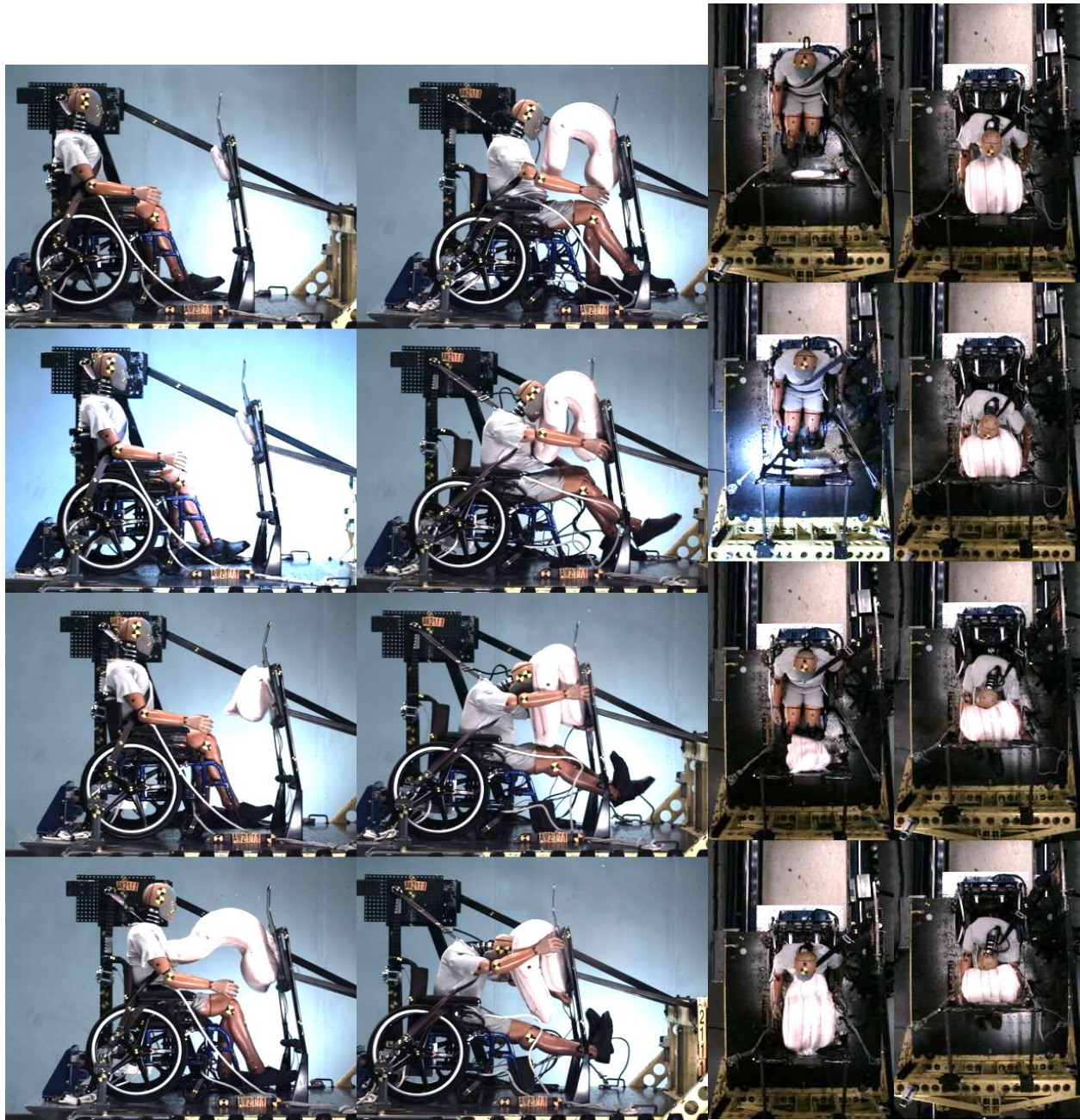
Figure C7. Right side and overhead camera views every 20 ms for test AW2111.
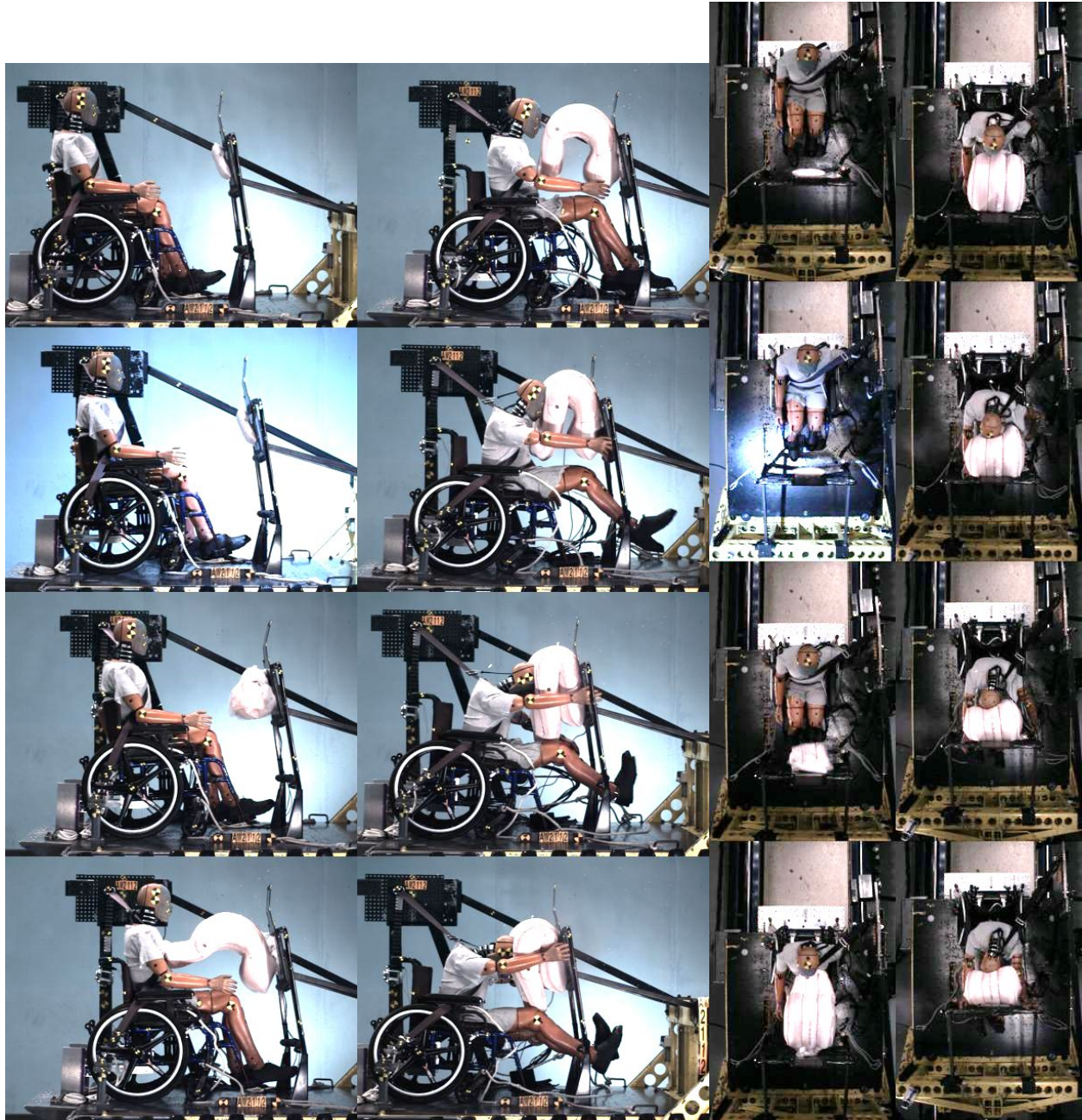
Figure C8. Right side and overhead camera views every 20 ms for test AW2112.
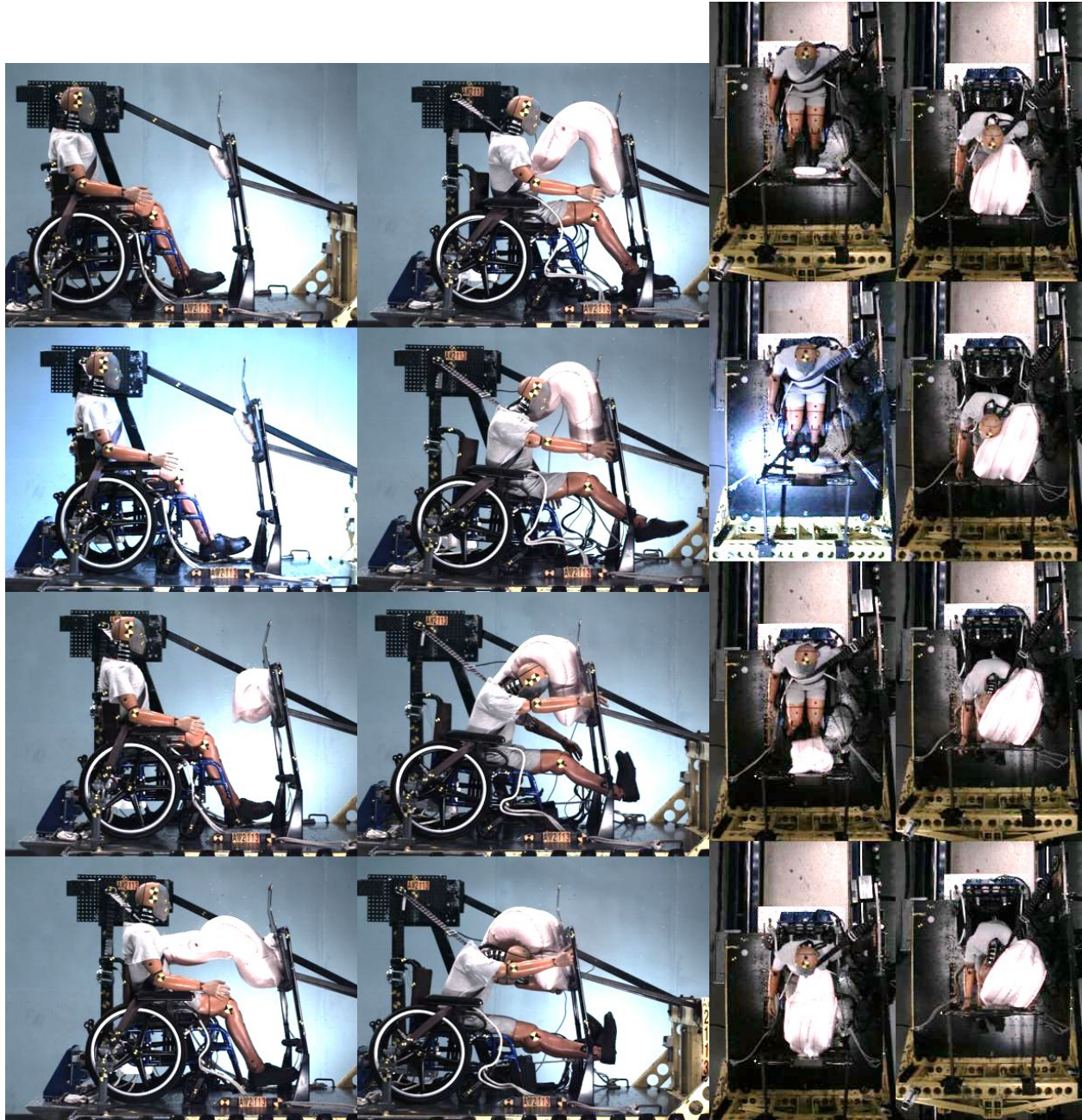
Figure C9. Right side and overhead camera views every 20 ms for test AW2113.
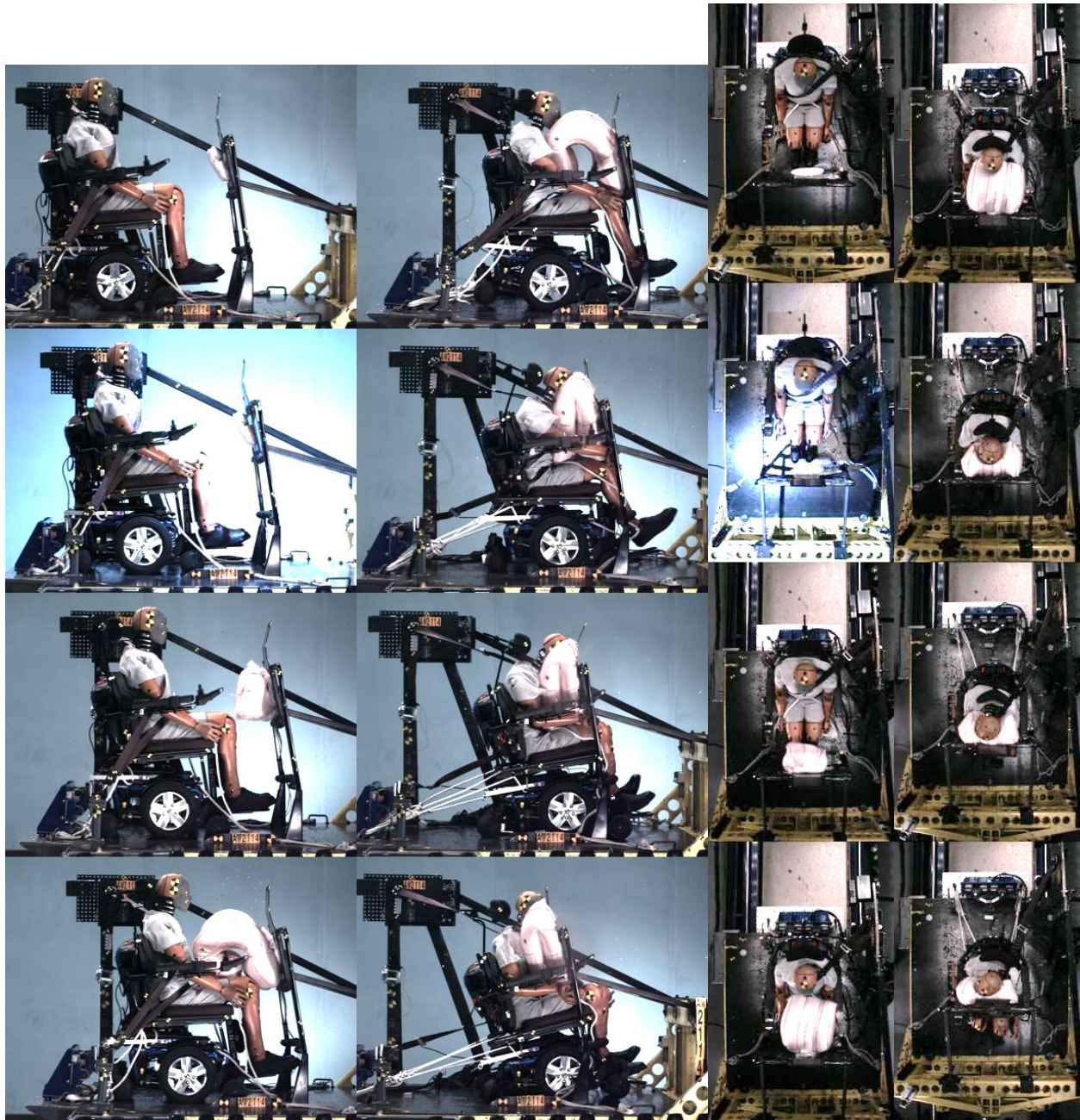
Figure C10. Right side and overhead camera views every 20 ms for test AW2114.
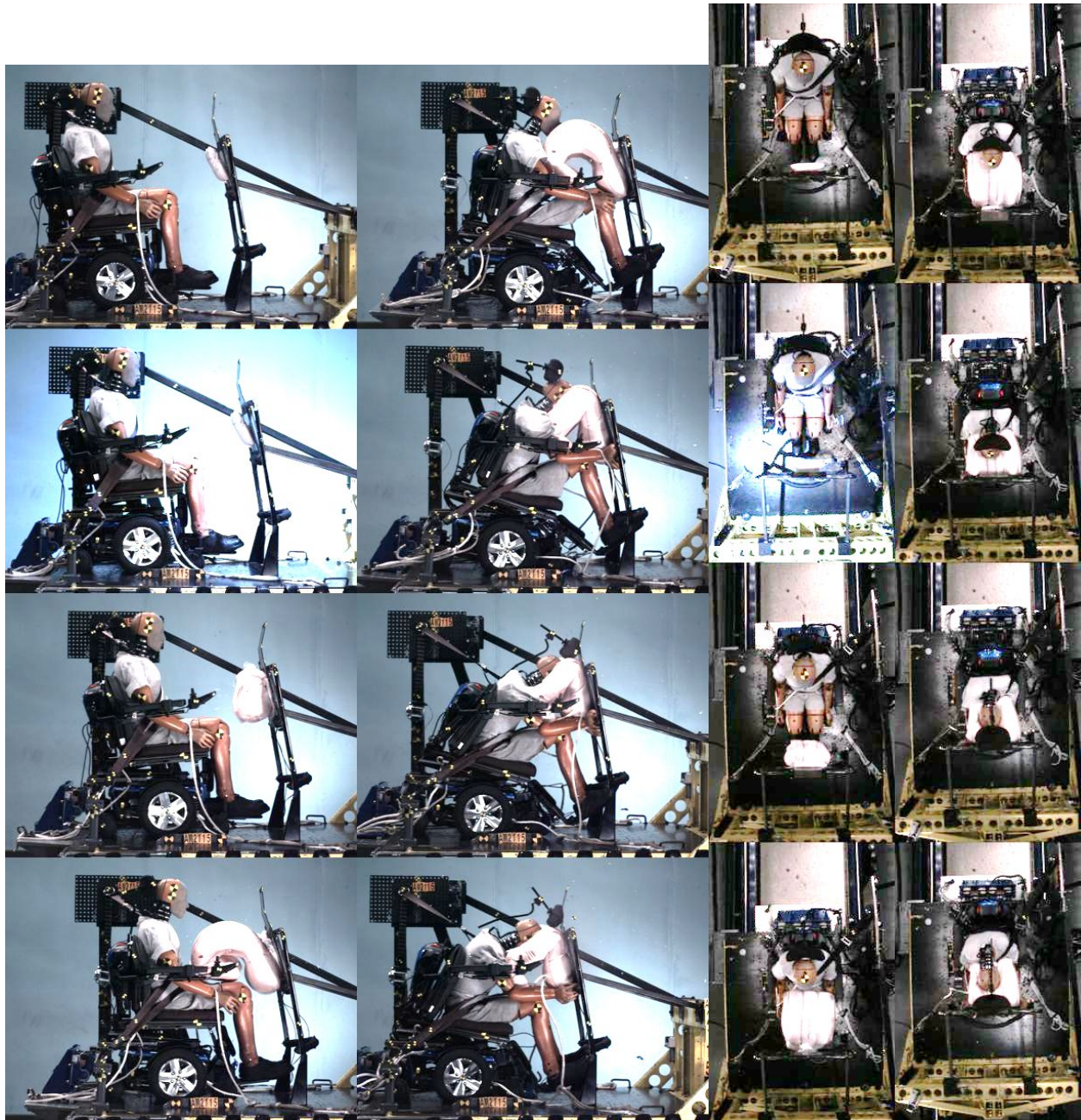
Figure C11. Right side and overhead camera views every 20 ms for test AW2115.

Side Impact Tests
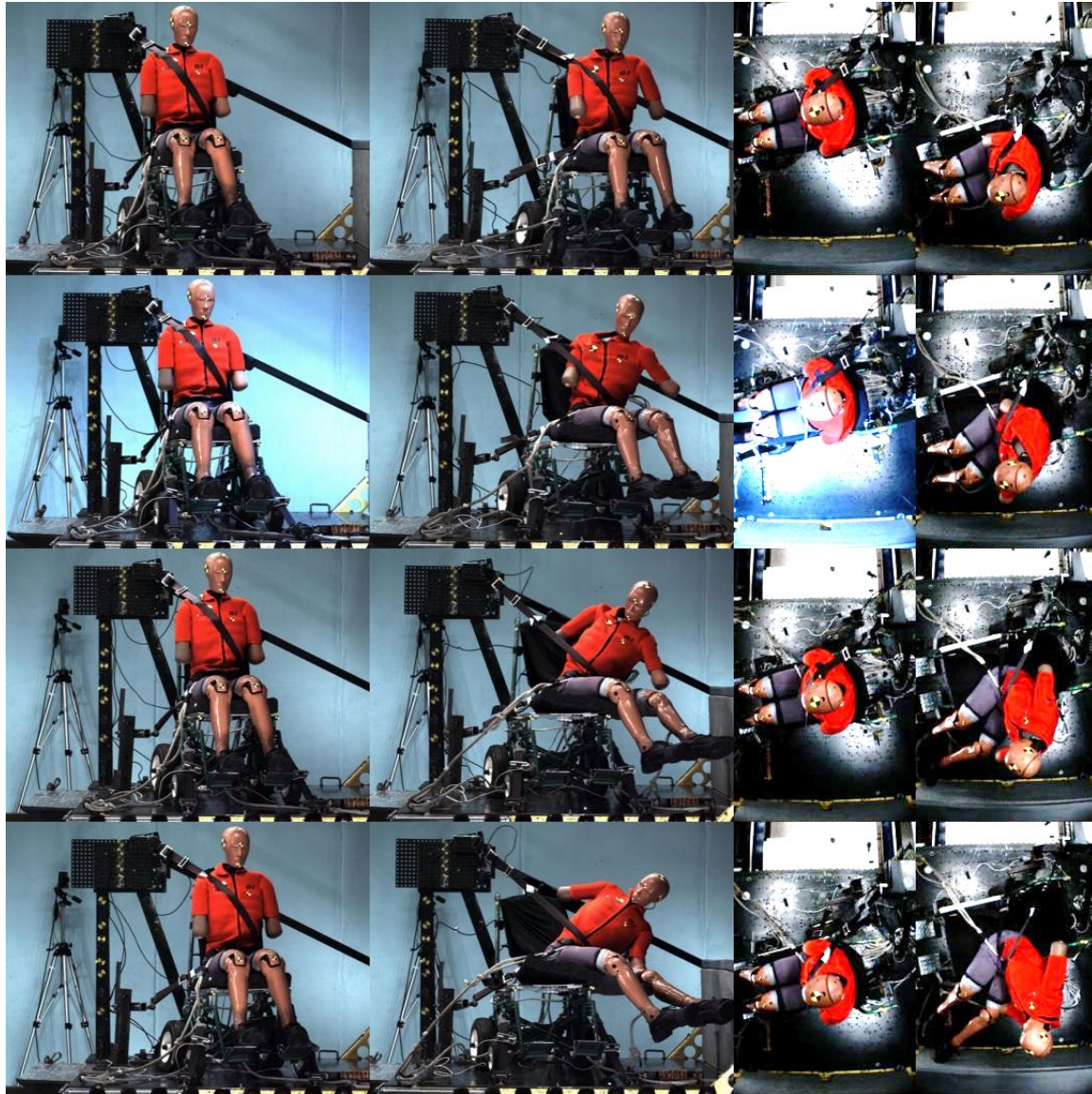
Figure C12. Right side and oblique camera views every 20 ms for test AW2011, baseline with 4-point strap tiedown.

Figure C13. Right side and oblique camera views every 20 ms for test AW2009, baseline with UDIG.

Figure C14. Right side and oblique camera views every 20 ms for test AW2107.

Figure C15. Right side and oblique camera views every 20 ms for test AW2108.

Figure C16. Right side and oblique camera views every 20 ms for test AW2110.

Figure C17. Right side and oblique camera views every 20 ms for test AW2116.

Figure C18. Right side and oblique camera views every 20 ms for test AW2117.

Figure C19. Right side and oblique camera views every 20 ms for test AW2118.

Figure C20. Right side and oblique camera views every 20 ms for test AW2119.

Appendix D: Extra Sled Tests

Because contractor expenses were less than budgeted, we performed four additional sled tests to address some unanswered questions. Table 1 shows the matrix for these tests. All tests were farside impacts, using the ES2-RE, belt geometry D, and the CATCH-V' airbag. Test AW2120 shifted the wheelchair forward relative to the airbag as shown in Figure 1; this shifted position was used in all four tests. Test AW2121 was performed with a manual wheelchair, to evaluate in farside impact the lighter attachment design that successfully tested in frontal impact in test AW2113. The goal of AW2122 was to evaluate the durability of the stronger attachments designed for the power wheelchair (tested in AW2115 in frontal impact) during side impact. Finally, test AW2123 evaluated a modified version of the lighter anchors, previously tested in AW2112 in frontal impact, in side impact conditions. The modifications consisted of reinforced side panels and a means of closing off the open hooks. Table 37 lists key measures from each test, while Table 38 reports excursions.

Table 36. Matrix of additional farside impact tests

Test ID	ATD	Belt Geometry	WC	Airbag	Goal
AW2120	ES2-RE	D	SWCB	CATCH-V'	Shifted WC forward relative to airbag
AW2121	ES2-RE	D	Manual	CATCH-V'	Lite attachments
AW2122	ES2-RE	D	Power	CATCH-V'	Strong attachments
AW2123	ES2-RE	D	SWCB	CATCH-V'	Upgraded lite anchors
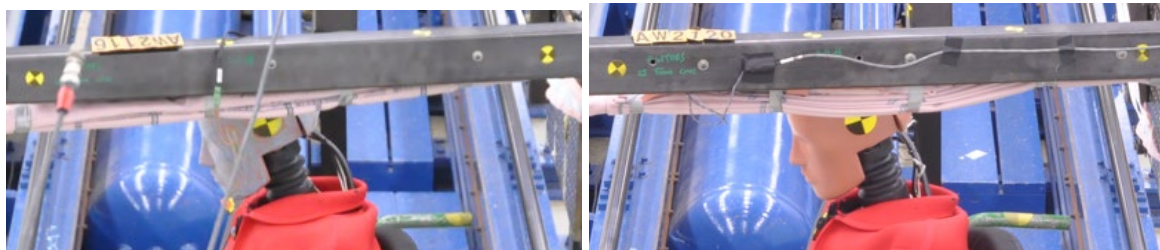
Figure 141. Comparison of head position relative to airbag in test AW2116 (left) and AW2120 (right).

Table 37. Summary of key measures from additional tests.

	2120:V'	2121: V'	2122: V'	2123: V'
Peak Sled accel (g)	23.8	22.9	24.6	23.9
Delta V (km/hr)	18.6	18.9	19.0	18.7
Peak Head R (g)	44.8	44.6	37.7	41.8
HIC 15	87	144	69	137
HIC 36	138	206	117	237
Upper Neck Fr R (N)	724	546.3	964.2	1279.1
Upper Neck Mo R (Nm)	69.5	71.4	60.1	64.8
Upper rib D (mm)	7.2	4.2	-4.4	5.8
Middle rib D (mm)	5.6	8	5.8	-35.8
Lower rib D (mm)	-5.3	5.6	3.7	-6.7
Lower spine R (g)	17	24.8	18.3	17.8
Front Ab Fy (N)	-31.6	519	1033.4	91.9
Middle Ab Fy (N)	-29.2	187.8	440.1	56.2
Rear Ab Fy (N)	44.9	186.1	210.6	88.8
Pubic force min (N)	-1140.1	-152.4	-727.2	-907.8
Pubic force max (N)	1615.1	1724.6	2215.9	1801.6
Pev R (g)	28.3	34.4	29.5	35.3
UDIG Left Res (N)	22537	1666	12937	
UDIG Left C Res (N)	5225	4073	5054	
UDIG Rt C Res (N)	10458	2471	9709	
UDIG Rt Res (N)	17496	3513	11346	

Table 38. ATD and wheelchair excursions from additional tests.

Test	ATD	WC	Restraint	WC ex (mm)	Head ex (mm)	Shld ex (mm)	Hip ex (mm)	Knee ex (mm)
AW2120	ES2-RE	SWCB	CATCH-V'	108	439	441	465	562
AW2121	ES2-RE	Manual	CATCH-V'	179	425	324	279	507
AW2122	ES2-RE	Power	CATCH-V'	530	479	427	624	911
AW2123	ES2-RE	SWCB	CATCH-V'	220	481	434	419	692

Side and overhead views of the kinematics in test AW2120 are shown in Figure 142. Kinematics do not look substantially different from AW2116 with the airbag in a more forward fore-aft location. In addition, as shown in Figure 3, when using the SWCB, the ATD's head contacted a similar location on the airbag.

Figure 142. Right side and oblique camera views every 20 ms for test AW2120.

Figure 143. Comparison of head contact location between AW2116 change test comparison (left) and AW2120 (right).

Kinematics from test AW2121 with the manual wheelchair are shown in Figure 4. In addition, Figure 5 compares the head location from test AW2118 to AW2121. The head striking the rear

part of the airbag in AW2118 was the motivation for trying the alternative location. The photo from AW2121 shows that the goal of obtaining a more central loading position was achieved.

Figure 144. Right side and oblique camera views every 20 ms for test AW2121.

Figure 145. Comparison of head contact points in manual chair in original and shifted locations.

One of the objectives of test AW2121 was to evaluate the lighter UDIG attachments, which were tested successfully in frontal impact in test AW2112. Figure 6 shows views of the attachments post-test from the rear on the left and from the bottom on the right. The attachments did not break but did deform. Some bending of the lower components of the wheelchair is also visible in the right-side picture. For this test, because it was not possible to procure a new manual wheelchair before the time available to run the sled test, we used components of the wheelchairs used in frontal tests AW2111-13 that were not visibly damaged to assemble a wheelchair for this test. There was no significant damage other than the bending, even though these wheelchair components had been previously tested.

Figure 146. Deformation to UDIG attachments during side impact in AW2121. Rear view (left), bottom view (right).

Kinematics for test AW2122 are shown in Figure 7. The purpose of this test was to evaluate the strength of the stronger UDIG attachments for the power wheelchair, tested successfully in frontal impact in test AW2115, in side impact. Figure 8 shows that the left UDIG vertical component remained intact, but the right vertical component sheared off at the top bolt and the lower cross member broke as well. Since we are unaware of previous tests run with a power chair in side impact using UDIG attachment, data collected from the UDIG loadcells during this test can be used to improve future UDIG attachment designs.

Figure 147. Right side and oblique camera views every 20 ms for test AW2122.
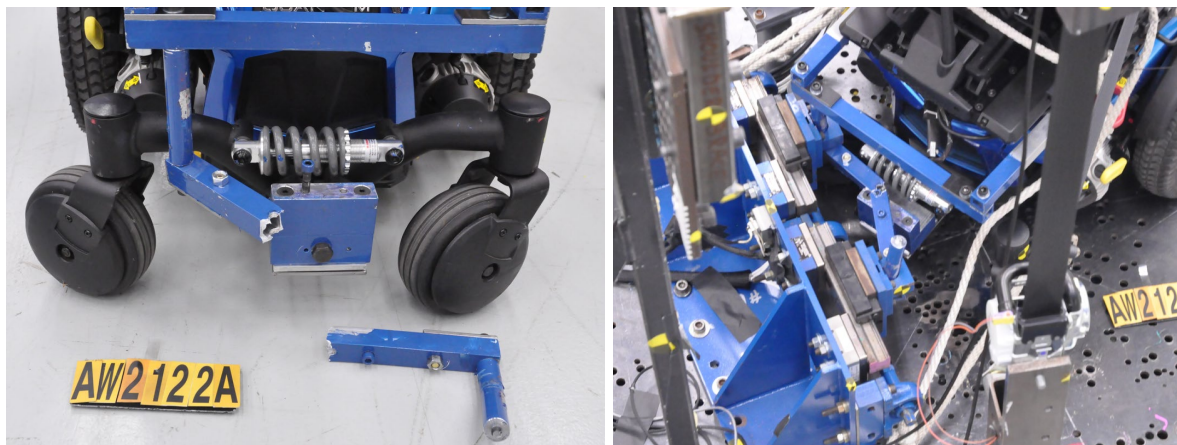
Figure 148. Deformation to UDIG attachments during side impact in AW2122. Rear view of wheelchair (left), and oblique view relative to docking station (right).

Kinematics from the last extra test, AW2123, are shown in Figure 9. This test evaluated the strength of lighter weight UDIG anchors similar to those used in volunteer testing. In addition to greater lateral reinforcement of the whole structure, we added a component to the hooks (shown in Figure 10 and Figure 11) that rotates into place as the hooks move outward to engage the attachments. During testing, the right-side hook broke off as shown in Figure 12. Force data from the UDIG loadcells measured in this test can help improve future designs.

Figure 149. Right side and oblique camera views every 20 ms for test AW2123.
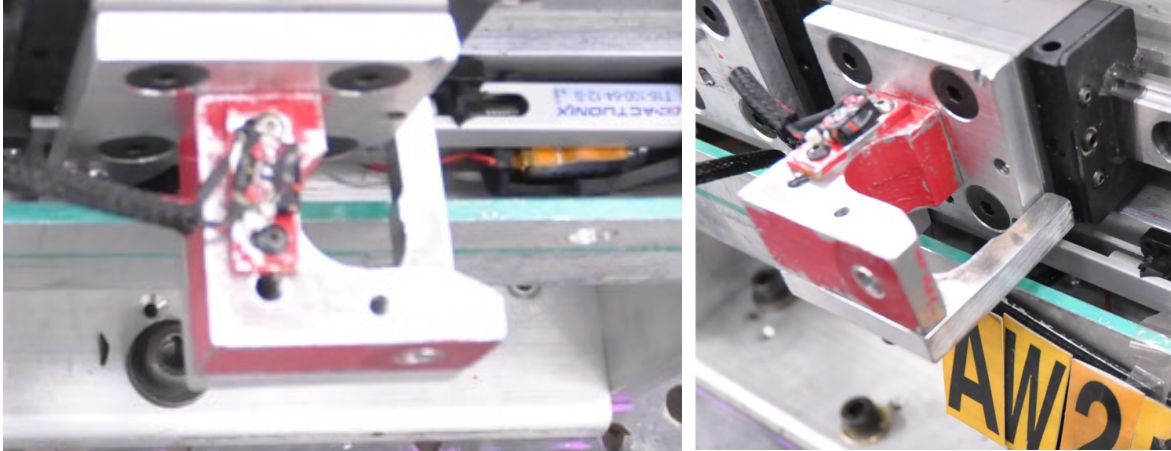
Figure 150. Extra hook component that rotates into place as hooks move outboard.
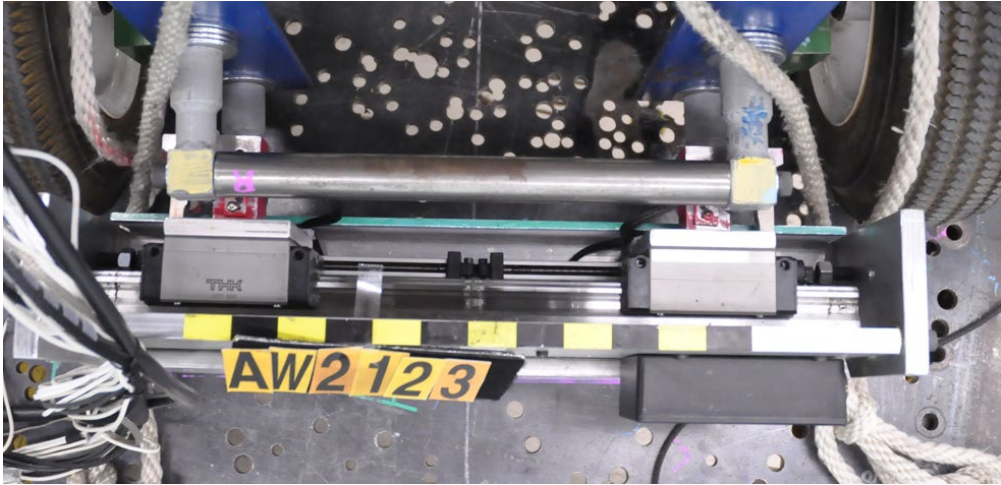
Figure 151. Top view of UDIG anchors with new hook components.
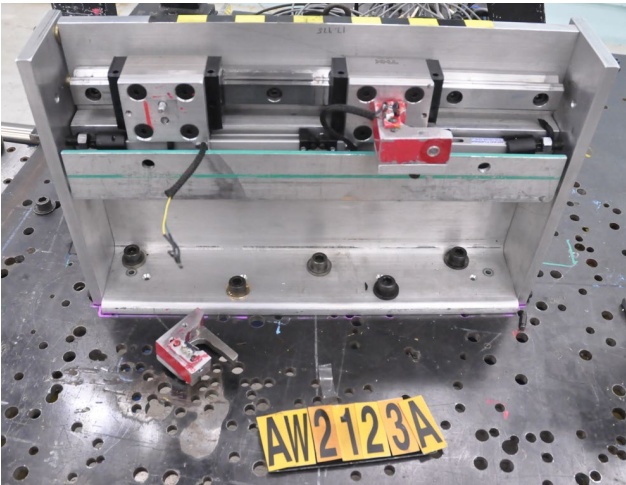
Figure 152. Hook damaged during test AW2123.

Appendix E. Dual-retractor seatbelt

For our volunteer testing, ZF provided us with a seatbelt equipped with a retractor that had their strongest spring available, and the longest length possible that would spool up with that spring strength. It was still of insufficient length to allow maneuvering into the wheelchair stations, so we spliced an additional 18" of webbing to the belt for volunteer testing. This meant that the volunteers had to snug the belt on themselves after donning.

To explore possible solutions to this problem, we asked ZF to provide us with a longer seatbelt and dual retractors that would be mounted to the D-ring and the outboard lap-belt anchor. Figure 13 shows the seatbelt installed in the Braun van, as well as providing a snug belt fit on a pilot volunteer.

Figure 153. Seatbelt with dual retractors installed (left) and providing snug belt tension on pilot volunteer (right).

Preliminary assessment of the system seems promising in addressing the issue. The belt remained snug during the donning process, with the pilot volunteer needing to pull the belt out slightly when routing it behind the armrests. The belt tension also slightly pulled the donning arm inboard towards the seatbelt station, with the potential to catch on the right wheelchair wheel if the person was located closer to that side of the station. This seatbelt was equipped with a standard latchplate; in our previous volunteer installation, we had increased the slot width to allow the webbing to slide more easily as it was donning. This initial trial with dual retractors indicates that it could be an effective way of improving belt tension with additional work to optimize the spring tension of each retractor.

Appendix F: Hardware Drawings

B

B

A

A

INTERPRET GEOMETRIC TOLERANCING PER:	UNLESS OTHERWISE SPECIFIED:		NAME	DATE
	DIMENSIONS ARE IN INCHES TOLERANCES: FRACTIONAL± ANGULAR: MACH± BEND ± TWO PLACE DECIMAL ± THREE PLACE DECIMAL ±	DRAWN BY:	KJB	
		COMMENTS:		
MATERIAL	FINISH			

M UMTRI

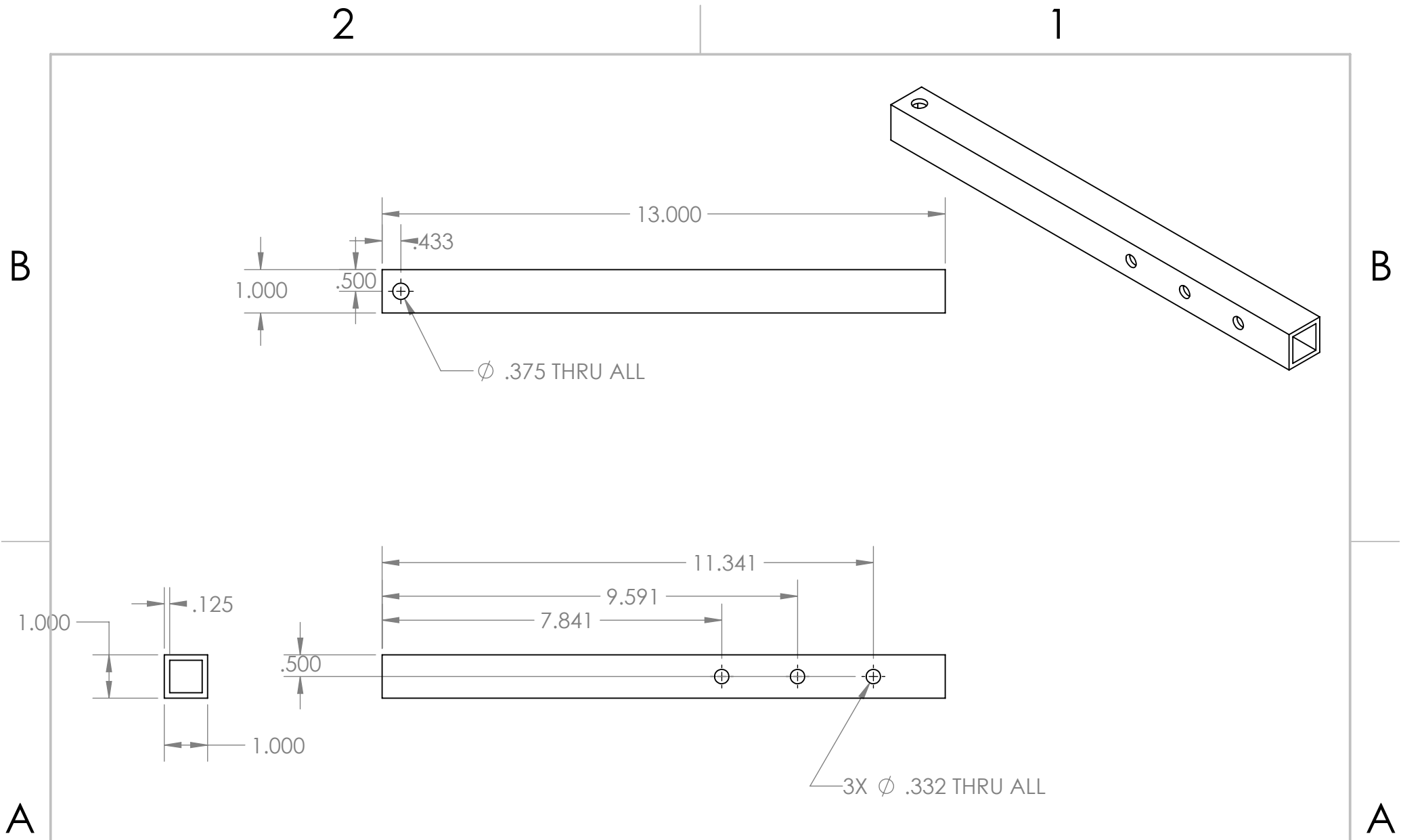TITLE: UDig_Assem_final

SIZE **A**   DWG. NO.   REV

SCALE: 1:8   WEIGHT: SHEET 1 OF 4

ITEM NO.	PART NUMBER	DESCRIPTION	QTY.
1	6709K61	Bearing rail	1
2	6709K180_BALL BEARING CARRIAGE	Bearing carriage	2
3	base_plate	Base plate	1
4	t16_100mm	Actuator	2
6	hookv3	Hook plate left	1
7	hookv3b	Hook plate right	1
8	base_plate2	Actuator mount	1
9	hook_end	UDig attachment hooks	2
10	udig_angle	Base angle	1
11	udig_side_plate	Reinforce side plates	2
12	udig_act_angle	Actuator protection angle	1
13	udig_act_angle_spacers	Angle spacers	4

			NAME	DATE	TITLE:	UDig_Assem_final	
INTERPRET GEOMETRIC TOLERANCING PER:	UNLESS OTHERWISE SPECIFIED:						
	DIMENSIONS ARE IN INCHES TOLERANCES: FRACTIONAL± ANGULAR: MACH ± BEND ± TWO PLACE DECIMAL ± THREE PLACE DECIMAL ±	DRAWN BY:	KJB				
		COMMENTS:			SIZE **A**	DWG. NO.	REV
MATERIAL	FINISH				SCALE: 1:4	WEIGHT:	SHEET 2 OF 4

ITEM NO.	PART NUMBER	DESCRIPTION	QTY.
1	6709K61	Bearing rail	1
2	6709K180_BALL BEARING CARRIAGE	Bearing carriage	2
3	base_plate	Base plate	1
4	t16_100mm	Actuator	2
6	hookv3	Hook plate left	1
7	hookv3b	Hook plate right	1
8	base_plate2	Actuator mount	1
9	hook_end	UDig attachment hooks	2
10	udig_angle	Base angle	1
11	udig_side_plate	Reinforce side plates	2
12	udig_act_angle	Actuator protection angle	1
13	udig_act_angle_spacers	Angle spacers	4

NAME | DATE

DRAWN BY: KJB

COMMENTS:

TITLE: UDig_Assem_final

SIZE **A**   DWG. NO.   REV

SCALE: 1:4   WEIGHT: SHEET 3 OF 4

B

ITEM NO.	PART NUMBER	DESCRIPTION	QTY.
1	6709K61	Bearing rail. McMaster part ID 6709K61 or 6709K63	1
2	6709K180_BALL BEARING CARRIAGE	Bearing carriage. McMaster part ID 6709K18	2
3	base_plate	Base plate	1
4	t16_100mm	Actuonix. T16-S Mini Track Actuator with Limit Switches - 100mm - 64:1 - 12 volts	2
6	hookv3	Hook plate left	1
7	hookv3b	Hook plate right	1
8	base_plate2	Actuator mount	1
9	hook_end	UDig attachment hooks	2
10	udig_angle	Base angle	1
11	udig_side_plate	Reinforce side plates	2
12	udig_act_angle	Actuator protection angle	1
13	udig_act_angle_spacers	Angle spacers	4

B

A

A

2

1

.500

18.000

.500

17.000

13.724

.500

10.575

.500

7.425

2.750

4.276

1.126

2.750

B

B

5.000

7.000

6X ⌀ .354 THRU ALL
M10X1.0 - 6H THRU ALL

7.250

9.000

9.500

5X ⌀ .257 ▽ 1.000
5/16-18 UNC ▽ .750

2.000

4.500

3/8-16 Tapped Hole

6.500

9.000

5X ⌀ .257 ▽ 1.000
5/16-18 UNC ▽ .750

11.500

13.500

A

16.000

A

2

1

2 1

B B

2.772
2.173
1.386
.598

.375

.869

1.494

1.969

2.538

3.325

3.443

.118

.354

2X ⌀ .266 THRU ALL
⌵ ⌀ .531 X 82°

4X ⌀ .354 THRU ALL
⌵ ⌀ .706 X 90°

4X ⌀ .118 THRU ALL

A A

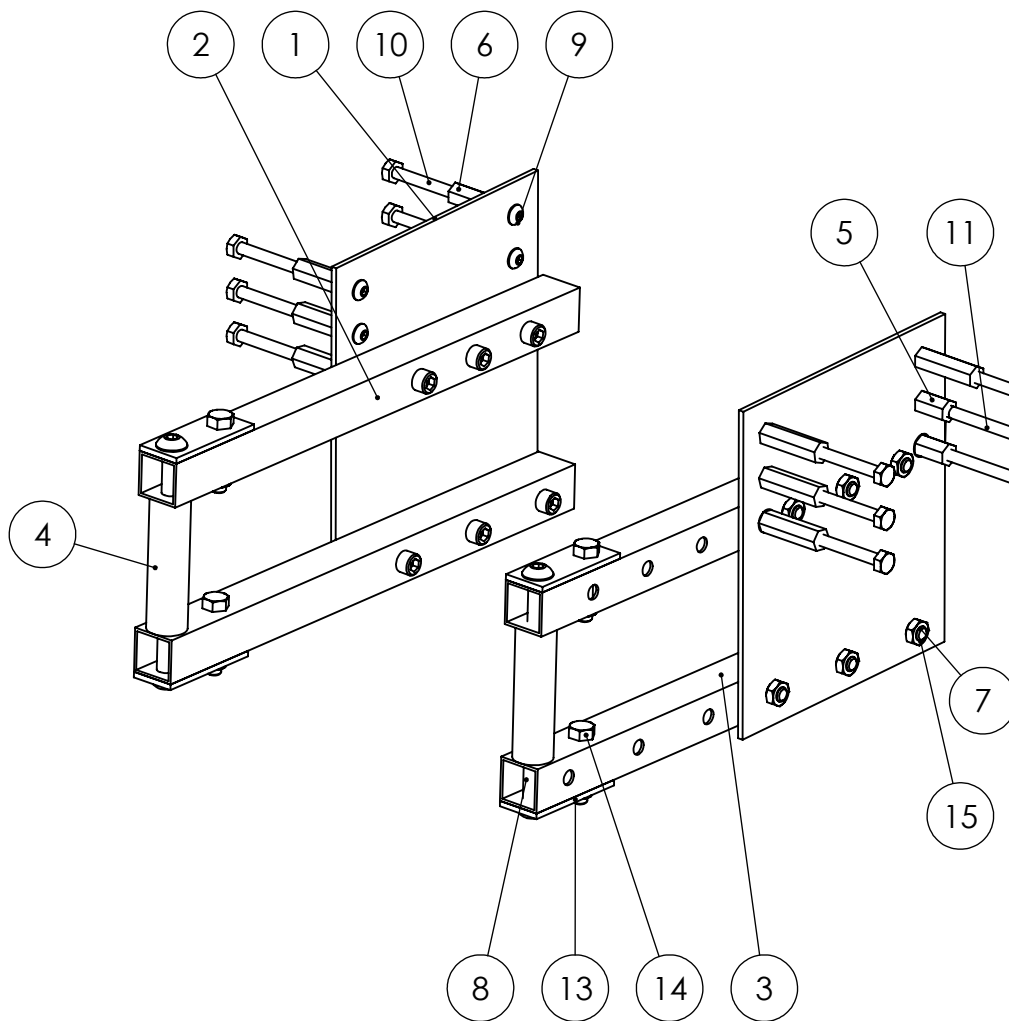| INTERPRET GEOMETRIC TOLERANCING PER:	UNLESS OTHERWISE SPECIFIED:		NAME	DATE	TITLE:	hookv3	
	DIMENSIONS ARE IN INCHES TOLERANCES: FRACTIONAL± ANGULAR: MACH± BEND ± TWO PLACE DECIMAL ± THREE PLACE DECIMAL ±	DRAWN BY:	KJB				
		COMMENTS:			SIZE **A**	DWG. NO.	REV
MATERIAL 6061 Al	FINISH				SCALE: 1:1	WEIGHT:	SHEET 1 OF 1

2 1

2

1

B

.375

2.772

2.173

1.386

.598

.394

.869

1.494

1.969

2.362

2.538

3.325

3.443

B

A

2X Ø .266 THRU ALL
⌵ Ø .531 X 82°

4X Ø .354 THRU ALL
⌵ Ø .706 X 90°

.118

.354

4X Ø .118 THRU ALL

A

2

1

2

1

B

18.000

5/16-18 Tapped Hole

1.000

1.500

5.000

13.000

16.500

1.000

3X ⌀ .332 THRU ALL

4X ⌀ .136 THRU ALL
8-32 UNC THRU ALL

1.250

.502   .625   1.000

.375

.953

8.823

9.000

9.177

17.047

17.625

A

B

A

M | UMTRI

2

1

2

1

B

B

2.250

1.000

1.718

1.218

1.000

.325

.575

2.000

1.075

1.525

R.500

.500

.1875

.8125

1/4-20 UNC

A

A

M | UMTRI

TITLE: hook_end

SIZE
A

DWG. NO.

REV

SCALE: 1:1 | WEIGHT: | SHEET 1 OF 1

2

1

2

1

B

B

16.000

13.500

11.500

9.000

6.500

4.500

2.000

1.000

3.000

6.000

.500

.250

4X ∅ .257 ▼ 1.000
5/16-18 UNC ▼ .750

8X ∅ .397 THRU ALL

.500
.750
3.000
4.250
6.000

A

A

M | UMTRI

2

1

5.250

.500

.500

12.500

9X ⌀ .332 THRU ALL

1.000

3.250

5.500

7.750

10.000

1.000

2.250

3.500

4.750

.500

4.000

12.000

15.500

16.000

2.125
2.500

4X ⌀ .332 THRU ALL

2.500

2.500

.250

16.000

2.500

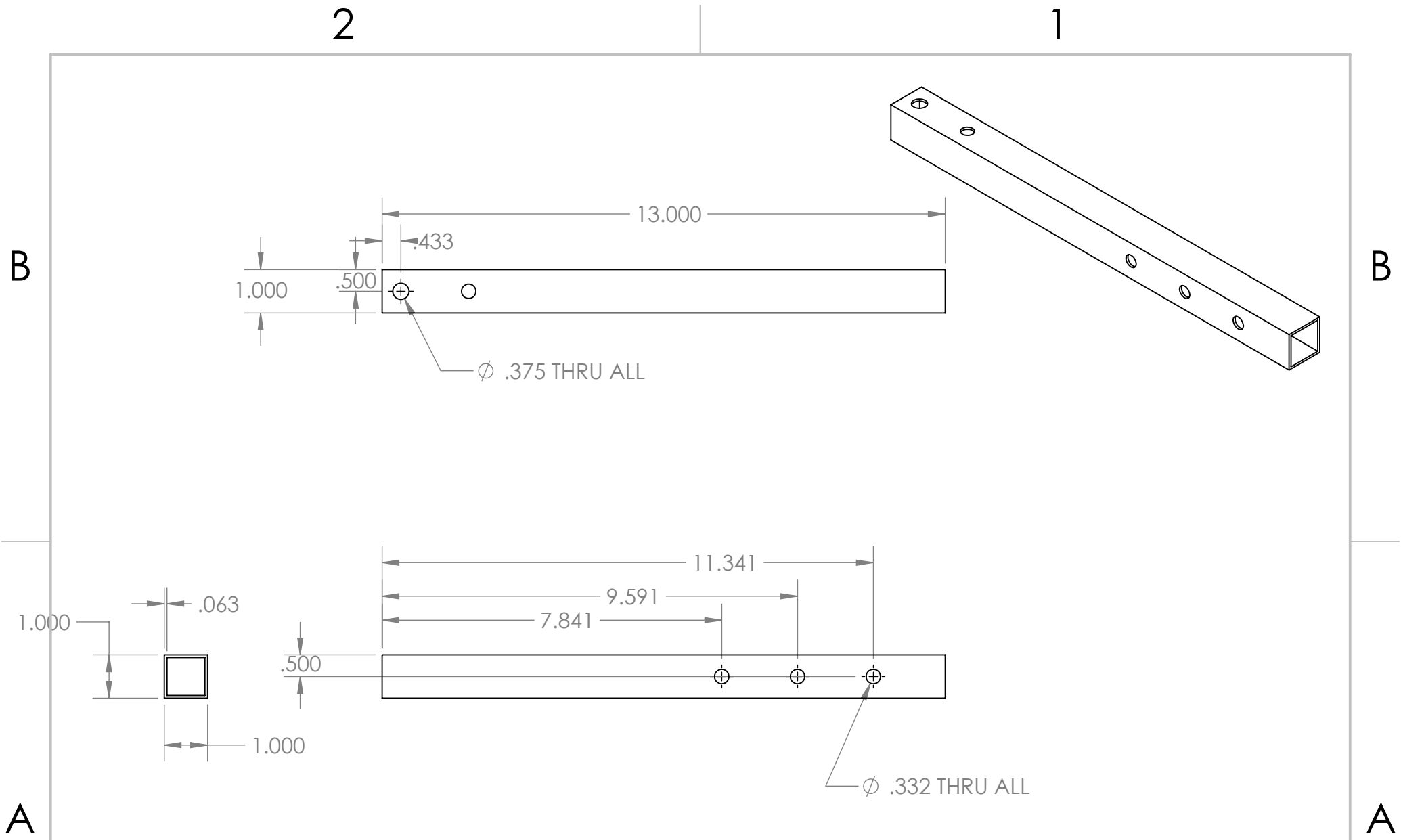|	INTERPRET GEOMETRIC TOLERANCING PER:	UNLESS OTHERWISE SPECIFIED:		NAME	DATE	TITLE:	udig_act_angle	
M | UMTRI		DIMENSIONS ARE IN INCHES TOLERANCES: FRACTIONAL± ANGULAR: MACH± BEND ± TWO PLACE DECIMAL ± THREE PLACE DECIMAL ±	DRAWN BY:	KJB				
			COMMENTS:			SIZE **A**	DWG. NO.	REV
	MATERIAL 6061 Al	FINISH				SCALE: 1:4	WEIGHT:	SHEET 1 OF 1

2

1

B

.500

Ø .875

Ø .875

Ø .332

A

UMTRI

2

1

INTERPRET GEOMETRIC TOLERANCING PER:		UNLESS OTHERWISE SPECIFIED:		NAME	DATE	TITLE: SWC_udig_attachments		
		DIMENSIONS ARE IN INCHES TOLERANCES: FRACTIONAL± ANGULAR: MACH± BEND ± TWO PLACE DECIMAL ± THREE PLACE DECIMAL ±	DRAWN BY:	KJB				
			COMMENTS:			SIZE A	DWG. NO.	REV
MATERIAL		FINISH				SCALE: 1:8	WEIGHT:	SHEET 1 OF 2

UMTRI

B

B
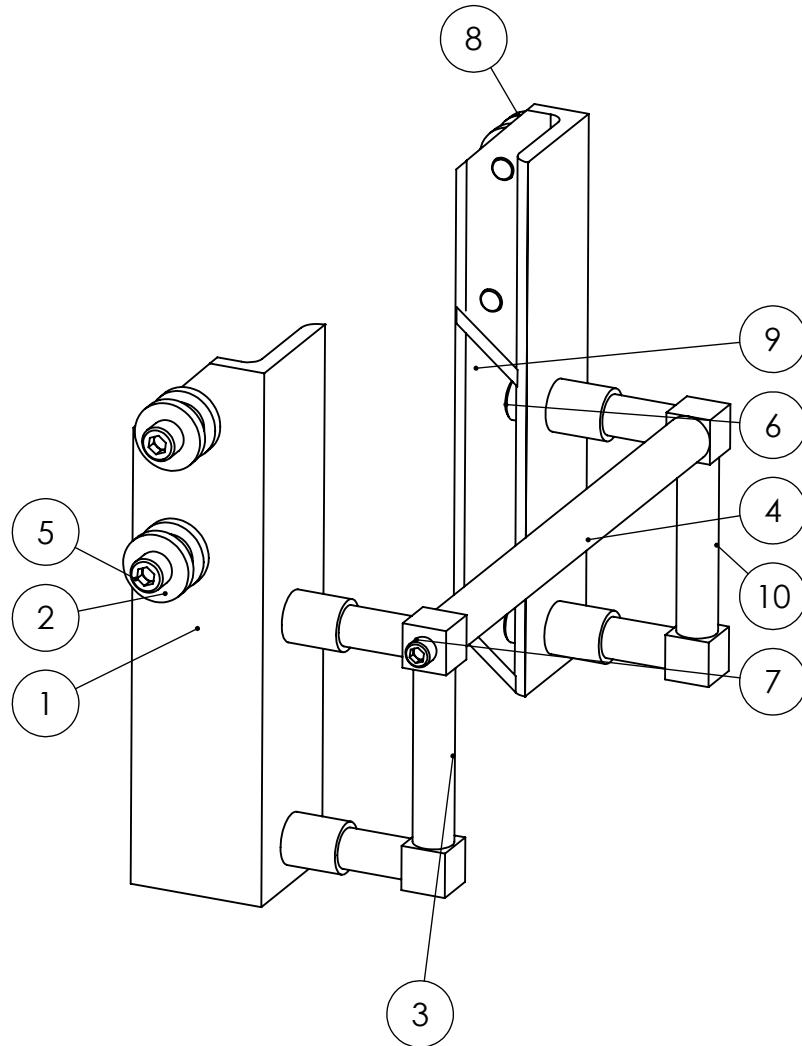
ITEM NO.	PART NUMBER	DESCRIPTION	QTY.
1	swc_attach_angle		1
2	swc_angle_reducer		4
3	swc_attach_handle		1
4	swc_attach_horiz_bar		1
5	HX-SHCS 0.5-20x1.5x1.5-N		4
6	HX-SHCS 0.625-18x1x1-N		4
7	HX-SHCS 0.375-16x1.5x1.5-N		2
8	Mirrorswc_angle_reducer		4
9	Mirrorswc_attach_angle		1
10	Mirrorswc_attach_handle		1

A

A

	INTERPRET GEOMETRIC TOLERANCING PER:	UNLESS OTHERWISE SPECIFIED:		NAME	DATE	TITLE SWC_udig_attachments		
M UMTRI		DIMENSIONS ARE IN INCHES TOLERANCES: FRACTIONAL± ANGULAR: MACH± BEND ± TWO PLACE DECIMAL ± THREE PLACE DECIMAL ±	DRAWN BY:	KJB				
			COMMENTS:			SIZE **A**	DWG. NO.	REV
	MATERIAL	FINISH				SCALE: 1:4 WEIGHT:		SHEET 2 OF 2

B

B

A

A

INTERPRET GEOMETRIC TOLERANCING PER:		UNLESS OTHERWISE SPECIFIED:		NAME	DATE	TITLE: manual_udig_attachments		
		DIMENSIONS ARE IN INCHES TOLERANCES: FRACTIONAL± ANGULAR: MACH± BEND ± TWO PLACE DECIMAL ± THREE PLACE DECIMAL ±	DRAWN BY:	KJB				
			COMMENTS:					
MATERIAL		FINISH				SIZE **A**	DWG. NO.	REV
						SCALE: 1:5	WEIGHT:	SHEET 1 OF 2

B

B

A

A

ITEM NO.	PART NUMBER	QTY.
1	side_manual_attach_plate	2
2	top_tube_manual_attach	2
3	bottom_tube_manual_attach	2
4	cyl_manual_attach	2
5	side_manual_attach_spacer_short	4
6	side_manual_attach_spacer_long	8
7	HX-SHCS 0.3125-18x1.375x1.375-N	12
8	SBHCSCREW 0.375-16x1.375-HX-N	4
9	SBHCSCREW 0.25-20x1-HX-N	8
10	HBOLT 0.2500-20x2x0.75-N	8
11	HBOLT 0.2500-20x2.5x0.75-N	4
12	SCHCSCREW 0.25-20x0.75x0.75-HX-N	4

		NAME	DATE		
INTERPRET GEOMETRIC TOLERANCING PER:	UNLESS OTHERWISE SPECIFIED:			TITLE: manual_udig_attachments	
	DIMENSIONS ARE IN INCHES TOLERANCES: FRACTIONAL ± ANGULAR: MACH ± BEND ± TWO PLACE DECIMAL ± THREE PLACE DECIMAL ±	DRAWN BY:	KJB		
		COMMENTS:			
MATERIAL	FINISH				

SIZE **A**   DWG. NO.   REV

SCALE: 1:3   WEIGHT: SHEET 2 OF 2

UMTRI

B

6.500

5.750
4.999
3.250
1.501
.750

.375

.750

2.826
2.765
2.887
2.750
1.750
2.765

7.500

.750 .671 .593

1.001

3.250

5.499

4X ⌀ .266 THRU ALL

2X ⌀ .266 THRU ALL
⌵ ⌀ .507 X 100°

6X ⌀ .257 THRU ALL
5/16-18 UNC THRU ALL

B

A

A

13.000

.433

1.000

.500

⌀ .375 THRU ALL

.125

1.000

1.000

11.341

9.591

7.841

.500

3X ⌀ .332 THRU ALL
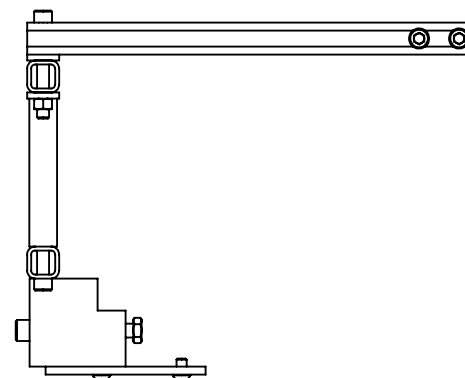
		INTERPRET GEOMETRIC TOLERANCING PER:	UNLESS OTHERWISE SPECIFIED:		NAME	DATE	TITLE: top_tube_manual_attach		
			DIMENSIONS ARE IN INCHES TOLERANCES: FRACTIONAL± ANGULAR: MACH± BEND ± TWO PLACE DECIMAL ± THREE PLACE DECIMAL ±0.005	DRAWN BY:	KJB				
M UMTRI				COMMENTS:			SIZE **A**	DWG. NO.	REV
		MATERIAL 6061 Al	FINISH				SCALE: 1:3	WEIGHT:	SHEET 1 OF 1

2

1

B

13.000

.433

1.000

.500

∅ .375 THRU ALL

1.000

.125

11.981

3X ∅ .332 THRU ALL

9.731

7.481

.500

1.000

A

	INTERPRET GEOMETRIC TOLERANCING PER:	UNLESS OTHERWISE SPECIFIED:		NAME	DATE	bottom_tube_manual_attach	
		DIMENSIONS ARE IN INCHES TOLERANCES: FRACTIONAL± ANGULAR: MACH± BEND ± TWO PLACE DECIMAL ± THREE PLACE DECIMAL ±0.005	DRAWN BY:	KJB			
			COMMENTS:			SIZE	DWG. NO.	REV
M UMTRI						**A**		
	MATERIAL 6061 Al	FINISH				SCALE: 1:3	WEIGHT:	SHEET 1 OF 1

2

1

2

1

B

3.000

Ø.866

Ø .313 ⤋ .940
3/8-16 UNC ⤋ .750

B

A

A

2

1

B

B

.500

⌀ .201 THRU ALL
1/4-20 UNC THRU ALL

.433

.750

A

A

		2		1	

.500

∅ .201 THRU ALL
1/4-20 UNC THRU ALL

.433

1.500

B

B

A

A

INTERPRET GEOMETRIC TOLERANCING PER:	UNLESS OTHERWISE SPECIFIED:		NAME	DATE	TITLE: manual_udig_attachments		
	DIMENSIONS ARE IN INCHES TOLERANCES: FRACTIONAL± ANGULAR: MACH± BEND ± TWO PLACE DECIMAL ± THREE PLACE DECIMAL ±	DRAWN BY:	KJB				
		COMMENTS:					
					SIZE **A**	DWG. NO.	REV
MATERIAL	FINISH				SCALE: 1:5	WEIGHT:	SHEET 1 OF 2

UMTRI

B

B

ITEM NO.	PART NUMBER	QTY.
1	side_manual_attach_plate	2
2	top_tube_manual_attach	2
3	bottom_tube_manual_attach	2
4	cyl_manual_attach	2
5	side_manual_attach_spacer_short	4
6	side_manual_attach_spacer_long	8
7	HX-SHCS 0.3125-18x1.375x1.375-N	12
8	SBHCSCREW 0.375-16x1.375-HX-N	4
9	SBHCSCREW 0.25-20x1-HX-N	8
10	HBOLT 0.2500-20x2x0.75-N	8
11	HBOLT 0.2500-20x2.5x0.75-N	4
12	SCHCSCREW 0.25-20x0.75x0.75-HX-N	4
13	manual_attach_tube_reinforcement_plate	4
14	HBOLT 0.3125-18x1.5x0.875-N	4
15	HJNUT 0.3125-18-D-N	16

A

A

2   1

B

6.500

5.750

4.999

3.250

1.501

.750

.125

.750

2.826   2.750   1.750

2.887   2.765

7.500

4X ⌀ .266 THRU ALL

2X ⌀ .266 THRU ALL
⌵ ⌀ .507 X 100°

6X ⌀ .257 THRU ALL
5/16-18 UNC THRU ALL

.750   .671   .593

1.001

3.250

5.499

A

2   1

2

1

B

B

13.000

.433

1.000

.500

⌀ .375 THRU ALL

.063

1.000

11.341

9.591

7.841

.500

1.000

1.000

⌀ .332 THRU ALL

A

A

M | UMTRI

2

1

2   1

B   B

13.000

.433

1.000   .500

Ø .375 THRU ALL

A   A

.063

1.000

.500

11.981

9.731

7.481

3X Ø .332 THRU ALL

1.000

INTERPRET GEOMETRIC TOLERANCING PER:	UNLESS OTHERWISE SPECIFIED:		NAME	DATE	bottom_tube_manual_attach	
	DIMENSIONS ARE IN INCHES TOLERANCES: FRACTIONAL± ANGULAR: MACH± BEND ± TWO PLACE DECIMAL ± THREE PLACE DECIMAL ±0.005	DRAWN BY:	KJB			
		COMMENTS:			SIZE DWG. NO. **A**	REV
MATERIAL 6061 Al	FINISH				SCALE: 1:3 WEIGHT:	SHEET 1 OF 1

UMTRI

2   1

B   B

3.000

Ø .866

Ø .313 ⤓ .940
3/8-16 UNC ⤓ .750

A   A

B

B

.500

$\varnothing$ .201 THRU ALL
1/4-20 UNC THRU ALL

.433

.750

A

A

UMTRI
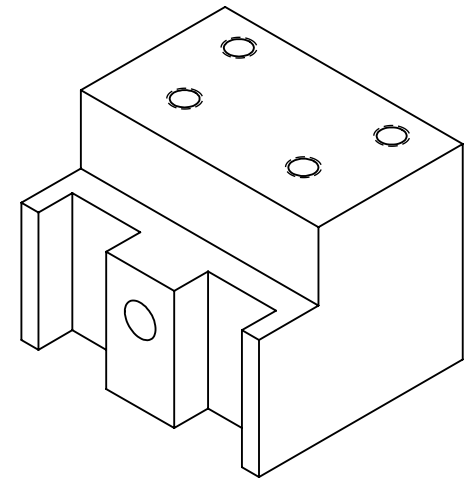
B

B

.500

$\varnothing$ .201 THRU ALL
1/4-20 UNC THRU ALL

.433

1.500

A

A

INTERPRET GEOMETRIC TOLERANCING PER:		UNLESS OTHERWISE SPECIFIED:		NAME	DATE	side_manual_attach_spacer_long
		DIMENSIONS ARE IN INCHES TOLERANCES: FRACTIONAL± ANGULAR: MACH± BEND ± TWO PLACE DECIMAL ± THREE PLACE DECIMAL ±0.005	DRAWN BY:	KJB		
			COMMENTS:			
MATERIAL 6061 Al		FINISH				

SIZE **A** DWG. NO.   REV

SCALE: 2:1   WEIGHT: SHEET 1 OF 1
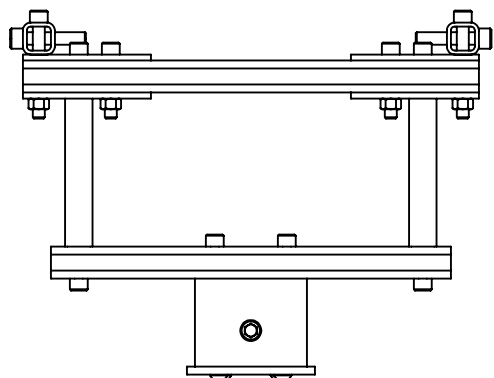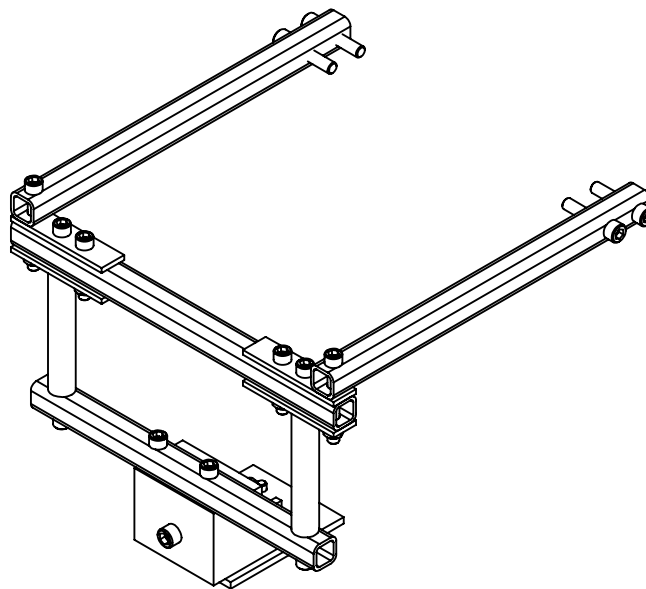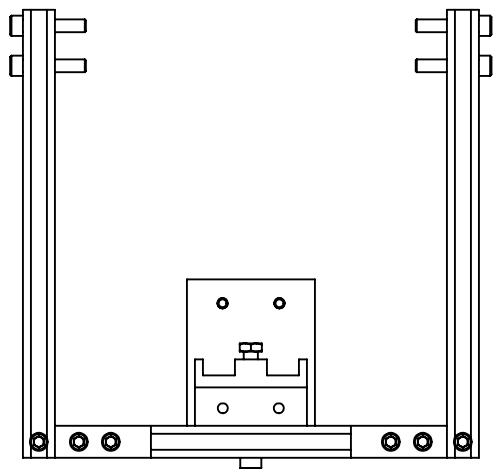
2

1

B

B

A

A

2

1

UMTRI

TITLE power_udig_attachments

SIZE **A** DWG. NO. REV

SCALE: 1:6 WEIGHT: SHEET 1 OF 2
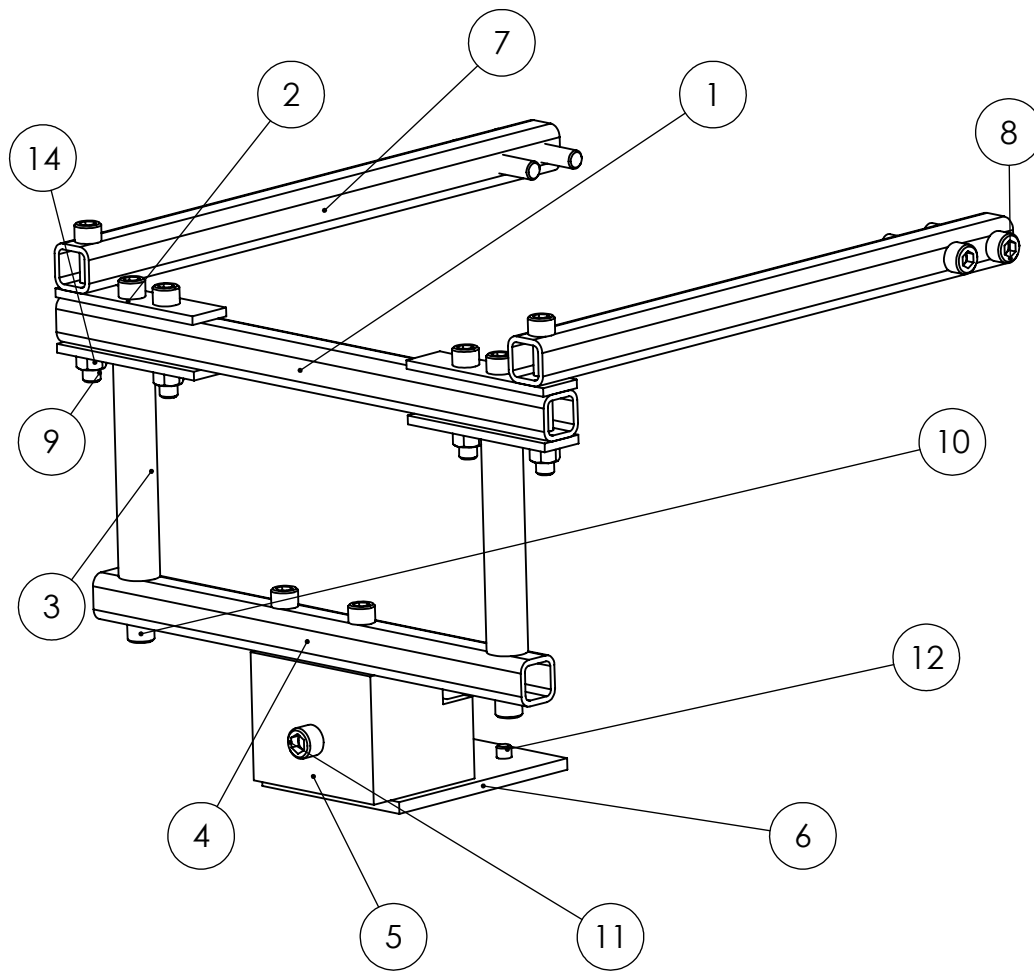
ITEM NO.	PART NUMBER	QTY.
1	rear_top_tube	1
2	power_attach_tube_reinforcement_plate	4
3	cyl_manual_attach	2
4	rear_bottom_tube	1
5	rear_lower_attach_block	1
6	rear_lower_attach_plate	1
7	side_attach_tube	2
8	B18.3.1M - 10 x 1.5 x 50 Hex SHCS -- 32NHX	4
9	HX-SHCS 0.375-16x3x1.5-N	2
10	HX-SHCS 0.375-16x2x1.5-N	8
11	HX-SHCS 0.4375-14x3.5x1.375-N	1
12	SBHCSCREW 0.3125-18x0.5-HX-N	4
13	HJNUT 0.4375-14-D-N	1
14	HNUT 0.3750-16-D-N	4

2

1

1.000

1.000

.125

1.000

.500

.500

1.750

2.750

6X ∅ .386 THRU ALL

14.250

11.500

12.500

13.750

B

B

A

A

TITLE: rear_top_tube

SIZE   DWG. NO.   REV
A

SCALE: 1:4   WEIGHT: SHEET 1 OF 1

2

1

2

1

B

B

4.000

.188

.188

2.750

1.750

.500

.500

1.000

3X ⌀ .397 THRU ALL

A

A

M UMTRI

2

1

2   1

3/8-16 Tapped Hole

$\emptyset$ .866

B   B

3/8-16 Tapped Hole

4.625

A   A

INTERPRET GEOMETRIC TOLERANCING PER:	UNLESS OTHERWISE SPECIFIED:		NAME	DATE
	DIMENSIONS ARE IN INCHES TOLERANCES: FRACTIONAL± ANGULAR: MACH± BEND ± TWO PLACE DECIMAL ± THREE PLACE DECIMAL ±0.005	DRAWN BY:	KJB	
		COMMENTS:		
MATERIAL 6061 Al	FINISH			

TITLE: cyl_power_attach

SIZE **A**

DWG. NO.

REV

SCALE: 1:1   WEIGHT: SHEET 1 OF 1

2   1

B

1.000

1.000

.125

.500

.875

5.125

4X ⌀ .386 THRU ALL

7.375

11.625

12.500

A

INTERPRET GEOMETRIC TOLERANCING PER:	UNLESS OTHERWISE SPECIFIED:		NAME	DATE
	DIMENSIONS ARE IN INCHES TOLERANCES: FRACTIONAL± ANGULAR: MACH± BEND ± TWO PLACE DECIMAL ± THREE PLACE DECIMAL ±0.005	DRAWN BY:	KJB	
		COMMENTS:		
MATERIAL Plain Carbon Steel	FINISH			

TITLE: rear_bottom_tube

SIZE **A**　DWG. NO.　　　　REV

SCALE: 1:3　WEIGHT:　　SHEET 1 OF 1

2

1

B

A

3.500
.625
.625
.421
1.471
2.125
2.500
3/8-16 Tapped Hole
.875
.875
3.000
2.125
.250
.250
1.250
1.250
1.000
2.750

1.625
Ø .453 THRU ALL

1.750

.750
.500
.750
5/16-18 Tapped Hole
2.750

4.000

3.000

2.894

1.117

1.000

.750

5.000

3.250

4X Ø .323 THRU ALL

UMTRI

TITLE: rear_lower_attach_plate

SIZE **A**   DWG. NO.   REV

SCALE: 1:2   WEIGHT: SHEET 1 OF 1
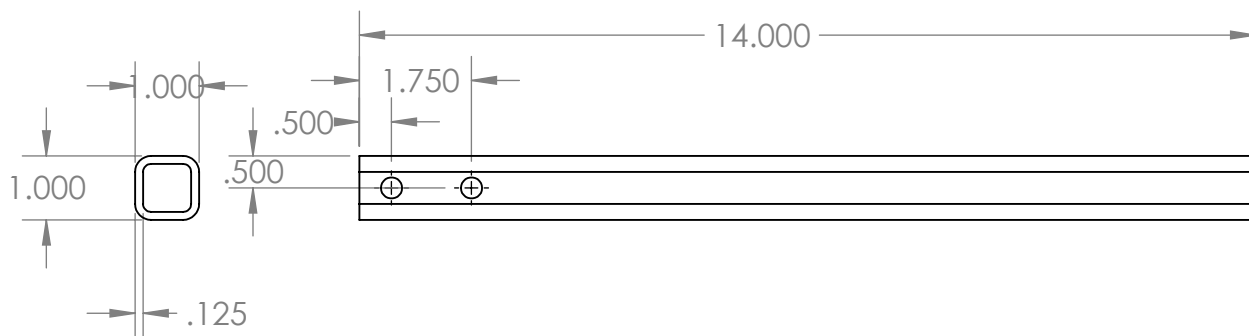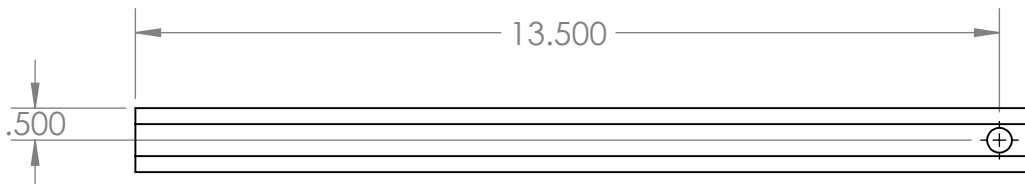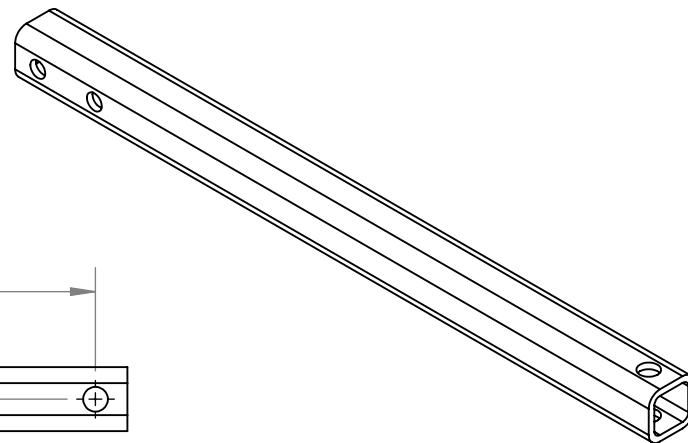
13.500

.500

14.000

1.750

.000

.500

.500

1.000

1.000

.125

			NAME	DATE
INTERPRET GEOMETRIC TOLERANCING PER:	UNLESS OTHERWISE SPECIFIED:			

UNLESS OTHERWISE SPECIFIED:

DIMENSIONS ARE IN INCHES
TOLERANCES:0.005
FRACTIONAL±
ANGULAR: MACH±   BEND ±
TWO PLACE DECIMAL   ±
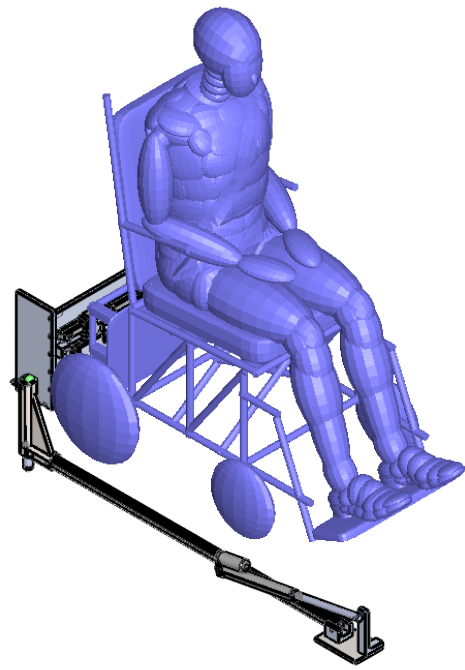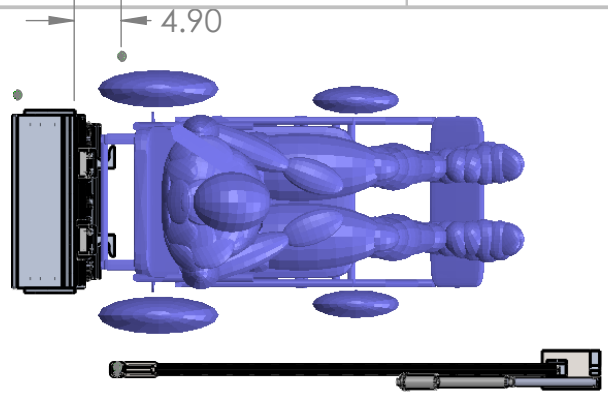THREE PLACE DECIMAL ±

DRAWN BY: KJB

COMMENTS:

MATERIAL
Plain Carbon Steel

FINISH

TITLE: side_attach_tube

SIZE **A**   DWG. NO.   REV

SCALE: 1:3   WEIGHT: SHEET 1 OF 1

2			1		

2   1

∅ .453

1.500

45.000

Electric Actuator
8in travel
225lb load capacity

B

9.250

∅ .516

5.375

1.625

1.500

4.750

4.000

Fixed Distance: Will depend on
actuator dimensions

A

2   1

2

1

4.90

B

B

11.10

5.97

49.82

50.25

15.11 — 17.21

A

A

INTERPRET GEOMETRIC TOLERANCING PER:	UNLESS OTHERWISE SPECIFIED:		NAME	DATE	TITLE: Assem_all_shifted		
	DIMENSIONS ARE IN INCHES TOLERANCES: FRACTIONAL± ANGULAR: MACH± BEND ± TWO PLACE DECIMAL ± THREE PLACE DECIMAL ±	DRAWN BY:	KJB				
		COMMENTS:			SIZE **A**	DWG. NO.	REV
MATERIAL	FINISH				SCALE: 1:20	WEIGHT:	SHEET 1 OF 1

2

1